SAPIENZA
UNIVERSITÀ DI ROMA

Doctoral Thesis

Aspects of BSM physics

Quality problem, axion detection and Naturalness

Scuola di dottorato Vito Volterra
Dottorato di ricerca in Fisica — XVIII ciclo

Candidate:
Pier Giuseppe Catinari
ID number 1652167
piergiuseppe.catinari@uniroma1.it

Thesis Advisors:
Prof. Angelo Esposito
Prof. Alfredo Leonardo Urbano

2026

A mia madre, Antonella

Our forefathers had civilization inside themselves, the wild outside.
We live in the civilization they created, but within us the wilderness still lingers.
What they dreamed, we live, and what they lived, we dream.
T. K. Whipple, Study Out the Land

Contents

Foreword

The material of the thesis is schematically organized as follows

- **Chapter 1** provides an overview of the Standard Model and its theoretical extensions, with a special emphasis on the Strong CP problem and the QCD axion as a possible solution, together with a discussion of the Higgs mass hierarchy problem.

- **Chapter 2** introduces the mathematical formulation of instantons as non-perturbative, finite-action solutions of the Yang–Mills equations in Euclidean spacetime and develops the formalism of 't Hooft vertex operators, which encode the effects of instanton-induced interactions on fermionic fields. Particular emphasis is placed on their role in the non-perturbative effects contributing to the QCD axion potential.

- **Chapter 3** is based on Ref. [1]:
  P. Catinari, A. Urbano,
  "Gravitational instantons and the quality problem of the QCD axion: Facts, speculations, and statements in between",
  Phys. Rev. D **111** (2025) no. 12, 125007, arXiv:2410.12741 [hep-th].

- **Chapter 4** is based on Ref. [2]:
  P. Catinari, A. Esposito, S. Pavaskar,
  "Effective field theory for anisotropic antiferromagnets: Gapped Goldstone bosons, pseudo-Goldstone excitations, and phase transitions",
  Phys. Rev. B **112** (2025) no. 6, 064408, arXiv:2411.09761 [cond-mat.str-el].

- **Chapter 5** is based on Ref. [3]:
  P. Catinari, A. Esposito, S. Pavaskar,
  "Hunting axion dark matter with antiferromagnets: A case study with nickel oxide",
  Phys. Rev. D **112** (2025) L121302, arXiv:2411.11971 [hep-ph].

- **Chapter 6** is based on Ref. [4]:
  P. Catinari, L. Del Grosso, L. Di Giovanni, A. Urbano,
  "Insights into the highest natural scale: Finite naturalness challenges inflationary dynamics",
  Phys. Rev. D **112** (2025) no. 6, 064408, arXiv:2504.17846 [hep-ph].

During the Ph.D. I have also coauthored the following preprint, which is not part of the thesis

- P. Catinari, R.T. D'Agnolo, P. Sesma,
  "Weak Scale Triggers in the SMEFT", arXiv:2512.11026 [hep-ph].

Abstract

The Standard Model (SM) successfully describes most of the known interactions among elementary particles, yet several fundamental questions remain unanswered. This Ph.D. thesis investigates theoretical and phenomenological aspects of physics Beyond the Standard Model (BSM), focusing on two central issues in high-energy physics: the strong CP problem and the naturalness of the Higgs boson mass.

This work addresses these challenges by combining non-perturbative methods in quantum field theory, effective field theory techniques, and phenomenologically motivated applications, with the goal of deepening our understanding of the mechanisms underlying BSM physics.

A central theme of the thesis is the study of the QCD axion, a theoretically well-motivated candidate for resolving the strong CP problem and a possible component of dark matter. Using the formalism of instantons and the corresponding 't Hooft vertex operators, we analyze the non-perturbative contributions to the axion potential, with particular attention to gravitational instanton effects.

The thesis also explores connections with condensed matter physics. By employing effective field theories for anisotropic antiferromagnets, we describe the emergence of gapped Goldstone and pseudo-Goldstone modes. Building on these insights, we investigate the potential of antiferromagnetic materials, such as nickel oxide (NiO), as experimental targets for axion dark matter detection, thereby creating a bridge between high-energy theoretical predictions and experimental approaches in solid-state physics.

Finally, the work examines the implications of the naturalness principle in a cosmological context, analyzing how naturalness considerations constrain inflationary dynamics and early-universe cosmology, particularly in models featuring super-Planckian field excursions.

Taken together, the results presented in this thesis provide a coherent contribution to the study of physics beyond the Standard Model. By integrating rigorous theoretical analysis, phenomenological relevance, and experimental considerations, this work advances the understanding of non-perturbative effects, axion physics, and the interplay between high-energy and condensed matter systems, offering new insights into some of the most compelling questions in particle physics today.

CHAPTER

1 Introduction

Although the Standard Model of particle physics has demonstrated remarkable success in describing the fundamental particles and their interactions, it is not without its limitations and unresolved questions. Despite its predictive power and extensive experimental validation, the Standard Model leaves several profound theoretical issues unexplained. Among the most significant are the Strong CP problem, which raises the question of why quantum chromodynamics (QCD) appears to preserve CP symmetry despite no theoretical requirement to do so, and the electroweak hierarchy problem, which concerns the unnatural fine-tuning required to keep the Higgs boson mass stable in the presence of large radiative corrections. This introductory chapter begins with a concise overview of the mathematical structure and foundational principles of the Standard Model, laying the groundwork for an examination of its limitations. In particular, the chapter will focus on the Strong CP problem and explore the axion as a proposed solution to this puzzling symmetry. Additionally, the electroweak hierarchy problem will be discussed, highlighting its implications for naturalness and the need for physics beyond the Standard Model.

1.1 The Standard Model (and beyond)

The Standard Model is a gauge theory that describes strong and electroweak interactions via the symmetry group $SU(3)_c \times SU(2)_L \times U(1)_Y$. The $SU(3)_c$ factor mediates what are known as the strong interactions, or Quantum Chromodynamics (QCD), while $SU(2)_L \times U(1)_Y$ represent the electroweak interactions. The strong and electroweak interactions are understood as arising due to the exchange of various spin-one bosons amongst the spin-half particles that make up matter. The specific gauge bosons associated with the generators of the algebra of the group are:

$$\begin{array}{ccccc} SU(3)_c & \times & SU(2)_L & \times & U(1)_Y \\ \downarrow & & \downarrow & & \downarrow \\ G^a_\mu & & W^i_\mu & & B_\mu \end{array}$$

where $a = 1, \ldots, 8$ and $i = 1, \ldots, 3$. The three forces described by the Standard Model are included in the Lagrangian density $\mathcal{L}_{\rm SM}$ as gauge interactions

$$\mathcal{L}_{\rm SM} \supset -\frac{1}{4}G^a_{\mu\nu}G^{a\mu\nu} - \frac{1}{4}W^i_{\mu\nu}W^{i\mu\nu} - \frac{1}{4}B_{\mu\nu}B^{\mu\nu} - \frac{g_s^2\theta^0_{\rm QCD}}{64\pi^2}\epsilon_{\mu\nu\rho\sigma}G^{a\mu\nu}G^{a\rho\sigma}$$
$$- \frac{g^2\theta_{\rm W}}{64\pi^2}\epsilon_{\mu\nu\rho\sigma}W^{i\mu\nu}W^{i\rho\sigma} - \frac{g'^2\theta_1}{64\pi^2}\epsilon_{\mu\nu\rho\sigma}B^{\mu\nu}B^{\rho\sigma} \equiv \mathcal{L}_{\rm gauge}\,, \qquad (1.1)$$

in which the gauge field-strengths are given by

$$
\begin{aligned}
B_{\mu\nu} &= \partial_\mu B_\nu - \partial_\nu B_\mu \,, \\
W^i_{\mu\nu} &= \partial_\mu W^i_\nu - \partial_\nu W^i_\mu - g\epsilon^{ijk} W^j_\mu W^k_\nu \,, \\
G^a_{\mu\nu} &= \partial_\mu G^a_\nu - \partial_\nu G^a_\mu - g_s f^{abc} G^b_\mu G^c_\nu \,,
\end{aligned} \tag{1.2}
$$

where g and g_s are the weak and strong gauge couplings and ϵ^{ijk} and f^{abc} are the structure constants of $SU(2)_L$ and $SU(3)_c$, respectively. Apart from spin-one particles, we are aware of a number of fundamental spin-half particles. The particle content (forces and matter) of the Standard Model can be summarized in Table 1.1.

Field	$SU(3)_C$	$SU(2)_L$	$U(1)_Y$	Name
A^a_μ	$\mathbf{8}$	$\mathbf{1}$	0	Gluons
W^k_μ	$\mathbf{1}$	$\mathbf{3}$	0	Weak SU(2) bosons
B_μ	$\mathbf{1}$	$\mathbf{1}$	0	Hypercharge boson
Q	$\mathbf{3}$	$\mathbf{2}$	$1/6$	Quark doublets
u^c	$\overline{\mathbf{3}}$	$\mathbf{1}$	$-2/3$	Up-type anti-quarks
d^c	$\overline{\mathbf{3}}$	$\mathbf{1}$	$1/3$	Down-type anti-quarks
L	$\mathbf{1}$	$\mathbf{2}$	$-1/2$	Lepton doublets
e^c	$\mathbf{1}$	$\mathbf{1}$	1	Charged anti-leptons
H	$\mathbf{1}$	$\mathbf{2}$	$1/2$	Higgs field

Table 1.1: Transformation properties of the SM fields under the SM gauge group. The matter fields (rows 4–8) are 3- vectors in the generation space: $Q = (Q_1, Q_2, Q_3) = \left(\begin{pmatrix} u_1 \\ d_1 \end{pmatrix}, \begin{pmatrix} u_2 \\ d_2 \end{pmatrix}, \begin{pmatrix} u_3 \\ d_3 \end{pmatrix}\right)$, $u^c = (u^c_1, u^c_2, u^c_3) \equiv (u^c, c^c, t^c)$, $d^c = (d^c_1, d^c_2, d^c_3) \equiv (d^c, s^c, b^c)$ and $L = (L_1, L_2, L_3) = \left(\begin{pmatrix} \nu_1 \\ e_1 \end{pmatrix}, \begin{pmatrix} \nu_2 \\ e_2 \end{pmatrix}, \begin{pmatrix} \nu_3 \\ e_3 \end{pmatrix}\right)$.

We are working in two-component notation following the notation of [5], where a four-component *Dirac spinor field* $\Psi(x)$ is made of two-component spinor fields $\psi_\alpha(x)$ and $\psi^c_\alpha(x)$, of opposite U(1)-charge as follows[1]

$$
\Psi(x) = \begin{pmatrix} \psi_\alpha(x) \\ \psi^{c\dagger\dot\alpha}(x) \end{pmatrix} . \tag{1.3}
$$

The kinetic term of the fermions and their gauge interactions are described by the term

$$
\begin{aligned}
\mathcal{L}_{\rm SM} &\supset \sum_{f\in Q,L} i f^\dagger \overline{\sigma}^\mu D_\mu f + \sum_{f\in u,d,e} i f^{c\dagger} \overline{\sigma}^\mu D^c_\mu f^{c\dagger} \equiv \mathcal{L}_{\rm kin} \,, \\
D_\mu \mathcal{X} &= \partial_\mu \mathcal{X} + i g_s G^a_\mu T^a_{R_\mathcal{X}} \mathcal{X} + i g W^i_\mu T^i_{R_\mathcal{X}} \mathcal{X} + i g' y_\mathcal{X} B_\mu \mathcal{X} \,.
\end{aligned} \tag{1.4}
$$

This is a good point to pause for a moment and introduce the logic of an Effective Field Theory (EFT) (see Sec. 1.4 for a more extended discussion). EFT provides a useful tool for organising the effects of any new physics in the SM field content. The basic observation is that although a Lagrangian density may in principle involve an infinite sum of interactions among the degrees of freedom of the theory, one

[1] The four-component chiral fermions are related to 2-component fermions via the dictionary – suppressing flavor index

$$
\begin{aligned}
q_L &= \begin{pmatrix} Q_\alpha \\ 0 \end{pmatrix}, u_R = \begin{pmatrix} 0 \\ u^{c\dagger\dot\alpha} \end{pmatrix}, d_R = \begin{pmatrix} 0 \\ d^{c\dagger\dot\alpha} \end{pmatrix}, l_L = \begin{pmatrix} L_\alpha \\ 0 \end{pmatrix}, e_R = \begin{pmatrix} 0 \\ e^{c\dagger\dot\alpha} \end{pmatrix}, \\
\overline{q}_L &= \left(0, Q^\dagger_{\dot\alpha}\right), \overline{u}_R = (u^{c\alpha}, 0), \overline{d}_R = (d^{c\alpha}, 0), \overline{l}_L = \left(0, L^\dagger_{\dot\alpha}\right), \overline{e}_R = (e^{c\alpha}, 0) \,.
\end{aligned}
$$

in fact only needs to deal with a finite subset of these when working in the deep infrared (at least in the perturbative regime of the theory). This is precisely why the Standard Model Lagrangian can be compact enough to fit on a t-shirt or a coffee mug. Concretely, when working in $D = 3+1$ spacetime dimensions, only those operatore of dimension 3 or less are *relevant*, those of dimension 4 are said to be *marginal*, while the rest are *irrelevant*. As a motivated illustration for this, let's consider the following example of a scalar field theory $D = 3+1$ spacetime

$$S = \int d^4x \left(\frac{1}{2}(\partial_\mu\phi)^2 - \frac{1}{2}m^2\phi^2 + \lambda\phi^4 + g\phi^6 + \cdots\right) = S^{\text{ren}} + S^{\text{non-ren}}\,, \tag{1.5}$$

where the ellipses stands for higher dimensional operators. Consider now a *dilation* transformation, *i.e.* a rescaling of the length scale

$$x^\mu \to \lambda x^\mu\,, \tag{1.6}$$

so that the volume element is rescaled by the factor λ^4. Under dilations, an operator with mass dimension $[\mathcal{O}]_{\rm m} = d_{\mathcal{O}}$, is rescaled by $\lambda^{-d_{\mathcal{O}}}$. Then, the contribution of this particular operator will be rescaled by a power $\lambda^{-d_{\mathcal{O}}}$, that is – under dilations

$$\mathcal{O}(x) \xrightarrow{x\to\lambda x} \lambda^{-d_{\mathcal{O}}}\mathcal{O}(x)\,. \tag{1.7}$$

In relativistic QFT, instead of distance scales L, it is more convenient to refer to energy scales E. The two are simply connected via the uncertainty relation $\text{E} \simeq 1/\text{L}$ (in natural units $\hbar = c = 1$), thus long distances translate into low energy, or infrared (IR) in our jargon, while short distances translate into high energy or ultraviolet (UV). As a result, under dilations

$$\mathcal{O}(x) \xrightarrow{x\to\lambda x} \Lambda^{d_{\mathcal{O}}}\mathcal{O}(x)\,, \tag{1.8}$$

where Λ is some energy scale. The higher-dimensional local operator $\mathcal{O}(x)$ will appear in the action in the form

$$S \supset \int d^4x\, c_{\mathcal{O}}\; \mathcal{O}(x)\,, \tag{1.9}$$

therefore, from dilations selection rules (or spurion analysis) we can write, being physics dilation invariant (or equivalently, being the action dimensionless)

$$\int d^4x\, c_{\mathcal{O}}\; \mathcal{O}(x) = \frac{c_{\mathcal{O}}}{\Lambda^{4-d_{\mathcal{O}}}} \int d^4x\, \mathcal{O}(x)\,, \tag{1.10}$$

for some numerical coefficient $c_{\mathcal{O}}$. The contribution of the operator $\mathcal{O}$ to some observable measured at low-energy E, will be then suppressed by a factor

$$(E/\Lambda)^{d_{\mathcal{O}}-4}\,,$$

where Λ denotes the scale of new physics (or the cutoff scale). At very longs scales, *i.e.* in the IR, we thus see that relevant operators (the first two in the action in Eq.(1.5)), will dominate the action, while the effect of the irrelevant one (the last term in Eq.(1.5), *i.e.* the ϕ^6) approaches zero. For marginal operators (the ϕ^4), one must carry out a more sophisticated quantum analysis – there is no guarantee that in strongly coupled the anomalous dimension is small, and so the naive dimension of an operator tells us nothing on its own. All the other interactions between the fields in Table 1.1 are obtained simply by symmetry under the gauge group and considering marginal and relevant operators. We have

$$\begin{aligned}\mathcal{L}_{\rm SM} &= \mathcal{L}_{\rm gauge} + \mathcal{L}_{\rm kin} \\ &\quad - \left(Q^\dagger \widetilde{H} Y_u u^{c\dagger} + Q^\dagger H Y_d d^{c\dagger} + L^\dagger H Y_e e^{c\dagger} + \text{h.c.}\right) + |D_\mu H|^2 + \frac{m_0^2}{2}|H|^2 - \frac{\lambda_0}{2}|H|^4\,,\end{aligned} \tag{1.11}$$

where the second line identifies the Yukawa interactions, given in terms of three complex matrices $Y_{u,d,l}$ and $\widetilde{H} = \epsilon H^*$, where ϵ is the Levi-Civita tensor in the $\mathrm{SU(2)_L}$ space. The Higgs potential is minimized at $v = m_0/\sqrt{2\lambda_0} \simeq 246$ GeV, where $H(x) = (0, (v + h(x))/\sqrt{2})^T$, giving rise to electroweak symmetry breaking. The gauge group is then spontaneously broken down to $\mathrm{U(1)_{em}}$, describing the electromagnetic interactions

$$SU(3)_c \times SU(2)_L \times U(1)_Y \xrightarrow{H} SU(3)_c \times U(1)_{em}\,.$$

The would-be Nambu-Goldstone bosons arising from the spontaneous symmetry breaking of the gauge group are eaten by the gauge bosons associated to the broken generators, giving rise to the massive $W^\pm$ and Z bosons. Furthermore, electroweak symmetry breaking is responsible for the generation of fermion masses. Splitting the $\mathrm{SU(2)_L}$ doublets as

$$Q = \begin{pmatrix} u \\ d \end{pmatrix} \text{ and } L = \begin{pmatrix} \nu \\ e \end{pmatrix}\,, \tag{1.12}$$

we find the mass terms

$$\mathcal{L}_m = -\frac{v}{\sqrt{2}} u^\dagger Y_u u^{c\dagger} - \frac{v}{\sqrt{2}} d^\dagger Y_d d^{c\dagger} - \frac{v}{\sqrt{2}} e^\dagger Y_e e^{c\dagger} + \text{h.c.}\,. \tag{1.13}$$

The physical masses are obtained upon performing a singular value decomposition of the Yukawa matrices in $\mathcal{L}_m$. Indeed, in full generality, one can decompose any matrix as $Y_f = L_f Y_f^{\text{diag}} R_f^\dagger$, where L_f and R_f are SU(3) matrices, and Y_f^{diag} is diagonal with complex entries. Then, we can rotate the quark fields via the SU(3) *flavor transformations*

$$u \to L_u u\,, d \to L_d d\,, e \to L_e e\,, \text{ and } u^c \to u^c R_u^\dagger\,, d^c \to d^c R_d^\dagger\,, e^c \to e^c R_e^\dagger\,. \tag{1.14}$$

This transformation leaves invariant most of the terms in the Lagrangian (1.11), in particular the R_fs cancel out completely, and we obtain

$$\mathcal{L}_m = -u^\dagger M_u u^{c\dagger} - d^\dagger M_d d^{c\dagger} - e^\dagger M_e e^{c\dagger} + \text{h.c.}\,, \tag{1.15}$$

where $M_f = v/\sqrt{2} Y_f^{\text{diag}}$. We can now make the entries of the diagonal matrices M_u, M_d, M_e real performing the phase transformations

$$u_j^c \to e^{i\phi_u^j} u_j^c\,,\; d_j^c \to e^{i\phi_d^j} d_j^c\,,\; e_j^c \to e^{i\phi_e^j} e_j^c\,, \tag{1.16}$$

and the Yukawa terms finally read

$$\mathcal{L}_m = -u_i^\dagger m_u^i u_i^{c\dagger} - d_i^\dagger m_d^i d_i^{c\dagger} - e_i^\dagger m_e^i e_i^{c\dagger}\,. \tag{1.17}$$

The only place where the L_fs emerge is in the charged current interactions between the W boson and left-handed quarks

$$\mathcal{L}_{\text{FV}} = -\frac{g}{\sqrt{2}} W_\mu^+ u^\dagger \overline{\sigma}^\mu V d + \text{h.c.}\,, \tag{1.18}$$

where the CKM matrix is related to the left rotations as $V = L_u^\dagger L_d$, and therefore is unitary. One can show that under CP transformations, $V \to V^*$, thus phases of the CKM matrix may lead to CP violation. A general unitary matrix has 9 free parameters: 3 angles and 6 phases, however most of the phases are removable. Indeed, we can make the *phase reparametrizations*

$$u_j \to e^{i\phi_j} u_j\,, u_j^c \to e^{-i\phi_j} u_j^c\,, d_j \to e^{i\eta_j} d_j\,, d_j^c \to e^{-i\eta_j} d_j^c\,, \tag{1.19}$$

which maintain real quark masses, and transform the CKM matrix elements as

$$V_{mn} \to e^{-i(\phi_m - \eta_n)} V_{mn} \,. \tag{1.20}$$

Physics cannot change under the above transformations (1.14) and (1.19), as these are merely change of variables in the functional integral that defines physical quantities. Therefore, CP-violating observables must be invariant under such transformations. Using the fact that, under CP $Y_f \xrightarrow{\text{CP}} Y_f^*$, quantities like

$$\mathrm{Tr}(Y_u Y_u^\dagger) \quad \text{or} \quad \det(Y_u^\dagger Y_u)\,,$$

that are reparametrization invariant, are suitable for describing CP-violating observables, since are CP-even.
To build a CP-odd quantity, one needs to go at quartic order in the Yukawas. Since, under CP

$$Y_u Y_u^\dagger Y_d Y_d^\dagger \xrightarrow{\text{CP}} \left(Y_d Y_d^\dagger Y_u Y_u^\dagger\right)^T \,,$$

then

$$\det\left[Y_u Y_u^\dagger, Y_d Y_d^\dagger\right] \xrightarrow{\text{CP}} -\det\left[Y_u Y_u^\dagger, Y_d Y_d^\dagger\right] \,. \tag{1.21}$$

Therefore, the QCD Lagrangian density $\mathcal{L}_{\text{QCD}}$

$$\mathcal{L}_{\text{SM}} \supset \mathcal{L}_{\text{QCD}} = -\frac{1}{4} G^a_{\mu\nu} G^{a\mu\nu} - \frac{g_s^2 \theta^0_{\text{QCD}}}{64\pi^2} \epsilon_{\mu\nu\rho\sigma} G^{a\mu\nu} G^{a\rho\sigma} - \left(Q^\dagger \widetilde{H} Y_u u^{c\dagger} + Q^\dagger H Y_d d^{c\dagger} + \text{h.c.}\right) \,, \tag{1.22}$$

contains the CP-violating phase

$$\boxed{\delta_{\text{CKM}} = \arg\ \det\left[Y_u Y_u^\dagger, Y_d Y_d^\dagger\right] \simeq \mathcal{O}(1)\,.} \tag{1.23}$$

There is however, another CP-violating phase in $\mathcal{L}_{\text{QCD}}$. The simultaneous rotation of all quarks under the *axial* transformation

$$\begin{aligned} u_j &\to e^{i\alpha_j} u_j \,, & u_j^c &\to e^{i\alpha_j} u_j^c \,, \\ d_j &\to e^{i\beta_j} d_j \,, & d_j^c &\to e^{i\beta_j} d_j^c \,, \end{aligned} \tag{1.24}$$

$j = 1\,, \ldots\,, N_f$ transforms the Yukawa matrices as

$$Y_u^{mn} \to e^{-i(\alpha_m + \alpha_n)} Y_u^{mn} \,, \quad Y_d^{mn} \to e^{-i(\beta_m + \beta_n)} Y_d^{mn} \,,$$

that is to say

$$\det(Y_u) \to e^{-2i \sum_j \alpha_j} \det(Y_u) \,,\ \det(Y_d) \to e^{-2i \sum_j \beta_j} \det(Y_d) \,, \tag{1.25}$$

which can be easily proven in the basis where $Y_{u,d}$ are diagonal. Moreover, using the fact that, under an axial transformation

$$Q \to e^{i\alpha \mathcal{Q}} Q \,, \tag{1.26}$$

$$q^c \to e^{-i\alpha \mathcal{Q}} q^c \,, \tag{1.27}$$

where $\mathcal{Q}$ is a matrix in flavor space, we have

$$\boxed{\delta \mathcal{L}_{\text{QCD}} = 2\alpha\, \mathrm{Tr}\, \mathcal{Q} \frac{g_s^2}{64\pi^2} \epsilon_{\mu\nu\rho\sigma} G^{a\mu\nu} G^{a\rho\sigma} \,,} \tag{1.28}$$

we find that, under (1.24) – being $\mathcal{Q} = \text{diag}\left(\alpha_1, \ldots, \alpha_{N_f}, \beta_1, \ldots, \beta_{N_f}\right)$

$$\delta \mathcal{L}_{\text{QCD}} = 2 \sum_j (\alpha_j + \beta_j) \frac{g_s^2}{64\pi^2} \epsilon_{\mu\nu\rho\sigma} G^{a\mu\nu} G^{a\rho\sigma} \,, \tag{1.29}$$

that is to say, under (1.24), we have the shift $\theta^0_{\rm QCD} \to \theta^0_{\rm QCD} + 2\sum_j(\alpha_j+\beta_j)$. We thus have found another CP-odd phase in $\mathcal{L}_{\rm QCD}$ that is invariant under phase transformations (1.24)

$$\boxed{\theta_{\rm QCD} = \arg\left[e^{i\theta^0_{\rm QCD}}\det Y_u Y_d\right]\,.} \tag{1.30}$$

It is worth noting that, if either Y_u or Y_d has a vanishing eigenvalue, then a chiral transformation can reabsorb θ_0. The phase $\theta_{\rm QCD}$ is CP-odd, since under CP

$$e^{i\theta_{\rm QCD}}\det Y_u Y_d \xrightarrow{\rm CP} e^{-i\theta_{\rm QCD}}\det Y_u^* Y_d^*\,,$$

and will enter in the expression of CP-odd observables (like the electric dipole moment of the neutron). The SM is a well-established basis of particle physics, with experimental results almost universally matching the theoretical predictions. Why, then, do we particle theorist and phenomenologists spend our lives looking for new states Beyond the SM (BSM)? Though there are many motivations, the present work has been fueled by the following subset

- **The Strong CP problem,**
- **the Naturalness problem of the Higgs boson mass.**

In the rest of this Introduction, we shall discuss each of these problems in turn.

1.2 The strong CP problem

In non-relativistic quantum mechanics, the neutron electric dipole moment is encoded in the Hamiltonian as

$$H_{\rm NR} \supset -d_n \boldsymbol{E}\cdot\boldsymbol{S}_n\,, \tag{1.31}$$

where $\boldsymbol{E}$ stands for the electric field and $\boldsymbol{S}_n$ is the spin-density of the neutron. In relativistic Quantum Field Theory, the analogous observable is induced by the Lagrangian density – in the 4-component notation of Dirac spinors

$$\mathcal{L} \supset -\frac{i}{2} d_n \overline{n}\sigma^{\mu\nu}\gamma_5 n\, F_{\mu\nu}\,, \tag{1.32}$$

where $n(x)$ is the neutron Dirac field. We can give a spurionic estimate for d_n using the following argument. We know that $\overline{\theta}$ becomes unphysical if any of the quark masses is zero. Therefore, d_n should be suppressed by at least one power of the lightest quark masses, in this case m_u. Since $[d_n]_{\rm m} = -1$, we must account for its mass dimension with the only other relevant scale at our disposal, m_n. Finally, being d_n CP-odd, it should be proportional to the only CP-odd parameter that we have at disposal in the IR, *i.e.* $\theta_{\rm QCD}$, and – being a dipole – to the electric charge. Therefore, our estimate can be expressed as

$$d_n \simeq c_n e \frac{m_u}{m_n^2}\theta_{\rm QCD}\,, \tag{1.33}$$

for some undetermined, at this stage, constant c_n. Plugging in the most recent data (see Ref. [6]), we get $d_n \lesssim 10^{-26}{\rm cm}\times{\rm e}$, from which we constrain $\theta_{\rm QCD}$ to be

$$\boxed{|\theta_{\rm QCD}| \lesssim 10^{-10}\,.} \tag{1.34}$$

We have argued that in the Standard Model there are two phases

$$\begin{aligned} \delta_{\rm CKM} &= \arg\ \det\left[Y_u Y_u^\dagger, Y_d Y_d^\dagger\right]\,, \\ \theta_{\rm QCD} &= \arg\left[e^{i\theta^0_{\rm QCD}}\det Y_u Y_d\right]\,. \end{aligned} \tag{1.35}$$

This remarkably small magnitude, ensures that low-energy QCD is approximately P and CP conserving; the puzzle of why the value of $\theta_{\rm QCD}$ should be so small is called *the strong CP problem*.
One might ask: what is wrong with simply choosing $\theta_{\rm QCD} = 0$? Within the Standard Model, this choice must be made at a particular scale, for instance somewhere above the Z or top quark mass. Since the weak interactions also break C and CP, $\theta_{\rm QCD}$ will renormalize (or run) due to loops involving Standard Model particles [7], and so will be nonzero at low energies where neutron dipole moments are measured. Within the Standard Model, the resulting nonzero value is less than 10^{-15}, however, and so is too small to be detected in existing experiments. This shows that it is consistent simply to choose the value of $\theta_{\rm QCD}$ to be small within the Standard Model, ant that phenomenologically-small values for $\theta_{\rm QCD}$ do not pose a naturalness problem for the standard model itself. Such a small value for $\theta_{\rm QCD}$ is nevertheless rather surprising. Furthermore, the small size of $\theta_{\rm QCD}$ often does become a naturalness problem once the Standard Model is embedded into a more microscopic theory, such as within the supersymmetric extensions. For this reason we describe in this Section a fairly mild modification of the Standard Model for which the small size of $\theta_{\rm QCD}$ could be made to *relax* to zero. It can do so because in the modified theory, $\theta_{\rm QCD}$ is related to the expectation value for an almost-massless new scalar field (called the QCD *axion*), for which the dynamics favors configurations [8] with $\theta_{\rm QCD} = 0$. Although the particle associated with this axion field is very light, it could have escaped detection so far because it couples to the other Standard Model fields only through small non-renormalizable (irrelevant) interactions.
Another motivation for studying the strong CP problem is that it offers a useful framework for exploring key features of the QCD vacuum, which are of intrinsic theoretical interest. In what follows, we will compute the axion chiral Lagrangian, following the seminal works [9, 10]. This requires constructing the QCD chiral Lagrangian, taking into account both the explicit breaking due to the $\rm U(1)_A$ anomaly and the quark masses. To do so consistently, we work at leading order in the large-N expansion of QCD. In the large-N limit, QCD exhibis both confinement and chiral symmetry breaking [11]. We have, for a $SU(N)$ QCD

$$\mathcal{L} = -\frac{1}{4} G^a_{\mu\nu} G^a_{\mu\nu} + i q^\dagger \overline{\sigma}^\mu D_\mu q + i q^{c\dagger} \overline{\sigma}^\mu D_\mu q^c + q^c M q + \text{h.c.} + \frac{\theta {g'_s}^2}{32\pi^2} G^a_{\mu\nu} \widetilde{G}^{a\mu\nu} \,, \tag{1.36}$$

where, for simplicity we redefined $\theta_{\rm QCD} \equiv \theta$ and with quarks transforming under the fundamental representation of $SU(N)$ and $G^a_{\mu\nu} = \epsilon_{\mu\nu\rho\sigma} G^{a\rho\sigma}/2$. That is

$$D_\mu = \partial_\mu + i g'_s A^a_\mu T^a \,. \tag{1.37}$$

To have a smooth large N limit, we have to replace $g'_s \to g_s/\sqrt{N}$, so that the anomaly is absent for $N \to \infty$. At $N \to \infty$, ignoring the quark masses, QCD with N_f flavors has the chiral symmetry

$$U(N_f) \times U(N_f) \to U_V(N_f) \,, \tag{1.38}$$

spontaneously broken by the chiral condensate

$$\langle q_i q^c_j \rangle = \Lambda^3 \delta_{ij} \,, i,j = 1,\ldots,N_f \,, \tag{1.39}$$

where Λ is a mass scale and the quarks transform under $U(N_f) \times U(N_f)$ as

$$q_i \to A_{ij} q_j \,, \quad q^c_i \to q^c_j B^\dagger_{ji} \,, \tag{1.40}$$

where A and B are two independent $U(N_f)$ matrices, *i.e.* $A^\dagger A = B^\dagger B = \mathbf{1}$. Under the above transformation, we have

$$\langle q_i q^c_j \rangle \to A_{ik} \langle q_k q^c_l \rangle B^\dagger_{lj}$$

therefore we introduce the Goldstone boson matrix

$$U(x) \equiv \frac{F_\pi}{\sqrt{2}} e^{i\sqrt{2}\Phi(x)/F_\pi} \,, \;\; \Phi(x) = T^a \pi^a(x) + \frac{\mathbf{1}_{N_f}}{\sqrt{N_f}} \eta'(x) \,, \tag{1.41}$$

where T^a are $SU(N_f)$ generators, normalized as $\mathrm{Tr}(T^aT^b) = \delta^{ab}$, such that under $U(N_f) \times U(N_f)$ transforms as $U \sim qq^c$, *i.e.*

$$U(x) \to AU(x)B^\dagger\,. \tag{1.42}$$

At the level of two-derivative terms, there are two possible invariants

$$\mathcal{I}_1 = \mathrm{Tr}(\partial_\mu U^\dagger \partial_\mu U)\,,\ \mathcal{I}_2 = \Big|\mathrm{Tr}(U^\dagger\partial_\mu U)\Big|^2\,. \tag{1.43}$$

Expanding we find, at the lowest order in the derivative expansion

$$\mathcal{I}_1 = F_\pi^2(\partial_\mu\eta')^2 + F_\pi^2(\partial_\mu\pi^a)^2 + \dots\,,\quad \mathcal{I}_2 = F_\pi^4(\partial_\mu\eta')^2 + \dots\,, \tag{1.44}$$

therefore, the most general kinetic term allowed by chiral symmetry is

$$\mathcal{L}_{\text{kin}} = \frac{1}{2}\,\mathrm{Tr}(\partial_\mu U^\dagger\partial_\mu U) + \frac{c}{2F_\pi^2}\Big|\mathrm{Tr}(U^\dagger\partial_\mu U)\Big|^2 = \frac{1}{2}(\partial_\mu\pi^a)^2 + \frac{1}{2}(1 + cN_f)(\partial_\mu\eta')^2 + \dots\,, \tag{1.45}$$

where the ellipsis stands for higher derivative terms. We now proceed to compute the decay constants of the π^a and η' mesons by evaluating the matrix elements

$$\begin{aligned}\langle 0|J_A^{\mu\,a}(x)|\pi^b\rangle &= ip^\mu e^{-ip\cdot x}F_\pi\delta^{ab}\,,\\ \langle 0|J_A^{\mu}(x)|\eta'\rangle &= ip^\mu e^{-ip\cdot x}F_{\eta'}\,,\end{aligned} \tag{1.46}$$

where $a = 1, \dots, N_f^2 - 1$; we thus need to compute the axial currents $J_A^{\mu a}$ and J_A^μ, associated to $SU(3)_A$ and $U(1)_A$ respectively. Under $SU(N_f)_A$ we have

$$q \to e^{i\alpha^aT^a}q\,,\ q^c \to e^{i\alpha^aT^a}q^c\ \Rightarrow U \xrightarrow{SU(N_f)_A} e^{i\alpha^aT^a}Ue^{i\alpha^aT^a} \simeq U + i\alpha^a\,(UT^a + T^aU) + \mathcal{O}(\alpha^2)\,, \tag{1.47}$$

from which we get the Noether current

$$J_A^{\mu a} = i\,\mathrm{Tr}\Big[T^a(U\partial_\mu U^\dagger - U^\dagger\partial_\mu U)\Big] = \sqrt{2}F_\pi\partial_\mu\pi^a + \dots\,. \tag{1.48}$$

Under a $U(1)_A$ transformation, we have

$$q \to e^{i\alpha}q\,, q^c \to e^{i\alpha}q^c \Rightarrow\ U \xrightarrow{U(1)_A} e^{2i\alpha}U\,, \tag{1.49}$$

from which we find the Noether current

$$J_A^\mu = \sqrt{2N_f(1 + cN_f)}F_\pi\partial_\mu\eta'. \tag{1.50}$$

From Eq. (1.46), we extract the decay constant $F_{\eta'} = \sqrt{2N_f(1 + cN_f)}F_\pi$. However, we know from large-N counting, that meson correlation functions at leading order in $1/N$ are given by diagrams with a single quark loop. Annihilation graphs, such as those on the right panel of Fig. 1.1, have two quark loops and are thus suppressed by one power of N. The suppression of annihilation graphs is known as Zweig's or OZI rule. One consequences of this is that mesons occur in nonets for three light quark flavors. There are nine possible meson states, which are divided into flavor octects $\overline{q}T^aq$, there T^a is a $SU(N_f)|_{N_f=3}$ *flavor* matrix, and a singlet $\overline{q}q$. Usually, the singlet and octet mesons are not related, because the singlet meson can mix with gluons. In the large N limit, this mixing is suppressed. The singlet and octet meson couplings are related by treating them as members of a $U(N_f)$ multiplet. That is to say, in the large N limit, the vector meson octet of $\{\rho, \omega, \phi, K^*\}$ all have the same mass, and the decay constants of the π^a's and η' are *equal*, *i.e.* $F_\pi = F_{\eta'}$. Therefore, $\mathcal{I}_2$ violates the OZI rule, since

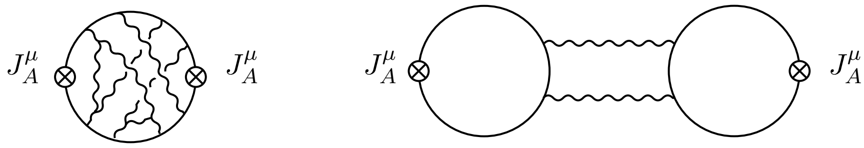

Figure 1.1: *The diagram in the right panel represents an annihilation process that violates the OZI rule and is therefore suppressed by a factor of* $1/N$ *relative to the leading, OZI-allowed diagram shown in the left panel.*

splits $F_{\eta'} = \sqrt{2N_f(1+cN_f)}F_\pi$ from F_π, so is absent and the effective Lagrangian for large N and in the absence of explicit chiral symmetry breaking must be

$$\mathcal{L}_{\rm kin} = \frac{1}{2}\,\mathrm{Tr}(\partial_\mu U^\dagger \partial_\mu U) + \mathcal{O}(1/N)\,. \tag{1.51}$$

Taking into account the quark masses, we get

$$\mathcal{L}_0(U,U^\dagger) \equiv \frac{1}{2}\,\mathrm{Tr}(\partial_\mu U^\dagger \partial_\mu U) + \frac{F_\pi}{2\sqrt{2}}\,\mathrm{Tr}\left[\mu^2(U+U^\dagger)\right]\,, \tag{1.52}$$

where μ^2 is proportional to the quar mass matrix which, without loss of generality, can be taken to be real, diagonal and non-negative (provided a θ-term is added). More precisely, in terms of the quark masses m_i and chiral condensate, the meson mass matrix, μ^2 is defined by

$$\mu^2_{ij} = \mu_i\delta_{ij} = -\frac{2m_i}{F_\pi^2}\langle q q^c\rangle \delta_{ij}\,. \tag{1.53}$$

The above Lagrangian density has to be modified in order to include the effect of the $\mathrm{U}(1)_\mathrm{A}$ anomaly. We know that, under the axial transformation – in the UV

$$q(x) \to \exp(i\beta\gamma_5\mathcal{Q})q(x)\,,\quad \delta\mathcal{L}_{\rm QCD} = 2\beta\,\mathrm{Tr}\,\mathcal{Q}\,\underbrace{\frac{g_s^2}{64\pi^2}\epsilon^{\mu\nu\rho\sigma}F^a_{\mu\nu}F^a_{\rho\sigma}}_{=q(x)}\,, \tag{1.54}$$

where $\mathcal{Q}$ is an $N_f\times N_f$ matrix, with $\mathcal{Q} = \mathrm{Tr}\,\mathcal{Q}/N_f\mathbf{1} + 2T^a\,\mathrm{Tr}(T^a\mathcal{Q})$. We can also write the topological charge $q(x)$ as the Hodge dual of the exterior derivative of a 3-form field, the Chern-Simons 3-form $\mathcal{C}_3$, defined as

$$q(x) = *\mathcal{F}_4\,,\quad \mathcal{F}_{\mu\nu\rho\sigma} = \frac{1}{4}\left(\partial_\mu\mathcal{C}_{\nu\rho\sigma} - \partial_\nu\mathcal{C}_{\mu\rho\sigma} - \partial_\rho\mathcal{C}_{\nu\mu\sigma} - \partial_\sigma\mathcal{C}_{\nu\rho\mu}\right)\,, \tag{1.55}$$

where

$$\mathcal{C}_3 = \frac{1}{8\pi^2}\,\mathrm{Tr}\left[A\wedge dA + \frac{2ig_s}{3}A\wedge A\wedge A\right]\,. \tag{1.56}$$

Because of confinement, the chiral Lagrangian density should not contain color degrees of freedom, but it can contain fields such as A^a_μ or $F^a_{\mu\nu}$ only through the color signlet combination $q(x)$. If we add to the chiral Lagrangian density

$$\mathcal{L}_{\rm anomaly} = \frac{i}{2}q(x)\,\mathrm{Tr}\left[\log U - \log U^\dagger\right]\,, \tag{1.57}$$

it will transform under the $\mathrm{U}(1)_\mathrm{A}$ transformation (1.54), $U \to e^{-i\beta\mathcal{Q}}Ue^{-i\beta\mathcal{Q}}$ as

$$\delta\mathcal{L}_{\rm anomaly} = 2\beta\,\mathrm{Tr}\,\mathcal{Q}\,q(x)\,, \tag{1.58}$$

i.e. in this way, $\mathcal{L}_{\text{anomaly}}$ explicltly breaks $\mathrm{U}(1)_{\mathrm{A}}$ as in the UV. Therefore, taking into account the explicit breaking due to the quark masses and to the anomaly, we find – in full generality

$$\mathcal{L}_{\text{tentative}} = \mathcal{L}_0(U, U^\dagger) + \frac{i}{2} q(x)\, \mathrm{Tr}\left[\log U - \log U^\dagger\right] + \sum_{k=1}^{\infty} \mathcal{L}_k(U, U^\dagger) q^k(x)\,, \tag{1.59}$$

where

- $\mathcal{L}_{\text{tentative}}$ is invariant under $SU(N_f) \times SU(N_f)$ and should transform as (1.58) under $U(1)_A$,
- $\mathcal{L}_{\text{tentative}}$ is CP-even, except for a term proportional to the QCD vacuum angle θ,
- $\mathcal{L}_{\text{tentative}}$ does not contain more than two derivatives of the fields U and $\mathcal{C}_3$.

The above requirements imply

$$\mathcal{L}_{2k+1}(U, U^\dagger) = 0\,,\ \ k = 1, 2, \dots\,, \tag{1.60a}$$

$$\mathcal{L}_{2k}(U, U^\dagger)\ \text{ is invariant under CP and under } U(N_f) \times U(N_f),\ \ k = 1, 2, \dots\,, \tag{1.60b}$$

thus restricting $\mathcal{L}_{\text{tentative}}$ to

$$\mathcal{L}_{\text{tentative}} = \mathcal{L}_0(U, U^\dagger) + \frac{i}{2} q(x)\, \mathrm{Tr}\left[\log U - \log U^\dagger\right] + \sum_{k=1}^{\infty} \mathcal{L}_{2k}(U, U^\dagger) q^{2k}(x)\,. \tag{1.61}$$

Up to here we have made no use of the large-N limit. If we demand that the Lagrangian density (1.61) follows from QCD in the large-N limit, we find the following N dependences (see also Ref. [12])

$$F_\pi^2 = \mathcal{O}(N)\,, \tag{1.62}$$
$$\langle \mathcal{L}_2 \rangle_0 = \mathcal{O}(1)\,, \tag{1.63}$$
$$\langle \mathcal{L}_{2k} \rangle_0 = \mathcal{O}(N^{2-2k})\,, \tag{1.64}$$

where we have used that the topological charge scales as $\propto 1/N$ (since $g_s^2 \propto 1/N$), while the vacuum energy scales as[2] $\propto N^2$. Therefore, two insertions of the topological charge in the vacuum yield, for instance

$$\langle \mathcal{L}_2 \rangle_0 = \mathcal{O}(1) \text{ in } 1/N\,.$$

$$\begin{aligned}\mathcal{L} = {} & \mathcal{L}_{\text{kin}}(U, U^\dagger) + \frac{F_\pi}{2\sqrt{2}}\, \mathrm{Tr}\left[\mu^2 (U + U^\dagger)\right] \\ & + \frac{i}{2} q(x)\, \mathrm{Tr}\left[\log U - \log U^\dagger\right] - \theta q(x) + \frac{N}{a F_\pi^2} q^2(x)\,,\end{aligned} \tag{1.65}$$

where a, if not zero, is of $\mathcal{O}(1)$ in $1/N$, and hence proportional to Λ_{QCD}^2. An immediate consequence of the $q^2(x)$ term is to give the topological susceptibility[3]

$$\chi_{\text{YM}} = \int d^4x\ \langle q(x) q(0) \rangle|_{\theta=0} = \frac{a F_\pi^2}{2N}\,, \tag{1.66}$$

[2]The diagrams contributing to the vacuum energy are vacuum-to-vacuum bubble diagrams, which are of order $\mathcal{O}(N^2)$ in the $1/N$ expansion, since any of the N^2 gluon species can circulate in the loop.

[3]We are tacitly assuming to work with Euclidean quantities.

in pure Yang-Mills (YM) theory (*i.e.* in absence of quarks). After the elimination of the field $q(x)$ – since it appears quadratically, and can be integrated out exactly, obtaining

$$q(x) = \frac{aF_\pi^2}{2N}\left(\theta - \frac{i}{2}\,\mathrm{Tr}\left[\log U - \log U^\dagger\right]\right)\,, \tag{1.67}$$

thus obtaining the Lagrangian density [10]

$$\mathcal{L} = \mathcal{L}_{\mathrm{kin}}(U, U^\dagger) + \frac{F_\pi}{2\sqrt{2}}\,\mathrm{Tr}\left[\mu^2(U + U^\dagger)\right] - \frac{aF_\pi^2}{4N}\left(\theta - \frac{i}{2}\,\mathrm{Tr}\left[\log U - \log U^\dagger\right]\right)^2\,, \tag{1.68}$$

from which we obtain the η' mass, for massless quarks

$$\boxed{m_{\eta'}^2 = \frac{aN_f}{2N} = \frac{N_f}{F_\pi^2}\chi_{\mathrm{YM}}\,,} \tag{1.69}$$

which is the celebrated Veneziano-Witten relation. That is to say, in the chiral limit, not all the pseudoscalar mesons are massless. The dependence of the vacuum structure on θ can be found by minimizing the potential. The most general background, given that $U^\dagger U = \frac{F_\pi^2}{2}$, is diagonal and can be parametrized as

$$\langle U\rangle = \frac{F_\pi}{\sqrt{2}}\mathrm{diag}(e^{i\phi_1}, \ldots, e^{i\phi_{N_f}})\,. \tag{1.70}$$

Inserting this background in the Lagrangian density (1.68), we find the potential

$$V(\phi_i) = \frac{aF_\pi^2}{4N}\left(\theta - \sum_{i=1}^{N_f}\phi_i\right)^2 - \frac{F_\pi^2}{2}\sum_{i=1}^{N_f}\mu_i^2\cos\phi_i\,, \tag{1.71}$$

from which the phases ϕ_i are determined by minimizing Eq. (1.71), and therefore satisfy the minimization equations

$$\mu_i^2\sin\phi_i = \frac{a}{N}\left(\theta - \sum_{j=1}^{N_f}\phi_j\right)\,,\; i = 1, \ldots, N_f\,. \tag{1.72}$$

The general solution of this equation is not tractable analytically. If Eq. (1.72) has only one solution, this solution must vary periodically in θ with periodicity 2π. However, it may happen that Eq. (1.72) has more than one solution. In this case, the physics is described by the solution that corresponds to the lowest energy. It could happen that two solutions "cross" in energy as θ is varied. For θ less than some critical value, one solution has the lower energy; for θ greater than the critical value, a different solution has lower energy. We can study Eq. (1.72) in various limits. In the realistic values of the parameters (although we should be careful that we haven't justified the large-N approximation as applied to the real QCD to be able to ignore the higher order corrections):

$$\mu_{u,d}^2 \ll \mu_s^2 \ll \frac{a}{N}\,, \tag{1.73}$$

this equation can be solved and Eq. (1.72)

$$\mu_u^2\sin\phi_u = \mu_d^2\sin\phi_d = \mu_s^2\sin\phi_s = \frac{a}{N}\left(\theta - \phi_u - \phi_d - \phi_s\right)\,, \tag{1.74}$$

reduces to

$$\mu_u^2\sin\phi_u = \mu_d^2\sin\phi_d \tag{1.75}$$

$$\phi_u + \phi_d = \theta\,, \tag{1.76}$$

$$\phi_s = 0\,. \tag{1.77}$$

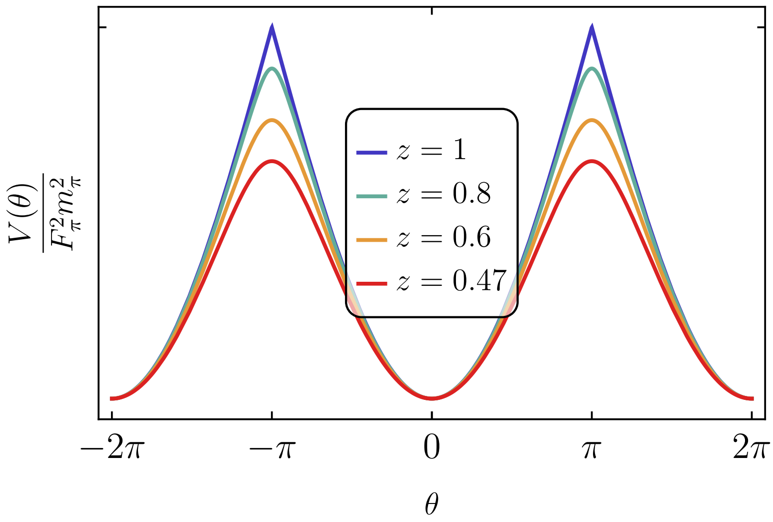

Figure 1.2: *Vacuum energy as a function of the vacuum angle θ for two quark flavors ($N_f = 2$), where $z = m_u/m_d$. The phenomenologically relevant value is $z \simeq 0.47$. The blue line shows the hypothetical situation if $z = 1$, where there is a cusp at $\theta = \pi$.*

That is to say, we find the CP-even solution

$$\begin{aligned} \sin\phi_u = \sin\overline{\phi}_u &= \frac{m_d \sin\theta}{\left[m_u^2 + m_d^2 + 2m_u m_d \cos\theta\right]^{1/2}}\,, \\ \sin\phi_d = \sin\overline{\phi}_d &= \frac{m_u \sin\theta}{\left[m_u^2 + m_d^2 + 2m_u m_d \cos\theta\right]^{1/2}}\,, \end{aligned} \tag{1.78}$$

which plugged in Eq. (1.71), gives the potential

$$\boxed{V(\theta) = -\frac{F_\pi^2}{2}\left(\mu_u^2 \cos\overline{\phi}_u + \mu_d^2 \cos\overline{\phi}_d\right) = -F_\pi^2 m_\pi^2 \sqrt{1 - \frac{4m_u m_d}{(m_u+m_d)^2}\sin^2\frac{\theta}{2}}\,,} \tag{1.79}$$

where we used $m_\pi^2 = (\mu_u^2 + \mu_d^2)/2$. The fact that the solution in Eq. (1.78) is CP-even follows from the fact that, under a CP trasnformation $U \to U^\dagger$, that is in terms of the ϕ_i (see Eq. (1.70)), $\phi_i \to -\phi_i$, and $\theta \to -\theta$. Let us now consider again Eq. (1.74) in the approximation (1.73) at $\theta = \pi$. We have

$$\phi_u + \phi_d + \phi_s = \pi\,, \tag{1.80}$$

$$\mu_u^2 \sin\phi_u = \mu_d^2 \sin\phi_d = \mu_s^2 \sin\phi_s\,. \tag{1.81}$$

From the equation $\mu_u^2 \sin\phi_u = \mu_d^2 \sin\phi_d$ we find

$$\sin\phi_d = \sin\overline{\phi}_d = \frac{m_u \sin\phi_s}{\sqrt{m_u^2 + m_d^2 - 2m_u m_d \cos\phi_s}}\,, \tag{1.82}$$

$$\sin\phi_u = \sin\overline{\phi}_u = \frac{m_d \sin\phi_s}{\sqrt{m_u^2 + m_d^2 - 2m_u m_d \cos\phi_s}}\,, \tag{1.83}$$

while, from $\mu_u^2 \sin\phi_u = \mu_s^2 \sin\phi_s$, we find

$$\frac{m_u m_d \sin\phi_s}{\sqrt{m_u^2 + m_d^2 - 2m_u m_d \cos\phi_s}} \equiv \frac{m_u m_d \sin\phi_s}{\sqrt{(m_u - m_d)^2 + 2m_u m_d(1-\cos\phi_s)}} = m_s \sin\phi_s\,. \tag{1.84}$$

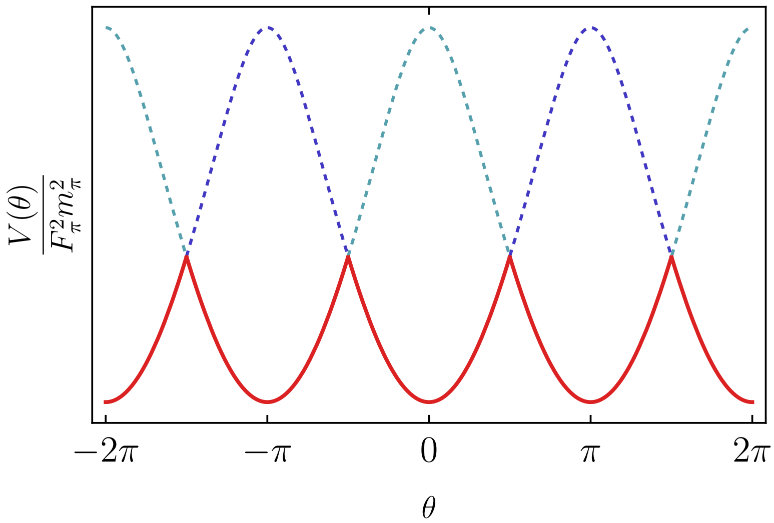

Figure 1.3: *The vacuum energy as a function of θ may have several branches, which cross at particular values of θ. The red line shows the (minimal) vacuum energy.*

Eq. (1.84) can have more than one vacuum solution. Indeed, there is always one CP-even solution $\sin\phi_s = 0$. Furthermore, when

$$m_s\,|m_u - m_d| < m_u m_d\,, \tag{1.85}$$

there are two additional CP-odd solutions

$$\cos\phi_s = 1 + \frac{m_s^2(m_u-m_d)^2 - m_u^2 m_d^2}{2m_u m_d m_s^2}\,, \tag{1.86}$$

since it does not determine the sign of ϕ_s, even though they correspond to the same value of $\cos\phi_s$; hence the two solutions of Eq. (1.86) transform into each other under CP, and – corresponding to the same value of $\cos\phi_s$ – have the same energy (see Eq. (1.71)). This means that at $\theta = \pi$, CP is *spontaneously broken*, since there are two inequivalent degenerate vacua that transform one into each other under CP. The possibility of spontaneous CP-breaking in the QCD vacuum was already pointed out by Dashen prior to the discovery of QCD (see Ref. [13]). Such occurrence thus goes under the name of Dashen's phenomenon.

By varying θ in a neighbourhood of π one can see that one of the two CP-odd solutions has the lowest value of the energy and that the two solutions cross at $\theta = \pi$. In the real world, the condition in Eq. (1.85) is not satisfied, and Dashen's phenomenon does not take place.

Among the various solutions of the Strong CP problem proposed so far, the so-called Peccei-Quinn (PQ) solution is arguably the most robust and model independent, because it only relies on the requirement of a new $U(1)$ *global* symmetry with a chiral anomaly under $SU(3)_c$ and on the low energy properties of QCD – in particular on its vacuum structure.

The basic idea is that the θ-angle is unphysical if there exists a global and continuous transformation, parametrized by a parameter α, that leaves the UV theory invariant up to a shift of the gluon topological term

$$\delta S = \frac{\alpha_s}{8\pi}\alpha G^a_{\mu\nu}\widetilde{G}^{a\mu\nu}\,, \tag{1.87}$$

where $\alpha_s = g_s^2/4\pi$. The easiest way to realize this setup is to introduce a $U(1)_{\rm PQ}$ global symmetry acting on the fields as $\phi \to \phi_\alpha$ under which the UV action is invariant, $S_{\rm UV}[\phi_\alpha] = S_{\rm UV}[\phi]$, but anomalous under $SU(3)_c$, so that the path integral changes as $[d\phi_\alpha] = [d\phi]\exp(i\frac{\alpha_s}{8\pi}\alpha G^a_{\mu\nu}\widetilde{G}^{a\mu\nu})$. Unfortunately

such a global symmetry is not present in the SM. As a consequence, the PQ solution requires new physics beyond the SM [14–16].
Whatever the physics is, the 't Hooft anomaly matching condition gives us a handle on how the low-energy physics should look like. Indeed, for consistency of the theory, if there is an anomalous global symmetry in the UV, the low-energy theory – even when the gauge group confines – should include the same global anomaly. We notice that the anomaly in the IR sector can be carried by

- massless (composite) fermions, if the symmetry with the global anomaly is linearly realized in the IR (in the case of the $U(1)_{\rm PQ}$ they should be colored),
- Nambu-Goldstone bosons (NGBs), if the symmetry with the global anomaly is non-linearly realized in the IR.

Since massless colored fermions are actually experimental excluded, the only option is that $U(1)_{\rm PQ}$ is spontaneously broken and in the low-energy theory its NGB, called the QCD *axion* $a(x)$, reproduces the anomaly by transforming non-linearly under PQ as

$$a(x) \xrightarrow{U(1)_{\rm PQ}} a(x) + \alpha f_a \,, \tag{1.88}$$

and coupling to the gluon topological term as

$$\mathcal{L}_{\rm IR} \supset \frac{\alpha_s}{8\pi}\frac{a}{f_a} G^a_{\mu\nu}\widetilde{G}^{a\mu\nu} \,. \tag{1.89}$$

The axion decay constant f_a defined in Eq. (1.89) is related to the scale of spontaneous symmetry breaking of the $U(1)_{\rm PQ}$. The rest of the low-energy Lagrangian invariant under the shift $a \to a + \alpha f_a$ in order to reproduce the anomaly in the UV (*i.e.* above f_a). At energies below the scale of PQ breaking, the SM+axion effective Lagrangian will be [17]

$$\mathcal{L}_{\rm IR} = \mathcal{L}_{\rm SM}^{(\theta=0)} - \theta_{\rm QCD}\frac{\alpha_s}{8\pi} G^a_{\mu\nu}\widetilde{G}^{a\mu\nu} + \frac{1}{2}(\partial_\mu a)^2 + \frac{\alpha_s}{8\pi}\frac{a}{f_a} G^a_{\mu\nu}\widetilde{G}^{a\mu\nu} + \dots \,, \tag{1.90}$$

where the dots represent additional terms that do not break the axion shift symmetry (and thus proportional to inverse powers of f_a). While the coupling to gluons in Eq. (1.90) is model independent and can be argued on the basis of anomaly matching only, the rest of the low-energy Lagrangian depends on the particular model under consideration. Couplings that can appear at order f_a^{-1} in Eq. (1.90) include

$$\mathcal{L}_{\rm IR} \supset \frac{g^0_{a\gamma\gamma}}{4} a F_{\mu\nu}\widetilde{F}^{\mu\nu} + \frac{\partial_\mu a}{2 f_a}\sum_i c_i^0 \overline{\psi}_i \gamma^\mu \gamma_5 \psi_i \,, \tag{1.91}$$

where $g^0_{a\gamma\gamma} \propto f_a^{-1}$ represents the coupling to the photons and the second term is the coupling to the fermion axial current, where ψ_i could be either a quark or a lepton. Although the coefficients $g^0_{a\gamma\gamma}$ and c_i^0 in Eq. (1.91) are model dependent, their value is important experimentally because they allow to probe and possibly detect the QCD axion (see Figures 1.5 and 1.6). From Eq. (1.79) and (1.90), we immediately get the axion potential (generated from QCD non-perturbative dynamics)

$$\boxed{V(a) = -F_\pi^2 m_\pi^2 \sqrt{1 - \frac{4 m_u m_d}{(m_u+m_d)^2}\sin^2\left(\frac{\theta}{2} - \frac{a}{2 f_a}\right)}\,,} \tag{1.92}$$

from which we get the relation

$$m_a = \frac{m_\pi F_\pi}{f_a}\frac{\sqrt{m_u m_d}}{m_u + m_d} \approx 5.7\mu\text{eV}\left(\frac{10^{12}\text{GeV}}{f_a}\right) \,. \tag{1.93}$$

To conclude, we notice that from the axion potential in Eq. (1.92) follows that, $\langle a \rangle = f_a \theta$, therefore the neutron electric dipole moment is relaxed to zero, *i.e.*

$$d_n \simeq c_n e \frac{m_u}{m_n^2}\left(\theta - \frac{\langle a \rangle}{f_a}\right) = 0 \,. \tag{1.94}$$

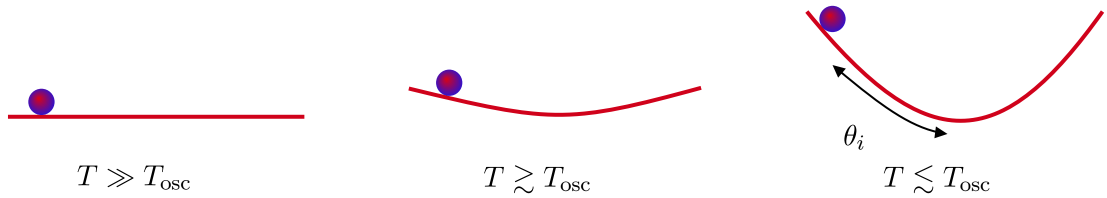

Figure 1.4: *Schematic illustration of the misalignment mechanism.*

1.3 Axions in Cosmology

A few years after the introduction of the QCD axion as a tool for solving the strong CP problem, it was realized that axions, if they exist, could also explain the observed dark matter density. The axion can obtain its dark matter abundance from either the misalignment mechanism or topological defects. The misalignment mechanism operates when PQ symmetry is broken during inflation and is never restored after inflation. Axions with masses above 10^{-2}eV (see Fig.) are constrained by stellar cooling, since such particles would lead to excessive energy loss from stars. Consequently, these astrophysical limits imply that axion dark matter must predominantly consist of very light, weakly interacting particles. When bosonic dark matter particles are light, it becomes more appropriate to treat them as a classical field. A heuristic justification for this transition is as follows (see Ref. [18] for a more detailed analysis). Consider a cubic volume of dark matter, with dimensions set by the de Broglie wavelenght of the axion, $\lambda_{\rm dB} = 1/m_a v_{\rm DM}$, where $v_{\rm DM} \simeq 10^{-3}$ is the local dark matter velocity. Using the fact that the energy density of dark matter in our galaxy is measured to be $\rho_{\rm DM} \simeq 0.4\,{\rm GeV\,cm^{-3}}$, the number density of dark matter is determined from $n = \rho/m_{\rm DM}$, whereas a rough measure for the volume occupied by each (quantum) state is the de Broglie volume $V_{\rm dB} = \lambda_{\rm dB}^3$. Accordingly, the dark matter states overlap when $nV_{\rm dB} = \rho_{\rm DM}/m_{\rm DM}^4 v_{\rm DM}^3 \gtrsim 1$. As quantum states begin to overlap, the system becomes coherent and can be described as a classical field. In this regime, it is more appropriate to treat dark matter collectively as a classical wave rather than as individual quantum particles. The *classical* equations of motion for an axion in an FRW spacetime are given by

$$\ddot{a}(t,\boldsymbol{x}) + 3H\dot{a}(t,\boldsymbol{x}) - \frac{1}{R^2}\nabla_{\boldsymbol{x}}^2 a(t,\boldsymbol{x}) + \frac{\partial V(a,T)}{\partial a} = 0\,, \tag{1.95}$$

where the dots denote time derivatives, R is the scale factor of the universe, $H = \dot{R}/R$ is the Hubble constant and spatial derivatives are taken with respect to comoving coordinates. This equation may simply be derived from the Euler-Lagrange equation for the axion in the presence of an FRW metric. Note that the zero-temperature axion potential $V(a, T = 0)$ is given in Eq. (1.92) as calculated in chiral perturbation theory. The temperature dependence arises from the fact that the QCD axion's potential is generated by QCD instantons, and QCD is at finite temperature T in the early universe. For simplicity, we will ignore the periodic behaviour of the axion potential and take the small-angle limit, for which

$$\frac{\partial V(a,T)}{\partial a} \approx m_a^2(T) a(t,\boldsymbol{x})\,, \tag{1.96}$$

- Early in the universe when the $T > \Lambda_{\rm QCD} \simeq 200$MeV and QCD is deconfined, the axion potential is negligible and the axion is massless (see Fig.).
- After $T < \Lambda_{\rm QCD}$, the axion gains a temperature dependent mass and the dynamics of the axion field begins to unfold (see Fig. 1.4).

There are two distinct possibilities for the subsequent evolution of the axion field, depending on whether or not PQ symmetry is broken after inflation. We will focus on the case of PQ symmetry broken before inflation (*i.e.* at a scale higher than the scale of inflation), and is not subsequently restored after inflation. In particular, this requires the reheating temperature to be smaller than the PQ scale

$$f_a \gg H_{\text{inflation}}, T_{\text{RH}}\,. \tag{1.97}$$

Each Hubble patch starts with a random initial misalignment angle for the axion field in the range $0 \leq \theta_i \leq 2\pi$; since the potential is flat, all values are equally likely. After PQ breaking, inflation stretches all Hubble patches and establishes homogeneous initial conditions, ensuring that the axion's initial misalignment angle is uniform everywhere post-inflation. Consequently, we can omit the gradient term in Eq. (1.95), and the equation of motion becomes

$$\ddot{a}(t,\boldsymbol{x}) + 3H\dot{a}(t,\boldsymbol{x}) + m_a^2(T)a = 0\,, \tag{1.98}$$

We will assume that the following dynamics occur during the radiation domination epoch of the universe, *i.e.* a(t) as the axion should act as dark matter before the matter-radiation equality.
When $H > m_a(T)$, the axion is overdamped and frozen at its initial misalignment angle. The axion field is thus stuck on its initial condition

$$a = a_0 \equiv f_a\theta_i\,,\; H \gg m_a(T) \;\text{ or at } T > T_{\text{osc}}\,. \tag{1.99}$$

The Hubble rate scales as $H(T) \simeq T^2/M_{\text{Pl}}$ and eventually becomes of order of the axion mass

$$H(T_{\text{osc}}) \simeq m_a(T_{\text{osc}})\,, \tag{1.100}$$

when this occurs, at temperature T_{osc}, then the axion field starts oscillating around its minimum. in the late time-universe can now solve the equation of motion (1.98) using the WKB approximation, assuming a radiation-dominated universe where $H = \frac{1}{2t}$. *i.e.* we assume the solution to factor as the product of slowly varying amplitude times a quickly varying phase

$$a(t) = f_a\mathcal{A}(t)e^{i\phi(t)}\,. \tag{1.101}$$

Plugging this ansatz into Eq. (1.98), we find two equations for the real and imaginary part

$$3H\frac{\dot{\mathcal{A}}}{\mathcal{A}} + \frac{\ddot{\mathcal{A}}}{\mathcal{A}} + m_a^2(T) - \dot{\phi}^2 = 0\,, \tag{1.102}$$

$$3H + 2\frac{\dot{\mathcal{A}}}{\mathcal{A}} + \frac{\ddot{\phi}}{\dot{\phi}} = 0\,. \tag{1.103}$$

Using the WKB approximation, Eq. (1.102) reduces to

$$m_a^2(T) - \dot{\phi}^2 = 0 \Rightarrow \phi(t) = \int_{t_0}^{t} dt'\, m_a(t) + \text{const}\,, \tag{1.104}$$

which inserted in Eq. (1.103) gives

$$3H + 2\frac{\dot{\mathcal{A}}}{\mathcal{A}} + \frac{\dot{m}_a}{m_a} = 0 \Rightarrow \mathcal{A}(t) = \frac{f_a\mathcal{C}}{R^{3/2}(t)m_a^{1/2}(t)}\,. \tag{1.105}$$

All in all, we have the solution of Eq. (1.98)

$$\boxed{a(t) = f_a\theta_i\left(\frac{m_a(T_{\text{osc}})}{m_a(T)}\right)^{1/2}\left(\frac{R(T_{\text{osc}})}{R(T)}\right)^{3/2}\cos\left[\int_{t_0}^{t} dt' m_a(t')\right]\,,} \tag{1.106}$$

where $\mathcal{C} = \theta_i$, from patching the solutions at the crossover point T_{osc} when the axion starts to oscillate. We can now examine this solution in two limiting regimes

- when $H > m_a(T)$, or $T > T_{\rm osc}$, the axion is overdamped and frozen at its initial misalignment angle. We find the energy density in the axion field $\rho_a = \frac{1}{2}m_a^2 a^2 + \frac{1}{2}\dot{a}^2$ to be

$$\rho_a = \frac{1}{2}m_a^2 a_0^2 = \frac{1}{2}m_a^2 f_a^2 \theta_i^2\,; \tag{1.107}$$

- in the opposite limit, as $H < m_a(T)$, or $T < T_{\rm osc}$, the axion begins to oscillate around the minimum of its potential, and the energy density scales as

$$\langle\rho_a\rangle \simeq \frac{1}{2}m_a^2(T) f_a^2 \theta_i^2 \frac{m_a(T_{\rm osc})}{m_a(T)}\frac{T^3}{T_{\rm osc}^3}\,, \tag{1.108}$$

  where the averaging is over the fast oscillations and used $R \propto T^{-1}$. We thus notice that, at late times, the axion redshifts like cold non-relativistic matter.

Equivalently, we can explicitly solve (1.98), assuming that the axion mass simply turns on at the QCD phase transition (see Ref. [19] for a more refined analysis, where the temperature dependence of m_a is taken into account) obtaining, for a radiation-dominated universe

$$a(t) = \frac{1}{t^{1/4}}\left[c_1 J_{1/4}(m_a t) + c_2 J_{-1/4}(m_a t)\right]\,,\quad \frac{\dot{R}}{R} = \frac{1}{2t}\,, \tag{1.109}$$

and for a matter-dominated universe

$$a(t) = \frac{1}{t^{1/2}}\left[\tilde{c}_1 J_{1/2}(m_a t) + \tilde{c}_2 J_{-1/2}(m_a t)\right]\,,\quad \frac{\dot{R}}{R} = \frac{2}{3t}\,. \tag{1.110}$$

Therefore, at late times (*i.e.* for $t \gg m_a^{-1}$),

$$a(t) \overset{t\gg m_a^{-1}}{\sim} a_0 (m_a t)^{-3/4}\sin(m_a t) = f_a\theta_i (m_a t)^{-3/4}\sin(m_a t)\,,\quad \frac{\dot{R}}{R} = \frac{1}{2t}\,, \tag{1.111}$$

and

$$a(t) \overset{t\gg m_a^{-1}}{\sim} a_0 (m_a t)^{-1}\sin(m_a t) = f_a\theta_i (m_a t)^{-1}\sin(m_a t)\,,\quad \frac{\dot{R}}{R} = \frac{2}{3t}\,, \tag{1.112}$$

from which we find – at late times

$$\langle\rho_a\rangle \overset{t\gg m_a^{-1}}{\simeq} \begin{cases} (m_a t)^{-3/2}\,, & \text{radiation domination}\,,\\ (m_a t)^{-2}\,, & \text{matter domination}\,,\end{cases} \tag{1.113}$$

and, in either cases, $\langle\rho_a\rangle \propto R^{-3}$ for large times. Therefore, comparing with the dark matter density today, we have from Eq. (1.108)

$$\frac{\rho_{a,0}}{\rho_{DM,0}} \simeq \frac{m_{a,0}\, m_a(T_{\rm osc}) f_a^2\theta_i^2\, T_0^3/T_{\rm osc}^3}{\text{eV}\, T_0^3} \equiv \frac{m_{a,0}\, m_a(T_{\rm osc}) f_a^2\theta_i^2}{\text{eV}\, T_{\rm osc}^3} = \frac{m_{a,0} f_a^2\theta_i^2}{\text{eV}\, m_a^{1/2}(T_{\rm osc}) M_{\rm Pl}^{3/2}}\,, \tag{1.114}$$

where we made use of the fact that, $H \simeq T^2/M_{\rm Pl}$ and at $T = T_{\rm osc}$, $H \simeq m_a(T_{\rm osc})$ and $m_{a,0}$ is the axion mass today, where we can use its zero-temperature value

$$m_{a,0}^2 \equiv m_a^2 = \frac{m_u m_d}{(m_u+m_d)^2}\frac{m_\pi^2 f_\pi^2}{f_a^2}\,. \tag{1.115}$$

We now turn to the temperature dependence of the axion mass. At finite temperature [20], the dilute instanton gas approximation provides a reliable framework to compute the axion potential from instanton-induced effects. For example, for three light quarks, the instanton effects can be encoded in the 't Hooft effective operator (see Eq. (2.194))

$$\Delta\mathcal{L}(T,x) = -C_{N_c}\int d\rho\,\rho^{-5+3N_f}\left(\frac{8\pi^2}{g^2(1/\rho)}\right)^{2N_c} e^{-\frac{8\pi^2}{g^2(1/\rho)}-\pi^2T^2\rho^2}e^{i\theta+i\frac{a}{f_a}} \times \prod_{\psi=u,d,s}\overline{\psi}_R(x)\psi_L(x) + \text{h.c.}\,, \tag{1.116}$$

where g is the strong coupling and the temperature enters as a scale in the instanton exponential, see Ref.s [21, 22], cutting off the integral over the instanton size ρ at $\rho \simeq 1/T$. We thus get, the contribution to the axion potential (see Section 2.1.3), or equivalently the axion free energy

$$\begin{aligned} F(\theta,T) &= C_3\int\frac{d\rho}{\rho^5}\left(\frac{8\pi^2}{g^2(1/\rho)}\right)^6 e^{i\theta+i\frac{a}{f_a}-\pi^2\rho^2T^2}(\rho\Lambda_{\text{QCD}})^{b_0}\prod_{i=u,d,s}m_i\rho + \text{h.c.} \\ &= C_3 e^{i\theta+i\frac{a}{f_a}}\Lambda^9_{\text{QCD}}\,m_um_dm_s\int d\rho\,\rho^7\left(\frac{8\pi^2}{g^2(1/\rho)}\right)^6 e^{-\pi^2\rho^2T^2} + \text{h.c.} \\ &\simeq C\left(\frac{8\pi^2}{g^2(T)}\right)^6\Lambda^9_{\text{QCD}}\frac{m_um_dm_s}{T^8}\cos\left(\theta+\frac{a}{f_a}\right)\,, \end{aligned} \tag{1.117}$$

where $b_0 = -\beta_0 = \frac{11}{3}N_c - \frac{4}{3}N_f d(\mathcal{C}_q) = 9$, for three light flavors in the fundamental representation and the constant $C = 2.4\times10^{-2}$ is obtained from a numerical integration of an expression for the instanton density [20] (see also [23] for a more recent discussion). We thus get the axion mass

$$m_a^2(T) = \frac{1}{f_a^2}\frac{d^2}{d^2\theta}F(T,\theta)\bigg|_{\theta=0} \sim \frac{m_um_dm_s}{f_a^2}\frac{\Lambda^9_{\text{QCD}}}{T^8}\,. \tag{1.118}$$

We thus distinguish the following cases

- $T_{\text{osc}} > \Lambda_{\text{QCD}}$ we have to use in Eq. (1.114) the temperature-dependent axion mass in (1.118) and plugging all the numbers, Eq.(1.114) gives

$$\frac{\rho_{a,0}}{\rho_{DM,0}} \simeq \mathcal{O}(1)\left(\frac{f_a}{10^{12}\,\text{GeV}}\right)^{\frac{7}{6}}\theta_i^2\,. \tag{1.119}$$

- $T_{\text{osc}} < \Lambda_{\text{QCD}}$ we can use in Eq. (1.114) the axion zero-temperature mass, then obtaining

$$\frac{\rho_{a,0}}{\rho_{DM,0}} \simeq \mathcal{O}(1)\left(\frac{f_a}{10^{12}\,\text{GeV}}\right)^{\frac{3}{2}}\theta_i^2\,. \tag{1.120}$$

Thus, QCD axion can account for the totality of cold dark matter in the universe, provided $f_a \simeq 10^{12}$ GeV.

1.4 Naturalness – with the gloves off: dimensional analysis

As understood long time ago by giants as Wilson [24] and Weinberg [25], the changes in complexity of a QFT as we move toward lower energies can be formulated in the language of "integrating out the UV degrees of freedom". The concept is perhaps most succintly incarnated by a path-integral approach. There are, at present, many kinds of evidence for the existence of physics above the electroweak scale.

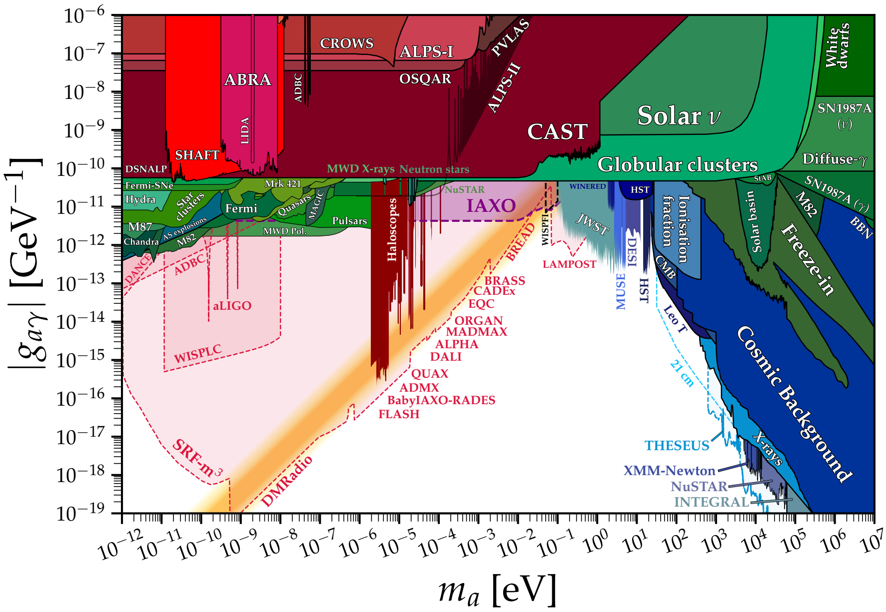

Figure 1.5: Current upper limits on the axion-photon coupling as a function of the axion mass from astrophysical and laboratory probes, with the QCD axion band indicated.

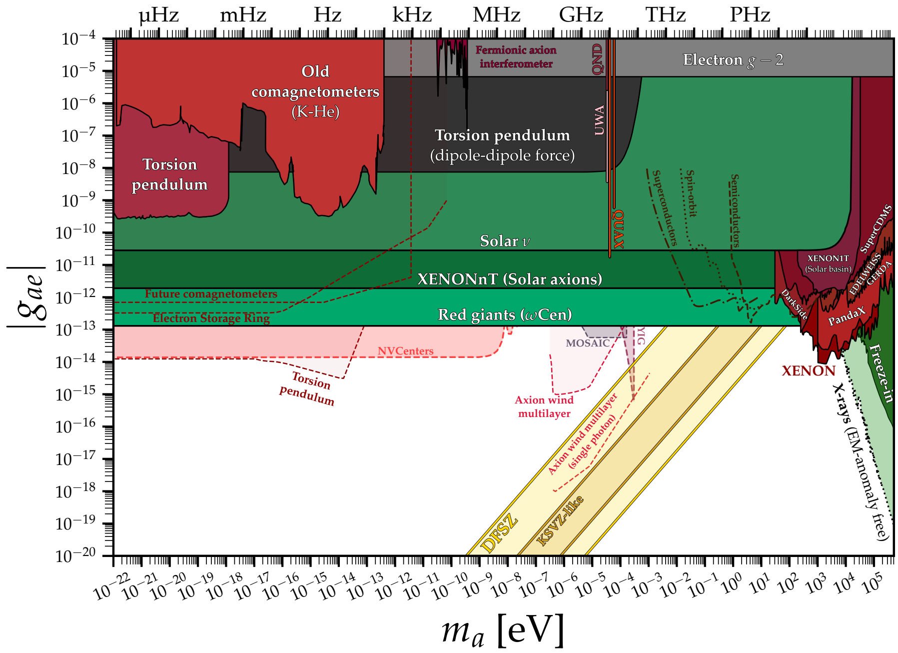

Figure 1.6: Current upper limits on the axion-electron coupling as a function of the axion mass from astrophysical and laboratory probes, with the QCD axion band indicated.

The strongest of these comes from gravity, which is characterized by a single dimensionful quantity: Newton's constant, G_N. Newton's constant defines an enormous scale

$$\bar{M}_{\rm Pl} = \frac{1}{\sqrt{G_N}} \simeq 10^{18}\text{GeV}\,, \tag{1.121}$$

which is characteristic of gravitational physics, being gravity the weakest force – e.g. $G_N/G_F \simeq 10^{-33}$ – precisely because this scale is so large compared with the other scales we know in physics. Since

Netwon's constant is an inverse power of mass (in units where $[\hbar] = 1$), the gravitational interactions are non-renormalizable, and so are likely the low-energy effective theory for some new physics which intervenes at some energy $v \ll E \lesssim \bar{M}_{\text{Pl}}$.
A second indication that nature involves physics at larger scales than $v = 246$GeV comes from the analysis of neutrino masses in terms of dimension-4 interactions (or in terms of the seesaw mechanism). In this picture, neutrino masses are light because they are inversely related to a very heavy mass, $m_\nu \propto v^2/M_{\text{NP}}$. Neglecting dimensionless factors, this implies a new scale $M_{\text{NP}} \simeq 10^{14}$GeV.
Now, imagine the theory is valid up to a scale Λ. If you only need to make a prediction for a measured quantity at energy scales $E \ll \Lambda$, it is not necessary to include in the computation all the details of the dynamics at the high scale. For example, you can describe the energy levels of the Hydrogen atom with excellent accuracy, without knowing anything about the mass of the top quark. The error that you are making is of order

$$\delta \simeq \alpha_{\text{em}} \frac{m_e}{m_t}$$

and if your experimental precision is inferior, this is perfectly acceptable. Some of the low-energy parameter that you need for the calculation are more sensitive to m_t, for example the proton mass and the fine structure constant α. However these are all quantities that you can measure at low energy, forgetting about their ultraviolet origin. If we could not describe the low-energy dynamics only in terms of low-energy degrees of freedom, at least to some finite precision, we would not have been able to make predictions for any physical system. However this does not mean that every trace of the UV dynamics disappears in the low-energy theory. There are very non-trivial consequences of UV physics that survive at low-energy. One classic example of this is the spin-statistics theorem. In non-relativistic quantum mechanics it is just a (measured) fact of life, but in quantum field theory it emerges from causality. Other than symmetry constraints, the UV dynamics also leaves behind small corrections to low-energy observables (the $\alpha m_e/m_t$ error in case of the Hydrogen atom).
These effects arise because, although the heavy degrees of freedom have been integrated out, their influence remains encoded in higher-dimensional operators suppressed by powers of the heavy scale. To see how effective field theories (EFTs) work in practice, we take a scale M and split the degrees of freedom in the path integral into two parts, the high-energy and low-energy modes

$$\int \mathcal{D}\phi\, e^{iS[\phi]} = \int \mathcal{D}\phi_L \mathcal{D}\phi_H\, e^{iS[\phi_L,\phi_H]}\,, \tag{1.122}$$

where the typical energy of the field configuration ϕ_L is $E_{\phi_L} < \Lambda$ (*light modes* or *low-energy modes*), while the energy of the field configuration ϕ_H is $E_{\phi_H} > \Lambda$ (*heavy modes* or high-energy modes). If we know how to do the path integral over the high-energy modes we obtain a description of the system in terms of the low-energy degrees of freedom

$$\int \mathcal{D}\phi_L \left(\mathcal{D}\phi_H\, e^{iS[\phi_L,\phi_H]}\right) = \int \mathcal{D}\phi_L e^{iS_{\text{EFT}}(\phi_L)}\,. \tag{1.123}$$

This is all we need and we have not even restricted the validity of the theory. In principle, we can use $S_{\text{EFT}}(\phi_L)$ to make predictions up to energy scales $E \lesssim \Lambda$. In practice, this suggests that we have not really gained anything and in fact most of the times the path integral cannot be performed exactly. However, even when this is not possible, we can always write $S_{\text{EFT}}(\phi_L)$ as an infinite sum of operators built from the low-energy fields and consistent with all the low-energy symmetries of the problem

$$S_{\text{EFT}}(\phi_L) = \sum_i \int d^D x\, c_i \mathcal{O}_i(\phi_L)\,, \tag{1.124}$$

where $\mathcal{O}_i(\phi_L)$ are local operators built from the low-energy fields ϕ_L. It might seem that this infinite sum requires the full knowledge of $S(\phi_L, \phi_H)$ to be useful. However here the power of broken symmetries

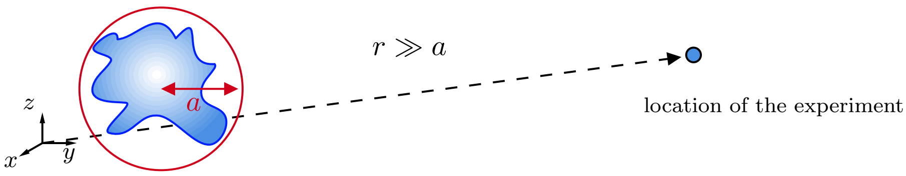

Figure 1.7: *A charge distribution of size a and a distant experiment at $r \gg a$; only a finite number of multipoles contribute appreciably to the potential at the observer's location.*

comes to our rescue. This is familiar from classical and quantum mechanics. Even in systems that are not rotationally invariant, for example, selection rules (or spurions) of the rotational symmetry are extremely useful to predict relations between matrix elements. If you prefer a quantum field theory equivalent, you can think about chiral symmetry in QCD and its breaking by the quark masses or flavor symmetries in the Standard Model and their breaking by the Yukawa matrices. In our case we need an even simpler symmetry. We can just use dimensional analysis, which should more appropriately be called the selection rules of the dilatation operator.
If we set $\hbar = c = 1$, our operators have some dimension δ_i in units of energy

$$[\mathcal{O}_i] = \mathrm{E}^{\delta_i} \,. \tag{1.125}$$

Since in this units the action is dimensionless, we must have $[c_i] = \mathrm{E}^{D-\delta_i}$ and therefore, factoring out the dimensionful quantities from the c_i's, we find

$$S_{\mathrm{EFT}}(\phi_L) = \sum_i \int d^D x \, \frac{c_i}{\Lambda^{\delta_i - D}} \mathcal{O}_i(\phi_L) \,. \tag{1.126}$$

Now we are in a position to estimate the contribution of each term in the sum in Eq. (1.126) to low-energy observables. Using again dimensional analysis, we have

$$\int d^D x \, \mathcal{O}_i(x) \approx E^{\delta_i - D} \,, \tag{1.127}$$

where E is some low-energy scale (*i.e.* the typical energy of an IR experiment); therefore each term in the sum contributes to a low-energy measurement an amount

$$\frac{c_i}{\Lambda^{\delta_i - D}} \int d^D x \, \mathcal{O}_i(\phi_L) \approx \left(\frac{E}{\Lambda}\right)^{\delta_i - D} \,. \tag{1.128}$$

We see immediately that operators with $\delta_i > D$ are suppressed when $E \ll \Lambda$, so if we are interested in a finite level of precision we need only a finite number of operators for our calculation. A classical analog is the multipole expansion in Electrodynamics (see Fig. 1.7). The multipole expansion involves taking an arbitrary distribution of charges and performing a Taylor series on the potential in the long-distance limit

$$V(r) = \frac{1}{r} \sum_{l,m} \left(\frac{a}{r}\right)^l \mathcal{C}_{l,m} \, Y_{l,m}(\Omega) \,, \tag{1.129}$$

where a is the size of the charge distribution (UV scale in the quantum field theory analog). For $r \gg a$, and at finite precision, only a finite number of multipoles are needed to accurately describe the potential $V(r)$, being higher-order terms suppressed by powers of a/r. The largest scale in our low-energy theory is Λ, and we can always write

$$\begin{aligned} c_i &= \gamma_0 \Lambda^{d-\delta_i} + \gamma_1 M_2^{d-\delta_i} + \gamma_2 M_2^{d-\delta_i} + \dots \\ &= \Lambda^{d-\delta_i} \left[\gamma_0 + \gamma_1 \left(\frac{M_1}{\Lambda}\right)^{d-\delta_i} + \gamma_2 \left(\frac{M_2}{\Lambda}\right)^{d-\delta_i} + \dots \right] \equiv g_i \Lambda^{d-\delta_i} \,, \end{aligned} \tag{1.130}$$

where $M_1\,, M_2\,, \cdots \ll \Lambda$. This just means that even if the c_i receive contributions from multiple scales, we can always parametrize them in terms of the largest scale in the theory times some dimensionless coefficient. From simple dimensional analysis we expect $g_i = \mathcal{O}(1)$ unless some extra symmetry (or dynamics) is at work.

Particle physicists formalize the statement that such dimensional analysis estimates are accurate with the term "naturalness".

The first example of naturalness is encountered in the kindergarten, *i.e.*how to estimate the time it takes for a ball that has been dropped to hit the floor. Because this depends only on the distance to the floor, d, and the strength of gravity, g, the simple dimensional analysis estimate gives $t \simeq \sqrt{d/g}$. However, if all of the relevant physics has not been identified, an incorrect result can be obtained. For example, if the coefficient of the air resistance, b, is important then the time would instead be estimated as $t \simeq bd/(mg)$.

Another application of naturalness is anticipating the scale of quantum mechanics à la Weisskopf [26] (see also [27, 28]). The first step in this line of reasoning is obtaining the classical electron radius. Consider the mass of the electron. Einstein's most famous equation, $E = mc^2$, shows that the energy and mass are one and the same. Thus, any source of potential energy associated with the electron should contribute to its mass. One source of potential energy is the electron self-energy. At the classical level, this energy is infinite. Indeed, the charge density distribution will be $\rho(\boldsymbol{x}) = \delta^{(3)}(\boldsymbol{x})$, and the electric field generated by this distribution will carry an energy

$$U = \frac{\varepsilon_0}{2}\int d^3\boldsymbol{x}|\boldsymbol{\mathcal{E}}(\boldsymbol{x})|^2\,,\ \boldsymbol{\mathcal{E}}(\boldsymbol{x}) = -\boldsymbol{\nabla}\Phi(\boldsymbol{x})\,, \tag{1.131}$$

where Φ is the electrostatic potential, *i.e.* $\Phi(r) = e/(4\pi\varepsilon_0 r)$. At the classical level, U is infinite. Assuming that at some distance R, one of the assumptions breaks down (*i.e.* $1/r^2$ electric field, point-like electron), we get[4] from dimensional analysis

$$\delta m_e|_{\text{Coulomb}} \propto \alpha_{\text{em}}/R\,. \tag{1.132}$$

In the extreme limit, where the entirety of the electron mass is due to electromagnetic self-energy

$$m_e \simeq \delta m_e|_{\text{Coulomb}} \Rightarrow R = R_{\text{cl}} \simeq \frac{\alpha_{\text{em}}}{m_e} = \frac{e^2}{4\pi\varepsilon_0 m_e c^2} \simeq 2.8\times 10^{-15}\,\text{m}\,, \tag{1.133}$$

where R_{cl} is also known as the *classical radius of the electron.* If the electron were modelled as a charged ball, R_{cl} would be the smallest the radius of the electron could possibly be. An analogous way to see this, is that – taking into account the electromagnetic correction in Eq. (1.132)

$$(m_e c^2)_{\text{obs}} = (m_e c^2)_{\text{bare}} + \delta m_e|_{\text{Coulomb}}\,, \tag{1.134}$$

where $(m_e c^2)_{\text{bare}}$ corresponds to the value of the electron mass appearing in the Hamiltonian. Experimentally, we know that the "size" of the electron is small, *i.e.*

$$R \lesssim \text{few TeV} \simeq 10^{-17}\text{cm}\,, \tag{1.135}$$

therefore the contribution to $(m_e c^2)_{\text{obs}}$ due to the self-energy would give $\delta m_e|_{\text{Coulomb}} \gtrsim 10\,\text{GeV}$, and hence the bare electron mass must be negative to obtain the observed mass of the electron, with a fine cancellation like

$$0.511\,\text{MeV} = (-9999.49 + 10000)\,\text{MeV}\,. \tag{1.136}$$

[4]Indeed, the regularized electromagnetic energy of a point charge is – assuming the electron to have a "size" R

$$U = \frac{\varepsilon_0}{2}\int_{r>R} dr\ 4\pi r^2 \frac{e^2}{(4\pi\varepsilon_0)^2 r^4} = \frac{e^2}{8\pi\varepsilon_0 R} = \frac{e^2}{8\pi R}\,,$$

where in the last equality we restored to natural units, where $\varepsilon_0 = \mu_0 = 1$.

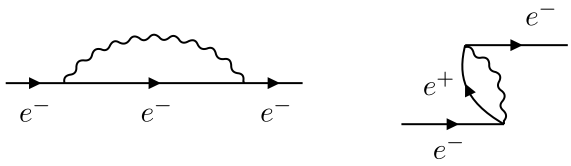

Figure 1.8: *Old-fashioned Feynman diagrams for the electron self-energy, at first order in perturbation theory. In modern Feynman diagram notation, the two diagrams would be combined into a single one, incorporating both effects.*

Even setting a conceptual problem with a negative mass aside, such a fine-cancellation between the bare mass of the electron and the Coulomb self-energy appears ridiculous. In order for such a cancellation to be absent, we conclude that the classical electromagnetism cannot be applied to distance scales shorter than $R_{\rm cl}$. An important point is that the above argument does not specify what actually happens at the scale $R_{\rm cl}$. Dimensional analysis simply informs the physicist when something will happen, not what will happen at said location. Indeed, when

$$R \simeq c\Delta t \simeq c\hbar/\Delta E \simeq \hbar c/(m_e c^2) \simeq 100\, R_{\rm cl} \tag{1.137}$$

quantum mechanics kicks in and completely changes the computation. While dimensional analysis cannot predict what will occur at $R_{\rm cl}$, it does correctly predict that one of the assumptions will break down. Today, we know that the actual resolution is that the classical Coulomb self-energy is supplemented by another contribution that is intrinsically relativistic and quantum mechanical. The total self-energy calculation to first order in perturbation theory can be depicted in "old-fashioned" Feynman diagram notation as in Fig. 1.8. The diagram in the left panel of Fig. 1.8 includes the linear divergent classical Coulomb self-energy (which behaves as $1/R$ as $R \to 0$). The right diagram involving the intermediate virtual positron is a new feature introduced in the relativistic quantum mechanical theory of the electron. This is precisely the computation that Weisskopf performed, and found that the positron contribution to the electron self-energy is negative and cancels the leading piece in the Coulomb self-energy

$$\delta m_e|_{\rm pair} = -\frac{1}{4\pi\varepsilon_0}\frac{e^2}{R}\,. \tag{1.138}$$

After the linearly divergent piece $1/R$ is canceled, the leading contribution in the $R \to 0$ limit is given by

$$\delta m_e = \delta m_e|_{\rm Coulomb} + \delta m_e|_{\rm pair} = \frac{3\alpha_{\rm em}}{4\pi} m_e c^2 \log\frac{\hbar}{m_e c R}\,, \tag{1.139}$$

meaning that

$$\boxed{(\delta m_e c^2)_{\rm obs} = (m_e c^2)_{\rm bare}\left(1 + \frac{3\alpha_{\rm em}}{4\pi}\right)\,.} \tag{1.140}$$

There are two important important things to be said about Eq. (1.140):

- the correction δm_e to the electron mass is proportional to the electron mass itself, therefore we are talking about the "percentage" of the correction, rather than a huge additive constant,

- the correction δm_e depends only *logarithmically* on the size of the electron. As a result, even if – in natural units $R \simeq 1/M_{\rm Pl}$, the correction is $\delta m_e = 0.085 \simeq 9\%$.

The fact that the correction is proportional to the bare mass is a consequence of a new symmetry present in the theory with the positron, *i.e.* chiral symmetry. Therefore, the doubling of the degrees of freedom (with an explicitly broken new global symmetry) and the cancellation of the power divergences

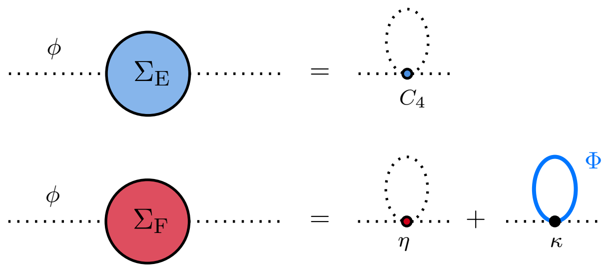

Figure 1.9: Diagrams contributing to the ϕ self-energy in the EFT ($\Sigma_{\rm E}$) and the full theory ($\Sigma_{\rm F}$).

lead to a sensible theory of the electron applicable to very short distance scales.
The last example of naturalness we will review is estimating the energy scale where the description of the chiral Lagrangian describing charged pions must be modified. The correction to the mass of the pion is, from dimensional analysis

$$\delta m_\pi^2 \propto \alpha_{\rm em}\Lambda^2 \tag{1.141}$$

As above, this can give an estimate of the energy scale where something new happens to be $\Lambda^2 \lesssim m_\pi^2/e^2$, which turns out to be within $\mathcal{O}(1)$ the mass of the ρ-meson. As in the case of the electron, dimensional analysis has been used to estimate the scale at which something happens.
We are finally at the point where we can describe the gauge hierarchy problem. The question is "At what energy scale does our description of the Higgs field break down?". Experimentally we know that the Higgs field is charged under the electroweak and hypercharge gauge groups, it also gives a mass to the top quark and is thus coupled to it via a Yukawa coupling y_t, therefore we find - from dimensional analysis

$$\delta m_h^2 \propto \max\left(g^2, g'^2, y_t^2\right)\Lambda_{\rm Higgs}^2 \Rightarrow \Lambda_{\rm Higgs} \lesssim \frac{m_h}{\max\left(g^2, g'^2, y_t^2\right)} \simeq 10^2 \div 10^3\,{\rm GeV}\,. \tag{1.142}$$

The Naturalness problem of the Higgs boson mass is simply to understand what happens at the scale $\Lambda_{\rm Higgs}$; if the answer is nothing, then what did we do wrong when estimating this energy scale? *i.e.* what goes wrong with dimensional analysis? To be as concrete as possible, and to clarify why scalar fields generally suffer a UV-sensitivity, it is useful to examine a specific model of (part of) what the UV physics might be [29, 30]. To this end, consider a theory consisting of two scalar fields: a light degree of freedom, ϕ, and a heavy degree of freedom, Φ; the full theory is (assuming a Z_2 symmetry acting on both ϕ and Φ)

$$\mathcal{L}_{\rm FULL} = \frac{1}{2}(\partial_\mu\phi)(\partial^\mu\phi) - \frac{1}{2}m_{\rm F}^2\phi^2 + \frac{1}{2}(\partial_\mu\Phi)(\partial^\mu\Phi) - \frac{1}{2}M^2\Phi^2 - \frac{1}{4}\kappa\phi^2\Phi^2 - \frac{1}{4!}\eta\phi^4\,, \tag{1.143}$$

where m_F^2 and M^2 are, respectively, the (renormalized) mass parameters for the scalar fields ϕ and Φ in the full theory, and we ignored self-interactions of the heavy scalar Φ. In deep IR, neglecting irrelevant operators, the EFT Lagrangian density for the scalar field ϕ will be

$$\mathcal{L}_{\rm EFT} = \frac{1}{2}(\partial_\mu\phi)(\partial^\mu\phi) - \frac{1}{2}m_{\rm E}^2\phi^2 - \frac{1}{4!}C_4\phi^4 + \mathcal{O}\left(\phi^6/M^2\right)\,, \tag{1.144}$$

where we are being careful to distinguish the full theory mass parameter $m_{\rm F}^2$ from the EFT mass parameter $m_{\rm E}^2$.

Now, suppose that we measure some pole mass for the scalar field ϕ, m_ϕ; from the Källen-Lehmann spectral decomposition

$$\begin{aligned}\frac{i}{p^2 - m_{\rm E}^2 - \Sigma_{\rm E}(p^2 = m_\phi^2) + i\epsilon} &= \frac{i}{p^2 - m_{\rm F}^2 - \Sigma_{\rm F}(p^2 = m_\phi^2) + i\epsilon} \\ &= \frac{iZ}{p^2 - m_\phi^2 + i\epsilon} + \text{terms regular at } p^2 = m_\phi^2\,,\end{aligned} \tag{1.145}$$

where Σ stands for the sum off all non-trivial 1PI diagrams. We thus find the pole equation

$$m_\phi^2 = m_{\mathrm{E}}^2 + \Sigma_{\mathrm{E}}(p^2 = m_\phi^2) = m_{\mathrm{F}}^2 + \Sigma_{\mathrm{F}}(p^2 = m_\phi^2)\,. \tag{1.146}$$

In the IR, (see Fig. 1.9) we find in the $\overline{\mathrm{MS}}$ scheme

$$m_\phi^2 = m_{\mathrm{E}}^2 - \frac{C_4 m_{\mathrm{E}}^2}{32\pi^2}\left(\log\frac{\mu^2}{m_{\mathrm{E}}^2} + 1\right)\,, \tag{1.147}$$

while in the UV

$$m_\phi^2 = m_{\mathrm{F}}^2 - \frac{\eta m_{\mathrm{F}}^2}{32\pi^2}\left(\log\frac{\mu^2}{m_{\mathrm{F}}^2} + 1\right) - \frac{\kappa M^2}{32\pi^2}\left(\log\frac{\mu^2}{M^2} + 1\right)\,, \tag{1.148}$$

then, since at the tree level we have the matching condition $C_4 = \eta$, we find at one-loop

$$m_{\mathrm{E}}^2(\mu) = m_{\mathrm{F}}^2(\mu) - \frac{\kappa M^2}{32\pi^2}\left(\log\frac{\mu^2}{M^2} + 1\right)\,. \tag{1.149}$$

We observe that in Eq. (1.147) the loop corrections in the low-energy EFT involve only light fields. Consequently, these loop contributions are suppressed relative to the tree-level term by the small factor $C_4/32\pi^2$, so that in the low-energy theory one finds $m_{\mathrm{E}}^2 \simeq m_\phi^2$. This is not the case for the coupling m_{F}^2 in the UV theory: as shown in Eq. (1.148), it receives a contribution of order κM^2. As a result, m_{F}^2 must be finely tuned in Eq. (1.149) with high precision in order to reproduce the observed low-energy value $m_{\mathrm{E}}^2 \simeq m_\phi^2$. In the absence of such a precise choice, Eq. (1.149) would instead give $m_{\mathrm{E}}^2 \sim m_{\mathrm{F}}^2$ and so would predict $m_\phi \sim M$. In the UV theory a huge hierarchy like $m_\phi \ll M$ between the two values of two masses is controlled by an extremely precise choice for the RG trajectory that is large at all scales except at the very low energies where it is measured to be small.

1.5 Appendix: CP transformations

Charge conjugation (C) and parity (P) are badly violated in the SM. Their combination, CP, is not a symmetry of the Lagrangian either. However, due to certain accidents of nature, the observable effects of the SM sources of CP violation are *feeble*. Let us begin by discussing how CP acts on the quantum fields in the SMEFT Lagrangian. The Higgs field H is a scalar and the transformation is quite simple. In the case of a scalar field $\Phi(t, \boldsymbol{x})$, we have

$$\Phi(t,x) = \int \frac{d^3p}{(2\pi)^3 2\omega_{\boldsymbol{p}}} \left[a_{\boldsymbol{p}} e^{-ip\cdot x} + b^\dagger_{\boldsymbol{p}} e^{ip\cdot x}\right] , \tag{1.150}$$

where $a_{\boldsymbol{p}}$ ($b_{\boldsymbol{p}}$) annihilates particles (anti-particles) associated with the field Φ. Charge conjugation exchanges particles and anti-particles, so we want it to act as

$$\mathrm{C} a_{\boldsymbol{p}} \mathrm{C}^{-1} = b_{\boldsymbol{p}} \,, \quad \mathrm{C} b_{\boldsymbol{p}} \mathrm{C}^{-1} = a_{\boldsymbol{p}} \,, \tag{1.151}$$

therefore, the action of C on $\Phi(t, \boldsymbol{x})$ is simply

$$\mathrm{C}\Phi(t,\boldsymbol{x})\mathrm{C}^{-1} = \Phi^\dagger(t,\boldsymbol{x}) \,. \tag{1.152}$$

Parity acts on $a_{\boldsymbol{p}}$ and $b_{\boldsymbol{p}}$ as

$$\mathrm{P} a_{\boldsymbol{p}} \mathrm{P}^{-1} = \eta_P a_{-\boldsymbol{p}} \,, \quad \mathrm{P} b_{\boldsymbol{p}} \mathrm{P}^{-1} = \eta_P^* b_{-\boldsymbol{p}} \,, \tag{1.153}$$

where $\eta_P = \pm 1$ is the intrinsic parity. Therefore, under P

$$\begin{aligned}
\mathrm{P}\Phi(t,\boldsymbol{x})\mathrm{P}^{-1} &= \int \frac{d^3p}{(2\pi)^3 2\omega_{\boldsymbol{p}}} \left[\mathrm{P} a_{\boldsymbol{p}} \mathrm{P}^{-1} e^{-ip\cdot x} + \mathrm{P} b^\dagger_{\boldsymbol{p}} \mathrm{P}^{-1} e^{ip\cdot x}\right] = \eta_P \int \frac{d^3p}{(2\pi)^3 2\omega_{\boldsymbol{p}}} \left[a_{-\boldsymbol{p}} e^{-ip\cdot x} + b^\dagger_{-\boldsymbol{p}} e^{ip\cdot x}\right] \\
&\equiv \eta_P \int \frac{d^3p}{(2\pi)^3 2\omega_{\boldsymbol{p}}} \left[a_{-\boldsymbol{p}} e^{-i\omega_{\boldsymbol{p}} x_0 + i\boldsymbol{p}\cdot\boldsymbol{x}} + b^\dagger_{-\boldsymbol{p}} e^{i\omega_{\boldsymbol{p}} x_0 - i\boldsymbol{p}\cdot\boldsymbol{x}}\right] \\
&= \eta_P \int \frac{d^3p}{(2\pi)^3 2\omega_{\boldsymbol{p}}} \left[a_{\boldsymbol{p}} e^{-i\omega_{\boldsymbol{p}} x_0 - i\boldsymbol{p}\cdot\boldsymbol{x}} + b^\dagger_{\boldsymbol{p}} e^{i\omega_{\boldsymbol{p}} x_0 + i\boldsymbol{p}\cdot\boldsymbol{x}}\right] = \eta_P \Phi(t,-\boldsymbol{x}) \,,
\end{aligned} \tag{1.154}$$

i.e. parity acts trivially on scalars, and flips signs for pseudo-scalars. We then understand that, under a CP transformation

$$\boxed{(\mathrm{CP})\Phi(t,\boldsymbol{x})(\mathrm{CP})^{-1} = \eta_P \Phi^\dagger(t,-\boldsymbol{x}) \,.} \tag{1.155}$$

In the 2-component notation, we have

$$\Psi(t,\boldsymbol{x}) = \begin{pmatrix} \psi_\alpha(t,\boldsymbol{x}) \\ \psi^{c\dagger\dot\alpha}(t,\boldsymbol{x}) \end{pmatrix} , \tag{1.156}$$

where ψ and $\psi^{c^\dagger}$ describes a left-handed and a right-handed fermion, respectively. Parity exchanges left- and right- fermions, therefore[5]

$$\mathrm{P}\psi_\alpha(t,\boldsymbol{x})\mathrm{P}^{-1} = i\sigma^0_{\alpha\dot\beta}\psi^{c\dagger\dot\beta}(t,-\boldsymbol{x}) \,, \quad \mathrm{P}\psi^{c\dagger\dot\alpha}(t,\boldsymbol{x})\mathrm{P}^{-1} = i\overline{\sigma}^{0\dot\alpha\beta}\psi_\beta(t,-\boldsymbol{x}) \,, \tag{1.157}$$

that is to say

$$\mathrm{P}\Psi(t,\boldsymbol{x})\mathrm{P}^{-1} = i\gamma^0\Psi(t,-\boldsymbol{x}) \,. \tag{1.158}$$

[5] We use the conventions of [5, 31]

To obtain the transformation properties of the other spinors, we simply raise and lower the undotted/dotted indices. Indeed

$$\mathrm{P}\psi^{\alpha}(t,\boldsymbol{x})\mathrm{P}^{-1} = \epsilon^{\alpha\beta}\mathrm{P}\psi_{\beta}(t,\boldsymbol{x})\mathrm{P}^{-1} = i\,\underbrace{\epsilon^{\alpha\beta}\sigma^{0}_{\beta\dot{\gamma}}}_{\epsilon_{\dot{\gamma}\dot{\beta}}\overline{\sigma}^{0\dot{\beta}\alpha}}\psi^{c\dagger\dot{\gamma}}(t,-\boldsymbol{x}) = -i\overline{\sigma}^{0\dot{\beta}\alpha}\psi^{c\dagger}_{\dot{\beta}}(t,-\boldsymbol{x})\,,$$

where we used the identity

$$\epsilon^{\alpha\beta}\sigma^{\mu}_{\beta\gamma} = \epsilon_{\dot{\alpha}\dot{\beta}}\overline{\sigma}^{\mu\dot{\beta}\alpha}\,.$$

In this way, we find

$$\boxed{\mathrm{P}\psi^{\alpha}(t,\boldsymbol{x})\mathrm{P}^{-1} = -i\overline{\sigma}^{0\dot{\beta}\alpha}\psi^{c\dagger}_{\dot{\beta}}(t,-\boldsymbol{x})\,,\quad \mathrm{P}\psi^{c\dagger}_{\dot{\alpha}}(t,\boldsymbol{x})\mathrm{P}^{-1} = -i\sigma^{0}_{\beta\dot{\alpha}}\psi^{\beta}(t,-\boldsymbol{x})\,.} \tag{1.159}$$

Making use of Eq. (1.157), (1.159), we now work out the transformation under P of the bilinears

$$\psi_i\sigma^{\mu}\psi^{\dagger}_j\,,\quad \psi^{\dagger}_i\overline{\sigma}^{\mu}\psi_j\,,\quad \psi_i\sigma^{\mu\nu}\psi_j\,,\quad \psi^{\dagger}_i\overline{\sigma}^{\mu\nu}\psi^{\dagger}_j\,, \tag{1.160}$$

where i and j are flavor indices. For instance, we have

- $\psi_i\sigma^{\mu}\psi^{\dagger}_j$

  $$\psi^{\alpha}_i\sigma^{\mu}_{\alpha\dot{\alpha}}\psi^{\dagger\dot{\alpha}}_j(t,\boldsymbol{x}) \xrightarrow{\mathrm{P}} -i\overline{\sigma}^{0\dot{\beta}\alpha}\psi^{c\dagger}_{i\dot{\beta}}\sigma^{\mu}_{\alpha\dot{\alpha}}\;i\sigma^{0\dot{\alpha}\beta}\psi^{c}_{\beta j}(t,\boldsymbol{x}) = \psi^{c\dagger}_{i\dot{\beta}}\overline{\sigma}^{0\dot{\beta}\alpha}\sigma^{\mu}_{\alpha\dot{\alpha}}\overline{\sigma}^{0\dot{\alpha}\beta}\psi^{c}_{\beta j}(t,\boldsymbol{x})\,,$$

  we now make use of the identity

  $$\overline{\sigma}^{0\dot{\beta}\alpha}\sigma^{\mu}_{\alpha\dot{\alpha}}\overline{\sigma}^{0\dot{\alpha}\beta} = (-1)^{\mu}\overline{\sigma}^{\mu\dot{\beta}\beta} \equiv \mathcal{P}^{\mu}_{\nu}\overline{\sigma}^{\nu\dot{\beta}\beta}\,, \tag{1.161}$$

  where we defined

  $$(-1)^{\mu} \equiv \begin{cases} 1\,, & \mu = 0\,, \\ -1\,, & \mu = i\,, \end{cases} \qquad \mathcal{P}^{\mu}_{\nu} \equiv \mathrm{diag}(1,-1,-1,-1)\,. \tag{1.162}$$

  Roughly speaking, for deriving (1.161), we used the fact that the factor $(-1)^{\mu}$ converts σ^{μ} to $\overline{\sigma}^{\mu}$, while the spinor index structure is preserved by the multiplication of the appropriate factors of the identity matrix (either σ^0 or $\overline{\sigma}^0$). Therefore, we find

  $$\psi_i\sigma^{\mu}\psi^{\dagger}_j(t,\boldsymbol{x}) \xrightarrow{\mathrm{P}} (-1)^{\mu}\psi^{c\dagger}_{i\dot{\alpha}}\overline{\sigma}^{\mu\dot{\alpha}\alpha}\psi^{c}_{\alpha j}(t,-\boldsymbol{x}) = (-1)^{\mu}\psi^{c\dagger}_{i}\overline{\sigma}^{\mu}\psi^{c}_{j}(t,-\boldsymbol{x})\,. \tag{1.163}$$

- $\psi_i\sigma^{\mu\nu}\psi_j$

  $$\psi^{\alpha}_i(\sigma^{\mu\nu})^{\beta}{}_{\alpha}\psi_{j\beta}(t,\boldsymbol{x}) \xrightarrow{\mathrm{P}} -i\overline{\sigma}^{0\dot{\beta}\alpha}\psi^{c\dagger}_{i\dot{\beta}}(\sigma^{\mu\nu})_{\alpha}{}^{\beta}\;i\sigma^{0}_{\beta\dot{\beta}}\psi^{c\dagger\dot{\beta}}_{j}(t,-\boldsymbol{x}) = \psi^{c\dagger}_{i\dot{\beta}}\;\overline{\sigma}^{0\dot{\beta}\alpha}(\sigma^{\mu\nu})_{\alpha}{}^{\beta}\sigma^{0}_{\beta\dot{\beta}}\psi^{c\dagger\dot{\beta}}_{j}(t,-\boldsymbol{x})$$

  we now make use of the identity

  $$\overline{\sigma}^{0\dot{\beta}\alpha}(\sigma^{\mu\nu})_{\alpha}{}^{\beta}\sigma^{0}_{\beta\dot{\beta}} = (-1)^{\mu+\nu}(\overline{\sigma}^{\mu\nu})^{\dot{\beta}}{}_{\dot{\alpha}}\,, \tag{1.164}$$

  where, again, the $(-1)^{\mu+\nu}$ sign converts $\sigma^{\mu\nu}$ to $\overline{\sigma}^{\mu\nu}$. Therefore

  $$\psi_i\sigma^{\mu\nu}\psi_j(t,\boldsymbol{x}) \xrightarrow{\mathrm{P}} \psi^{c\dagger}_i\overline{\sigma}^{\mu\nu}\psi^{c\dagger}_j(t,-\boldsymbol{x})\,. \tag{1.165}$$

All in all, we find the transformation properties

$$\psi_i \sigma^\mu \psi_j^\dagger(t,\boldsymbol{x}) \xrightarrow{\mathrm{P}} (-1)^\mu \psi_i^{c\dagger} \overline{\sigma}^\mu \psi_j^c(t,-\boldsymbol{x})\,, \tag{1.166}$$
$$\psi_i^\dagger \overline{\sigma}^\mu \psi_j(t,\boldsymbol{x}) \xrightarrow{\mathrm{P}} (-1)^\mu \psi_i^{c} \sigma^\mu \psi_j^{c\dagger}(t,-\boldsymbol{x})\,, \tag{1.167}$$
$$\psi_i \sigma^{\mu\nu} \psi_j(t,\boldsymbol{x}) \xrightarrow{\mathrm{P}} (-1)^{\mu+\nu} \psi_i^{c\dagger} \overline{\sigma}^{\mu\nu} \psi_j^{c\dagger}(t,-\boldsymbol{x})\,, \tag{1.168}$$
$$\psi_i^\dagger \overline{\sigma}^{\mu\nu} \psi_j^\dagger(t,\boldsymbol{x}) \xrightarrow{\mathrm{P}} (-1)^{\mu+\nu} \psi_i^{c} \sigma^{\mu\nu} \psi_j^{c}(t,-\boldsymbol{x})\,. \tag{1.169}$$

Using the fact that C acts as

$$\mathrm{C}\psi(t,\boldsymbol{x})\mathrm{C}^{-1} = \psi^c(t,\boldsymbol{x})\,, \quad \mathrm{C}\psi^c(t,\boldsymbol{x})\mathrm{C}^{-1} = \psi(t,\boldsymbol{x})\,, \tag{1.170}$$

we are ready to investigate how CP acts on the Yukawa terms

$$\begin{aligned}
(\mathrm{CP}) \int d^4xh \left[y\psi^c\psi + y^*\psi^\dagger\psi^{c\dagger}\right](t,\boldsymbol{x})(\mathrm{CP})^{-1} &= (\mathrm{CP}) \int d^4xh \left[y\psi^{c\alpha}\psi_\alpha + y^*\psi^\dagger_{\dot\alpha}\psi^{c\dagger\dot\alpha}\right](t,\boldsymbol{x})(\mathrm{CP})^{-1} \\
&= \int d^4xh \left[y\psi^{c\dagger}_{\dot\alpha}\psi^{\dagger\dot\alpha} + y^*\psi^\alpha\psi^c_\alpha\right](t,-\boldsymbol{x}) \\
&= \int d^4xh \left[y^*\psi^c\psi + y\psi^\dagger\psi^{c\dagger}\right](t,-\boldsymbol{x}) \\
&= \int d^4xh \left[y^*\psi^c\psi + y\psi^\dagger\psi^{c\dagger}\right](t,\boldsymbol{x})\,,
\end{aligned} \tag{1.171}$$

where we used the property for which $\psi\eta = -\eta_\alpha\psi^\alpha = -\epsilon_{\alpha\beta}\eta^\beta\psi^\alpha = \eta\psi$ and changed the integration variable $\boldsymbol{x} \to -\boldsymbol{x}$. Therefore, under CP, the Yukawa coupling y transforms as

$$\boxed{y \xrightarrow{\mathrm{CP}} y^*\,.} \tag{1.172}$$

For gauge fields, P and C act as (see for instance [32])

$$\mathrm{P}V^\mu(t,\boldsymbol{x})\mathrm{P}^{-1} = \mathcal{P}^\mu_\nu V^\nu(t,-\boldsymbol{x})\,, \tag{1.173}$$
$$\mathrm{C}V^\mu(t,\boldsymbol{x})\mathrm{C}^{-1} = -V^\nu(t,\boldsymbol{x})\,. \tag{1.174}$$

The action of parity is the usual one for vectors. For electromagnetic fields it implies the well known fact that the electric field $\boldsymbol{E}$ is P-odd, while the magnetic field $\boldsymbol{B}$ is P-even. The minus in the action of C is intuitive: changing a particle into anti-particle flips the electric charge and thus the sign of the potential.

We now consider the charge conjugation which operates on some unitary representation of a compact Lie Group G. Let us denote the N-dimensional fundamental representation of a group G by $\square$ and its complex conjugate representation (anti-fundamental) by $\overline{\square}$. The operation of charge conjugation C exchanges $\square$ and $\overline{\square}$. For simplicity, we discuss a scalar field (the extension to fermion fields is immediate)

$$\Phi = \begin{pmatrix}\phi_1\\ \vdots \\ \phi_N\end{pmatrix} \text{ in the representation } \square\,, \quad \Phi^* = \begin{pmatrix}\phi_1^\dagger\\ \vdots \\ \phi_N^\dagger\end{pmatrix} \text{ in the representation } \overline{\square}\,,$$

Where, under the action of the Lie group G

$$\begin{pmatrix}\Phi\\ \Phi^*\end{pmatrix} \xrightarrow{G} U(g)\begin{pmatrix}\Phi\\ \Phi^*\end{pmatrix} = \begin{pmatrix}e^{-i\omega^a T^a} & 0 \\ 0 & e^{-i\omega^a(-T^{aT})}\end{pmatrix}\begin{pmatrix}\Phi\\ \Phi^*\end{pmatrix}\,, \tag{1.175}$$

where $U(g)$ is the matrix representation of the group element g. Under C, we have

$$\mathrm{C}\begin{pmatrix}\Phi\\ \Phi^*\end{pmatrix}\mathrm{C}^{-1}\equiv\mathcal{C}\begin{pmatrix}\Phi\\ \Phi^*\end{pmatrix}=\begin{pmatrix}\Phi^*\\ \Phi\end{pmatrix}. \tag{1.176}$$

For instance, we have the transformation of the Higgs doublet

$$H(t,\boldsymbol{x})_i=\begin{pmatrix}\chi^+(t,\boldsymbol{x})\\ \frac{1}{\sqrt{2}}\left[v+h(t,\boldsymbol{x})+i\chi^0(t,\boldsymbol{x})\right]\end{pmatrix}\xrightarrow{\mathrm{C}}\epsilon^{ij}H_j^\dagger(t,-\boldsymbol{x})=\begin{pmatrix}\chi^-(t,-\boldsymbol{x})\\ -\frac{1}{\sqrt{2}}\left[v+h(t,-\boldsymbol{x})-i\chi^0(t,-\boldsymbol{x})\right]\end{pmatrix}.$$

Furthermore, for a gauge field $\boldsymbol{A}_\mu=A_\mu^aT^a$,

$$T^a\xrightarrow{\mathrm{C}}-T^{aT} \tag{1.177}$$

i.e., under charge conjugation, we have the transformation of a gauge field

$$\boxed{\boldsymbol{A}_\mu\xrightarrow{\mathrm{C}}-\boldsymbol{A}_\mu^T=-\boldsymbol{A}_\mu^*\,.} \tag{1.178}$$

We notice that, in this way, the Yang-Mills Lagrangian is C-even. Indeed, we have

$$\mathcal{L}_{\mathrm{YM}}\supset-g_sq^\dagger\overline{\sigma}_\mu\boldsymbol{A}_\mu q-g_sq^{c\dagger}\overline{\sigma}_\mu(-\boldsymbol{A}_\mu^*)q^c\,, \tag{1.179}$$

indeed, under C

$$q^\dagger\overline{\sigma}_\mu\boldsymbol{A}_\mu q\xrightarrow{\mathrm{C}}q^{c\dagger}\overline{\sigma}_\mu(-\boldsymbol{A}_\mu^*)q^c\,,\quad q^{c\dagger}\overline{\sigma}_\mu(-\boldsymbol{A}_\mu^*)q^c\xrightarrow{\mathrm{C}}q^\dagger\overline{\sigma}_\mu\boldsymbol{A}_\mu q\,. \tag{1.180}$$

Using the fact that

$$\boldsymbol{G}_{\mu\nu}=\partial_\mu\boldsymbol{A}\nu-\partial_\nu\boldsymbol{A}\mu-ig[\boldsymbol{A}_\mu,\boldsymbol{A}_\nu]\xrightarrow{\mathrm{C}}-(\partial_\mu A_\nu^a-\partial_\nu A_\mu^a)T^{a*}-ig\underbrace{[T^{a*},T^{b*}]}_{-if^{abc}T^{c*}}A_\mu^aA_\nu^b=-G_{\mu\nu}^aT^{a*} \tag{1.181}$$

from which follows that

$$(\mathrm{C})\boldsymbol{G}_{\mu\nu}(t,\boldsymbol{x})(\mathrm{C})^{-1}=-G_{\mu\nu}^a(t,\boldsymbol{x})T^{a*}\,, \tag{1.182}$$

$$(\mathrm{P})\boldsymbol{G}_{\mu\nu}(t,\boldsymbol{x})(\mathrm{P})^{-1}=(-1)^{\mu+\nu}G_{\mu\nu}^a(t,-\boldsymbol{x})T^a\,, \tag{1.183}$$

$$(\mathrm{CP})\boldsymbol{G}_{\mu\nu}(t,\boldsymbol{x})(\mathrm{CP})^{-1}=-(-1)^{\mu+\nu}G_{\mu\nu}^a(t,-\boldsymbol{x})T^{a*}\,. \tag{1.184}$$

It is easy to show that the kinetic term $G_{\mu\nu}^aG^{a\mu\nu}$ is CP-even, while $G_{\mu\nu}^a\widetilde{G}^{a\mu\nu}$ is CP-odd. Indeed, we have the transformation

$$\begin{aligned}(\mathrm{CP})\int d^4xG_{\mu\nu}^a\widetilde{G}^{a\mu\nu}(t,\boldsymbol{x})(\mathrm{CP})^{-1}&=\frac{1}{2}\underbrace{(-1)^{\mu+\nu+\rho+\sigma}\epsilon^{\mu\nu\rho\sigma}}_{=-\epsilon^{\mu\nu\rho\sigma}}\int d^4xG_{\mu\nu}^aG_{\rho\sigma}^a(t,-\boldsymbol{x})\\&=-\int d^4xG_{\mu\nu}^a\widetilde{G}^{a\mu\nu}(t,\boldsymbol{x})\,.\end{aligned} \tag{1.185}$$

Part I

The Strong CP problem: quality problem

CHAPTER

2

Instanton calculus

This chapter introduces the mathematical formulation of instantons, which are non-perturbative, finite-action solutions to the Yang–Mills equations in Euclidean spacetime that play a fundamental role in understanding topological effects in gauge theories. Building upon this foundation, we develop the formalism of 't Hooft vertex operators, which encapsulate the effects of instanton-induced interactions on fermionic fields. These operators provide a powerful tool to describe how instantons violate certain classical symmetries, such as axial U(1) symmetry, and generate effective multi-fermion interactions. Through detailed derivations and examples, this chapter aims to equip the reader with a solid grasp of the instanton calculus framework and the significance of 't Hooft vertices in addressing non-perturbative phenomena such as the Strong CP problem and the dynamics of chiral symmetry breaking.

2.1 Instanton calculus

In the presence of an extended field configuration A^a_μ (so far the instanton solution is a classical one), the quantum system is described by a *wave functional* (see [33–36])

$$\Psi[A_\mu]\,, \tag{2.1}$$

where $\Psi[A_\mu]$ can be interpreted as the probability to measure the field profile A_μ. The *vacuum state*, in particular, is characterized by a wave functional with *vanishing energy*.
Since the topological effects to be discussed are rooted in the gluonic sector, to simplify the following discussion we restrict ourselves to $SU(N_c)$ pure Yang-Mills (i.e. without quarks)

$$\mathcal{L} = -\frac{1}{4}G^a_{\mu\nu}G^{a,\mu\nu}, \quad D_\mu G^{a\mu\nu} = 0, \tag{2.2}$$

where

$$D_\mu = \partial_\mu - ig[A_\mu,\ \cdot\ ] \quad \leftrightarrow \quad (D_\mu)_{ab} = \partial_\mu\delta_{ab} - gf_{abc}A^c_\mu. \tag{2.3}$$

In the following we will conveniently work in the temporal (or Weyl) gauge

$$A_0(\mathbf{x},t) = 0, \quad G^a_{0i} = \partial_0 A^a_i. \tag{2.4}$$

The gauge fixed Yang-Mills Lagrangian is therefore

$$\mathcal{L} = -\frac{1}{4}G^a_{\mu\nu}G^{a,\mu\nu} = \frac{1}{2}(\partial_0 A^a_i)^2 - \frac{1}{4}G^a_{ij}G^a_{ij}, \tag{2.5}$$

and we see that the first term in the right-hand side of (2.5) corresponds to a "kinetic" gluon energy density, while the second term to a "potential" gluon energy density. In terms of the color-electric and -magnetic fields

$$E_a^i = G_a^{i0}, \; B_a^i = -\frac{1}{2}\varepsilon^{ijk} G_{ajk} = \varepsilon^{ijk}\partial_j A^{ak} - \frac{g}{2} f^{abc} \varepsilon^{ijk} A_b^j A_c^k \; (G_{ij}^a = \varepsilon_{ijk} B^{a,k}), \tag{2.6}$$

that is

$$\mathbf{E}_a = -\frac{\partial \mathbf{A_a}}{\partial t}, \quad \mathbf{B}_a = \boldsymbol{\nabla} \times \mathbf{A} - \frac{g}{2} f^{abc} \mathbf{A}_b \mathbf{A}_c, \tag{2.7}$$

the Yang-Mills Lagrangian is

$$\mathcal{L} = \frac{1}{2}\left(\mathbf{E}_a^2 - \mathbf{B}_a^2\right). \tag{2.8}$$

The canonical variables, in the temporal gauge, are the spatial components A_i^a and their conjugate momenta

$$\pi_i^a = \frac{\delta \mathcal{L}}{\delta(\partial_0 A_i^a)} = G_{0i}^a = -E_i^a, \tag{2.9}$$

then the Hamiltonian reads

$$H = \int d^3x \left(\pi_i^a \partial_0 A_i^a - \mathcal{L}\right) = \frac{1}{2}\int d^3x \left(\mathbf{E}_a^2 + \mathbf{B}_a^2\right) = \int d^3x \left(\frac{(\partial_0 A_i^a)^2}{2} + \frac{(G_{ij}^a)^2}{4}\right), \tag{2.10}$$

where again we can interpret $(\partial_0 A_i)^2/2$ and $(G_{ij})^2/4$ respectively as "kinetic" and "potential" energies. When the obvious canonical commutation relations

$$\begin{aligned} \left[A_a^i(\mathbf{x},t), A_b^j(\mathbf{x}',t)\right] &= 0 \\ \left[E_a^i(\mathbf{x},t), E_b^j(\mathbf{x}',t)\right] &= 0 \\ \left[E_a^i(\mathbf{x},t), A_b^j(\mathbf{x}',t)\right] &= i\delta_{ij}\delta^{ab}\delta^{(3)}(\mathbf{x}-\mathbf{x}') \end{aligned} \tag{2.11}$$

are imposed, the Hamiltonian equation of motion are

$$\frac{\partial A_a^i}{\partial t} = i[H, A_a^i] = -E_a^i, \tag{2.12}$$

reproducing the definition of E_i^a, and

$$\frac{\partial E_a^i}{\partial t} = i[H, E_a^i] = \varepsilon^{ijk}\left(\partial_j - g f_{abc} A_{jc}\right) B^{bk} = \varepsilon^{ijk} D_j^{ab} B_b^k, \tag{2.13}$$

that is

$$\frac{\partial \mathbf{E}^a}{\partial t} = \mathbf{D}^{ab} \times \mathbf{B}^b, \tag{2.14}$$

which is the Yang-Mills version of the Ampère's law (the spatial component of the Yang-Mills equation (2.2)). However Gauss' law (the time component of the Yang-Mills equation (2.2))

$$\mathbf{D}^{ab} \cdot \mathbf{E^b} = 0, \tag{2.15}$$

it is not found in the canonical formalism. In a sense, the Hamiltonian theory is a larger than the Yang-Mills one: it gives rise to an entirely consistent quantum mechanics which, however, does not coincide with the desired Yang-Mills theory since Gauss' law is not incorporated. How should one then implement the Yang-Mills dynamics in the Hamiltonian formulation? Eq. (2.15) cannot be incorporated just imposing it as an operator equation: it would lead to inconsistencies (see for example the Gupta-Bleuler quantization of QED). Instead, Eq. (2.15) must be incorporated as a constraint on the Fock space, restricting the physical states to those eigenstates of H which satisfy

$$\begin{aligned} \mathbf{D}^{ab} \cdot \mathbf{E^b} \Psi[\mathbf{A}] = 0, \\ H\Psi[\mathbf{A}] = E\Psi[\mathbf{A}], \end{aligned} \tag{2.16}$$

where $\Psi[\mathcal{A}]$ is the wave-functional in the Schrödinger picture; in this scheme the operators are time-independent and we are working in the "position" basis $A^i_a(\mathbf{x})$, where

$$\mathbf{p} = -i\boldsymbol{\nabla} \leftrightarrow \; E^i_a(\mathbf{x}) = i\frac{\delta}{\delta A^i_a(\mathbf{x})}. \tag{2.17}$$

Let us now establish the appearance of the θ angle as a consequence of the nontrivial topology of the gauge group G (i.e. $\pi_3(G) = Z$) in this framework. The temporal gauge leaves a residual gauge invariance under time-independent gauge transformations, in matrix form

$$A_\mu \to {}^U A_\mu = U A_\mu U^\dagger + \frac{i}{g} U \partial_\mu U^\dagger, \tag{2.18}$$

indeed if $U = U(\mathbf{x})$, the gauge condition $A_0(\mathbf{x}, t) = 0$ is preserved. That is, we have invariance under the gauge transformations

$$U(\omega^a(\mathbf{x})) = e^{i\omega^a(\mathbf{x})t^a}. \tag{2.19}$$

If $\omega^a(\mathbf{x})$ is infinitesimal,

$$A_\mu \to A_\mu + i\left[\omega(\mathbf{x}), A_\mu\right] + \frac{1}{g}\partial_\mu \omega(\mathbf{x}),$$

in components

$$\delta A^a_\mu = \frac{1}{g}\partial_\mu \omega^a(\mathbf{x}) - f^{abc}\omega^b(\mathbf{x}) A^c_\mu.$$

Under such a gauge transformation, the wave-functional transforms as, using (2.17) and (2.16)

$$\begin{aligned} \Psi[\mathbf{A} + \delta\mathbf{A}] - \Psi[\mathbf{A}] &= \int d^3x \frac{\delta\Psi[\mathbf{A}]}{\delta A^a_i(\mathbf{x})}\delta A^a_i(\mathbf{x}) = \int d^3x \big(-iE^a_i(\mathbf{x})\Psi[\mathbf{A}]\big)\delta A^a_i(\mathbf{x}) \\ &= -\frac{i}{g}\int d^3x \left(\partial_i \omega^a(\mathbf{x}) - g f^{abc}\omega^b(\mathbf{x})A^c_i\right) E^a_i(\mathbf{x})\Psi[\mathbf{A}] \\ &= \frac{1}{g}\int d^3x \left[\partial_i(\omega^a E^a_i) - \omega^a \partial_i E^a_i - g f^{abc}\omega^b A^c_i E^a_i\right]\Psi[\mathbf{A}] \\ &= -\frac{i}{g}\int d^3x \Big[\partial_i(\omega^a E^a_i) \underbrace{-\omega^a \partial_i E^a_i + g f^{abc}\omega^a A^c_i E^b_i}_{=-\omega_a D^{ab}_i E^b_i}\Big]\Psi[\mathbf{A}] \\ &= -\frac{i}{g}\int d^3x \partial_i(\omega^a E^a_i) = -\frac{i}{g}\int d\mathbf{S}\cdot \mathbf{E^a}\omega^a(\mathbf{x}). \end{aligned} \tag{2.20}$$

Now comes the point. For a gauge transformation which can be continuously deformed to the identity, i.e. with winding number $n = 0$,

$$\omega^a(\mathbf{x}) \xrightarrow[|\mathbf{x}|\to\infty]{} 0, \tag{2.21}$$

that is, from Eq. (2.20), we see that the wave functional $\Psi[\mathbf{A}]$ is invariant under $n = 0$ gauge transformations, i.e. $\Psi[\boldsymbol{A}]$ is invariant under "small" gauge transformations. However, this is not true in general. Indeed there are gauge transformations which cannot be continuously deformed to the identity transformation, i.e. with winding number $n \neq 0$. The classic example of a gauge transformation with $n = 1$ (in the group $SU(2)$ which is embedded in the gauge group $SU(N)$) is

$$U^{(1)}(\mathbf{x}) = \exp\left(\frac{i\pi\mathbf{x}\cdot\tau}{\sqrt{\mathbf{x}^2+c^2}}\right) \equiv e^{i\omega^a_{(1)}(\boldsymbol{x})t^a} = e^{i\hat{\boldsymbol{x}}\cdot\boldsymbol{\tau} f_{(1)}(r)}, \tag{2.22}$$

where $\boldsymbol{\tau}$ are the $SU(2)$ generators and c is a real constant. We notice that

(i) the $\omega(\boldsymbol{x})$ corresponding to this gauge transformation,

$$\omega^a_{(1)}(\boldsymbol{x}) = \frac{\pi x^a}{\sqrt{\boldsymbol{x}^2+c^s}}, \tag{2.23}$$

does not vanish at spatial infinity,

(ii) $\omega^a_{(1)}(\boldsymbol{x})$ contains a singularity (here a branch cut),

(iii) $f(0) = 0$, $f(\infty) = \pi$ and correspondingly the limiting value of $U^{(1)}(\boldsymbol{x})$ for $r \to \infty$ is angle-independent

$$U^{(1)}(\boldsymbol{x}) \xrightarrow[|\boldsymbol{x}|\to\infty]{} -1. \tag{2.24}$$

This is characteristic for topologically non-trivial gauge transformations, since the exponential can neither be smoothly deformed into the unit element nor expanded for all $\mathbf{x}$. A representative for the class n can be immediately obtained from $U^{(1)}$ by using the addidivity of the winding number under group multiplication

$$U^{(n)}(\mathbf{x}) = \left[U^{(1)}(\boldsymbol{x})\right]^n = \exp\left(\frac{n\pi x^a}{\sqrt{\boldsymbol{x}^2+c^s}}\right) \equiv e^{i\hat{\boldsymbol{x}}\cdot\boldsymbol{\tau} f_{(n)}(r)}, \tag{2.25}$$

where now

$$f_{(n)}(0) = 0,\ f_{(n)}(\infty) = n\pi. \tag{2.26}$$

Therefore we have discovered that $\Psi[\mathbf{A}]$ is in general *not* gauge invariant, i.e. is not invariant under “large" gauge transformations (to wit those that cannot be continuously deformed into the indentity). However, the gauge-fixed hamiltonian (2.10) H is invariant under the time-independent gauge transformations $U(\mathbf{x})$. This implies, after quantization, that the Hamilton operator commutes with the operators $\mathcal{U}(\omega(\mathbf{x}))$ which furnish a unitary representation of the group on the $\Psi[\mathbf{A}]$:

$$[H,\mathcal{U}(\omega(\mathbf{x}))] = 0. \tag{2.27}$$

Thus the energy eigenfunctions can be chosen to be simultaneous eigenstates of H and $\mathcal{U}(\omega(\mathbf{x}))$. Since the eigenvalues of unitary operators must be phases

$$\mathcal{U}^{(n)}(\omega(\mathbf{x}))\Psi[\mathbf{A}] = \Psi\left[{}^{U^{(n)}(\omega(\mathbf{x}))}\mathbf{A}\right] = e^{i\beta_n(\omega(\mathbf{x}))}\Psi[\mathbf{A}]. \tag{2.28}$$

Concatenating two gauge transformations and using the additivity of the winding number

$$\mathcal{U}^{(n)}(\omega)\mathcal{U}^{(m)}(\chi)\Psi[\mathbf{A}] = \Psi\left[{}^{U^{(n)}(\omega)U^{(m)}(\chi)}\mathbf{A}\right] = \Psi\left[{}^{U^{(n+m)}(\xi)}\mathbf{A}\right] = \mathcal{U}^{(n+m)}(\xi)\Psi[\boldsymbol{A}], \tag{2.29}$$

where the group parameters ω, χ and ξ depend on $\mathbf{x}$; therefore

$$e^{i(\beta_n(\omega)+\beta_m(\chi))}\Psi[\boldsymbol{A}] = e^{i\beta_{n+m}(\xi)}\Psi[\boldsymbol{A}] \Longleftrightarrow \beta_n(\omega)+\beta_m(\chi) = \beta_{n+m}(\xi). \tag{2.30}$$

However, rewriting the unit element as

$$\mathbf{1} = \mathcal{U}^{(0)}(\zeta)\mathcal{U}^{(0)\dagger}(\zeta),$$

where $U^{(0)}(\zeta(\boldsymbol{x}))$ is some gauge transformation with winding number $n = 0$, we get - using the invariance of $\Psi[\mathbf{A}]$ under "small" gauge transformations

$$\mathcal{U}^{(n)}(\omega)\Psi[\mathbf{A}] = e^{i\beta_n(\omega)}\Psi[\mathbf{A}] = \mathcal{U}^{(0)}(\zeta)\mathcal{U}^{(0)\dagger}(\zeta)\mathcal{U}^{(n)}(\omega)\Psi[\mathbf{A}] = \mathcal{U}^{(0)}(\zeta)\mathcal{U}^{(n)}(\omega')\Psi[\mathbf{A}] = e^{i\beta_n(\omega')}\Psi[\mathbf{A}], \tag{2.31}$$

that is

$$\beta_n(\omega'(\mathbf{x})) = \beta_n(\omega(\mathbf{x})), \tag{2.32}$$

but $\zeta(\boldsymbol{x})$ is arbitrary, and we conclude that the phases β cannot depend on the details of the gauge transformation (including its $\mathbf{x}$ dependence coming only through $\omega(\boldsymbol{x})$)

$$\beta_n(\omega) = \beta_n. \tag{2.33}$$

As a consequence, (2.30) simplifies to

$$\beta_n + \beta_m = \beta_{n+m}, \tag{2.34}$$

which in turn implies

$$\beta_n = n\theta, \quad \text{with an arbitrary real and state independent angle } \theta \in [0, 2\pi]. \tag{2.35}$$

Altogether, we have therefore established

$$\mathcal{U}^{(n)}(\omega)\Psi[\boldsymbol{A}] = e^{in\theta}\Psi[\boldsymbol{A}], \tag{2.36}$$

for any ω and for *any physical state (not just the vacuum).*

Let us now describe in greater detail the nature of the vacuum wave functional. Considering the field configuration (in matrix form)

$$\mathbf{A}^{(n)}(\mathbf{x}) = iU^{(n)}(\mathbf{x})^\dagger \boldsymbol{\nabla} U^{(n)}(\mathbf{x}), \tag{2.37}$$

which corresponds to a vacuum configuration (indeed it has vanishing F_{ij} cfr. (2.10)) labelled by the winding number n, *neglecting tunneling effects*, we may expect the vacuum to be of the form

$$\chi_n[\boldsymbol{A}] = \varphi[\mathbf{A} - \mathbf{A}^{(n)}], \tag{2.38}$$

where the wave-functional φ is peaked about zero and has a spread due to quantum fluctuations; the χ_n's are like wave functions that peak about a particular potential minimum of a periodic potential in quantum mechanics. However, one can show that a finite action field configuration with winding number m can interpolate between the two vacua $\mathbf{A}^{(n)}(\mathbf{x})$ at $t_i = -\infty$ and $\mathbf{A}^{(n+m)}(\mathbf{x})$ at $t_f = +\infty$ (the (anti-)instanton interpolates between $\mathbf{A}^{(n)}$ and $\mathbf{A}^{(n\mp1)}$), that is

$$\mathcal{U}^{(m)}\chi_n[\boldsymbol{A}] = \chi_{n+m}[\boldsymbol{A}], \tag{2.39}$$

therefore giving origin to tunneling between different vacua $\mathbf{A}^{(n)}$. The correct wave-functional describing the vacuum state is (in the crystal problem the analogous approach is called the "tight binding" approximation)

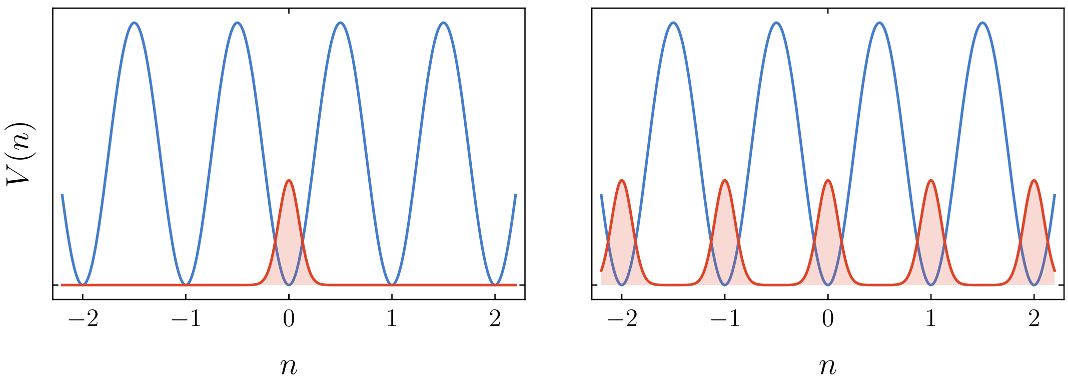

Figure 2.1: *Wave functionals of the system in the absence (left) and presence (right) of tunneling processes, illustrating the modification of the quantum state due to tunneling between classically inaccessible regions.*

Vacuum state wave functional (θ-vacuum)

$$\Psi_\theta[\boldsymbol{A}] = \sum_{m=-\infty}^{\infty} e^{-i\theta m}\chi_m[\boldsymbol{A}], \tag{2.40}$$

or, in a shorthand notation

$$|\theta\rangle = \sum_{m=-\infty}^{\infty} e^{-i\theta m}\,|m\rangle\,, \tag{2.41}$$

indeed, under a generic “large" gauge transformation

$$\mathcal{U}^{(n)}\Psi_\theta[\boldsymbol{A}] = \sum_{m=-\infty}^{\infty} e^{-i\theta m}\chi_{m+n}[\mathbf{A}] = \sum_{m=-\infty}^{\infty} e^{-i(m-n)\theta}\chi_m[\mathbf{A}] = e^{in\theta}\Psi_\theta[\boldsymbol{A}], \tag{2.42}$$

accordingly to the transformation of physical states under “large" gauge transformations in (2.36). Furthermore, theories based on the different $\Psi_\theta[\mathbf{A}]$ states (i.e. with different values of θ) are physically different from each other; indeed the parameter θ is a *constant of motion*, since it does not change in the precess of time evolution

$$\mathcal{U}^{(n)}\left(e^{iHt}\Psi_\theta[\mathbf{A}]\right) = e^{iHt}\left(\mathcal{U}^{(n)}\Psi_\theta[\mathbf{A}]\right) = e^{in\theta}\left(e^{iHt}\Psi_\theta[\mathbf{A}]\right), \tag{2.43}$$

where we used the gauge invariance of H under both “small" and “large" gauge transformations (2.27). Moreover, physical states obtained by acting on the θ-vacuum with a gauge invariant operator $\mathcal{O}$ will be characterized by the same value of θ

$$\mathcal{U}^{(n)}\left(\mathcal{O}\Psi_\theta[\mathbf{A}]\right) = \mathcal{O}\left(\mathcal{U}^{(n)}\Psi_\theta[\mathbf{A}]\right) = e^{in\theta}\mathcal{O}\Psi_\theta[\mathbf{A}]. \tag{2.44}$$

That is, the value of θ characterizes the theory (observables like the vacuum energy will depend on θ) and different values of θ will define different worlds, the so called $\boldsymbol{\theta}$ **worlds**. This can be expressed in terms of a *superselection rule*

$$\langle\theta'|\mathcal{O}|\theta\rangle = \langle\theta'|\mathcal{U}^{(n)\dagger}\mathcal{O}\,\mathcal{U}^{(n)}|\theta\rangle = e^{i(\theta-\theta')}\,\langle\theta'|\mathcal{O}|\theta\rangle\,, \tag{2.45}$$

hence

$$\langle\theta'|\mathcal{O}|\theta\rangle = \delta(\theta-\theta')\,\langle\theta|\mathcal{O}|\theta\rangle\,. \tag{2.46}$$

In the euclidean path-integral representation, we have the tunneling probability

$$\begin{aligned}\langle n|e^{-Ht}|m\rangle \xrightarrow[t\to+\infty]{} & \int[\mathcal{D}A_{(n-m)}\dots]\exp\left(-\int d^4x[\mathcal{L}(A_\mu,\dots)+\mathcal{L}_{\text{g.f.}}(A_\mu,\dots)]\right)\\ &=\int[\mathcal{D}A_{(n-m)}\dots]\exp\left(-S_{\text{E}}[A,\dots]\right)\end{aligned} \tag{2.47}$$

where in the dots all the other relevant fields are included and we are integrating over finite action field configurations which can connect the two vacua $|n\rangle$ and $|m\rangle$, i.e. field configurations with winding number $n-m$. Therefore, we have the transition probability

$$\langle\theta'|e^{-Ht}|\theta\rangle \xrightarrow[t\to+\infty]{} \delta(\theta-\theta')Z(\theta), \tag{2.48}$$

$$\begin{aligned}Z(\theta)=\langle\theta|e^{-Ht}|\theta\rangle=e^{-E(\theta)V_4}&=\sum_{n,m=-\infty}^{\infty}e^{-i\theta(m-n)}\langle n|e^{-Ht}|m\rangle\\ &=\sum_{n,m=-\infty}^{\infty}e^{-i\theta(m-n)}\int[\mathcal{D}A_{(n-m)}\dots]\exp\left(-S_{\text{E}}[A,\dots]\right)\\ &=\sum_{\nu=-\infty}^{\infty}e^{i\theta\nu}\int[\mathcal{D}A_\nu\dots]\exp\left(-S_{\text{E}}[A,\dots]\right),\end{aligned} \tag{2.49}$$

where in the second equality we introduced the vacuum energy-density $E(\theta)$, being $V_4=Vt$ the four-dimensional Euclidean volume. In the Euclidean we can express the winding number n as

$$n=\frac{g^2}{32\pi^2}\int d^4x G^a_{\mu\nu}\tilde{G}^a_{\mu\nu}, \tag{2.50}$$

where, again

$$\tilde{G}^a_{\mu\nu}=\frac{1}{2}\varepsilon_{\mu\nu\rho\sigma}F^a_{\rho\sigma},\quad \varepsilon_{1234}=+1. \tag{2.51}$$

Therefore, we can write

$$\begin{aligned}Z(\theta)&=\sum_n e^{i\theta n}\int[\mathcal{D}A_n\dots]\exp\left(-\int d^4x[\mathcal{L}(A_\mu,\dots)+\mathcal{L}_{\text{g.f.}}(A_\mu,\dots)]\right)\\ &=\sum_n\int[\mathcal{D}A_n\dots]\exp\left(-\int d^4x[\mathcal{L}(A_\mu,\dots)-i\frac{g^2\theta}{32\pi^2}G^a_{\mu\nu}\tilde{G}^a_{\mu\nu}+\mathcal{L}_{\text{g.f.}}(A_\mu,\dots)]\right)\\ &=\int[\mathcal{D}A\dots]\exp\left(-\int d^4x[\mathcal{L}(A_\mu,\dots;\theta)+\mathcal{L}_{\text{g.f.}}(A_\mu,\dots)]\right),\end{aligned} \tag{2.52}$$

where

$$\mathcal{L}(A_\mu,\dots;\theta)=\mathcal{L}(A_\mu,\dots)-i\frac{g^2\theta}{32\pi^2}G^a_{\mu\nu}\tilde{G}^a_{\mu\nu}, \tag{2.53}$$

and, in the third line, all gauge field topologies are summed over, that is

$$\mathcal{D}A=\sum_n\mathcal{D}A_n. \tag{2.54}$$

Continuing back to the Minkowskian space-time and working for simplicity in the temporal gauge, denoting the Euclidean quantities with an hat

$$\begin{gathered}\hat{x}_4\equiv ix_0,\quad \hat{x}_i\equiv x^i,\quad d^4x_{\text{E}}\equiv d^4\hat{x}=id^4x,\\ A^0=i\hat{A}_4,\quad A^i=-\hat{A}_i\end{gathered} \tag{2.55}$$

$$\hat{G}^a_{\mu\nu}\hat{\tilde{G}}^a_{\mu\nu} = \frac{1}{2}\hat{\varepsilon}_{\mu\nu\rho\sigma}\hat{G}^a_{\mu\nu}\hat{G}^a_{\rho\sigma} = \hat{\varepsilon}_{4ijk}\hat{G}^a_{4i}\hat{G}^a_{jk} = \hat{\varepsilon}_{4ijk}\frac{\partial \hat{A}^a_i}{\partial \hat{x}_4}\hat{G}^a_{jk} = \hat{\varepsilon}_{4ijk}\left(-i\frac{\partial A^a_i}{\partial x_0}\right)G^a_{jk}$$
$$= -i\hat{\varepsilon}_{4ijk}G^a_{0i}G^a_{jk}, \tag{2.56}$$

now, we use the fact that the total anti-symmetric symbols in Euclidean and Minkowskian space-times differ for a minus sign, indeed

$$\hat{\varepsilon}_{1234} = +1, \quad \varepsilon^{0123} = +1, \tag{2.57}$$

and we finally get

$$\hat{F}^a_{\mu\nu}\hat{\tilde{F}}^a_{\mu\nu} = i\varepsilon^{0ijk}F^a_{0i}F^a_{jk} = \frac{i}{2}\varepsilon^{\mu\nu\rho\sigma}F^a_{\mu\nu}F^a_{\rho\sigma} = iF^a_{\mu\nu}\tilde{F}^{a\mu\nu}. \tag{2.58}$$

Thus we have discovered that the dynamical effects of the vacuum structure of a Yang-Mills theory are captured in the Lagrangian formalism through the presence of a θ-term

$$\mathcal{L} = -\frac{1}{4}F^{a,\mu\nu}F^a_{\mu\nu} + \theta\frac{g^2}{32\pi^2}F_{a,\mu\nu}\tilde{F}^a_{\mu\nu}. \tag{2.59}$$

Another way to understand the emergence of the θ term is based on causality considerations [37]

2.1.1 Instanton gas in pure Yang-Mills

We consider the euclidean generating functional for a pure Yang-Mills $SU(2)$ theory

$$Z(\theta) = \sum_n \int [\mathcal{D}A]_n e^{-S_{\mathrm{E}}[A]+in\theta} = \sum_n \langle 0|0\rangle_n \ , \tag{2.60}$$

where

$$S_{\mathrm{E}}[A] = \frac{1}{4}\int d^4x G^a_{\mu\nu}G^a_{\mu\nu} = \frac{1}{2}\int d^4x\, \mathrm{Tr}(G_{\mu\nu}G_{\mu\nu}),$$
$$G_{\mu\nu} = G^a_{\mu\nu}t^a, \quad G^a_{\mu\nu} = \partial_\mu A^a_\nu - \partial_\nu A^a_\mu + g\varepsilon_{abc}A^b_\mu A^c_\nu,$$
$$D_\mu = \partial_\mu - igA^a_\mu t^a \quad , \quad [D_\mu, D_\nu] = -igG_{\mu\nu}$$

and $\mathrm{Tr}(t^a t^b) = 1/2\delta^{ab}$. In the following we will focus on the one instanton sector, i.e. to the sector with winding number $n = 1$

$$Z[J]\big|_{n=1} = \int [\mathcal{D}A]_1 e^{-S_{\mathrm{E}}[A]+i\theta}. \tag{2.61}$$

As in the quantum mechanical analog, we shall perform small oscillations around the classical solution, namely around the BPST instanton

$$A^{\mathrm{inst},a}_\mu \quad \rightarrow \quad S[A^{\mathrm{inst},a}_\mu] \equiv S_0 = \frac{8\pi^2}{g^2},$$

that is we will expand the configuration A^a_μ on which we integrate in (2.61) as

$$A^a_\mu = A^{\mathrm{inst},a}_\mu + a^a_\mu \ \longleftrightarrow \ A_\mu = A^{\mathrm{inst}}_\mu + a_\mu, \tag{2.62}$$

where a_μ is the fluctuation. Working at the quadratic order in the fluctuation (there is no linear order in the fluctuation a^a_μ, since $A^{\mathrm{inst,a}}_\mu$ is a solution of the equations of motion), we get

$$G_{\mu\nu} = \partial_\mu A_\nu - \partial_\nu A_\mu - ig[A_\mu, A_\nu] = \mathcal{G}_{\mu\nu} + \mathcal{D}_\mu a_\nu - \mathcal{D}_\nu a_\mu - ig[a_\mu, a_\nu], \tag{2.63}$$

where $\mathcal{G}_{\mu\nu}$ is the field strenght computed in the instanton solution and we introduced the covariant derivative respect to the background field A^{inst}

$$\mathcal{D}_\mu = \partial_\mu - ig[A_\mu^{\text{inst}}, \cdot].$$

Therefore we get

$$\operatorname{Tr}(G_{\mu\nu}G_{\mu\nu}) = \operatorname{Tr}(\mathcal{G}_{\mu\nu}\mathcal{G}_{\mu\nu}) + 2\operatorname{Tr}(\mathcal{D}_\mu a_\nu \mathcal{D}_\mu a_\nu) - 2\operatorname{Tr}(\mathcal{D}_\mu a_\nu \mathcal{D}_\nu a_\mu) - 2ig\operatorname{Tr}(\mathcal{G}_{\mu\nu}[a_\mu, a_\nu]) + \dots$$

and substituting into the action, doing the traces and integrating by parts

$$\begin{aligned}
S_{\mathrm{E}}[A] &= S_0 + \int d^4x \left\{\operatorname{Tr}(\mathcal{D}_\mu a_\nu \mathcal{D}_\mu a_\nu) - \operatorname{Tr}(\mathcal{D}_\mu a_\nu \mathcal{D}_\nu a_\mu) - ig\operatorname{Tr}(\mathcal{G}_{\mu\nu}[a_\mu, a_\nu])\right\} + \dots \\
&= S_0 + \int d^4x \operatorname{Tr}\left\{\mathcal{D}_\mu a_\nu \mathcal{D}_\mu a_\nu - \mathcal{D}_\mu a_\nu \mathcal{D}_\nu a_\mu - ig\mathcal{G}_{\mu\nu}[a_\mu, a_\nu]\right\} \\
&= S_0 - \int d^4x \operatorname{Tr}\left\{a_\mu(\mathcal{D}^2\delta_{\mu\nu} - \mathcal{D}_\mu\mathcal{D}_\nu)a_\nu + 2ig\mathcal{G}_{\mu\nu}a_\mu a_\nu\right\} \\
&= S_0 - \int d^4x \operatorname{Tr} a_\mu[\mathcal{D}^2\delta_{\mu\nu} - \mathcal{D}_\mu\mathcal{D}_\nu + 2ig\mathcal{G}_{\mu\nu}]a_\nu \\
&= S_0 - \int d^4x \operatorname{Tr} a_\mu \Delta_{\mu\nu}^{\text{gauge}}(A^{\text{inst}})a_\nu
\end{aligned} \tag{2.64}$$

where in the fifth line we have introduced the operator

$$\Delta_{\mu\nu}^{\text{gauge}}(A^{\text{inst}}) \equiv \mathcal{D}^2\delta_{\mu\nu} - \mathcal{D}_\mu\mathcal{D}_\nu + 2ig\mathcal{G}_{\mu\nu}. \tag{2.65}$$

Therefore,

$$Z(\theta)|_{n=1} = \int [\mathcal{D}A]_1 e^{-S_{\mathrm{E}}[A]+i\theta} \propto e^{i\theta}e^{-S_0} \times \sqrt{\frac{1}{\det \Delta_{\mu\nu}^{\text{gauge}}(A^{\text{inst}})}}, \tag{2.66}$$

however, not surprisingly, the operator $\Delta_{\mu\nu}^{\text{gauge}}(A^{\text{inst}})$ has zero modes, indeed for an arbitrary $\lambda(x)$

$$\Delta_{\mu\nu}^{\text{gauge}}(A^{\text{inst}})(\mathcal{D}_\nu\lambda) = [\mathcal{D}^2, \mathcal{D}_\mu]\lambda + 2ig\mathcal{G}_{\mu\nu}\mathcal{D}_\nu\lambda = -ig\mathcal{D}_\nu\mathcal{G}_{\nu\mu}\lambda + ig\mathcal{G}_{\nu\mu}\mathcal{D}_\nu\lambda + 2ig\mathcal{G}_{\mu\nu}\mathcal{D}_\nu\lambda = 0,$$

after integrating by parts. There are two main differences with respect to the quantum-mechanical case:

- the redundancy under *small* gauge transformations, i.e. gauge transformation which shuffle among gauge configurations with a fixed winding number, must be fixed. To this aim we introduce a gauge-fixing term and this will introduce a ghost determinant $\det \Delta^{\text{ghost}}$. Therefore, schematically, denoting the ghost fields as c and $\bar{c}$

$$Z(\theta)|_{n=1} = \int [\mathcal{D}A]_1[\mathcal{D}c][\mathcal{D}\bar{c}]e^{-S[A]} \propto e^{i\theta}e^{-S_0}\sqrt{\frac{1}{\det \Delta_{\mu\nu}^{\text{gauge}}(A^{\text{inst}})}}\det \Delta^{\text{ghost}}(A^{\text{inst}}),$$

  where $S = S_{\text{YM}} + S_{\text{g.f.}} + S_{\text{ghost}}$.

- the second difference with respect to quantum mechanics is that the the determinants of Δ^{ghost} and $\Delta_{\mu\nu}^{\text{gauge}}$ are UV-divergent and must be regularized. One possible choice is a Pauli-Villars regulator of mass M (both for ghosts and gauge fields). In the Pauli-Villars regularization one has

$$\begin{aligned}
\det \Delta_{\mu\nu}^{gauge} &\to (\det \Delta_{\mu\nu}^{gauge})^{\text{reg}} = \frac{\det \Delta_{\mu\nu}^{gauge}}{\det(\Delta_{\mu\nu}^{gauge} + M^2\delta_{\mu\nu})}, \\
\det \Delta^{ghost} &\to (\det \Delta^{ghost})^{\text{reg}} = \frac{\det(\Delta^{ghost})}{\det(\Delta^{ghost} + M^2)}
\end{aligned}$$

  obtaining

$$Z(\theta)|_{n=1} \propto e^{i\theta}e^{-S_0}\sqrt{\frac{\det(\Delta_{\mu\nu}^{gauge} + M^2\delta_{\mu\nu})}{\det \Delta_{\mu\nu}^{gauge}}}\frac{\det(\Delta^{ghost})}{\det(\Delta^{ghost} + M^2)}$$

The first step to evaluate the determinants is that of separating out the contribution from the zero modes (otherwise we would get an infinite result). In the case of the Pauli-Villars determinant, formally

$$\begin{aligned}\det(\Delta^{\text{gauge}}_{\mu\nu} + M^2\delta_{\mu\nu}) &= \prod_n(\varepsilon_n + M^2) = \underbrace{M^2 \dots M^2}_{\sharp \text{ of zero modes}} \prod_{\substack{\text{non-zero}\\ \text{modes}}} (\varepsilon_n + M^2)\\ &= \underbrace{M^2 \dots M^2}_{\sharp \text{ of zero modes}} \det{}'(\Delta^{\text{gauge}}_{\mu\nu}),\end{aligned}$$

where $\det'$ is the determinant without zero modes. Excluding zero modes in $\det(\Delta^{\text{gauge}}_{\mu\nu})$ implies a factor of $\sqrt{S_0}$ for each zero mode and an integration over it. In our case there are eight zero modes (the instanton solution has eight collective coordinates), and we finally have

$$\begin{aligned}Z(\theta)|_{n=1} \propto \int d^4x_0 \int dR \int d\phi \sin\phi d\psi d\omega R^3 M^8 (\sqrt{S_0})^8 \times\\ \times e^{i\theta} e^{-S_0} \sqrt{\frac{\det'(\Delta^{\text{gauge}}_{\mu\nu} + \mathrm{M}^2\delta_{\mu\nu})}{\det' \Delta^{\text{gauge}}_{\mu\nu}}} \frac{\det(\Delta^{ghost})}{\det(\Delta^{ghost} + M^2)},\end{aligned} \tag{2.67}$$

where

(i) x_0 is the instanton center, R is the instanton size;

(ii) $0 \leq \phi \leq \pi$, $0 \leq \psi,\ \omega \leq 2\pi$ are the three Euler angles parametrizing the $SU(2)_c$ manifold and the $SU(2)_c$ measure is, up to irrelevant numerical normalization factors

$$d\mu_{SU(2)} \propto \sin\phi d\phi d\psi d\omega$$

and the factor R^3 comes from the Jacobian of the change of variables from changing integration over zero-modes to collective coordinates. The factor R^3 could have been established on dimensional grounds, since at zero order $Z(\theta)|_{n=1} = e^{i\theta}e^{-S_0}$, therefore to render $Z(\theta)|_{n=1}$ dimensionless we have to multiply for a factor R^3.

The integral over d^4x_0 gives $V\tau$, ant the one over the $SU(2)_c$ manifold is just a constant factor that is not interesting for us. Hence we can write

$$Z(\theta)|_{n=1} \propto (V\tau) \int_0^\infty \frac{dR}{R^5} \left(\frac{8\pi^2}{g_0^2}\right)^4 e^{i\theta - \frac{8\pi^2}{g_0^2} + 8\log(MR)} \sqrt{\frac{\det'(\Delta^{\text{gauge}}_{\mu\nu} + \mathrm{M}^2\delta_{\mu\nu})}{\det' \Delta^{\text{gauge}}_{\mu\nu}}} \frac{\det(\Delta^{ghost})}{\det(\Delta^{ghost} + M^2)}, \tag{2.68}$$

where $g_0 \equiv g(M)$ is the *bare* gauge coupling. Notice that the contribution from the zero modes is purely non-perturbative, since it is $\propto \left(\frac{8\pi^2}{g_0^2}\right)^4$. The contribution from the non-zero modes, on the other hand, can be computed by resorting to ordinary perturbation theory. An explicit calculation gives at 1-loop

$$\sqrt{\frac{\det'(\Delta^{\text{gauge}}_{\mu\nu} + \mathrm{M}^2\delta_{\mu\nu})}{\det' \Delta^{\text{gauge}}_{\mu\nu}}} \frac{\det(\Delta^{ghost})}{\det(\Delta^{ghost} + M^2)} = \exp -\frac{N_c}{3} \left(\frac{g_0^2}{8\pi^2}\right) \log(MR) S_0 (1 + \mathcal{O}(g^2)), \tag{2.69}$$

then, since $N_c = 2$

$$\begin{aligned}Z(\theta)|_{n=1} &\propto (V\tau) \int_0^\infty \frac{dR}{R^5} \left(\frac{8\pi^2}{g_0^2}\right)^4 \exp\Big\{ i\theta \underbrace{- \frac{8\pi^2}{g_0^2} + 8\log(MR) - \frac{2}{3}\log(MR)}_{-\frac{8\pi^2}{g^2(M)} + \frac{22}{3}\log(MR)} \Big\}\\ &= (V\tau) \int_0^\infty \frac{dR}{R^5} \left(\frac{8\pi^2}{g_0^2}\right)^4 \exp i\theta - \frac{8\pi^2}{g^2(1/R)},\end{aligned} \tag{2.70}$$

where in the second line we used the formula for the running of the gauge coupling

$$\frac{1}{g^2(\mu)} = \frac{1}{g^2(M)} + \frac{\beta_0}{8\pi^2}\log(\frac{M}{\mu}), \quad \beta_0 = -\frac{11}{3}N_c.$$

Anti-screening effect of the vacuum in a non-Abelian gauge theory

We notice as an aside the following. One way to physically understand the running of the electric charge in QED

$$\frac{1}{e^2(\mu)} = \frac{1}{e_0^2} + \frac{1}{12\pi^2}\log(\frac{\Lambda^2}{\mu^2}),$$

is to say that the QED vacuum (pictorially visualized as a cloud of electron-positron pairs) shields the original charge, so it appears reduced to someone sitting far away. How does the story go with a non-Abelian vacuum? We have seen that the allowance for the zero and non-zero modes has the consequence that $8\pi^2/g_0^2$ in the argument of the exponential in (2.70) is replaced by the effective coupling constant $\frac{8\pi^2}{g^2(1/R)}$:

$$\frac{8\pi^2}{g^2(1/R)} = \frac{8\pi^2}{g_0^2} - 8\log MR + \frac{2}{3}\log(MR) = \frac{8\pi^2}{g_0^2} - \frac{22}{3}\log(MR).$$

This explains that the “anti-screening" contribution to the β function - i.e. the negative contribution to β_0 - comes, in this instanton calculation, entirely from zero modes (which are, as said, connected with purely non-perturbative effects), while non-zero modes contribute to the positive correction to β_0 and we understand the “anti-screening" role of the Yang-Mills vacuum.

We notice as an aside the following. One way to physically understand the screening However, the factor g^{-8} in the pre-exponent in (2.66) remains unrenormalized in this approximation, i.e. to 1-loop order. To see its renormalization explicitly one should perform a 2-loop calculation in the instanton background, obtaining

$$\left(\frac{8\pi^2}{g^2(M)}\right)^4 \to \left(\frac{8\pi^2}{g^2(1/R)}\right)^4.$$

Therefore, for a $SU(2)$ pure Yang-Mills theory we have

One-instanton contribution to the euclidean generating functional $Z(\theta)$ in $SU(2)$ pure Yang-Mills

$$Z(\theta)|_{n=1} \propto (V\tau)\int_0^\infty \frac{dR}{R^5}\left(\frac{8\pi^2}{g^2(1/R)}\right)^4 e^{i\theta-\frac{8\pi^2}{g(1/R)^2}} \equiv (V\tau)\int_0^\infty \frac{dR}{R^5}e^{i\theta}d(R), \tag{2.71}$$

$$d(R) = const \times \left(\frac{8\pi^2}{g^2(1/R)}\right)^4 \exp\left(\frac{-8\pi^2}{g^2(1/R)}\right), \tag{2.72}$$

where $d(R)$ is the *instanton density*. How to generalize (2.71) for a $SU(N)$ Yang-Mills theory? To construct an $SU(N_c)$, $N_c > 2$ instanton

$$A_\mu^{\text{inst,a}}, \; a = 1, \ldots, N_c^2 - 1,$$

one can set three of the $(N_c^2 - 1)$ gauge field components $A_\mu^{\text{inst,a}}$ to be equal to those of the $SU(2)$ instanton, and let the other vanish. This procedure is obviously not unambiguous; for instance we consider the so-called *minimal embedding*, in which we choose to label the $SU(N_c)$ generators in a way such that the first three generators are

$$T^1 = \frac{1}{2}\left(\begin{array}{cc|c} 0 & 1 & \cdot \\ 1 & 0 & \cdot \\ \hline \cdot & \cdot & \cdot \end{array}\right), \quad T^2 = \frac{1}{2}\left(\begin{array}{cc|c} 0 & -i & \cdot \\ i & 0 & \cdot \\ \hline \cdot & \cdot & \cdot \end{array}\right), \quad T^3 = \frac{1}{2}\left(\begin{array}{cc|c} 1 & 0 & \cdot \\ 0 & -1 & \cdot \\ \hline \cdot & \cdot & \cdot \end{array}\right), \tag{2.73}$$

where the dots in the above definition represent zero matrices of appropriate dimensions. Next, we define the $SU(N_c)$ instanton field, using this basis of generators, as follows

$$A_\mu^{SU(N_c)\ \text{inst}} = \sum_{a=1}^{3} A_\mu^{\text{inst,a}}(x) T^a, \tag{2.74}$$

where in (2.74) $A_\mu^{\text{inst,a}}$ is the $SU(2)$ instanton. In other words, the instanton “lives" in the 2×2 upper left block of the $N_c \times N_c$ matrix carachterizing the gauge field

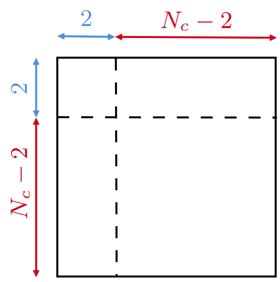

(2.75)

from which we immediately find

$$G_{\mu\nu}^{SU(N_c),\text{inst}} = \sum_{a=1}^{3} G_{\mu\nu}^{\text{inst,a}}(x) T^a. \tag{2.76}$$

Using the general definitions it is not difficult to see that the above $SU(N_c)$ instanton solution

(i) is self-dual,

(ii) has unit topological charge,

(iii) has minimal (non-trivial) action $8\pi^2/g^2$.

The instanton obtained in this basis of generators is called the $SU(N_c)$ BPST instanton. Actually we can apply $SU(N_c)$ transformations to this solution to generate new instantons, *except* for those $SU(N_c)$ rotations that leave the instanton solution invariant. These rotations consist of ones affecting the lower right $(N_c - 2) \times (N_c - 2)$ sub-block and ones trivially commuting with this instanton solution, in other words the generators corresponding to zero modes are those that do not live in the bottom-right $(N_c - 2) \times (N_c - 2)$ sub-block or do not belong to the Cartan sub-algebra. For completeness, we remember that given a Lie algebra, its Cartan sub-algebra is formed by the largest set of commuting generators; in the case under analysis, i.e. $SU(N_c)$, the Cartan subalgebra is formed by traceless diagonal generators with real entries (that are in total $N_c - 1$) and for instance we may choose a basis in which the $N_c - 1$ Cartan generators are

$$H_1 = \frac{1}{2}\begin{pmatrix} 1 & 0 & \dots \\ 0 & -1 & \dots \\ \vdots & \vdots & \ddots \end{pmatrix}, \; H_2 = \frac{1}{\sqrt{12}}\begin{pmatrix} 1 & 0 & 0 & \dots \\ 0 & 1 & 0 & \dots \\ 0 & 0 & -2 & \dots \\ \vdots & \vdots & \vdots & \ddots \end{pmatrix},$$

$$H_3 = \frac{1}{\sqrt{24}}\begin{pmatrix} 1 & 0 & 0 & 0 & \dots \\ 0 & 1 & 0 & 0 & \dots \\ 0 & 0 & 1 & 0 & \dots \\ 0 & 0 & 0 & -3 & \dots \\ \vdots & \vdots & \vdots & \vdots & \ddots \end{pmatrix}, \dots$$

However, in the decomposition (2.74), some Cartan generators may have non-zero diagonal entries only in the $(N_c - 2) \times (N_c - 2)$ sub-block, therefore the number of zero modes will be

$$(N_c^2 - 1) - [(N_c - 2)^2 - 1] - \{(N_c - 1) - [(N_c - 2) - 1] - 1\} = 3 + 4(N_c - 2), \tag{2.77}$$

since $N_c^2 - 1$ is the total number of generators, $[(N_c - 2)^2 - 1]$ is the number of generators in the $(N_c - 2) \times (N_c - 2)$ sub-block, $(N_c - 1) - [(N_c - 2) - 1]$ is the number of Cartans not belonging to the $(N_c - 2) \times (N_c - 2)$ sub-block and we have subtracted one generator of $SU(2)$ already in the Cartan sub-algebra (it does not commute with (2.74)). Clearly, the $4 + 1$ zero modes associated with translations and dilations are not touched and the total number of zero modes of the BPST instanton is thus

$$5 + 3 + 4(N_c - 2) = 4N_c. \tag{2.78}$$

Since each additional zero mode gives a factor $(RM)\sqrt{S_0}$, the instanton density becomes

$$\left(\frac{8\pi^2}{g_0^2}\right)^{2N_c} \exp -\frac{8\pi^2}{g_0^2} + 4N_c \log(MR) - \frac{N_c}{3}\log(MR) = \left(\frac{8\pi^2}{g_0^2}\right)^{2N_c} \exp -\frac{8\pi^2}{g^2(1/R)}, \tag{2.79}$$

where we used

$$-4N_c + \frac{N_c}{3} = -\frac{11}{3}N_c = \beta_0.$$

That is, for a $SU(N_c)$ pure Yang-Mills theory we have

One-instanton contribution to the euclidean generating functional $Z(\theta)$ in $SU(N_c)$ pure Yang-Mills

$$Z(\theta)|_{n=1} \propto (V\tau)\int_0^\infty \frac{dR}{R^5}\left(\frac{8\pi^2}{g^2(1/R)}\right)^{2N_c} e^{i\theta - \frac{8\pi^2}{g(1/R)^2}} \equiv (V\tau)\int_0^\infty \frac{dR}{R^5} e^{i\theta} d(R), \tag{2.80}$$

$$d(R) = K \times \left(\frac{8\pi^2}{g^2(1/R)}\right)^{2N_c} \exp\left(\frac{-8\pi^2}{g^2(1/R)}\right), \tag{2.81}$$

where K is a numerical constant (for details see [38, 39])

$$\begin{gathered} K = \frac{C_1}{(N_c - 1)!\,(N_c - 2)!} e^{-C_2 N_c}, \\ C_1 = \frac{2e^{5/6}}{\pi^2} \approx 0.466, \;\; C_2 = \frac{5}{3}\log(2) - \frac{17}{36} + \frac{1}{3}(\log(2\pi) + \gamma) + \frac{2}{\pi^2}\sum_{s=1}^{\infty}\frac{\log s}{s^2} \approx 1.296. \end{gathered} \tag{2.82}$$

However the constant C_2 depends on the renormalization scheme, ideed the value of C_2 in (2.82) stands for the one in PV regularization. In the MS scheme one can show that [38]

$$C_2^{\mathrm{MS}} = C_2 - 3.888, \tag{2.83}$$

and one must simultaneously use

$$\exp\left(\frac{-8\pi^2}{g^2(1/R)}\right) \to \exp\left(\frac{-8\pi^2}{g^2_{\mathrm{MS}}(1/R)}\right). \tag{2.84}$$

By using the expression of the gauge coupling at 1-loop, the integrand in (2.80) can be written as

$$\propto \frac{dR}{R^5}\exp\left(\frac{-8\pi^2}{g^2(1/R)}\right),$$

using the expression for the gauge coupling at 1-loop level

$$g^2(1/R) = \frac{8\pi^2}{\beta_0\log(\Lambda_c R)},$$

where Λ_c is the $SU(N_c)$ dynamical scale, we obtain

$$\frac{dR}{R^5}\exp\left(\frac{-8\pi^2}{g^2(1/R)}\right) = dRR^{-5}(\Lambda_c R)^{-\beta_0} \propto dR(\Lambda_c R)^{-5-\beta_0}. \tag{2.85}$$

Since $-5-\beta_0 = -5+\frac{11}{3}N_c > 0$ for any $N_c \geq 2$, this means that the integral over the instanton size

(i) converges for small instantons $\Lambda_c R \ll 1$,

(ii) diverges for large instantons $\Lambda_c R \gg 1$.

In other words, we have encountered an **infrared divergence**. Thus, any ensemble of instantons will be dominated by the large-R instantons, unless the instanton density is somehow cut-off in the IR, to wit at long distances. At large R the gauge coupling constant becomes strong, and we completely lose theoretical control: quasiclassical methods are no longer applicable. Then, this divergence is an embarrassmente but not a catastrophe. It would be a catastrophe if we obtained a divergent answer in a regime in which we trusted our approximations. This is not the situation here; the divergence arises in the regime of large coupling constant, where all small-coupling approximations are certainly wrong. Phrased another way, the fact that it the integrand has the wrong behavior for large R is overshadowed by the fact that it is the wrong integrand. Following [40], we assume that the phenomena associated with large R reduce effectively to the appearance of an upper limit R_m in the integral over R, and for all $R < R_m$ one can use the one-instanton formula (2.81) for the instanton density $d(R)$. In the dilute gas approximation (*DIGA*), i.e. in the hypothesis in which the instanton and anti-instanton centers are widely separated,

$$\langle l|e^{-H\tau}|m\rangle = \sum_{n,\bar{n}=0}^{\infty}\frac{(V\tau)^{n+\bar{n}}}{n!\,\bar{n}!}\left[\int^{R_M}\frac{dR}{R^5}d(R)\right]^{n+\bar{n}}\delta_{l-m,n-\bar{n}}, \tag{2.86}$$

that is

$$\begin{aligned} Z(\theta) &= \sum_{l,m=-\infty}^{\infty} e^{i\theta(l-m)}\langle l|e^{-H\tau}|m\rangle = \sum_{n,\bar{n}=0}^{\infty}\frac{(V\tau)^{n+\bar{n}}}{n!\,\bar{n}!}e^{i\theta(n-\bar{n})}\left[\int^{R_M}\frac{dR}{R^5}d(R)\right]^{n+\bar{n}} \\ &= \exp\left(V\tau e^{i\theta}\int^{R_M}\frac{dR}{R^5}d(R)\right)\exp\left(V\tau e^{-i\theta}\int^{R_M}\frac{dR}{R^5}d(R)\right) \\ &= \exp\left(2V\tau\cos(\theta)\int^{R_M}\frac{dR}{R^5}d(R)\right), \end{aligned} \tag{2.87}$$

therefore using (2.48), we finally obtain the vacuum energy-density

Vacuum energy-density in $SU(N_c)$ pure Yang-Mills

$$E(\theta) = -2K\cos(\theta)\int^{R_M}\frac{dR}{R^5}\exp\left(\frac{-8\pi^2}{g^2(1/R)}\right)\left(\frac{8\pi^2}{g^2(1/R)}\right)^{2N_c}. \tag{2.88}$$

How can this result be generalized in the presence of (massive) quarks?

2.1.2 Fermions in an instanton background

For the time being we will limit ourselves to Dirac spinors in Euclidean space-time. We will focus on fermions in the fundamental representation of the gauge group, which, for simplicity will be assumed to be $SU(2)$. There are no conceptual difficulties in generalizing the results to other groups, e.g. $SU(N)$ with arbitrary N. To analitically continue the fermionic Lagrangian to Euclidean space-time we define the Euclidean γ matrices as follows

$$\gamma^0 \equiv \hat{\gamma}_4, \quad \gamma^i \equiv i\hat{\gamma}_i \quad \Rightarrow \quad \{\hat{\gamma}_\mu, \hat{\gamma}_\nu\} = 2\delta_{\mu\nu}, \; \mu,\nu = 1,\ldots,4, \tag{2.89}$$

and we notice that the Euclidean gamma matrices $\hat{\gamma}_\mu$ are Hermitian - while in the Minkowskian γ^0 is Hermitian and γ^i are anti-Hermitian. Using (2.55), since

$$D_\mu = \partial_\mu - igA^a_\mu t^a, \tag{2.90}$$

we have

$$D_0 = \frac{\partial}{\partial x_0} - igA^a_0 t^a = i\frac{\partial}{\partial \hat{x}_4} + g\hat{A}^a_4 t^a = i\hat{D}_4, \tag{2.91}$$

moreover

$$D^i = \frac{\partial}{\partial x_i} - igA^{ia}t^a = -\frac{\partial}{\partial x^i} + ig\hat{A}^a_i t^a = -\frac{\partial}{\partial \hat{x}_i} + ig\hat{A}^a_i t^a = -D_i = -\hat{D}_i, \tag{2.92}$$

where we introduced

$$\hat{D}_\mu = \frac{\partial}{\partial \hat{x}_\mu} - ig\hat{A}^a_\mu t^a. \tag{2.93}$$

In Euclidean space the fields ψ and $\bar{\psi}$ over which we integrate in the path integral must be regarded as independent anticommuting variables. It is convenient to define the Euclidean variables $\hat{\psi}$ and $\hat{\bar{\psi}}$ as follows:

$$\hat{\psi} = \psi, \quad \bar{\psi} = -i\hat{\bar{\psi}}, \tag{2.94}$$

therefore the Dirac action yields

$$\begin{aligned} S_F &= \int d^4x\bar{\psi}(i\gamma^\mu D_\mu - m)\psi = -i\int d^4\hat{x}i\hat{\bar{\psi}}\Big(i\hat{\gamma}_4\times(i\hat{D}_4) - \hat{\gamma}_i\times(\hat{D}_i) - m\Big)\hat{\psi} \\ &= i\int d^4\hat{x}\hat{\bar{\psi}}(\hat{\gamma}_\mu\hat{D}_\mu + m)\hat{\psi}, \end{aligned} \tag{2.95}$$

and using $iS = -S_{\rm E} \equiv -\hat{S}$, we find the fermionic Euclidean action

$$\hat{S}_F = -\int d^4\hat{x}\hat{\bar{\psi}}(i\hat{\gamma}_\mu\hat{D}_\mu + im)\hat{\psi}, \tag{2.96}$$

or omitting the hats, since we will be working with Euclidean quantities

$$S_F = -\int d^4\, x\bar{\psi}(i\gamma_\mu D_\mu + im)\psi. \tag{2.97}$$

Therefore, since ψ and $\bar{\psi}$ are Grassmann variables, integrating them out gives the fermionic measure

$$\mu_F = \int [\mathcal{D}\psi][\mathcal{D}\bar{\psi}]e^{-S_F} = \det\left(i\gamma_\mu D_\mu + im\right). \tag{2.98}$$

In order to compute the determinant, we restrict the Euclidean space-time to a large but finite box, so that the eigenvalues of $i\not{D} + im$ form a discrete spectrum, and therefore

$$\det\left(i\gamma_\mu D_\mu + im\right) = \prod_n (\lambda_n + im), \tag{2.99}$$

where the real numbers λ_n's are the eigenvalues of the Hermitian operator $i\not{D}$ determined from the equations

$$i\gamma_\mu D_\mu u_n(x) = \lambda_n u_n(x), \tag{2.100}$$

with appropriate boundary conditions. We now notice the following

(i) ***Non-zero eigenvalues of*** $i\not{D}$ ***come into pairs*** $(\lambda_n, -\lambda_n)$.
To prove this statement, let us define the Euclidean γ_5 matrix as

$$\hat{\gamma}_5 \equiv -\hat{\gamma}_1\hat{\gamma}_2\hat{\gamma}_3\hat{\gamma}_4 = i\gamma_0\gamma_1\gamma_2\gamma_3. \tag{2.101}$$

If in Minkowksy we choose the Weyl basis of γ matrices, to wit

$$\gamma^\mu = \begin{pmatrix} 0 & \sigma^\mu \\ \bar{\sigma}^\mu & 0 \end{pmatrix}, \quad \sigma^\mu = (I, \sigma^i), \quad \bar{\sigma}^\mu = (I, -\sigma^i), \tag{2.102}$$

which in the Euclidean reads[1]

$$\hat{\gamma}_\mu = \begin{pmatrix} 0 & -i\sigma^-_\mu \\ i\sigma^+_\mu & 0 \end{pmatrix}, \quad \sigma^\pm_\mu = (\sigma, \mp i), \tag{2.103}$$

we find

$$\hat{\gamma}_5 = \begin{pmatrix} -I & 0 \\ 0 & I \end{pmatrix}, \tag{2.104}$$

from which $\hat{\gamma}_5$ is Hermitian and anti-commutes with $\hat{\gamma}_\mu$. Returning to omit the hats, if

$$i\gamma_\mu D_\mu u_n(x) = \lambda_n u_n(x), \tag{2.105}$$

then

$$\lambda_n \gamma_5 u_n = \gamma_5 (i\gamma_\mu D_\mu) u_n = -i\gamma_\mu D_\mu (\gamma_5 u_n), \tag{2.106}$$

that is, $\gamma_5 u_n$ is an eigenfunction of $i\not{D}$ with eigenvalue $-\lambda_n$.

(ii) ***Eigenfunctions of*** $i\not{D}$ ***with zero eigenvalue can always be chosen to be eigenfunctions of*** γ_5***.***
Since $\gamma_5^2 = 1$, its eigenvalues are ± 1. Suppose that u_n is an eigenfunction of $i\not{D}$ with zero eigenvalue but not an eigenfunction of γ_5, that is

$$\gamma_\mu D_\mu u_n = 0, \quad \gamma_5 u_n = \tilde{u}_n, \tag{2.107}$$

however,

$$\gamma_\mu D_\mu \tilde{u}_n = \gamma_\mu D_\mu \gamma_5 u_n = -\gamma_5 \gamma_\mu D_\mu u_n = 0. \tag{2.108}$$

So, if we consider $u_n \pm \tilde{u}_n$, we have found eigenfunctions of $\gamma_\mu D_\mu$ with zero eigenvalue that are also eigenfunctions of γ_5 with eigenvalue ± 1 respectively.

[1] These $\sigma^\pm_\mu$ matrices are Euclidean analogs of the Minkowski matrices $(\sigma_\mu)_{\alpha\dot{\alpha}}$ and $(\bar{\sigma}_\mu)^{\dot{\alpha}\alpha}$: $\sigma^- \leftrightarrow \sigma$, $\sigma^+ \leftrightarrow \bar{\sigma}$.

It is very important to establish, in the limit $m \to 0$, the possible existence of eigenfunctions with zero eigenvalue, in particulare those that are **normalizable** in the limit of infinite Euclidean space-time. We will call such eigenfunctions as (Euclidean) **zero-modes** of the Dirac operator $\not{D}$.
Let us study the zero modes of the Dirac operator in the instanton field background, that is, let us study

$$i\gamma_\mu \mathcal{D}_\mu u_0(x) = 0, \tag{2.109}$$

where (see [39] for details)

$$\begin{aligned} \mathcal{D}_\mu &= \partial_\mu - igA_\mu^{\text{inst,a}}(x)t^a\,, \\ A_\mu^{\text{inst}}(x) = A_\mu^{\text{inst,a}}(x)\frac{\tau^a}{2}, &\quad A_\mu^{\text{inst,a}}(x) = \frac{2}{g}\eta_{a\mu\nu}\frac{(x-x_0)_\nu}{(x-x_0)^2+\rho^2}\,, \\ G_{\mu\nu}^{\text{inst}}(x) = G_{\mu\nu}^{\text{inst,a}}(x)\frac{\tau^a}{2}, &\quad G_{\mu\nu}^{\text{inst,a}}(x) = -\frac{4}{g}\eta_{a\mu\nu}\frac{\rho^2}{[(x-x_0)^2+\rho^2]^2}\,, \end{aligned} \tag{2.110}$$

where in (2.110) $\eta_{a\mu\nu}$ is the 't Hooft symbol and we introduced the notation for which the Pauli matrices acting on color indices are denoted with $\boldsymbol{\tau}$. For later use we write some useful identities involving the 't Hooft symbols $\eta_{a\mu\nu}$ and $\bar{\eta}_{a\mu\nu}$. We have the definitions,

$$\eta_{a\mu\nu} = \begin{cases} \varepsilon_{a\mu\nu} & \mu,\nu = 1,2,3, \\ -\delta_{a\nu} & \mu = 4, \nu = 1,2,3\,, \\ \delta_{a\mu} & \nu = 4, \mu = 1,2,3\,, \\ 0 & \mu = \nu = 4. \end{cases} \quad , \quad \bar{\eta}_{a\mu\nu} = \begin{cases} \varepsilon_{a\mu\nu} & \mu,\nu = 1,2,3, \\ \delta_{a\nu} & \mu = 4, \nu = 1,2,3\,, \\ -\delta_{a\mu} & \nu = 4, \mu = 1,2,3\,, \\ 0 & \mu = \nu = 4. \end{cases} \quad , \tag{2.111}$$

from which it is easy to check that

$$\sigma_\mu^+ \sigma_\nu^- = \delta_{\mu\nu} + i\eta_{a\mu\nu}\sigma^a\,, \tag{2.112}$$

$$\sigma_\mu^- \sigma_\nu^+ = \delta_{\mu\nu} + i\bar{\eta}_{a\mu\nu}\sigma^a\,. \tag{2.113}$$

We give a short list of relations for the symbols $\eta_{a\mu\nu}$ and $\bar{\eta}_{a\mu\nu}$

$$\begin{aligned} \eta_{a\mu\nu} &= \frac{1}{2}\varepsilon_{\mu\nu\rho\sigma}\eta_{a\rho\sigma} \quad (\eta_{a\mu\nu} \text{ is self-dual})\,, \\ \eta_{a\mu\nu} &= -\eta_{a\nu\mu} \quad (\text{anti-symmetry in } \mu,\nu)\,, \\ \eta_{a\mu\nu}\eta_{b\mu\nu} &= 4\delta_{ab}\,, \\ \eta_{a\mu\nu}\bar{\eta}_{b\mu\nu} &= 0\,, \\ \eta_{a\mu\nu}\eta_{b\mu\lambda} &= \delta_{ab}\delta_{\nu\lambda} + \varepsilon_{abc}\eta_{c\nu\lambda}. \end{aligned} \tag{2.114}$$

To pass from the relations for $\eta_{a\mu\nu}$ to those for $\bar{\eta}_{a\mu\nu}$, it is necessary to make the substitution

$$\eta_{a\mu\nu} \to \bar{\eta}_{a\mu}, \quad \varepsilon_{\mu\nu\gamma\delta} \to -\varepsilon_{\mu\nu\gamma\delta}, \quad \text{from which follows that } \bar{\eta}_{a\mu\nu} \text{ is anti-self-dual.} \tag{2.115}$$

First of all, we notice that in the massless limit ($m = 0$), the left and right chiralities obey a pair of decoupled Weyl equations (equations for the zero modes). Indeed, writing

$$u_0(x) = \begin{pmatrix} \chi_L(x) \\ \chi_R(x) \end{pmatrix}, \tag{2.116}$$

the equation for the zero mode reads

$$i\gamma_\mu \mathcal{D}_\mu u_0(x) = 0 \Leftrightarrow \begin{cases} \sigma_\mu^- \mathcal{D}_\mu \chi_R = 0, \\ \sigma_\mu^+ \mathcal{D}_\mu \chi_L = 0. \end{cases} \tag{2.117}$$

We stress once again that both $\boldsymbol{\sigma}$ and $\boldsymbol{\tau}$ denote Pauli matrices and we use $\boldsymbol{\sigma}$ in connection with the Lorentz indices and $\boldsymbol{\tau}$ in connection with the color indices. We now start solving the equation

$$\sigma_\mu^+ \mathcal{D}_\mu \chi_L = 0. \tag{2.118}$$

Applying $\sigma_\mu^- \mathcal{D}_\mu$ gives, using (2.114)

$$\sigma_\mu^- \sigma_\nu^+ \mathcal{D}_\mu \mathcal{D}_\nu \chi_L = (\delta_{\mu\nu} + i\bar{\eta}_{a\mu\nu}\sigma^a)\mathcal{D}_\mu \mathcal{D}_\nu \chi_L = (\mathcal{D}_\mu)^2 \chi_L + \frac{i}{2}\bar{\eta}_{a\mu\nu}\sigma^a \underbrace{[\mathcal{D}_\mu, \mathcal{D}_\nu]}_{=-ig\, G^{\text{inst},\text{a}}_{\mu\nu}\tau^a/2} \chi_L = (\mathcal{D}_\mu)^2 \chi_L = 0. \tag{2.119}$$

Similarly, applying $\sigma_\mu^+ \mathcal{D}_\mu$ to

$$\sigma_\mu^- \mathcal{D}_\mu \chi_R = 0, \tag{2.120}$$

gives instead, using (2.114)

$$\begin{aligned}
\sigma_\mu^+ \sigma_\nu^- \mathcal{D}_\mu \mathcal{D}_\nu \chi_R = (\delta_{\mu\nu} + i\eta_{a\mu\nu}\sigma^a)\mathcal{D}_\mu \mathcal{D}_\nu \chi_R &= (\mathcal{D}_\mu)^2 \chi_R + \frac{i}{2}\eta_{a\mu\nu}\sigma^a \underbrace{[\mathcal{D}_\mu, \mathcal{D}_\nu]}_{=-ig\, G^{\text{inst},\text{a}}_{\mu\nu}\tau^a/2} \chi_R \\
&= (\mathcal{D}_\mu)^2 \chi_R + \frac{g}{4}\sigma^a \tau^b \eta_{a\mu\nu}\left(-\frac{4}{g}\eta_{b\mu\nu}\frac{\rho^2}{[(x-x_0)^2+\rho^2]^2}\right)\chi_R \\
&= (\mathcal{D}_\mu)^2 \chi_R - \left(4\boldsymbol{\sigma}\cdot\boldsymbol{\tau}\frac{\rho^2}{[(x-x_0)^2+\rho^2]^2}\right)\chi_R.
\end{aligned} \tag{2.121}$$

That is we have obtained

$$(\mathcal{D}_\mu)^2 \chi_L = 0, \quad -(\mathcal{D}_\mu)^2 \chi_R = -\left(4\boldsymbol{\sigma}\cdot\boldsymbol{\tau}\frac{\rho^2}{[(x-x_0)^2+\rho^2]^2}\right)\chi_R. \tag{2.122}$$

The operator $-(\mathcal{D}_\mu)^2 = (i\mathcal{D}_\mu)(i\mathcal{D}_\mu)$ is a sum of squares of Hermitian operators, and thence is positive-definite. From this follows that $-(\mathcal{D}_\mu)^2$ does not have vanishing eigenvalues, which yields

$$(\mathcal{D}_\mu)^2 \chi_L = 0 \Rightarrow \chi_L = 0, \tag{2.123}$$

therefore there are no zero modes with negative chirality in one-instanton background.
In the equation for χ_R, we use a basis of total "angular momentum", where the total "angular momentum" corresponds to the addition of ordinary spin (associated with the $\boldsymbol{\sigma}$'s) and color spin (associated with the $\boldsymbol{\tau}$'s); thence the total "angular momentum" is equal to zero or unity. We have

$$\mathbf{J}^2 = \left(\frac{\boldsymbol{\sigma}}{2} + \frac{\boldsymbol{\tau}}{2}\right)^2 = \frac{3}{2} + \frac{\boldsymbol{\sigma}\cdot\boldsymbol{\tau}}{2} \quad \Rightarrow \quad \boldsymbol{\sigma}\cdot\boldsymbol{\tau} = \begin{cases} -3, \; j=0, \\ \;\;\,1, \; j=1. \end{cases} \tag{2.124}$$

Howerver, since $-(\mathcal{D}_\mu)^2$ is positive-definite, we discard the case with $j=1$. Working in the total "angular momentum" basis

$$(\boldsymbol{\sigma} + \boldsymbol{\tau})\chi_R = 0, \tag{2.125}$$

in other words χ_R describes a state for which the color and usual spin add to each other to give a singlet. Writing explicitly the indices

$$\chi_R^{\alpha,a} = \underbrace{\chi_R^{(\alpha,a)}}_{j=1} + \underbrace{f(x-x_0)\varepsilon^{\alpha a}}_{j=0}, \tag{2.126}$$

we fix completely the dependence of χ_R on the indices

$$\chi_R^{\alpha,a} = f(x-x_0)\varepsilon^{\alpha a}, \tag{2.127}$$

that is, in matrix form

$$\chi_R = f(x-x_0)\varphi, \quad \varphi^{\alpha a} = \varepsilon^{\alpha a}. \tag{2.128}$$

To determine $f(x-x_0)$ we have to write explicitly $-(\mathcal{D}_\mu)^2$ and one finds the zero-mode solution

$$\boxed{u_0(x) = \frac{1}{\pi}\frac{\rho}{[(x-x_0)^2+\rho^2]^{3/2}}\begin{pmatrix}0\\1\end{pmatrix}\varphi, \quad \varphi^{\alpha a} = \varepsilon^{\alpha a},} \tag{2.129}$$

which is normalized to one

$$\int d^4x u_0^\dagger(x)u_0(x) = 1. \tag{2.130}$$

That is, we have explicitly shown that, in the instanton background, the operator $i\not{\mathcal{D}}$ has a zero mode with "+" chirality. Similarly, it is also possible to show that in the anti-instanton background, the operator $i\not{\mathcal{D}}$ has a zero mode with "$-$" chirality.

2.1.3 Instanton NDA

In the previous section we explicitly found a zero mode for a massless Dirac fermion in the instanton background. However there is another indirect way to prove that there is a zero eigenvalue of $i\not{\mathcal{D}}$ in the presence of a non topologically trivial background and it is based on the Atiyah-Singer index theorem (see [36, 41, 42]). Let $\phi_n(x)$ be the complete set of eigenfunction of the Hermitian eigenvalue problem

$$\begin{aligned} i\not{\mathcal{D}}\phi_n(x) &= \lambda_n\phi_n(x), \\ \int d^4x\phi_m(x)^\dagger\phi_n(x) &= \delta_{nm}, \\ \sum_n \phi_n(x)\phi_n^\dagger(y) &= \delta^{(4)}(x-y), \end{aligned} \tag{2.131}$$

where $D_\mu = \partial_\mu - igA_\mu$, with A_μ some background gauge field. One can show that, if the fermions belong to a representation of the gauge group with Dynkin index $T(\mathcal{C}_q)$

$$\sum_n \phi_n(x)^\dagger\gamma_5\phi_n(x) = \frac{g^2}{16\pi^2}\mathrm{Tr}\,(G_{\mu\nu}\tilde{G}_{\mu\nu}) = \frac{T(\mathcal{C}_q)g^2}{16\pi^2}G^a_{\mu\nu}\tilde{G}^a_{\mu\nu}\,, \tag{2.132}$$

where the sum on the LHS of (2.132) is ambiguous and it is defined as

$$\sum_n \phi_n(x)^\dagger\gamma_5\phi_n(x) \equiv \lim_{\Lambda\to\infty}\sum_n e^{-\lambda_n^2/\Lambda^2}\phi_n(x)^\dagger\gamma_5\phi_n(x). \tag{2.133}$$

Therefore, integrating (2.132), we readily get

$$\sum_n e^{-\lambda_n^2/\Lambda^2}\int d^4x\phi_n(x)^\dagger\gamma_5\phi_n(x) = 2T(\mathcal{C}_q)n, \tag{2.134}$$

the left-hand side, being well-defined by this cut-off procedure, recieves contributions only from the states with $\lambda_n = 0$, that is

$$\sum_n \int d^4x\phi_n(x)^\dagger\gamma_5\phi_n(x)\bigg|_{\text{zero modes}} = 2T(\mathcal{C}_q)n. \tag{2.135}$$

We notice that if we formally took into account the non-zero modes, despite the exponential suppression, as we had previously shown, ϕ_n and $\gamma_5\phi_n$ have respectively eigenvalues λ_n and $-\lambda_n$. Since eigenfunctions of an Hermitian operator with different eigenvalue are orthogonal,

$$\sum_n \int d^4x \phi_n(x)^\dagger \gamma_5 \phi_n(x)\Big|_{\text{non-zero modes}} = 0. \tag{2.136}$$

Using the fact that the eigenstates of $i\not{D}$ with zero eigenvalues have definite chirality, we find

$$n_+ - n_- = 2T(\mathcal{C}_q)n, \tag{2.137}$$

where n_+ and n_- are the number of zero modes of $i\not{D}$ which are eigenstates of γ_5 with eigenvalues $+$ and $-$ respectively. This is the celebrated Atiyah-Singer index theorem.
Using the fact that at the quantum level the gauge-invariant axial current is anomalous

$$\partial_\mu J^5_\mu(x) = \frac{N_f d(\mathcal{C}_q) g^2}{8\pi^2} F^a_{\mu\nu}\tilde{F}^a_{\mu\nu}(x) + 2\bar{q}M\gamma_5 q\,, \quad J^5_\mu(x) = \bar{q}\gamma_\mu\gamma_5 q \equiv \sum_{f=1}^{N_f} \bar{q}^f\gamma_\mu\gamma_5 q^f\,, \tag{2.138}$$

where M is the quark mass matrix in flavor space (we take the chiral limit, i.e. $M \to 0$), we see that the change in the axial charge

$$Q_5 = \int d^3x J^5_0(x), \tag{2.139}$$

between large negative and positive times

$$\Delta Q_5 = Q_5(t=+\infty) - Q_5(t=-\infty) = \int_{-\infty}^{+\infty} dt\dot{Q}_5 = \int d^4x\, \partial_0 J^5_0 = \int d^4x\, \partial_\mu J^5_\mu = 4N_f T(\mathcal{C}_q)n, \tag{2.140}$$

where we used the fact that, in the chiral limit and being J^5_μ gauge invariant, the charge is spatially localized, i.e.

$$\int dt \int_{\Sigma_\infty} d^3x\, \hat{\mathbf{n}}\cdot\mathbf{J^5} = 0. \tag{2.141}$$

Therefore we find

Atiyah-Singer index theorem

$$\Delta Q_5 = 2N_f(n_+ - n_-) = 4N_f T(\mathcal{C}_q)n, \tag{2.142}$$

which means that any field configuration with non-vanishing winding number n has at least one eigenfunction of vanishing eigenvalue and thus a vanishing Fermi determinant. This implies that the vacuum tunneling is suppressed when there are n massless fermions (and so physics becomes θ-independend). Indeed, the tunneling amplitude between two vacua with winding numbers differing by n units, in presence of massless fermions is

$$\begin{aligned}\langle m+n|e^{-HT}|m\rangle &= \int [\mathcal{D}A]_n[\mathcal{D}\bar{\psi}][\mathcal{D}\psi] \exp\left(-\left[\frac{1}{4}(G^a_{\mu\nu})^2 - \bar{\psi}i\not{D}\psi\right]\right) \\ &= \int [\mathcal{D}A]_n \det(i\not{D}) \exp\left(-\frac{1}{4}(G^a_{\mu\nu})^2\right),\end{aligned} \tag{2.143}$$

where $\det(i\not{D})$ is computed in the background of a gauge field with winding number n. Therefore, from (2.142),

$$\langle m+n|e^{-HT}|m\rangle = 0\,, \quad \text{for } n \neq 0, \tag{2.144}$$

meaning that we must not sandwich the functional integral expression between two vacuum states, because the initial and final charges Q_5 should be different: when the gauge field vacuum tunnels, chiral charge is created; the final state contains a chiral pair and is orthogonal to the Fermi vacuum. Furthermore, since no tunneling effects are present, we cannot anymore define a θ vacuum, instead there will be gauge equivalent n vacua, accordingly to the massless quark solution to the strong CP problem.
Only "virtual tunneling" can occur: an anti-instanton is needed to soak up the chirality created by the instanton. From (2.142), in the presence of an instanton

$$\Delta Q_5 = 2N_f(n_+ - n_-) = N_f \times 4T(\mathcal{C}_q), \tag{2.145}$$

that is the instanton transition (with $n = 1$) forces the chiral charge to change by $4T(\mathcal{C}_q)$ for each flavor and we have to incorporate this feature. *In other worlds, while instantons no longer give rise to vacuum tunnelling, they do still have a role to play for, they now violate axial charge.*
Pictorially we can then represent the instanton as an effective vertex

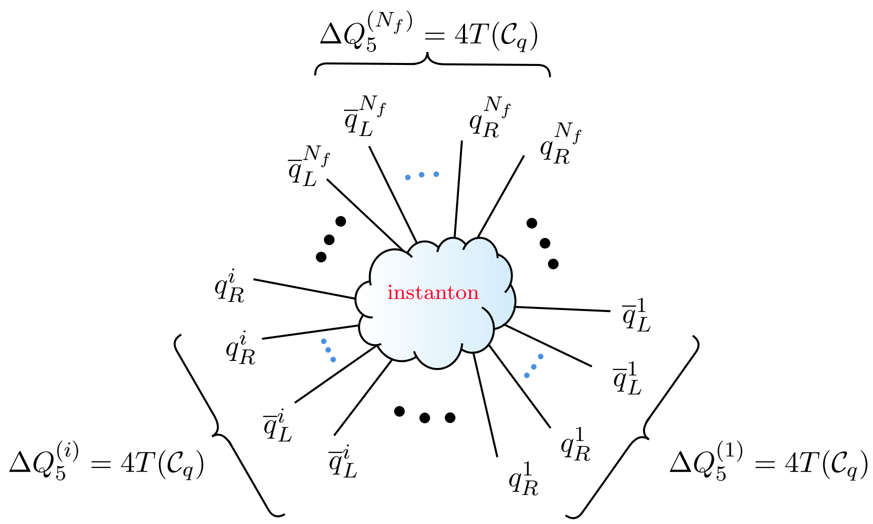

(2.146)

which gives a net violation of the chiral charge Q_5 of

$$\Delta Q_5 = N_f \times 4T(\mathcal{C}_q). \tag{2.147}$$

To unfold the structure of this effective vertex, we proceed as follows. First, to keep the discussion simple, we consider the one flavor case, $N_f = 1$, the Dirac fermions in the fundamental representation of the gauge group and the operator

$$\mathcal{O} = \bar{q}_L q_R(x), \quad \text{with chirality} \quad \chi = 2. \tag{2.148}$$

We compute the Euclidean expectation value

$$\langle \mathcal{O}(x) \rangle_A = \mathcal{N} \int [\mathcal{D}q][\mathcal{D}\bar{q}] e^{\int d^4\bar{q} i \not{D} q} \bar{q}_L q_R(x) \tag{2.149}$$

in the presence of an external gauge field A, where $\mathcal{N}$ is a normalization factor. Expanding in the basis (2.131),

$$q(x) = \sum_n a_n \phi_n(x), \quad \bar{q}(x) = \sum_n \bar{b}_n \phi_n^\dagger(x)\,, \tag{2.150}$$

where, since q and $\bar{q}$ are in the functional integration two independent Grassmann variables, a_n and $\bar{b}_n$ are two independent sets of anti-commuting variables (not carrying spinor indices, which are carried only by the ϕ_n's). Therefore, the path integral measure is

$$\mathcal{N}\int[\mathcal{D}q][\mathcal{D}\bar{q}]=\mathcal{N}\int\prod_n da_n d\bar{b}_n\equiv\mathcal{N}\int(da)(d\bar{b}), \tag{2.151}$$

and the fermionic action is

$$\int d^4x\bar{q}i\not{D}q=\int d^4x\sum_{n,m}\bar{b}_n a_m\left(\phi_n^\dagger i\not{D}\phi_m\right)=\sum_n\lambda_n\bar{b}_n a_n, \tag{2.152}$$

therefore

$$e^{-S_F}=\prod_n e^{\lambda_n\bar{b}_n a_n}=\prod_n(1+\lambda_n\bar{b}_n a_n), \tag{2.153}$$

moreover

$$\bar{q}_L q_R=\bar{q}\left(\frac{1+\gamma_5}{2}\right)q=\sum_{n,m}\bar{b}_n a_m\phi_n^\dagger\left(\frac{1+\gamma_5}{2}\right)\phi_m. \tag{2.154}$$

In terms of a_n's and $\bar{b}_n$'s the expectation value of $\mathcal{O}$ then becomes

$$\langle\mathcal{O}(x)\rangle_A=\mathcal{N}\int(da)(d\bar{b})\prod_n(1+\lambda_n\bar{b}_n a_n)\sum_{m,l}\bar{b}_m a_l\phi_m^\dagger\left(\frac{1+\gamma_5}{2}\right)\phi_l. \tag{2.155}$$

The Grassmannian integrals are performed according to the rules

$$\int da_n\begin{pmatrix}1\\a_m\end{pmatrix}=\int d\bar{b}_n\begin{pmatrix}1\\\bar{b}_m\end{pmatrix}=\begin{pmatrix}0\\\delta_{nm}\end{pmatrix}, \tag{2.156}$$

therefore the only non-vanishing contribution to $\langle\mathcal{O}\rangle_A$ are those in which each a_n and $\bar{b}_n$ appears exactly once, giving

$$\langle\mathcal{O}(x)\rangle_A\propto\prod_m\lambda_n\sum_n\frac{1}{\lambda_n}\phi_n^\dagger\left(\frac{1+\gamma_5}{2}\right)\phi_n(x). \tag{2.157}$$

We now ask what are the external gauge field configurations A_μ giving a non-vanishing $\langle\mathcal{O}\rangle_A$. That is, we consider the following cases

1. $i\not{D}$ has no zero modes.
   This means that, as previously shown, *all* the eigenvalues of $i\not{D}$ are paired

   $$i\not{D}\phi_n=\lambda_n\phi_n,\quad i\not{D}\gamma_5\phi_n=-\lambda_n\gamma_5\phi_n, \tag{2.158}$$

   and the sum appearing in (2.157) vanishes, i.e.

   $$\sum_n\frac{1}{\lambda_n}\phi_n^\dagger\left(\frac{1+\gamma_5}{2}\right)\phi_n(x)=0. \tag{2.159}$$

   That is from the index theorem, excluding $n_+=n_-$, $i\not{D}$ vanishes for topologically trivial gauge field configurations.

2. $i\not{D}$ has one "+" chirality zero mode: $n_+=1$.
   Calling ϕ_0 the corresponding eigenvector, i.e. $i\not{D}\phi_0=\lambda_0\phi_0$, $\lambda_0=0$, (2.157) becomes

$$\lambda_0\prod_n{}'\lambda_n\left(\frac{1}{\lambda_0}\phi_0^\dagger\left(\frac{1+\gamma_5}{2}\right)\phi_0(x)+\underbrace{\frac{1}{\lambda_1}\phi_1^\dagger\left(\frac{1+\gamma_5}{2}\right)\phi_1(x)+\dots}_{=0}\right)=\prod_n{}'\lambda_n\phi_0^\dagger\left(\frac{1+\gamma_5}{2}\right)\phi_0(x)$$
$$=\det{}'(\mathrm{i}\not{D})\phi_0^\dagger\left(\frac{1+\gamma_5}{2}\right)\phi_0(\mathrm{x})=\det{}'(\mathrm{i}\not{D})\phi_0^\dagger\phi_0(\mathrm{x}), \tag{2.160}$$

that is

$$\langle \mathcal{O}(x)\rangle_A \propto \det{}'(\mathrm{i}\not{D})\phi_0^\dagger\phi_0(\mathrm{x}) \neq 0, \tag{2.161}$$

where, as usual $\det'$ is the determinant computed excluding zero eigenvalues.

3. $i\not{D}$ has one "$-$" chirality zero mode: $n_- = 1$.
   Proceeding as in the previous point,

$$\langle \mathcal{O}(x)\rangle_A \propto \det{}'(\mathrm{i}\not{D})\phi_0^\dagger\left(\frac{1+\gamma_5}{2}\right)\phi_0(\mathrm{x}) = 0, \tag{2.162}$$

   which means that anti-instanton configurations give vanishing contribution to $\langle\mathcal{O}\rangle_A$.

4. $i\not{D}$ has more than one zero-mode

$$\not{D}\phi_0^{(n)} = \lambda_0^{(n)}\phi_0^{(n)}, \quad \lambda_0^{(n)} = 0\,. \tag{2.163}$$

   In this case (2.157) yields

$$\begin{aligned}&\langle \mathcal{O}(x)\rangle_A \\ &\propto \lambda_0^{(1)}\lambda_0^{(2)}\dots\lambda_0^{(n)}\det{}'(\mathrm{i}\not{D})\times \\ &\times\left(\frac{1}{\lambda_0^{(1)}}\phi_0^{(1)\dagger}\left(\frac{1+\gamma_5}{2}\right)\phi_0^{(1)}(x) + \frac{1}{\lambda_0^{(2)}}\phi_0^{(2)\dagger}\left(\frac{1+\gamma_5}{2}\right)\phi_0^{(2)}(x)+\dots\right) = 0,\end{aligned} \tag{2.164}$$

   that is gauge field configurations with $|n|\geq 2$ do not contribute to the expectation value of $\mathcal{O}$.

From the above analysis we conclude that[2]

$$\langle\bar{q}_L q_R\rangle_A \neq 0 \;\; \text{requires} \;\; n=1, \tag{2.165}$$

similarly

$$\langle\bar{q}_R q_L\rangle_A \neq 0 \;\; \text{requires} \;\; n=-1, \tag{2.166}$$

Therefore,

$$\begin{aligned}\langle\bar{q}_L q_R\rangle &= \mathcal{N}\sum_n\int[\mathcal{D}A]_n[\mathcal{D}\bar{q}][\mathcal{D}q]\,\exp\int d^4x\left(-\frac{1}{4}(G^a_{\mu\nu})^2 + \bar{q}i\not{D}q\right) + in\theta\bar{q}_L q_R(x) \\ &= \mathcal{N}\int[\mathcal{D}A]_1[\mathcal{D}\bar{q}][\mathcal{D}q]\,\exp\int d^4x\left(-\frac{1}{4}(G^a_{\mu\nu})^2 + \bar{q}i\not{D}q\right) + i\theta\bar{q}_L q_R(x) \\ &= \mathcal{N}\int[\mathcal{D}A]_1\exp -\frac{1}{4}\int d^4x (G^a_{\mu\nu})^2 e^{i\theta}\frac{\det'(\mathrm{i}\not{D})}{\det(i\not{\partial})}\phi_0^\dagger(x)\phi_0(x),\end{aligned} \tag{2.167}$$

where we have normalized respect to the case with $A_\mu = 0$. Expanding about the instanton solution and substituting the explicit expression for the zero-mode solution (2.129), we find

$$\begin{aligned}\langle\bar{q}_L q_R\rangle \propto \int\frac{d\rho}{\rho^5}\int d^4x_0\int d\Omega\left(\frac{8\pi^2}{g^2}\right)^{2N_c}&\exp(-\frac{8\pi^2}{g_0^2}+\frac{11}{3}N_c\log(M\rho))e^{i\theta}\times \\ \times\frac{\det'(\mathrm{i}\not{D})}{\det(i\not{\partial})}&\frac{\rho^3\varphi^\dagger\varphi}{\pi^2\left[(x-x_0)^2+\rho^2\right]^3},\end{aligned} \tag{2.168}$$

where $d\Omega$ is the differential corresponding to the color orientation of the instanton and it is normalized to unity. We notice that the g^2 factoring (2.168) is the bare coupling, which we expect to be renormalized

[2] To avoid confusion, n in(2.165) is the winding number.

by taking into account two-loop effects. Moreover, in (2.168) we have in the numerator a factor of ρ^3, two of which are carried by $\phi_0^\dagger\phi_0$ and an extra ρ is inserted for dimensional reasons (to match the dimentions of the LHS of (2.168)).
However the determinants must be regularized from loop divergences, to wit

$$\frac{\det'(\mathrm{i}\not{D})}{\det(i\not{\partial})} \to \left.\frac{\det'(\mathrm{i}\not{D})}{\det(i\not{\partial})}\right|_{\text{regulated}} = \frac{\det'(\mathrm{i}\not{D})}{i(M\rho)\times\det'(\mathrm{i}\not{D}+\mathrm{iM})}\frac{\det(\mathrm{i}\not{\partial})}{\det(\mathrm{i}\not{\partial}+\mathrm{iM})}, \tag{2.169}$$

where M is the mass of the PV regulator. As in the Yang-Mills case, the dependence on the regulator mass scale M must be such that M is removed by a renormalization of the coupling constant, i.e. the dependence on M must give the renormalization of the overall factor $\exp(-8\pi^2/g_0^2)$. Indeed it can be shown (see [38]) that the non-zero modes give

$$\frac{\det'(\mathrm{i}\not{D})}{\det'(\mathrm{i}\not{D}+\mathrm{iM})}\frac{\det(\mathrm{i}\not{\partial})}{\det(\mathrm{i}\not{\partial}+\mathrm{iM})} = \exp\left(\frac{1}{3}\log(M\rho)\right), \tag{2.170}$$

therefore

$$\left.\frac{\det'(\mathrm{i}\not{D})}{\det(i\not{\partial})}\right|_{\text{regulated}} = \exp - \log(M\rho) + \frac{1}{3}\log(M\rho). \tag{2.171}$$

Comparing this result with the pure gluonic case, we see that the situation has been changed because of the anticommutativity of the fermionic fields: the zero-frequency modes of the light quarks lead to “screening" of the charge, and the positive-frequency modes to “anti-screening". Using the formula for the running coupling

$$\frac{1}{g^2(\mu)} = \frac{1}{g^2(M)} + \frac{\beta_0}{8\pi^2}\log\left(\frac{M}{\mu}\right), \quad \beta_0 = -\left(\frac{11}{3}N_c - \frac{4}{3}N_f d(\mathcal{C}_q)\right), \tag{2.172}$$

we finally obtain

$$\langle \bar{q}_L q_R(x)\rangle \propto \left(\frac{8\pi^2}{g^2}\right)^{2N_c} \int \frac{d\rho}{\rho^5}\int d^4x_0 \left(\frac{8\pi^2}{g^2(1/\rho)}\right)^{2N_c} e^{-\frac{8\pi^2}{g^2(1/\rho)}} e^{i\theta} \frac{\rho^3}{[(x-x_0)^2+\rho^2]^3}. \tag{2.173}$$

Motivated by the picture (2.146), we now make the following observation (see [43, 44]); for small instanton size, the integrand of (2.173) goes like

$$(x-x_0)^{-6}, \tag{2.174}$$

and the Euclidean propagator for massless Dirac fermions in coordinate space reads

$$S_F(x-x_0) = \frac{\gamma_\mu(x-x_0)_\mu}{2\pi^2(x-x_0)^4} \propto (x-x_0)^{-3}, \tag{2.175}$$

therefore, for large x^2, the amplitude (2.173) has exactly the space-time structure of the amplitude generated by the effective vertex at x_0

$$-C\left(\frac{8\pi^2}{g^2}\right)^{2N_c} \int \frac{d\rho}{\rho^5}\,\rho^3 e^{i\theta}\, e^{-\frac{8\pi^2}{g(1/\rho)}}\,\bar{q}_R q_L(x_0) + \text{h.c.}, \tag{2.176}$$

where the minus sign comes from the Fermi statistics and the factor

$$(x-x_0)^6, \tag{2.177}$$

is precisely reproduced by the 2 propagators that connect x_0 with x and the integral over the collective coordinate x_0 will correspond to the integration in coordinate configuration over the vertex variable;

the Hermitian conjugate of (2.176) gives the anti-instantonic contribution to $\langle \bar{q}_R q_L(x) \rangle$. This can be visualized diagrammatically as

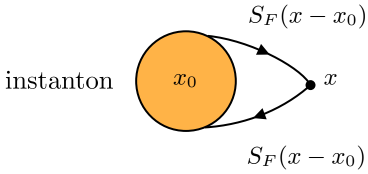

(2.178)

Summarizing what we have discussed so far, naively the theory with one massless quark is invariant under $U(1)_A$ transformations $q \to e^{i\alpha\gamma_5} q$ and therefore we would expect

$$\langle 0|\bar{q}_L q_R|0\rangle = 0, \quad \text{at any order in perturbation theory.} \tag{2.179}$$

However, we had explicitly shown that - due to non-perturbative effects,

$$\langle 0|\bar{q}_L q_R|0\rangle \neq 0\,, \tag{2.180}$$

and this can be encoded by adding to the QCD Lagrangian the extra term

$$\Delta\mathcal{L}(x) = -C \left(\frac{8\pi^2}{g^2}\right)^{2N_c} \int \frac{d\rho}{\rho^5}\, e^{i\theta}\, \rho^3 e^{-\frac{8\pi^2}{g(1/\rho)}}\, \bar{q}_R q_L(x) + \text{h.c.}\,, \tag{2.181}$$

which explicitly breaks $U(1)_A$ symmetry. We notice that the effective Lagrangian appearing in (2.181) is apparently not gauge invariant, since each fermion in the RHS of (2.181) carries its own color index, i.e. denoting with i_t, $t = 1, \ldots, N_f$ the color index, (2.181) has to be rewritten as

$$\Delta\mathcal{L}(x) = -\int d\rho \rho^{-5+3}\, d_{N_c}(\rho) e^{i\theta}\, (\mathcal{K}^{(1)}_{N_c})^{i_1 i_2} (\bar{q}_R q_L(x))_{i_1 i_2} + \text{h.c.}\,, \tag{2.182}$$

where the function $d_{N_c}(\rho)$ and the tensor $(\mathcal{K}^{(1)}_{N_c})^{i_1 i_2}$ are obtained computing the fermionic correlation function $\langle \bar{q}_L q_R(x) \rangle$ with the effective 't Hooft vertex and matching the result with the instanton background computation in (2.167). For instance (see [44])

$$\begin{aligned} (\mathcal{K}^{(1)}_{N_c})^{i_1 i_2} &= 2\pi^2 \delta^{i_1 i_2}, \quad N_c = 2, \\ (\mathcal{K}^{(1)}_{N_c})^{i_1 i_2} &= \frac{4}{3}\pi^2 \delta^{i_1 i_2}, \quad N_c = 3, \end{aligned} \tag{2.183}$$

and in PV regularization

$$d_{N_c}(\rho) = \frac{C_1}{(N_c-1)!(N_c-2)!} \left(\frac{8\pi^2}{g^2}\right)^{2N_c} e^{-\frac{8\pi^2}{g^2(1/\rho)} - C_2 N_c + 0.292 N_f} \equiv C_{N_c} \left(\frac{8\pi^2}{g^2}\right)^{2N_c} e^{-\frac{8\pi^2}{g^2(1/\rho)}}, \tag{2.184}$$

where in MS renormalization the 0.292 is replaced by -0.495 and in $\overline{\text{MS}}$ renormalization by 0.153. Doing the same analysis for $N_f > 1$, we now consider

$$\langle \bar{q}^1_L q^1_R(x_1) \ldots \bar{q}^{N_f}_L q^{N_f}_R(x_{N_f}) \rangle_A. \tag{2.185}$$

Doing the same steps done with $N_f = 1$ we find ($i\not{D}$ is flavor blind, and so its eigenvectors)

$$\bar{q}^t_L q^t_R(x_t) = \bar{q}^t \left(\frac{1+\gamma_5}{2}\right) q^t(x_t) = \sum_{n,m} \bar{b}^t_n a^t_m \phi^\dagger_n \left(\frac{1+\gamma_5}{2}\right) \phi_n(x_t), \quad t = 1, \ldots, N_f. \tag{2.186}$$

Thence

$$\langle \bar q_L^1 q_R^1(x_1)\dots \bar q_L^{N_f} q_R^{N_f}(x_{N_f})\rangle_A = \mathcal{N}\prod_{t=1}^{N_f}\int (da^t)(d\bar b^t)\prod_n (1+\lambda_n \bar b_n^t a_n^t)\sum_{m,l}\bar b_m^t a_l^t \phi_m^\dagger\left(\frac{1+\gamma_5}{2}\right)\phi_l(x_t)$$
$$\propto \prod_{t=1}^{N_f}\prod_m \lambda_n \sum_n \frac{1}{\lambda_n}\phi_n^\dagger\left(\frac{1+\gamma_5}{2}\right)\phi_n(x_t), \tag{2.187}$$

and to get a non-vanishing expectation value we need a zero mode per each flavor. Equivalently the only gauge field configuration for which the expectation value (2.185) is non-zero is the one for which $n_+ = N_f$ and $n_- = 0$, that is from the Atiyah-Singer theorem (2.142),

$$n_+ - n_- = N_f \Leftrightarrow \; n = 1, \tag{2.188}$$

$$\langle \bar q_L^1 q_R^1(x_1)\dots \bar q_L^{N_f} q_R^{N_f}(x_{N_f})\rangle_A \neq 0 \;\text{ requires }\; n=1, \tag{2.189}$$

similarly

$$\langle \bar q_R^1 q_L^1(x_1)\dots \bar q_R^{N_f} q_L^{N_f}(x_{N_f})\rangle_A \neq 0 \;\text{ requires }\; n=-1. \tag{2.190}$$

Therefore, ignoring two-loop effects

$$\langle \bar q_L^1 q_R^1(x_1)\dots \bar q_L^{N_f} q_R^{N_f}(x_{N_f})\rangle$$
$$= \mathcal{N}\sum_n \int [\mathcal{D}A]_n[\mathcal{D}\bar q][\mathcal{D}q]\,\exp\int d^4x\left(-\frac14 (G^a_{\mu\nu})^2 + \bar q i \not{D} q\right) + in\theta \prod_{t=1}^{N_f}\bar q_L^t q_R^t(x_t)$$
$$= \mathcal{N}\int [\mathcal{D}A]_1[\mathcal{D}\bar q][\mathcal{D}q]\,\exp\int d^4x\left(-\frac14 (G^a_{\mu\nu})^2 + \bar q i \not{D} q\right) + i\theta \prod_{t=1}^{N_f}\bar q_L^t q_R^t(x_t)$$
$$= \mathcal{N}\int \frac{d\rho}{\rho^5}\int d^4x_0 \int d\Omega \left(\frac{8\pi^2}{g^2}\right)^{2N_c}\exp\left(-\frac{8\pi^2}{g_0^2}+\frac{11}{3}N_c\log(M\rho)\right)e^{i\theta}\times$$
$$\times\left(\frac{\det'(\mathrm{i}\not{D})}{\det(i\not\partial)}\right)^{N_f}\prod_{t=1}^{N_f}\frac{\rho^3\varphi^\dagger\varphi}{\pi^2\left[(x_t-x_0)^2+\rho^2\right]^3}$$
$$= \mathcal{N}\langle\varphi^\dagger\varphi\rangle^{N_f}\pi^{-2N_f}\int d\rho\int d^4x_0 \rho^{-5+3N_f}\,e^{i\theta}\left(\frac{8\pi^2}{g^2}\right)^{2N_c}\exp\left\{\underbrace{\left(-\frac{8\pi^2}{g_0^2}+\log(M\rho)\left[\frac{11}{3}N_c-\frac23 N_f\right]\right)}_{=-8\pi^2/g^2(1/\rho^2)}\right\}\times$$
$$\times\prod_{t=1}^{N_f}\frac{1}{\left[(x_t-x_0)^2+\rho^2\right]^3}, \tag{2.191}$$

Again, for small instanton sizes, the integrand of (2.191) goes like

$$\prod_{t=1}^{N_f}(x_t-x_0)^{-6}, \tag{2.192}$$

which is reproduced by $2N_f$ fermion propagators, that is the amplitude (2.191) has the same space-time structure of the amplitude generated by the effective vertex at x_0

$$-C\int d\rho\,\rho^{-5+3N_f}\left(\frac{8\pi^2}{g^2}\right)^{2N_c} e^{-\frac{8\pi^2}{g^2(1/\rho)}}\,e^{i\theta}\bar q_R^1 q_L^1(x_0)\dots \bar q_R^{N_f} q_L^{N_f}(x_0) + \text{h.c.}\,, \tag{2.193}$$

where the minus sign comes from the Fermi statistics and the Hermitian conjugate of (2.193) gives the anti-instantonic contribution to $\langle \bar{q}_R^1 q_L^1(x_1)\ldots \bar{q}_R^{N_f} q_L^{N_f}(x_{N_f})\rangle$. However, owing to Fermi statistics, we can equivalently express (2.193) as - up to a constant factor

't Hooft effective operator

$$\Delta\mathcal{L}(x) = -\int d\rho\, \rho^{-5+3N_f}\, d_{N_c}(\rho)(\mathcal{K}_{N_c}^{(N_f)})^{i_1 i_2\ldots i_{2N_f}}\, e^{i\theta}\, \det_{s,t}\left(\bar{q}_R^s(x) q_L^t(x)\right)_{i_1 i_2\ldots i_{2N_f}} + \text{h.c.}\,, \quad (2.194)$$

where the determinant goes over flavor indices and the Hermitian conjugate results from the anti-instanton configuration. As in the case with one flavor, the integration over the collective coordinate $x_{0\mu}$ in (2.191) simply corresponds to the integration in coordinate configuration over the vertex variable. The effective vertex generated by field configuration with winding number $|n| = 1$ is the so-called *'t Hooft operator* [43]. Diagrammatically, the contribution of (2.194) to the Green function $\langle \bar{q}_L^1 q_R^1(x_1)\ldots \bar{q}_L^{N_f} q_R^{N_f}(x_{N_f})\rangle$ can be depicted with the "daisy" diagram

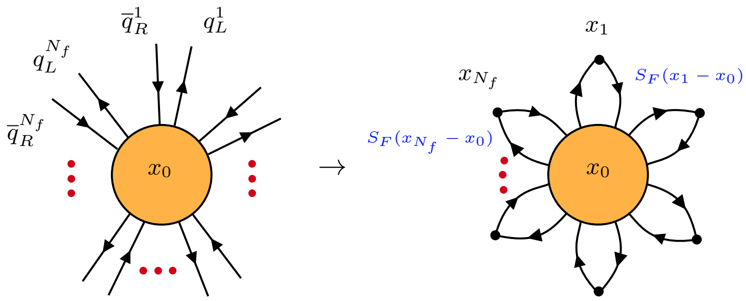

(2.195)

As an application of (2.194) we may give an estimate of the axion potential [45]. As we did in (2.88), to compute the vacuum energy-density, we have to evaluate vacuum-to-vacuum transition amplitudes, i.e. $Z(\theta)$ which can be seen diagrammatically as the sum of **vacuum bubbles**, i.e. as the sum of diagrams without external legs. We focus on the one-instanton contribution $Z(\theta)|_{n=1}$ which is obtained closing up the fermion legs of the 't Hooft operator (diagrammatically depicted in the left of (2.195)) using all available couplings, as for an ordinary vacuum-to-vacuum amplitude. Another ingredient to the axion potential estimate is based on the fact that the strong couling, if the particle content is the one of the Standard Model, is a decreasing function of $1/\rho$, therefore the factor $\exp[-8\pi^2/g^2(1/\rho)]$ gives an exponential suppression of the small size instantons. We consider instanton contributions within an energy range $[M_{\text{IR}}, M_{\text{UV}}]$, where M_{IR} is well above the strong coupling scale, i.e. $M_{\text{IR}} \gg \Lambda_{\text{QCD}}$, while M_{UV} is below the mass of the charm quark. The 't Hooft operator (2.194) is therefore

$$\Delta\mathcal{L}(x) \approx \int_{1/M_{\text{UV}}}^{1/M_{\text{IR}}} \frac{d\rho}{\rho^5}\rho^9\, d_3(\rho) e^{i\theta}\bar{u}_R(x) u_L(x)\bar{d}_R(x) d_L(x)\bar{s}_R(x) s_L(x) + \text{h.c.}, \quad (2.196)$$

which can be depicted as

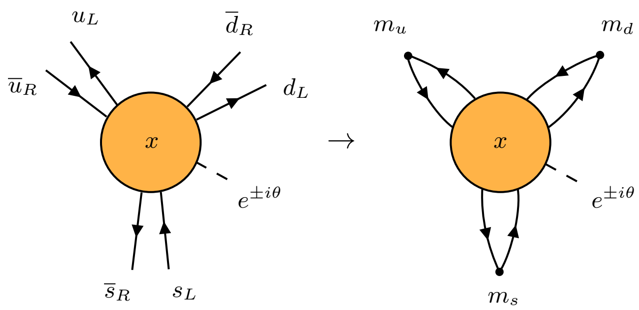

(2.197)

and we have the one-instanton estimate

$$\begin{aligned} & m_u m_d m_s e^{i\theta}\int_{1/M_{\rm UV}}^{1/M_{\rm IR}}\frac{d\rho}{\rho^5}\rho^3 d_3(\rho)\approx m_u m_d m_s e^{i\theta}\left(\frac{8\pi^2}{g^2(M_{\rm IR})}\right)^6 e^{-\frac{8\pi^2}{g^2(M_{\rm IR})}}\int_{1/M_{\rm UV}}^{1/M_{\rm IR}}\frac{d\rho}{\rho^5}\rho^3(M_{\rm IR}\rho)^9 \\ & = e^{i\theta}\left(\frac{8\pi^2}{g^2(M_{\rm IR})}\right)^6 e^{-\frac{8\pi^2}{g^2(M_{\rm IR})}}\frac{m_u m_d m_s M_{\rm IR}}{8}, \end{aligned} \tag{2.198}$$

therefore we have the estimate axion potential in the dilute-gas approximation, up to $\mathcal{O}(1)$ factors

$$V(a) = -2\cos(\frac{a(x)}{f_a}+\theta_{\rm QCD})\times\frac{1}{8}\left(\frac{8\pi^2}{g^2(M_{\rm IR})}\right)^6 e^{-\frac{8\pi^2}{g^2(M_{\rm IR})}} m_u m_d m_s M_{\rm IR}. \tag{2.199}$$

To confirm that closing legs of the 't Hooft operator with mass insertion gives simply masses, i.e. not loops or propagators, we have to do an explicit computation of the one-instanton contribution to $Z(\theta)|_{n=1}$. We have, normalizing to the case with $A_\mu^{\rm cl}=0$

$$Z(\theta)=\sum_n\langle 0|0\rangle_n = \frac{\sum_n\int[\mathcal{D}A]_n[\mathcal{D}\eta][\mathcal{D}\bar\eta][\mathcal{D}\psi][\mathcal{D}\bar\psi]\exp(-S_E)}{\int[\mathcal{D}A][\mathcal{D}\eta][\mathcal{D}\bar\eta][\mathcal{D}\psi][\mathcal{D}\bar\psi]\exp(-S_E)\big|_{A_\mu^{\rm cl}=0}}\,, \tag{2.200}$$

where the Euclidean action is given by (we are now considering massless fermions)

$$S_E = S_{\rm G}+S_\psi\,, \tag{2.201}$$

$$S_{\rm G} = \int d^4x\left[\frac{1}{4}F^a_{\mu\nu}F^a_{\mu\nu} - i\theta\frac{g^2}{32\pi^2}F^a_{\mu\nu}\tilde F^a_{\mu\nu}+\mathcal{L}_{\rm ghost}(\eta,\bar\eta,A)\right]\,, \tag{2.202}$$

$$S_\psi = \sum_f\int d^4x\bar\psi_f(-i\gamma_\mu\mathcal{D}_\mu)\psi_f\,. \tag{2.203}$$

Focusing on the one-instanton sector (see [38, 43] or [46, 47] for a more recent discussion) and expanding as usual around the instanton solution

$$A^a_\mu = A_\mu^{\rm instanton,a}+a^a_\mu\,, \tag{2.204}$$

we get, at the quadratic order in the quantum fields

$$S_E = S_0+\int d^4x\left[\frac{1}{2}a_\mu M_{\rm G}^{\mu\nu}a_\nu+\bar\eta M_{\rm ghost}\eta+\bar\psi_f M_\psi^{ff'}\psi_{f'}\right],\quad S_0\equiv S[A_\mu^{\rm inst}]=\frac{8\pi^2}{g^2}-i\theta\,, \tag{2.205}$$

therefore, treating the fermion mass term as an interaction

$$W_{SU(N_c)}\equiv Z(\theta)|_{n=1}=\langle 0|0\rangle_1 = \frac{\sum_n\int[\mathcal{D}A]_n[\mathcal{D}\eta][\mathcal{D}\bar\eta][\mathcal{D}\psi][\mathcal{D}\bar\psi]\exp(-S_E)}{\int[\mathcal{D}A][\mathcal{D}\eta][\mathcal{D}\bar\eta][\mathcal{D}\psi][\mathcal{D}\bar\psi]\exp(-S_E)\big|_{A_\mu^{\rm cl}=0}}. \tag{2.206}$$

Reassembling what we have done so far, the gauge sector gives

$$\int\prod_{i=1}^{4N_c}d\gamma_i J(\gamma)e^{-S_0}I_\psi(\gamma)\left.\frac{(\det'{\rm M_G})^{-1/2}\det'{\rm M_{ghost}}}{[\det(M_G)^{-1/2}\det(M_{\rm ghost})]\big|_{A_\mu^{\rm cl}=0}}\right|_{\rm regulated}\,, \tag{2.207}$$

where γ_i, $i=1,\ldots,4N_c$ are the collective coordinates of the BPST instanton, namely

$$\gamma_i = \begin{cases}(x_0)_i & i=1,\ldots,4\\ \rho & i=5,\\ T^a & T^a\in SU(N_c)/\mathcal{T},\quad \text{where } \mathcal{T} \text{ is the little group of the BPST instanton,}\end{cases} \tag{2.208}$$

and the integration over corresponding eigenmodes must be considered separately: it must be replaced by an integration over the collective coordinates including an appropriate Jacobian $J(\gamma)$ for this transformation. $I_\psi(\gamma)$ encodes the contribution from fermion sector (depending on the instanton collective coordinates). We get, in PV regularization

$$C_{N_c}\left(\frac{8\pi^2}{g^2}\right)^{2N_c}\int d^4x_0\int\frac{d\rho}{\rho^5}e^{-\frac{8\pi^2}{g_0^2}+\log(M\rho)\frac{11}{3}N_c}e^{i\theta}I_\psi(\gamma). \tag{2.209}$$

Analogously to the bosonic contributions to vacuum-vacuum amplitude, we can isolate the fermionic zero-modes in the integration over the fermionic fields, obtaining

$$I_\psi(\gamma)=\int\prod_f\rho^{1/2}da_f^{(0)}\prod_{f'}\rho^{1/2}d\bar{b}_{f'}^{(0)}\int[\mathcal{D}'\psi][\mathcal{D}'\bar{\psi}]\exp-\int d^4x\bar{\psi}_fM_\psi^{ff'}\psi_{f'}, \tag{2.210}$$

where $M_\psi^{ff'}=-i\gamma_\mu\mathcal{D}_\mu\delta_{ff'}$. Furthermore we used the fact that the Grassmann integration measures have mass dimension $[da_f^{(0)}]=[d\bar{b}_f^{(0)}]=1/2$, indeed from (2.129), $[\phi_0]=+2$, but

$$\psi_f(x)=\sum_n a_f^{(n)}\phi_n(x)\Rightarrow[a_f^{(n)}]=-1/2, \tag{2.211}$$

finally

$$\int da_f^{(n)}a_f^{(n)}=1\Rightarrow[da_f^{(n)}]=+1/2, \tag{2.212}$$

and since $I_\psi(\gamma)$ is dimensionless, we have to insert a factor $\rho^{1/2}$ per each fermion zero-mode.
For chiral fermions in the fundamental representation we have only one zero mode with positive chirality for each flavor, yielding

$$\begin{aligned}I_\psi(\gamma)&=\int\prod_{f=1}^{N_f}\rho^{1/2}da_f^{(0)}\prod_{f'=1}^{N_f}\rho^{1/2}d\bar{b}_{f'}^{(0)}\int[\mathcal{D}'\psi][\mathcal{D}'\bar{\psi}]\exp-\int d^4x\bar{\psi}_fM_\psi^{ff'}\psi_{f'}\\&=\int\prod_{f=1}^{N_f}\rho^{1/2}da_f^{(0)}\prod_{f'=1}^{N_f}\rho^{1/2}d\bar{b}_{f'}^{(0)}\left.\frac{\det'\mathrm{M}_\psi}{\det M_\psi|_{A_\mu^{\mathrm{cl}}=0}}\right|_{\text{regulated}}=\rho^{N_f}e^{-\frac{2}{3}\log(M\rho)}\int\prod_{f=1}^{N_f}da_f^{(0)}d\bar{b}_f^{(0)},\end{aligned} \tag{2.213}$$

therefore, in absence of interactions among fermions, considering instanton contributions within an energy-range $[M_{\mathrm{IR}},M_{\mathrm{UV}}]$ which is well above the strong coupling scale Λ_{N_c} defined as

$$\Lambda_{N_c}^{b_0}=\rho^{-b_0}e^{-\frac{8\pi^2}{g^2(1/\rho)}},\quad b_0\equiv-\beta_0. \tag{2.214}$$

This restriction ensures that instanton effects are calculable even when those are IR dominated, since the coupling $g(\mu)$ is still perturbative. Therefore

Vacuum-to-vacuum amplitude

$$W_{SU(N_c)}=C_{N_c}\left(\frac{8\pi^2}{g^2}\right)^{2N_c}e^{i\theta}\int d^4x_0\int_{1/M_{\mathrm{UV}}}^{1/M_{\mathrm{IR}}}\frac{d\rho}{\rho^5}(\rho\Lambda_{N_c})^{b_0}\rho^{N_f}\int\prod_{f=1}^{N_f}da_f^{(0)}d\bar{b}_f^{(0)}. \tag{2.215}$$

If we have a mass interaction, i.e. a *relevant* coupling

$$-S_\psi^{\mathrm{int}}=\sum_{f=1}^{N_f}\int d^4x\bar{\psi}_f(x)im_f\psi_f(x), \tag{2.216}$$

since the integral over zero modes projects onto the zero mode wavefunction of fermion field, i.e. writing $\psi_f(x) = \sum_n a_f^{(n)}\phi_n(x)$, then, for instance

$$\int da_f^{(0)}\psi_f(x) = \phi_0(x),$$

the integral over zero modes yields

$$\begin{aligned}\int \prod_{f=1}^{N_f} da_f^{(0)} d\bar{b}_f^{(0)} e^{i\int d^4x \bar{\psi}_f(x) m_f \psi_f(x)} &= \frac{i^{N_f}}{N_f!}\prod_{f=1}^{N_f} m_f N_f! \int d^4x_f \int da_f^{(0)} d\bar{b}_f^{(0)} \bar{\psi}_f \psi_f(x_f) \\ &= i^{N_f}\prod_{f=1}^{N_f} m_f \underbrace{\int d^4x_f \phi_0^\dagger(x_f)\phi_0(x_f)}_{=1} \end{aligned} \tag{2.217}$$

therefore the mass interactions gives the one-instanton contribution to the vacuum functional

$$\boxed{\begin{aligned} W_{SU(N_c)} &= C_{N_c}\left(\frac{8\pi^2}{g^2}\right)^{2N_c} e^{i\theta}\int d^4x_0 \int_{1/M_{\rm UV}}^{1/M_{\rm IR}} \frac{d\rho}{\rho^5}(\rho\Lambda_{N_c})^{b_0}\rho^{N_f} i_f^N \prod_{f=1}^{N_f} m_f \\ &= V_4 C_{N_c}\left(\frac{8\pi^2}{g^2}\right)^{2N_c} i_f^N \prod_{f=1}^{N_f} m_f e^{i\theta}\int_{1/M_{\rm UV}}^{1/M_{\rm IR}} \frac{d\rho}{\rho^5}(\rho\Lambda_{N_c})^{b_0}\rho^{N_f}. \end{aligned}} \tag{2.218}$$

That is, with a full instanton calculus, we re-obtained - up to $\mathcal{O}(1)$ factors - the result given by closing the fermion legs of the 't Hooft operator with all the available interactions.
Up to now, we had been considering chiral fermions in the fundamental representation of the gauge group $SU(N_c)$.
What happens if other couplings are present? Let us assume that the theory contains a neutral scalar ϕ with Yukawa couplings to the fermions [45], that is the *marginal* coupling

$$-S_\psi^{\rm int} = i\sum_f \int d^4x\, y_n \varphi(x)\bar{\psi}_f(x)\psi_f(x), \tag{2.219}$$

where $\varphi(x)$ is some neutral scalar field. In this case, we may also close up the fermion legs of the 't Hooft operator with $\frac{1}{2}N_f$ loops of scalars, that is

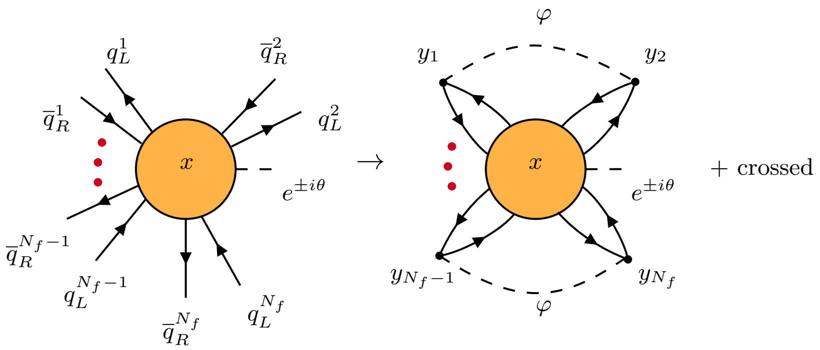

(2.220)

how do these diagrams contribute to the vacuum energy-density? The vacuum-to-vacuum, amplitude

(2.215) is

$$W_{SU(N_c)} = C_{N_c}\left(\frac{8\pi^2}{g^2}\right)^{2N_c} e^{i\theta}\int d^4x_0\int_{1/M_{\rm UV}}^{1/M_{\rm IR}}\frac{d\rho}{\rho^5}(\rho\Lambda_{N_c})^{b_0}\int[\mathcal{D}\varphi]e^{-S_0(\varphi)}\times$$
$$\times\int\prod_{f=1}^{N_f}\rho da_f^{(0)}d\bar{b}_f^{(0)}e^{i\int d^4x\sum_f y_f\varphi(x)\bar{\psi}_f(x)\psi_f(x)}\,. \tag{2.221}$$

We now focus on the integration over the zero modes

$$\begin{aligned}&\rho^{N_f}\int\prod_{f=1}^{N_f}da_f^{(0)}d\bar{b}_f^{(0)}\exp(i\int d^4x\sum_f y_f\varphi(x)\bar{\psi}_f(x)\psi_f(x))\\ &=i^{N_f}\rho^{N_f}\prod_{f=1}^{N_f}y_f\int d^4x_f\varphi(x_f)\phi_0^\dagger(x_f)\phi_0(x_f).\end{aligned} \tag{2.222}$$

Taking for simplicity $N_f = 2$

$$W_{SU(N_c)} = -\,C_{N_c}\left(\frac{8\pi^2}{g^2}\right)^{2N_c} e^{i\theta}\int d^4x_0\int_{1/M_{\rm UV}}^{1/M_{\rm IR}}\frac{d\rho}{\rho^5}(\rho\Lambda_{N_c})^{b_0}\int[\mathcal{D}\varphi]\times$$
$$\times\, e^{-S_0(\varphi)}y_1y_2\rho^2\int d^4x_1\int d^4x_2\varphi(x_1)\phi_0^\dagger(x_1)\phi_0(x_1)\varphi(x_2)\phi_0^\dagger(x_2)\phi_0(x_2), \tag{2.223}$$

where $S_0(\varphi)$ is the kinetic term of the φ field and the integration over φ gives the scalar propagator $\Delta_F(x_1 - x_2)$. Therefore for each loop we must evaluate the loop integral

$$\begin{aligned}I &= y_1y_2\rho^2\int d^4x_1d^4x_2\phi_0^\dagger(x_1)\phi_0(x_1)\Delta_F(x_1-x_2)\phi_0^\dagger(x_2)\phi_0(x_2)\\ &= y_1y_2\rho^2\int\frac{d^4k}{(2\pi)^4}d^4x_1d^4x_2\frac{2\rho^2}{\pi^2}\frac{1}{(x_1^2+\rho^2)^3}\frac{e^{-ik\cdot(x_1-x_2)}}{(k^2+m_s^2)}\frac{2\rho^2}{\pi^2}\frac{1}{(x_2^2+\rho^2)^3}\\ &= y_1y_2\rho^2\left(\frac{2\rho^2}{\pi^2}\right)^2\int\frac{d^4k}{(2\pi)^4}\frac{1}{(k^2+m_s^2)}\frac{d^4x_1e^{-ik\cdot x_1}}{(x_1^2+\rho^2)^3}\frac{d^4x_2e^{ik\cdot x_2}}{(x_2^2+\rho^2)^3}\,,\end{aligned} \tag{2.224}$$

where we used the explicit expression for (2.129). Using the result

$$\int d^4x\frac{e^{-ik\cdot x}}{(x^2+\rho^2)^3} = \frac{\pi^2}{2\rho^2}|k|\rho K_1\left(|k|\rho\right), \tag{2.225}$$

where $K_1(z)$ is a modified Bessel function, we obtain

$$I = y_1y_2\rho^2\int\frac{d^4k}{(2\pi)^4}\frac{(\rho|k|)^2}{k^2+m_s^2}\left(K_1\left(|k|\rho\right)\right)^2 = y_1y_2\frac{\rho^4}{8\pi^2}\int_0^\infty dk\,\frac{k^5}{k^2+m_s^2}\left(K_1\left(k\rho\right)\right)^2, \tag{2.226}$$

and that - from the behavior of $K_1(z)$ - the loop integral is cut-off at $|k|\sim\rho^{-1}$. Therefore we get, using $|k|\sim\rho^{-1}$,

$$I = \begin{cases}\frac{y_1y_2}{5\pi^2}\frac{1}{\rho^2m_s^2}, & \rho m_s\gg 1,\\ \frac{y_1y_2}{12\pi^2}, & \rho m_s\ll 1.\end{cases} \tag{2.227}$$

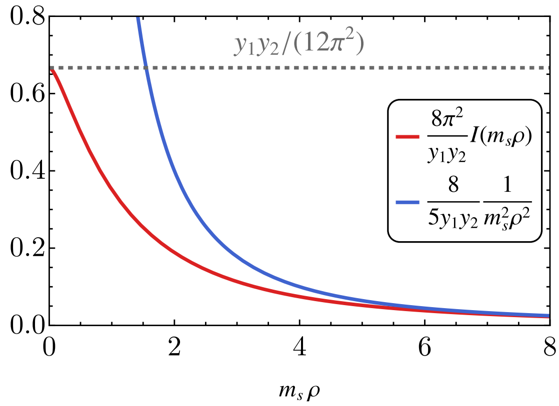

Figure 2.2: *Numerical evaluation of the Yukawa loop integral* $I(m_s\rho)$ *defined in* (2.224).

Then, if $\rho m_s \ll 1$, i.e. at energies for which the scalar $\varphi(x)$ may propagate freely, we have to multiply (2.215) for

$$\frac{y_{N_i}y_{N_j}}{12\pi^2} \tag{2.228}$$

for each loop. If $N_f = 2$, we get the vacuum amplitude

$$W_{SU(N_c)} = -V_4 C_{N_c}\left(\frac{8\pi^2}{g^2}\right)^{2N_c} e^{i\theta}\,\frac{y_1y_2}{12\pi^2}\int_{1/M_{\rm UV}}^{1/M_{\rm IR}}\frac{d\rho}{\rho^5}(\rho\Lambda_{N_c})^{b_0}\,. \tag{2.229}$$

The coupligs used to close the legs of the 't Hooft operator do not have to be masses or marginal couplings, but can also be higher-dimensional eeffective operators. For instance, we may take a four-fermion operator of the form

$$-S_\psi^{\rm int} = \frac{c_F}{\Lambda_F^2}\int d^4x\,\bar\psi_i(x)\psi_i(x)\bar\psi_{i+1}(x)\psi_{i+1}(x),\; i=1,\ldots,N_f-1, \tag{2.230}$$

tying-up the fermion legs with this effective vertex we get

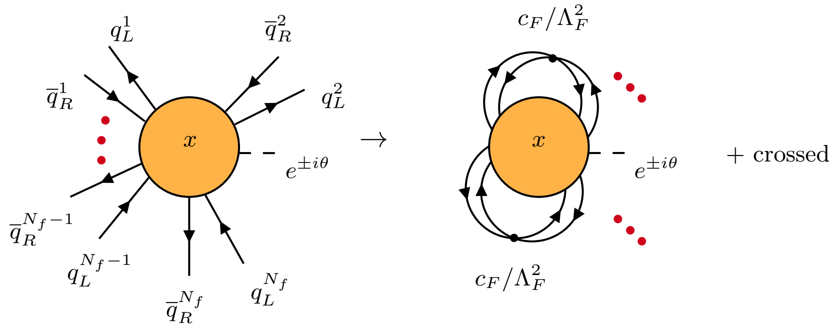

(2.231)

Again, to compute the contribution of this effective vertex, we have to compute the vacuum-to-vacuum amplitude, using the explicit expression for (2.129)

$$\begin{aligned}
W_{SU(N_c)} &= C_{N_c}\left(\frac{8\pi^2}{g^2}\right)^{2N_c} e^{i\theta}\int d^4x_0 \int_{1/M_{\rm UV}}^{1/M_{\rm IR}} \frac{d\rho}{\rho^5}(\rho\Lambda_{N_c})^{b_0}\rho^{N_f}\int\prod_{f=1}^{N_f} da_f^{(0)}d\bar{b}_f^{(0)}e^{-S_\psi^{\rm int}}\\
&= C_{N_c}\left(\frac{8\pi^2}{g^2}\right)^{2N_c} e^{i\theta}\int d^4x_0 \int_{1/M_{\rm UV}}^{1/M_{\rm IR}} \frac{d\rho}{\rho^5}(\rho\Lambda_{N_c})^{b_0}\rho^{N_f}\left(\frac{4\rho^4}{\pi^4}\int\frac{d^4x}{(x^2+\rho^2)^6}\right)^{N_f/2}\left(\frac{c_F}{\Lambda_F^2}\right)^{N_f/2}\\
&= C_{N_c}\left(\frac{8\pi^2}{g^2}\right)^{2N_c} e^{i\theta}\int d^4x_0 \int_{1/M_{\rm UV}}^{1/M_{\rm IR}} \frac{d\rho}{\rho^5}(\rho\Lambda_{N_c})^{b_0}\rho^{-N_f}\left(\frac{c_F}{5\pi^2\Lambda_F^2}\right)^{N_f/2}\\
&= V_4 C_{N_c}\left(\frac{8\pi^2}{g^2}\right)^{2N_c} e^{i\theta}\left(\frac{c_F}{5\pi^2\Lambda_F^2}\right)^{N_f/2}\int_{1/M_{\rm UV}}^{1/M_{\rm IR}} \frac{d\rho}{\rho^{5+N_f}}(\rho\Lambda_{N_c})^{b_0},
\end{aligned}\tag{2.232}$$

that is, we get the vacuum amplitude

$$\boxed{W_{SU(N_c)} = V_4 C_{N_c}\left(\frac{8\pi^2}{g^2}\right)^{2N_c} e^{i\theta}\left(\frac{c_F}{5\pi^2\Lambda_F^2}\right)^{N_f/2}\int_{1/M_{\rm UV}}^{1/M_{\rm IR}} \frac{d\rho}{\rho^{5+N_f}}(\rho\Lambda_{N_c})^{b_0}.}\tag{2.233}$$

We notice furthermore that (2.233) is consistent with (2.229). Indeed, for $1/\rho \ll m_s$, (2.229) becomes for $N_f = 2$

$$W_{SU(N_c)} = V_4 C_{N_c}\left(\frac{8\pi^2}{g^2}\right)^{2N_c} e^{i\theta}\frac{y_1y_2}{5\pi^2 m_s^2}\int_{1/M_{\rm UV}}^{1/M_{\rm IR}} \frac{d\rho}{\rho^{5+2}}(\rho\Lambda_{N_c})^{b_0}\,,\tag{2.234}$$

consistently with the fact that, at energies $E \ll m_s$, we can integrate out the scalar $\varphi(x)$ obtaining an effective operator of the form

$$\mathcal{O}^F_{1,2}(x) = \frac{y_1y_2}{m_s^2}\bar{\psi}_1(x)\psi_1(x)\bar{\psi}_2(x)\psi_2(x).\tag{2.235}$$

For the following, it is useful to derive a rule for computing the QCD instanton contribution - up to $\mathcal{O}(1)$ factors to the low-energy axion potential. To compute the vacuum energy (2.206) in the presence of interactions, we have to do a perturbative expansion in the couplings up to an order that is enough to provide one fermion field for each fermion zero mode. All additional fields that appear in the interactions only survive the path integral if they can be fully Wick-contracted, yielding propagators. Up to $\mathcal{O}(1)$ factors, these yield the following factors of π

$$\text{zero}-\text{mode} \propto \frac{1}{\pi}\,,\ \text{vertex} \propto \pi^2\,,\ \text{propagator } \Delta_{\rm F} \propto \frac{1}{\pi^2}\,,\tag{2.236}$$

where we used the explicit expression for a fermionic zero-mode (2.129), that a vertex involves a space-time integration $\int d^4x \propto \pi^2\int dx\,x^3$ and that a Feynman propagator involves an integral over four-momenta $\int\frac{d^4p}{(2\pi)^4} \propto \frac{1}{\pi^2}\int dp\,p^3$. Writing this in powers of 4π, we get the rule

$$\text{add a factor of } (4\pi)^{-\alpha},\ \alpha = \#\text{ of zero-modes - }2(\#\text{ of vertices}) + 2(\#\text{ of propagators})\,.\tag{2.237}$$

We thus have shown the following rules in instanton calculus (or instanton NDA, see Ref. [47])

- Identify the 't Hooft operator, containing one leg for each fermionic zero-mode. The number of zero modes for each fermion is given by $2k$, where k is the Dynkin index of the representation under the gauge group.

- Treat the 't Hooft operator as a $2k$-point vertex in a Feynman diagram and close the fermion legs using any available coupling. Particles with mass $m < 1/\rho$ propagate freely, and can appear in loops, those of mass $m > 1/\rho$ should be integrated out, and the resulting effective operators can be used to close fermion legs.
- Combine the couplings used to close the 't Hooft operator with the instanton density and the integral over the instanton size, which corresponds to an overall factor

$$C_N \left(\frac{8\pi^2}{g_2^2}\right)^{2N} \int \frac{d\rho}{\rho^5} \left(\Lambda_G \rho\right)^{b_0} \,, \tag{2.238}$$

  and add appropriate powers of ρ, the only available dimensionful parameter to get the right dimensions (*i.e.* those of a potential V). Propagators should not be added to the estimate.
- Add a factor of $(4\pi)^{-\alpha}$, where α is given by

$$\alpha = \#\text{ of zero-modes - } 2(\#\text{ of vertices}) + 2(\#\text{ of propagators})\,. \tag{2.239}$$

CHAPTER

3

The axion quality problem and gravitational instantons

3.1 Gravity and global symmetries

The Peccei-Quinn (PQ) mechanism addressing the strong CP problem faces a significant challenge: it depends on a global $U(1)_{\mathrm{PQ}}$ symmetry spontaneously broken. This symmetry is introduced to dynamically solve the strong CP problem by promoting the CP-violating θ-parameter in QCD to a dynamical field, the axion, which adjusts itself to cancel the CP violation. Although this symmetry is broken at low energies by the QCD anomaly, it must remain an exceptionally precise symmetry at high-energy scales. This issue is commonly referred to as the PQ quality problem. This fact seems to contradict the modern effective field theory understanding that global symmetries are not fundamental but rather emerge as accidental symmetries, namely symmetries of the renormalizable Lagrangian whose violation occurs through irrelevant operators.

This conceptual problem is further exacerbated by the widely held belief that gravity explicitly breaks global symmetries. If true, this would imply that any global symmetry present in a low-energy effective theory would be violated by gravitational interactions, potentially undermining the robustness of such symmetries at high-energy scales.In the aforementioned context, the quality problem can be readily quantified as follows. If Planck-scale physics is the sole source of PQ-violating effects, then at energies below the Planck scale, the effect of gravitational interactions is encoded by the effective operator in the axion Lagrangian [48]

$$\frac{1}{\sqrt{-g}}\mathcal{O}_g(x) = \sum_{n\geq 5} \frac{\lambda^2}{M_{\mathrm{Pl}}^{n-4}}\Phi^n(x) + \mathrm{h.c.} + \mathrm{c}, \tag{3.1}$$

where $\Phi(x) = f_a e^{ia/f_a}$, f_a is the scale at which the $U(1)_{\mathrm{PQ}}$ symmetry gets spontaneously broken, $\lambda = |\lambda|\exp(i\delta)$ is a dimensionless complex coupling and c is a constant chosen so that the minimum of the potential is zero. The effective operator $\mathcal{O}_g$ then induces the axion effective potential

$$V_g(a) = 2|\lambda|^2 M_{\mathrm{Pl}}^4 \sum_{n\geq 5}\left(\frac{f_a}{M_{\mathrm{Pl}}}\right)^n \left[1-\cos\left(n\frac{a}{f_a}+2\delta\right)\right], \tag{3.2}$$

therefore, for $O(1)$ values of the phase δ and $|\lambda|$, taking $f_a = 10^{12}$ GeV, the $U(1)_{\mathrm{PQ}}$ symmetry must be protected from explicit breaking effects caused by operators with dimensions up to $d \sim 14$, suggesting a highly non-trivial structure in the PQ dynamics. We refer to this situation, where explicit breaking effects are introduced through irrelevant operators whose scaling is determined by naive dimensional

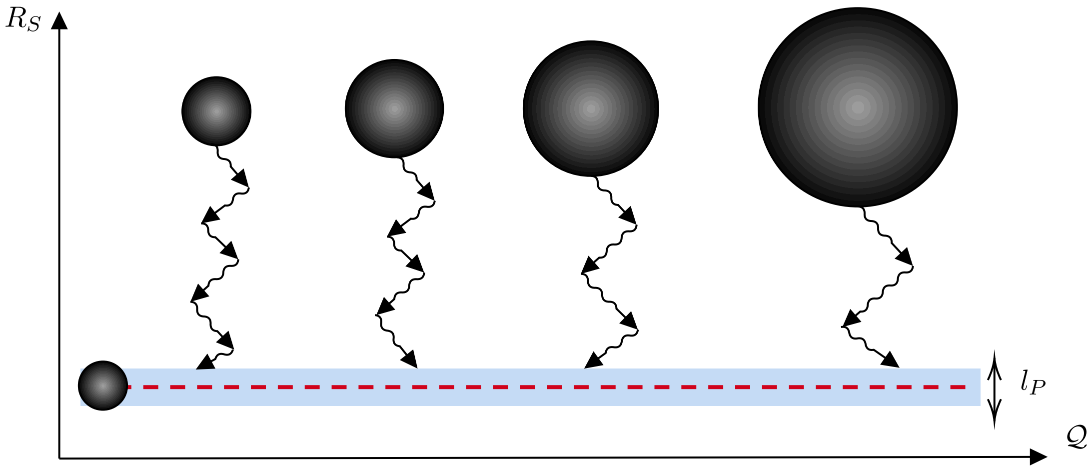

Figure 3.1: *Schematic representation of the Banks-Seiberg argument [49].*

analysis, as a case of perturbative breaking.
This specification is necessary, as it is by no means certain that gravity breaks global symmetries as described above. In fact, gravitational interactions are CP-conserving perturbatively, and the only conceivable source of CP violation is nonperturbative quantum gravity dynamics. Multiple indications indeed suggest that explicit breakings due to gravity have a nonperturbative origin.
Firstly, there are a series of arguments related to black hole physics that are often referred to as folklore theorems [49]. If a continuous global symmetry $\mathcal{G}$ is exactly conserved, a black hole could, in principle, carry a corresponding global charge. Indeed suppose that the lightest particle in the spectrum has positive mass m and transforms in an irreducible representation $\boldsymbol{r}$ of the global group. We can now consider multi-particle states, *i.e.* gas of $\mathcal{G}$-charged particles, transforming under an arbitrary representation $\boldsymbol{\mathcal{R}} \subset \boldsymbol{r} \otimes \boldsymbol{r} \otimes \boldsymbol{r} \otimes \ldots$ of the global symmetry group. By adiabatically shrinking this gas of $\mathcal{G}$-charged particles, it is possible to form Schwarzschild black holes with arbitrarily large global charge $\mathcal{Q}_{\text{global}}$ (see Fig. 3.1). As long as the semiclassical effective field theory of gravity remains valid—up to length scales of the order of $\mathcal{X} l_{\text{Pl}}$, where $\mathcal{X}$ is a order one number and l_{Pl} is the Planck length—these charged black holes will Hawking radiate, thereby losing mass while conserving their global charge $\mathcal{Q}_{\text{global}}$. Thus, if we start with a large black hole of arbitrarily large charge $\mathcal{Q}_{\text{global}}$ and wait enough, we will obtain a stable black hole remnant of charge $\mathcal{Q}_{\text{global}}$ and mass $\mathcal{X} M_{\text{Pl}}$. In this way we can generate an infinite number of macroscopic black hole states that are indistinguishable, *i.e.* with the same size and energy—respectively $\mathcal{X} l_{\text{Pl}}$ and $\mathcal{X} M_{\text{Pl}}$—but differing in their global charges $\mathcal{Q}_{\text{global}}$. Since in conventional statistical mechanics the entropy of a system originates in the counting of states that are macroscopically indistinguishable, these remnants will give an infinite entropy. Equivalently, a spacetime region of linear size of the order of the Planck length has infinite entropy, since it could store an information of the order $\log \mathcal{N}$, where $\mathcal{N} \to \infty$ is the number of Planck remnants. This would conflict with the finite entropy bound of a general spacetime region [50, 51], regardless of the density matrix of its matter content. Intuitively, for the generalized second law (GSL) [52] to hold, the entropy of a general system cannot be arbitrarily large. This is because the growth of the black hole's horizon area depends on the mass added to it [53], regardless of the entropy of the matter system. If systems with arbitrarily large entropy at a given mass and size were possible, the GSL could be violated, implying that the entropy of any general system must be bounded from above. To make this argument sharper, we employ the most general entropy bound applicable to Lorentzian geometries, known as the covariant entropy bound (CEB) [50, 51], which asserts that the entropy on any lightsheet $\mathcal{L}(B)$ [1] of a surface B

[1]A given surface B possesses four orthogonal null directions represented by null hypersurfaces $F_1, \ldots, F_4$ that border on B. Introducing the *expansion scalar*, $\theta(\lambda) \equiv \frac{d\mathcal{A}/d\lambda}{\mathcal{A}}$, where λ is an affine parameter for the light rays generating F_i,

cannot exceed its surface area

$$S[\mathcal{L}(B)] \leq \frac{A[B]}{4\,G_N\hbar}\,. \tag{3.3}$$

However, using the CEB, we can also constraint the entropy of the whole spacetime bulk using a background independent formulation of the holographic principle [54]. For this aim, we perform a null foliation, *i.e.* we slice the spacetime into a 1-parameter family of null hypersurfaces $\mathcal{H}(\tau)$. Next, on each null hypersurface $\mathcal{H}(\tau)$ we locate the two-dimensional spatial surface of maximal surface area $\mathcal{A}_{\max}(\tau)$; unless it lies on the spacetime boundary, this surface divides $\mathcal{H}(\tau)$ into two parts. By construction, this hypersurface of maximal area for a given τ has two lightsheets, implying that

$$S[\mathcal{H}(\tau)] \leq \frac{\mathcal{A}_{\max}(\tau)}{2\,G_N\hbar}\,. \tag{3.4}$$

Repeating this construction for all values of τ, one obtains a 2+1-dimensional hypersurface $\mathcal{A}$, called the *holographic screen* on which the entire spacetime information can be stored holographically, *i.e.* at a density not exceeding one bit for Planck area. Taking a causal diamond $\mathcal{D}$ whose past boundary is a portion of the remnant black hole event horizon, the CEB will imply that, in Planck units

$$S[\mathcal{H}_\diamond(\tau)] \leq \frac{\mathcal{A}_\diamond(\tau)}{2} \simeq O(1)\mathcal{X}^2\,, \tag{3.5}$$

where we introduced the null foliation $\mathcal{H}_\diamond(\tau)$ on $\mathcal{D}$ and $\mathcal{A}_\diamond \supset \mathcal{D}$ is the holographic screen of the causal diamond. Thus, the CEB implies that the information stored in a spacetime region with linear size of the order of $l_{\rm Pl}$ has to be finite, in contradiction with the existence of an infinite number of remnant states. The key point of this argument is that black hole thermodynamics is fundamentally incompatible with continuous global symmetries. This incompatibility lends support to the hypothesis that exact continuous global symmetries are not intrinsic to the frameworks of quantum gravity and black hole physics. Secondly, in the context of string theory, it can be shown that explicit breaking effects of continuous global symmetries are always due to non-perturbative effects, with candidates including worldsheet instantons, brane instantons and gauge instantons [55, 56]. The inability to preserve a global symmetry in string theory can be seen as a consequence of the fact that the effective field theories associated with classical vacua of superstring theories (regardless of whether they are spacetime supersymmetric) lack continuous global symmetries—all continuous symmetries are gauged [57]. Alternatively, in the context of the AdS/CFT correspondence, it can be demonstrated that any global symmetry, whether discrete or continuous, in a bulk quantum gravity theory would be inconsistent with entanglement wedge reconstruction on the CFT side of the correspondence [58].

We now briefly discuss some key aspects of a string-theoretic setup, as certain details will prove important in the continuation of our work. In the perturbative formulation of string theory, the string mass scale M_s and the string coupling g_s are fundamental parameters that govern both the physics of the strings themselves and their interactions. The string mass scale M_s is a measure of the energy at which stringy effects become significant. The string coupling g_s controls the strength of interactions between strings. In the weak-coupling regime, where $g_s \ll 1$, the interactions between strings are rare, and the perturbative expansion in powers of g_s is well-defined. The Planck mass of gravity in four-dimensional spacetime is related to M_s, g_s, and the six-dimensional volume of the compactified extra dimensions V. When six of the original ten dimensions of string theory are compactified, the four-dimensional Planck mass is related to the string scale by [59]

$$M_{\rm Pl}^2 \approx \frac{(VM_s^6)M_s^2}{g_s^2}\,. \tag{3.6}$$

we assume that λ increases in the direction away from B and $\mathcal{A}$ is the infinitesimal area spanned by two neighboring lightrays. If F_i is such that $\theta(\lambda) \leq 0$ everywhere, then F_i is said to be a lightsheet.

In addition to the string mass scale, another important energy scale in compactified string theories is the Kaluza-Klein (KK) mass scale. This scale arises from the compactification of extra dimensions, where the momentum modes of particles propagating in the compact dimensions are quantized due to the compact geometry. The KK mass scale is inversely related to the size R of the compactified dimensions and is typically given by $M_{\mathrm{KK}} \approx R^{-1} \approx V^{-1/6}$ (under the assumption that the compactified dimensions have a common radius R). We thus find

$$g_s M_{\mathrm{Pl}} \approx \left(\frac{M_s}{M_{\mathrm{KK}}}\right)^3 M_s\,. \tag{3.7}$$

It is important to emphasize that the two mass scales M_s (related to the fundamental string tension and controlling the onset of stringy effects—i.e., the energy scale at which the extended nature of strings becomes significant and point-particle approximations break down) and M_{KK} (determined by the size R of the compactified extra dimensions) are generally independent parameters in a string compactification,[2] although they can become comparable under certain conditions. If we consider the case $M_s \approx M_{\mathrm{KK}}$, the string mass scale, the string coupling and the four-dimensional Planck mass are related by

$$g_s M_{\mathrm{Pl}} \approx M_s\,, \tag{3.8}$$

with $M_s \ll M_{\mathrm{Pl}}$ in the weakly coupled regime. Under these circumstances, and based solely on dimensional analysis, the breaking effects due to non-perturbative stringy instantons are expected to contribute to the axion potential as in (3.2), now with $|\lambda|^2 = g_s^2 e^{-C/g_s}$ where $C = O(1)$ is an order 1 constant.

The key aspect is the exponential suppression given by the factor $e^{-S_{\mathrm{E}}} = e^{-C/g_s}$, where S_{E} is the Euclidean action of the string instanton generating the axion potential [60]. Consequently, if string theory is weakly coupled, i.e., if $g_s \ll 1$, all non-perturbative effects, and in particular the explicit symmetry-breaking effects of global symmetries, are exponentially suppressed. In this regard, it is worth emphasizing that there are strong semi-quantitative indications suggesting that quantum gravity is indeed ultraviolet (UV) completed at weak coupling. *i)* Imagine N species of quantum fields, with masses at the scale M, coupled to gravity. In this case, both perturbative renormalization arguments [61, 62] and non-perturbative black hole considerations [63, 64] suggest that in the presence of N-species the effective contribution to the Planck mass is parametrically given by $(N/16\pi^2)M^2 \approx M_{\mathrm{Pl}}^2$ which would imply $g_s \approx 4\pi/\sqrt{N}$. Consequently, the presence of a large number of particle species, $N \gg 1$, lowers the gravitational cutoff parametrically below the Planck mass. *ii)* In the Standard Model, flavor symmetries are approximate global symmetries explicitly broken by the Yukawa couplings. From the perspective of the UV theory, the smallness of certain Yukawa couplings appears to be compatible with the exponential suppression associated with the presence of weak coupling. *iii)* Inflation is a theoretical phase of rapid exponential expansion in the early universe, proposed to resolve issues like the horizon, flatness, and monopole problems. It is driven by the potential energy of a scalar field, the inflaton, which causes space to expand dramatically over a very short time. This expansion amplifies quantum fluctuations, stretching them to macroscopic scales and seeding the anisotropies observed in the cosmic microwave background (CMB). The energy scale of inflation is characterized by the Hubble parameter H, typically around $H = O(10^{13})$ GeV, though it varies with different inflationary models. The amplitude of the scalar power spectrum, which describes the density fluctuations in the early universe, is related to H; specifically, the larger H, the larger the predicted amplitude of these primordial fluctuations. The observed amplitude of the scalar power spectrum, $A_s \simeq 2.1 \times 10^{-9}$, provides constraints on the inflationary energy scale and potential. In string theory, the inflaton field can emerge from various

[2] For example, in large extra dimension scenarios, M_{KK} can be much smaller than M_s, allowing KK modes to become observable at lower energies.

configurations, such as the distance between branes or compactification moduli [65]. Most models of inflation in string theory are formulated under the condition $H \ll M_s \approx M_{\rm KK} \ll M_{\rm Pl}$, with the inflaton mass, m_ϕ, parametrically given by $m_\phi \approx \sqrt{\eta_V} H$, where $\eta_V = M_{\rm Pl}^2 V''(\phi)/V(\phi)$, with $V(\phi)$ being the inflaton potential. For slow-roll inflation to occur, the potential must be relatively flat, which means that the inflaton mass is typically smaller than or comparable to the Hubble scale, $\eta_V \ll 1$. Under these assumptions, the inflaton is the only light field, while the others have masses far above the Hubble scale; the heavy fields can then be integrated out, leaving a model of single-field inflation. Describing the dynamics of the inflaton within the context of an effective theory featuring only a single mass scale, M_s, and a fundamental coupling, g_s, leads to the result that the amplitude of the scalar power spectrum is intrinsically tied to the coupling g_s^2. This is a consequence of dimensional analysis. In the slow-roll approximation, we write $A_s = H^2/8\pi^2\epsilon \bar{M}_{\rm Pl}^2$, where ϵ is the first slow-roll parameter and $\bar{M}_{\rm Pl}$ the reduced Planck mass. The ratio $H^2/\bar{M}_{\rm Pl}^2$ has dimensions of a coupling squared, and the only possibility—given the assumptions under which we are working—is that $A_s \propto g_s^2$. Consequently, the measurement of A_s implies that the string coupling is in the weak regime. Throughout this work, we will assume that the UV completion of gravity is a string theory in the perturbative regime of weak coupling.

3.1.1 Symmetry breaking due to Euclidean wormholes

Finally, it has been conjectured that global symmetries are violated by Euclidean wormholes in the quantum gravity path integral [66–70]. If this claim were true, the breaking effect due to wormholes could pose a threat to the axion solution of the strong CP problem; it is indeed known that the scalar action describing the spontaneous breaking of a $U(1)$ symmetry admits wormhole solutions (dubbed Euclidean axion wormholes), whose explicit symmetry-breaking effects become particularly significant when the radial degree of freedom of the complex scalar field is treated as dynamic [68, 69, 71]. However, there are some very fundamental conceptual issues with Euclidean wormholes, cf. ref. [72] for a recent review. Specifically, it is not yet clear whether Euclidean wormholes actually contribute to the path integral. It is indeed crucial to ensure that the wormhole solutions are stable to small perturbations of their topology, an analysis which so far has not led to definitive conclusions. See, for example, the discussion in ref. [73], where it is concluded that wormholes are not relevant saddle points of the functional integral in quantum gravity.

Throughout this work, we will not take into account the presence of Euclidean wormholes, assuming that they do not contribute to the quantum gravity path integral.

3.1.2 Gravitational instantons

Given these premises, the perspective we choose to consider in this work is as follows. Let us first return to the case of QCD. Yang-Mills instanton solutions—non-perturbative solutions to the Yang-Mills equations that describe tunneling between different vacua of QCD with different topological charges [34, 40]—are essential for the axion solution to the strong CP problem since they provide the non-perturbative dynamics that generate the axion potential, allowing the axion field to dynamically cancel the θ-term and restore CP symmetry in QCD.

Remarkably, Einstein's theory of gravitation, in its Euclidean formulation, admits non-perturbative solutions, dubbed gravitational instantons, that strongly resemble the Yang-Mills instantons [74, 75]. Consequently, it is reasonable to expect that these gravitational instantons are the most likely candidates to play a significant role when considering gravitational effects in the context of the axionic solution to the strong CP problem. These solutions, in fact, persist even under the assumption that string theory is weakly coupled (see Eq. (3.8)) or when neglecting the effects of wormholes (cf. section 3.1.1), and, as we will demonstrate, provide a calculable contribution to the axion potential in the controlled setup of semi-classical gravity.

Let us try to clarify more precisely what a gravitational instanton actually is (cf. ref. [76] for a comprehensive discussion). In the fields of mathematical physics and differential geometry, a gravitational instanton refers to a non-singular, geodesically complete, four-dimensional Riemannian manifold that solves the vacuum Einstein equations $R_{\mu\nu} = 0$ (without a cosmological constant, also known as Ricci-flat metrics). These manifolds are called gravitational instantons due to their role as analogues to instantons from Yang–Mills theory, but in the realm of quantum gravity. Similar to self-dual Yang–Mills instantons, gravitational instantons are typically expected to behave like four-dimensional Euclidean space at large distances and possess a self-dual Riemann tensor. A self-dual Riemann tensor verifies the condition $R_{\mu\nu\rho\sigma} = \tilde{R}_{\mu\nu\rho\sigma}$ with $\tilde{R}_{\mu\nu\rho\sigma} = \epsilon_{\mu\nu}{}^{\alpha\beta} R_{\alpha\beta\rho\sigma}/2$ and $\epsilon_{\mu\nu\alpha\beta} = \sqrt{g}\varepsilon_{\mu\nu\alpha\beta}$ the totally antisymmetric Levi-Civita tensor (with $\epsilon^{\mu\nu\alpha\beta} = \varepsilon^{\mu\nu\alpha\beta}/\sqrt{g}$). We remark that this condition automatically guarantees the vanishing of the Ricci tensor, $R_{\mu\nu} = 0$. In addition, we focus on solutions that have the interesting property of approaching a flat metric at infinity. Since the Yang-Mills instanton potential approaches a pure gauge configuration at infinity, this class of Einstein solutions closely resembles the Yang-Mills case. Ricci-flat, self-dual metrics approaching a flat metric at infinity exhibit several notable characteristics. Firstly, they typically possess zero action, which highlights their importance in the path integral approach to quantum gravity.[3] Additionally, as these metrics tend toward flatness and effectively eliminate gravitational interactions at infinity, one can employ standard asymptotic-state techniques to investigate quantum effects. On the contrary, self-dual metrics that are regular and have finite action, but are not asymptotically flat, are characterized by a gravitational field that persists throughout spacetime, making it difficult to define the asymptotic plane-wave states necessary for ordinary scattering theory.

There are no non-trivial gravitational instantons that are truly asymptotically Euclidean [79, 80].[4] However, there are two important classes of gravitational instantons that approach flat space at infinity in a specific manner.

- Asymptotically locally Euclidean (ALE) metrics. These solutions are called ALE metrics because, despite their local flatness at large distances, their global topology at infinity differs from that of ordinary Euclidean space. More specifically, ALE metrics are asymptotically flat, but the boundaries are three-spheres with points identified under the action of some discrete group, namely $(S^3/\Gamma) \times \mathbb{R}$ where Γ is a finite group of isometries acting freely on S^3.

  Notable examples include the Eguchi-Hanson (EH) metric [82] and the Gibbons-Hawking multi-center metric in special configurations in which the centers are arranged symmetrically [83].

- Asymptotically locally flat (ALF) metrics. ALF spaces also approach flat space at infinity, but their asymptotic structure is more complicated. In ALF spaces, the geometry at infinity resembles a flat space with a circle fibration.

  Notable examples include the Taub-NUT space [84, 85], where the metric asymptotically approaches $\mathbb{R}^3 \times S^1$, and the Gibbons-Hawking multi-center metric in generic configurations.

In general, Ricci-flat ALE metrics—such as the EH metric—exhibit zero action, while Ricci-flat ALF metrics—such as the Taub-NUT metric (cf. ref. [75])—possess finite non-zero action due to their more complex asymptotic structure, which introduces a non-zero contribution from the boundary

[3] The Euclidean Einstein-Hilbert action is given by

$$S = \underbrace{\frac{1}{16\pi G_N}\int d^4x\sqrt{g}\,R}_{\equiv S_{\text{bulk}}} + S_{\text{boundary}}\,, \tag{3.9}$$

where R is the Ricci scalar, g is the determinant of the metric, and S_{boundary} represents the boundary contribution given by the Gibbons-Hawking-York boundary term [77, 78]. Ricci-flat gravitational instantons have $R = 0$, and the bulk part of the action vanishes. However, it is possible to get a non-vanishing contribution from the boundary term.

[4] More precisely, if the manifold has the topology of Euclidean space at infinity, that is, $S^3 \times \mathbb{R}$, and approaches the flat Euclidean metric sufficiently fast, then every self-dual solution is isometric to Euclidean space, cf. ref. [81].

term. In a semiclassical approach to quantum gravity, therefore, ALE instantons are often considered more relevant than ALF instantons due to their zero action. For this reason, we will focus on ALE gravitational instantons for the remainder of this work (we will provide a more detailed justification in section 3.2.2). Topologically speaking, there are three invariants of utmost importance: the Euler characteristic χ, the Hirzebruch signature τ, and the spin-$\frac{1}{2}$ index $I_{\frac{1}{2}}$. These three invariants are central in characterizing the properties of smooth manifolds and can be thought of as the gravitational analogs of the Yang-Mills topological invariants [86–88]. Gravitational instantons have been classified based on their topological properties in refs. [75, 76]. Gravitational instantons with non-zero spin-$\frac{1}{2}$ index are those that support non-trivial solutions to the massless Dirac equation for spin-$\frac{1}{2}$ fermions (called fermionic zero modes) in the background of the gravitational instanton. In this regard, there is once again a strong parallelism between gravity and Yang-Mills theories. In Yang-Mills theory, fermions couple to gauge fields, and their dynamics are governed by the Dirac equation in the background of the gauge field. For a given instanton solution of the Yang-Mills equations, the Dirac operator in that background may have zero modes-solutions to the Dirac equation with zero eigenvalue. These zero modes are essential because instantons induce processes that can violate chiral symmetry in theories with massless fermions. Therefore, we are particularly interested in gravitational instantons that possess a non-zero spin-$\frac{1}{2}$ index. However, most of the known gravitational instantons have a vanishing spin-$\frac{1}{2}$ index [76]. The only relevant exception is the gravitational instanton known as K3. The K3 surface is the only compact regular simply-connected manifold without boundary which admits a nontrivial metric with self-dual curvature. The spin-$\frac{1}{2}$ index is $I_{\frac{1}{2}}(\mathrm{K3}) = +2$. However, as just mentioned, K3 has no boundaries and does not approach a flat space at infinity. It is still possible to take K3-type gravitational instantons into account through a procedure that involves cutting out a 4-dimensional ball and gluing K3 into flat spacetime via a wormhole-type throat [89]. The downside is that K3 transitions from having a vanishing action to a Planckian action of the form $S_\mathrm{E} \sim \rho^2 M_\mathrm{Pl}^2$ [89], where ρ is the typical size of the wormhole throat, and its contribution to the gravitational path integral becomes automatically suppressed. For this reason, we will not further analyze this possibility in this work.[5]

However, there exists a second, natural possibility: one can seek and construct a combined solution to the Maxwell-Einstein equations in the presence of the gravitational instanton metric. Remarkably, introducing a gravitational instanton that also solves the Maxwell equations can lead to significant changes in the spin-$\frac{1}{2}$ index, often resulting in non-vanishing contributions due to the interplay between fermions and the electromagnetic field in the modified spacetime. In particular, this is the case for the ALE EH gravitational instanton [82]. The latter has Euler characteristic $\chi(\mathrm{EH}) = 2$, Hirzebruch signature $\tau(\mathrm{EH}) = -1$, spin-$\frac{1}{2}$ index $I_{\frac{1}{2}}(\mathrm{EH}) = 0$ and vanishing action. The EH gravitational instaton supports a non-zero Maxwell field strenght with $1/r^4$ asymptotic behavior. It is worth emphasizing that this asymptotic behavior is the same as that of Yang-Mills instantons.[6] These gravitational instantons are known as Abelian Eguchi-Hanson (AEH) instantons [88]. The AEH instantons possess two properties of great importance for our study. First, their action is no longer vanishing but non-zero, and it is controlled not by the Planck scale but by the electromagnetic coupling. Second, the AEH instantons can have a non-zero spin-$\frac{1}{2}$ index.

For these reasons, AEH instantons have been the subject of several studies in relation to the quality problem of the QCD axion. Before starting our analysis, it is therefore useful to summarize what has already been discussed in the literature. First, ref. [90] studied the gravitational analogues of CP violating effects in QCD, recognizing that they arise through the addition of terms $\theta_\mathrm{em} F_{\mu\nu}\tilde{F}^{\mu\nu}$ and $\theta_\mathrm{grav} R_{\mu\nu\rho\sigma}\tilde{R}^{\mu\nu\rho\sigma}$ to the Lagrangian density, where $R_{\mu\nu\alpha\beta}$ and $F_{\mu\nu}$ are the curvature tensor and Maxwell field tensor, respectively, with $\tilde{R}^{\mu\nu\rho\sigma}$ and $\tilde{F}^{\mu\nu}$ their Hodge dual. It was argued that both terms can

[5]Moreover, as already recognized in the analysis of ref. [89], it is unclear whether the stability problem of the wormhole mentioned earlier, if present, could give rise to any pathology in this patched solution as well.

[6]For instance, the self-dual ALF Taub-NUT metric supports a non-zero Maxwell field strength with $1/r^2$ asymptotic behavior (like a magnetic monopole).

be non-trivial in spacetimes with sufficiently complex topology. Refs. [91, 92] demonstrated that AEH gravitational instantons provide a concrete and calculable new source of intrinsic PQ symmetry breaking by quantum gravity. The results of refs. [91, 92] suggest that the gravitational contribution to the axion potential could saturate the current experimental bound on the neutron electric dipole moment. Ref. [93] (see also refs. [94, 95]) considers colored Eguchi-Hanson (CEH) gravitational instantons. CEH gravitational instantons are the non-abelian analogue of AEH instantons [96, 97]. Ref. [93] makes the bold claim that CEH gravitational instantons compromise the axion solution to the strong CP problem.

In this work, we will critically reanalyze the role of AEH and CEH gravitational instantons as responsible for the explicit gravitational breaking of the PQ symmetry. We anticipate that the effects we will find will be significantly smaller than those previously reported, and we will argue that there is no reason for the PQ symmetry to suffer from a quality problem due to gravity.

3.2 Gravitational instantons and the quality problem of the QCD axion

We investigate the gravitational contribution to the axion potential $V(a)$ arising from gravitational non-perturbative effects, specifically as the sole sources of CP violation induced by gravity.

In section 3.2.1, we will begin by making some perturbative comments regarding the axion's anomalous coupling to gravity, while in section 3.2.2 we will discuss the non-perturbative effects.

3.2.1 Perturbative considerations

The axion, a Goldstone boson (GB) of the non-linearly realized chiral $U(1)_{\rm PQ}$ symmetry, exhibits a mixed anomaly with QCD and gravity. These anomalies couple the axion to the QCD field strength and its dual, as well as to gravitons through the Riemann tensor and its dual [98]. The anomalous part of the axion effective Lagrangian reads

$$\mathcal{L}_a \supset -\frac{1}{32\pi^2 f_a}\, a\, G^a_{\mu\nu}\tilde{G}^{a,\mu\nu} - \frac{E}{32\pi^2 N f_a}\, a\, F_{\mu\nu}\tilde{F}^{\mu\nu} + \frac{G}{768\pi^2 N f_a}\, a\, R_{\mu\nu\rho\sigma}\tilde{R}^{\mu\nu\rho\sigma}\,, \tag{3.10}$$

where $\alpha_S \equiv g_S^2/4\pi$ (with g_S being the strong coupling), $\alpha \equiv e^2/4\pi$ (with e being the fundamental electric charge), while N, E and G are model-dependent anomaly coefficients of order one, which can be computed explicitly for a given UV-complete axion model. To provide an example, we calculate the value of these coefficients in the case of a UV-completion of the KSVZ type (cf. ref. [99] for a review). We consider the generalized KSVZ model described by the Lagrangian density

$$\begin{aligned}\mathcal{L}_{\rm KSVZ} =& (\partial_\mu\Phi)^*(\partial^\mu\Phi) - V(\Phi) + \sum_{\mathcal{Q}}\left[\overline{\mathcal{Q}} i \not{D}\mathcal{Q} - \left(\lambda_{\mathcal{Q}}\Phi\overline{\mathcal{Q}_L}\mathcal{Q}_R + \text{h.c.}\right)\right]\,,\\ V(\Phi) =& \lambda_\Phi\left(|\Phi|^2 - \frac{v_a^2}{2}\right)^2\,,\end{aligned} \tag{3.11}$$

with spontaneously broken global $U(1)_{\rm PQ}$ symmetry with order parameter v_a. We parametrize the complex scalar field as $\Phi = (v_a+\rho)e^{ia/v_a}/\sqrt{2}$, with the Goldstone field a that plays the role of the axion. In full generality, we consider vector-like fermions $\mathcal{Q}$ transforming according to the SM representation

$$\mathcal{Q} \sim (\mathcal{C}_{\mathcal{Q}}, \mathcal{I}_{\mathcal{Q}}, \mathcal{Y}_{\mathcal{Q}})_{SU(3)_{\rm C}\times SU(2)_{\rm L}\times U(1)_{\rm Y}}\,. \tag{3.12}$$

We find

$$N \equiv \sum_{\mathcal{Q}} \chi_{\mathcal{Q}} d(\mathcal{I}_{\mathcal{Q}}) T(\mathcal{C}_{\mathcal{Q}})\,,$$
$$E \equiv \sum_{\mathcal{Q}} \chi_{\mathcal{Q}} d(\mathcal{C}_{\mathcal{Q}}) \mathrm{Tr}(q_{\mathcal{Q}}^2)\,,$$
$$G \equiv \sum_{\mathcal{Q}} \chi_{\mathcal{Q}} d(\mathcal{I}_{\mathcal{Q}}) d(\mathcal{C}_{\mathcal{Q}})\,, \tag{3.13}$$

with $f_a \equiv v_a/2N$. $\chi_{\mathcal{Q}} = \pm 1$ with $\chi_{\mathcal{Q}} = +1$ for a Yukawa coupling of the form $\lambda_{\mathcal{Q}} \Phi \overline{\mathcal{Q}_L} \mathcal{Q}_R$ + h.c. and $\chi_{\mathcal{Q}} = -1$ for a Yukawa coupling of the form $\lambda_{\mathcal{Q}} \Phi \overline{\mathcal{Q}_R} \mathcal{Q}_L$ + h.c.; $T(\mathcal{C}_{\mathcal{Q}})$ is the colour Dynkin index for the representation $\mathcal{C}_{\mathcal{Q}}$ with $SU(3)_{\mathrm{C}}$ generators $T^a_{\mathcal{C}_{\mathcal{Q}}}$, and it is defined by the condition $\mathrm{Tr}(T^a_{\mathcal{C}_{\mathcal{Q}}} T^b_{\mathcal{C}_{\mathcal{Q}}}) = T(\mathcal{C}_{\mathcal{Q}})\delta_{ab}$; $d(\mathcal{I}_{\mathcal{Q}})$ denotes the dimension of the weak isospin representation $\mathcal{I}_{\mathcal{Q}}$. The electric charge operator is defined by $q_{\mathcal{Q}} \equiv T^3_{\mathcal{I}_{\mathcal{Q}}} + \mathcal{Y}_{\mathcal{Q}}$; notice that $\mathcal{Y}_{\mathcal{Q}}$ is to be understood as $\mathcal{Y}_{\mathcal{Q}}\, \mathbb{1}_{d(\mathcal{I}_{\mathcal{Q}}) \times d(\mathcal{I}_{\mathcal{Q}})}$ with $\mathcal{Y}_{\mathcal{Q}}$ a scalar number. It is possible to rewrite $\mathrm{Tr}(q^2_{\mathcal{Q}}) = \mathrm{Tr}[(T^3_{\mathcal{I}_{\mathcal{Q}}} + \mathcal{Y}_{\mathcal{Q}})(T^3_{\mathcal{I}_{\mathcal{Q}}} + \mathcal{Y}_{\mathcal{Q}})] = T(\mathcal{I}_{\mathcal{Q}}) + \mathcal{Y}^2_{\mathcal{Q}} d(\mathcal{I}_{\mathcal{Q}})$, where $T(\mathcal{I}_{\mathcal{Q}})$ is the Dynkin index of the $SU(2)_{\mathrm{L}}$ representation $\mathcal{I}_{\mathcal{Q}}$ and where we used $\mathrm{Tr}(T^3_{\mathcal{I}_{\mathcal{Q}}}) = 0$. The electromagnetic contribution, which is blind to $SU(3)_{\mathrm{C}}$, is proportional to the dimension of the representation $\mathcal{C}_{\mathcal{Q}}$ and to the trace of the charge operator $q^2_{\mathcal{Q}}$. On the other hand, the gravitational coupling, which is blind to both $SU(3)_{\mathrm{C}}$ and $SU(2)_{\mathrm{L}}$, is proportional to the dimension of the representation $\mathcal{C}_{\mathcal{Q}}$ and $\mathcal{I}_{\mathcal{Q}}$. Therefore, the gravitational coupling of the axion does not vanish even in the case in which one takes the vector-like fermions $\mathcal{Q}$ to be completely uncharged under the $SU(3)_{\mathrm{C}} \times SU(2)_{\mathrm{L}}$ gauge group (that is, $d(\mathcal{I}_{\mathcal{Q}}) = d(\mathcal{C}_{\mathcal{Q}}) = 1$).
In the infrared—that is, at the level of the chiral axion Lagrangian—a chiral rotation of the light quarks has the following effects: *i)* eliminates the effective axion-gluon coupling, *ii)* introduces a derivative axial-vector axion-quark coupling, and *iii)* modifies the effective axion-photon and axion-graviton couplings. As far as the latter are concerned, we find

$$\mathcal{L}_a \supset -\frac{1}{32\pi^2 f_a}\left[\frac{E}{N} - 6\mathrm{Tr}(Q\mathrm{q}^2)\right] a F_{\mu\nu}\tilde{F}^{\mu\nu} + \frac{1}{768\pi^2 f_a}\left(\frac{G}{N} - 6\right) a\, R_{\mu\nu\rho\sigma}\tilde{R}^{\mu\nu\rho\sigma}\,, \tag{3.14}$$

with $\mathrm{q} \equiv \mathrm{diag}(2/3, -1/3, -1/3)$ and $Q = (m_u^{-1} + m_d^{-1} + m_s^{-1})^{-1}\mathrm{diag}(1/m_u, 1/m_d, 1/m_s)$. We note that in the original KSVZ model with one vector-like pair of heavy fermions with $\mathcal{Q} \sim (3, 1, 0)$ we have $N = 1/2$ and $G = 3$. In this case, therefore, the effective axion-graviton coupling vanishes. More in general, in the case in which we have one single heavy fermion, we find, whatever $SU(2)_{\mathrm{L}} \times U(1)_{\mathrm{Y}}$ quantum numbers, $G/N = d(\mathcal{C}_{\mathcal{Q}})/T(\mathcal{C}_{\mathcal{Q}})$. This immediately implies that in the case of the fundamental representation of $SU(3)_{\mathrm{C}}$ for which $d(\mathcal{C}_{\mathcal{Q}}) = 3$ and $T(\mathcal{C}_{\mathcal{Q}}) = 1/2$ we have $G/N = 6$ and the gravitational coupling vanishes. However, in more general KSVZ models we have $G/N \neq 6$. For instance, in the non-minimal solution with $\mathcal{Q}_1 \sim (8, 1, 0)$, $\mathcal{Q}_2 \sim (6, 1, 0)$ and opposite $\chi_{\mathcal{Q}}$ charge (that is, the non-minimal model that gives $N_{\mathrm{DW}} = 1$) we get $G/N = 4$. Furthermore, following from the previous argument, in the case of a single $\mathcal{Q}$uark, $G/N \neq 6$ if $\mathcal{Q}$ transforms according to $SU(3)_{\mathrm{C}}$ irreps of dimension higher than the fundamental. To fix ideas, we consider some of the most relevant cases discussed in ref. [100]. In table 3.1, we show for which variations of the KSVZ model it is possible to obtain a non-zero value for the gravitational coupling $G/N - 6$. When non-zero, we observe that the value of the combination $G/N - 6$ remains of order one in realistic situations.

From a phenomenological standpoint, it is clear that the gravitational coupling of the QCD axion is of negligible relevance in perturbation theory. In the weak–field limit, the quantization of gravity amounts to expanding the metric around the Minkowski background $g_{\mu\nu} = \eta_{\mu\nu} + \kappa h_{\mu\nu}$. The inclusion of the factor $\kappa \equiv \sqrt{32\pi G_N}$ in the definition of the graviton field $h_{\mu\nu}$ gives this field a mass dimension of unity and results in a kinetic term (arising from the standard Einstein-Hilbert action) with standard

$\mathcal{Q}$ representation	R_1 $(3,1,-1/3)$	R_3 $(3,2,1/6)$	R_6 $(3,3,-1/3)$	R_8 $(3,3,-4/3)$	R_9 $(\bar{6},1,-1/3)$	R_{12} $(8,1,-1)$	$R_8 \ominus R_3$	$R_8 \oplus R_6 \ominus R_9$	$R_6 \oplus R_9$	$R_{12} \ominus R_9$
E/N	$2/3$	$5/3$	$14/3$	$44/3$	$4/15$	$8/3$	$122/3$	$170/3$	$23/12$	$44/3$
G/N	6	6	6	6	$12/5$	$8/3$	6	24	$15/4$	4
$N_{\rm DW}$	1	2	3	3	5	6	2	2	4	1

Table 3.1: *Numerical values for E/N, G/N and $N_{DW} = 2N$ for some of the most relevant $\mathcal{Q}$ representations discussed in ref. [100]. The symbol $\oplus$ refers to $\chi_{\mathcal{Q}} = +1$ while $\ominus$ to $\chi_{\mathcal{Q}} = -1$.*

normalization. For matter interactions, the order of κ keeps track of the number of gravitons involved in an interaction. Consequently, for a Lagrangian density of the form $\mathcal{L} = y\, a\, R_{\mu\nu\rho\sigma}\tilde{R}^{\mu\nu\rho\sigma}$ we find

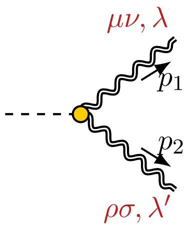

$$= 2yi\kappa^2 \varepsilon_{\mu\rho\alpha\beta} p_1^\alpha p_2^\beta \left[p_{1\,\sigma} p_{2\,\nu} - (p_1 \cdot p_2)\eta_{\nu\sigma} \right] , \tag{3.15}$$

while the interaction Lagrangian density $\mathcal{L} = k\, a\, F_{\mu\nu}\tilde{F}^{\mu\nu}$ generates the amplitude

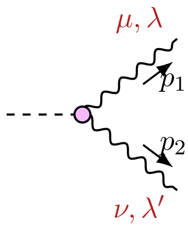

$$\equiv 4ik\varepsilon_{\mu\nu\rho\sigma} p_1^\rho p_2^\sigma \, . \tag{3.16}$$

The axion-graviton coupling, if compared to the axion-photon one, pays a huge suppression factor of the order of

$$\frac{a \to \text{gravitons}}{a \to \text{photons}} \sim \alpha^{-1} \left(\frac{m_a}{M_{\rm Pl}} \right)^2 , \tag{3.17}$$

where we have treated powers of momentum as the axion rest mass m_a. Based on dimensional analysis, the decay width of the axion into two gravitons can be estimated to be of the order of

$$\Gamma_{a\to gg} \approx \frac{G_N^2 m_a^7}{\pi^4 f_a^2} , \tag{3.18}$$

which is phenomenologically irrelevant.

From a model-building perspective, one might consider attempting to engineer a mechanism that leads to an amplification of the gravitational coupling of the axion (without altering that of QCD). A potentially interesting possibility is to implement a clockwork mechanism [101, 102], along the lines of that proposed in ref. [103]. In its original formulation, the clockwork mechanism is described by a renormalizable theory involving a sequence of $\mathcal{N} + 1$ complex scalar fields ϕ_i with a global $U(1)^{\mathcal{N}+1}$ symmetry that is spontaneously broken at the scale f. This global symmetry is further explicitly broken, but in a manner that leaves a residual $U(1)$ symmetry intact. The corresponding NG boson, which can be identified with the QCD axion as discussed in ref. [103], resides in a compact field space, where its effective decay constant is determined by $3^{\mathcal{N}} f \gg f$. The core idea presented in ref. [103] is as follows: new vector-like fermions responsible for generating the color anomaly are coupled to the final site $\mathcal{N}$ of the scalar chain. This setup still resolves the strong CP problem but with the key distinction that the scale $3^{\mathcal{N}} f$ can be significantly larger than the fundamental symmetry-breaking scale f. In the standard QCD axion model, the vector-like fermions that mediate the QCD anomaly also contribute to the axion-photon coupling. However, in the clockwork QCD axion framework, additional electromagnetically charged vector-like fermions are coupled to a site $\mathcal{M} < \mathcal{N}$ in the scalar chain. These fermions generate the axion-photon coupling, which is effectively decoupled from the solution to the strong CP problem. In its simplest realization, the clockwork axion model requires the existence of a single vector-like colored fermion in the fundamental representation of $SU(3)_{\mathrm{C}}$ and a single color neutral vector-like fermion with unit hypercharge and singlet under $SU(2)_{\mathrm{L}}$.

In our case, it is sufficient to introduce a single heavy vector-like fermion, even if completely neutral under the Standard Model gauge group, to contribute to the gravitational axion coupling. The setup we have in mind, therefore, takes the structure given by the following schematic

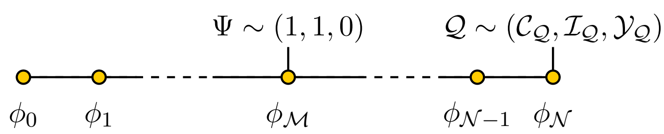

in which one vector-like fermions $\mathcal{Q}$ is coupled to the last site of the clockwork chain while a second vector-like fermion Ψ, uncharged under the Standard Model gauge group, is coupled to the site $\mathcal{M}$. The effective coupling of the axion to gluons and gravitons arises by performing a chiral rotation to remove the axion from the Yukawa coupling involving the fermions $\mathcal{Q}$ and Ψ. We find

$$\mathcal{L}_a \supset -\frac{1}{32\pi^2 f_a}\, a\, G^a_{\mu\nu}\tilde{G}^{a,\mu\nu} + \frac{G}{768\pi^2 N f_a}\, a\, R_{\mu\nu\rho\sigma}\tilde{R}^{\mu\nu\rho\sigma}\,, \tag{3.19}$$

with

$$\frac{G}{N} = \frac{d(\mathcal{I}_{\mathcal{Q}})d(\mathcal{C}_{\mathcal{Q}}) + 3^{\mathcal{N}-\mathcal{M}} d(\mathcal{I}_\Psi)d(\mathcal{C}_\Psi)}{d(\mathcal{I}_{\mathcal{Q}})T(\mathcal{C}_{\mathcal{Q}})}\,. \tag{3.20}$$

Even considering a fermion $\mathcal{Q} \sim (3,1,0)$ in the color fundamental and isospin singlet, we find that, at low energies, the gravitational coupling of the axion is non-zero and is given by

$$\frac{G}{N} - 6 = 2 \times 3^{\mathcal{N}-\mathcal{M}}\,, \tag{3.21}$$

where we used $d(\mathcal{I}_\Psi) = d(\mathcal{C}_\Psi) = 1$. The relation between the fundamental symmetry breaking scale f and the effective decay constant f_a is given by $f_a = 3^{\mathcal{N}} f$. Furthermore, we note that in this particular realization with $\mathcal{Q} \sim (3,1,0)$ and $\Psi \sim (1,1,0)$, the axion-photon coupling is entirely generated at low energies and is therefore controlled by the effective axion decay constant f_a.

We have thus found that the coupling to gravitons can be exponentially large, and its magnitude is controlled by the distance between the site coupled to the colored fermions and the site coupled to the uncharged ones. It is natural at this point to ask how large this enhancement can be. It is not difficult to realize that, at least within the context of this minimal setup, there is a fundamental obstruction to the attempt to make the gravitational coupling arbitrarily large. On the one hand, we would like to consider an axion mass as large as possible in order to minimize the ratio given by eq. (3.17). On the other hand, the axion mass generated by non-perturbative QCD effects is described by the scaling [23]

$$m_a \approx 5.7 \times 10^{-10} \left(\frac{10^{16}\,\mathrm{GeV}}{f_a}\right) \mathrm{eV}\,. \tag{3.22}$$

Consequently, increasing the axion mass implies decreasing the value of $f_a = 3^{\mathcal{N}} f$, and thus considering a small value of $3^{\mathcal{N}}$ (assuming a fixed value of f, for instance $f = O(100)$ GeV, which approximately corresponds to the smallest possible value, given that at the scale f the massive scalar gears produced by the clockwork mechanism are found). However, this latter factor is precisely what should contribute to the enhancement of the gravitational coupling.

To be a bit more concrete, if we consider a GUT-scale value $f_a \approx 10^{16}$ GeV and a spontaneous breaking scale $f \approx 100f$ GeV, we obtain an enhancement factor (we take $\mathcal{M} = 0$ to maximize the effect) $3^{\mathcal{N}} \approx 10^{14}$, which, however, is still too small to make the gravitational coupling phenomenologically relevant. Numerically, eq. (3.18) gives

$$\Gamma^{-1}_{a\to gg} \approx 10^{102} \left(\frac{f_a}{10^{16}\,\mathrm{GeV}}\right)^9 3^{-2\mathcal{N}}\,\mathrm{s} \gg \tau_{\mathrm{U}} \approx 10^{17}\,\mathrm{s}\,, \tag{3.23}$$

where τ_{U} is the age of the universe.
In perturbation theory, since $G\tilde{G} \equiv G^a_{\mu\nu}\tilde{G}^{a,\mu\nu}$ is a total derivative, the axion Lagrangian is shift-invariant. However, because of QCD non-perturbative effects, $G\tilde{G}$ will generate an axion potential. Analogously, $R\tilde{R} \equiv R_{\mu\nu\rho\sigma}\tilde{R}^{\mu\nu\rho\sigma}$, is a total derivative and, *in perturbation theory*, it does not spoil the axion shift-invariance. We now move to consider non-perturbative effects.

3.2.2 Non-perturbative breaking induced by gravity

We ask whether gravitational non-perturbative effects can induce $R\tilde{R}$ to generate an axion potential. This could be naturally interpreted as the axion potential induced by gravitational interactions. Mimicking the strong interactions [34–36, 40], where in the Euclidean functional integral $\mathcal{Z}_{\mathrm{E}}$ we have to sum over all the topologically distinct gauge sectors, we have the full (Euclidean) generating functional [104]

$$\mathcal{Z}_{\mathrm{E}} \equiv \lim_{\tau_{\mathrm{E}}\to\infty} {}_{\mathrm{out}}\langle 0|\, e^{-\hat{H}\tau_{\mathrm{E}}}\,|0\rangle_{\mathrm{in}} = \int [\mathcal{D}\mathcal{A}]\,[\mathcal{D}\Psi]\,[\mathcal{D}g]\, e^{-S_{\mathrm{E}}}\,, \tag{3.24}$$

where, $[\mathcal{D}\Psi]$ means summing over all the matter fields in the theory, $[\mathcal{D}\mathcal{A}]$ over all the topologically distinct sectors of the Yang-Mills theory and $[\mathcal{D}g]$ over all the gravitational sectors. At this stage, it is crucial to pause for an important remark. Regarding the gravitational part of the functional integral defining the vacuum persistence amplitude in eq. (3.24), one should sum over all 4-dimensional Riemannian spaces $\{M, g_{\mu\nu}\}$ with arbitrary topology for the manifold M and arbitrary metric $g_{\mu\nu}$, subject to the condition that M has a prescribed boundary ∂M, and that $g_{\mu\nu}$ induces some prescribed metric k_{ab} on ∂M. It seems plausible that the appropriate boundary condition for the vacuum persistence amplitude corresponds to metrics that are asymptotically Euclidean, with a boundary at infinity that can be interpreted as a 3-sphere equipped with its standard metric. We could thus attempt to imagine the contribution of a gravitational instanton as schematized in fig. 3.2.

From an operational standpoint, this sum can be organized as follows [105]. First, it is possible to divide the positive definite metrics $g_{\mu\nu}$ on M, which induce the given metric k_{ab} on the boundary ∂M, into equivalence classes under conformal transformations with a conformal factor Ω that is positive and equal to one on ∂M. Second, it is possible to select a metric from each conformal equivalence class that satisfies $R = 0$. One can then explicitly perform the integration over conformal deformations of this metric. This leaves the task of summing over all metrics that satisfy $R = 0$. In full generality, the action of these metrics is given by a boundary term (the bulk term vanishes).

At this point, in order for the functional integration to behave properly, one can invoke the so-called positive-action conjecture [105, 106]: all non-singular asymptotically flat metrics with $R = 0$ everywhere have non-negative action. It is further conjectured that the action is zero if and only if the space is flat. The validity of the positive action conjecture—which, we reiterate, must hold true in order to give meaning to the functional integration—has a striking consequence of great relevance to our discussion. In fact, the positive action conjecture requires that there are no Ricci-flat asymptotically Euclidean metrics other than flat space [81, 106]. Consequently, if we restrict ourselves to considering exclusively

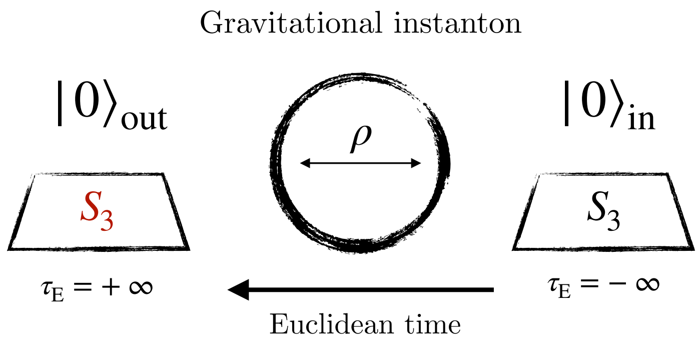

Figure 3.2: *Schematic representation of a gravitational instanton of size ρ, as a tunneling event between two disjoint vacua, intended as two flat Euclidean spacetimes.*

metrics that are asymptotically Euclidean, it would not be legitimate to include gravitational instantons (as defined in section 3.1.2) in the sum defining the vacuum persistence amplitude. This argument would resolve our issue at its root. The gravitational instantons discussed in refs. [91–93], which could potentially spoil the axion solution to the strong CP problem, simply must not be considered in the gravitational path integral.

However, in the remainder of our analysis, we choose to follow the discussion in ref. [81], in which an alternative asymptotic condition was proposed by introducing a fundamental group at infinity: the metric locally approaches the Euclidean one but a neighborhood of infinity has the topology of $(S^3/\Gamma) \times \mathbb{R}$ where Γ is a finite group of isometries acting on S^3. These are nothing but the ALE spaces discussed in section 3.1.2.

In the following, therefore, we will contemplate summing over ALE spaces. The reasoning behind this choice is to demonstrate, as we will explicitly do, that even in the case where ALE spaces are taken into consideration, the low-energy physics that is potentially sensitive to these geometries remains protected, even in the absence of Planck-scale suppression. In particular, as explained in section 3.1.2, we will focus on the contribution of the AEH gravitational instantons.

We have, in full generality, the Euclidean action

$$S_{\text{E}} = S_{\text{grav}} + S_{\text{gauge}} + S_{\text{matter}} + S_\theta \,, \tag{3.25}$$

in which

$$S_{\text{grav}} = -\frac{1}{16\pi G_N} \int_M d^4x \, \sqrt{g}\, R - \frac{1}{8\pi G_N} \int_{\partial M} d^3\vec{x} \, \sqrt{k}\, [K] \,,$$

where the volume integral of the Ricci scalar R is taken over M with boundary ∂M and $[K] \equiv K - K_0$ denotes the difference between the trace of the second fundamental form of the boundary ∂M in the metric $g_{\mu\nu}$ (denoted by K), and its value in the flat metric (denoted by K_0); k is the determinant of the induced metric on the boundary.
The second term in eq. (3.2.2), known as the Gibbons-Hawking-York boundary term, is an important term added to the Einstein-Hilbert action in the context of General Relativity (GR) when spacetime has boundaries, and is necessary because the variation of the Ricci scalar R, which contains second derivatives of the metric, leads to boundary terms involving first derivatives of the metric that must be canceled to ensure a well-posed variational principle [77, 78, 107]. In eq. (3.25), we further have

$$S_{\text{gauge}} + S_{\text{matter}} = \int_M d^4x \, \sqrt{g} \left\{ \frac{1}{4\, g_S^2} G^a_{\mu\nu} G^{a,\mu\nu} + \frac{1}{4\, e^2} F_{\mu\nu} F^{\mu\nu} + \mathcal{L}[\mathcal{A}, \Psi] \right\} ,$$

where $\mathcal{L}[\mathcal{A},\Psi]$, in which $\mathcal{A}$ and Ψ collectively representing the gauge and matter fields, respectively, and includes the axion Lagrangian $\mathcal{L}_a$. Finally, we have the topological terms (that are purely imaginary in Euclidean spacetime [44])

$$S_\theta = i\int_M d^4x\,\sqrt{g}\left\{\frac{\overline{\theta}}{32\pi^2}G^a_{\mu\nu}\tilde{G}^{a,\mu\nu}+\frac{\theta_{\rm em}}{32\pi^2}F_{\mu\nu}\tilde{F}^{\mu\nu}-\frac{\theta_{\rm grav}}{768\pi^2}R_{\mu\nu\rho\sigma}\tilde{R}^{\mu\nu\rho\sigma}\right\}, \tag{3.26}$$

where $\theta_{\rm em}$ is non-zero in non-topologically trivial backgrounds. In the following we will demonstrate that AEH instantons [88] (see Appendix 3.4) allow for an explicit and controlled computation of the gravitationally induced axion potential, identifying it as the dominant contribution from non-perturbative gravitational effects. Indeed, in the case of gravitational instantons, the one-instanton contribution to the Euclidean path integral will be

$$\begin{aligned}\mathcal{Z}_{\rm E}|_{1-\rm inst} &= \sum_{\overline{g}=\overline{g}_{\rm AEH}}\int [\mathcal{D}\mathcal{A}]\,[\mathcal{D}\Psi]\,[\mathcal{D}h]\,e^{-S_{\rm E}[\mathcal{A},\Psi,\overline{g},h]}\,,\\ g_{\mu\nu} &= \overline{g}_{\mu\nu}+h_{\mu\nu}/M_{\rm Pl}\,.\end{aligned} \tag{3.27}$$

The AEH instantons have Euclidean action (see appendix 3.4)

$$S_{\rm E}\left[\overline{g}_{\rm AEH}\right] = \frac{\pi p^2}{\alpha} - i\,\frac{p^2}{2}\theta_{\rm em} - i\frac{\theta_{\rm grav}}{16}\,, \tag{3.28}$$

where e is a $U(1)$ gauge charge that may naturally be interpreted as the electric charge and p is a real number. Consequently, eq. (3.27) becomes

$$\mathcal{Z}_{\rm E}|_{1-\rm inst} = \sum_p \int [\mathcal{D}\mathcal{A}]\,[\mathcal{D}\Psi]\,[\mathcal{D}h]\,e^{-\frac{\pi p^2}{\alpha}+i\,\frac{p^2}{2}\theta_{\rm em}+i\frac{\theta_{\rm grav}}{16}+\dots}+\mathcal{O}(e^{-M_{\rm Pl}^2\rho^2})\,, \tag{3.29}$$

where the ellipses stand for quantum fluctuations around the classical solution. At this point, after discussing the theoretical foundations of the semi-classical gravity approach within which we are operating, we can proceed to the calculation of the axion potential generated by gravitational instantons.

3.2.3 Contribution to the axion potential

In full analogy to the computation of the axion potential arising from QCD instanton effects, we will employ the method of 't Hooft operators to compute the axion potential induced by gravitational effects. In ref. [43], 't Hooft showed that (see the discussion in Section 2.1.3), at distances much larger than the instanton size—so that we can describe one instanton event in a local way—BPST instantons [108] produce effective interactions for a quark q_i^s with color index $i = 1,\dots,N_c$ and flavor index $s = 1,\dots,N_f$ with effective Lagrangian

$$\Delta\mathcal{L}_{\rm inst}(x) = c\,e^{i\overline{\theta}}\,\left(\mathcal{K}^{(N_f)}_{N_c}\right)^{i_1 i_1\dots i_{N_f}}\det_{s,t}\left[\overline{q}^s_R(x)q^t_L(x)\right]_{i_1 i_2\dots i_{2N_f}}+\text{h.c.}\,, \tag{3.30}$$

where

$$c = O(1)\exp[-S_{\rm E}(\mathcal{A}_{\rm inst})]\,. \tag{3.31}$$

We indicate with $\mathcal{A}_{\rm inst}$ the classical BPST instanton [108] whose action is given by $S_{\rm E}(\mathcal{A}_{\rm inst}) = 8\pi^2/g_S^2$ with g_S the strong coupling constant; in eq. (3.30), $\mathcal{K}^{(N_f)}_{N_c}$ is a tensor of the color group $SU(N_c)$.

The physics content of eq. (3.30) can be intuitively understood from the celebrated index theorem [109], which states that the violation of the chiral charge

$$Q_5 = \sum_{j=1}^{N_f}\int d^4x\,\overline{\Psi}_j\gamma_0\gamma_5\Psi_j\,,$$

in a background $\mathcal{A}$ is $\Delta Q_5 = 2(n_+ - n_-) = 4N_f T(\mathcal{C}_\Psi)n$, where n is the winding number, normalized as

$$n = \frac{1}{32\pi^2}\int d^4x\, \mathcal{G}^a_{\mu\nu}\tilde{\mathcal{G}}^{a,\mu\nu} = 0, \pm1, \pm2, \dots,$$

$\mathcal{G}^a_{\mu\nu} = G^a_{\mu\nu}(\mathcal{A})$ (that is, $\mathcal{G}^a_{\mu\nu}$ denotes $G^a_{\mu\nu}$ evaluated on the gauge configuration $\mathcal{A}$) and $n_+ - n_- =$ index $\left(\mathrm{i}\not{\mathcal{D}}\right)_{\mathcal{A}}$ is the index of the Dirac operator in the background of $\mathcal{A}$, *i.e.* the number of normalizable eigenvectors with zero eigenvalue of $i\not{\mathcal{D}}_{\mathcal{A}}$ (the so-called *zero modes*). Under a chiral transformation, we have $q_R \to q_R e^{-i\alpha}$, $q_L \to q_L e^{i\alpha}$. Furthermore, for simplicity, we have assumed that all the fermions Ψ_j's are in the same representation of the color group with Dynkin index $T(\mathcal{C}_\Psi) = 1/2$. From the index theorem, in the background of one instanton (for which $n = 1$), the chiral charge is violated by $\Delta Q_5 = 2N_f$ units. That is to say, each flavor violates the chiral charge by 2 units. This effect of non-perturbative chiral charge violation in presence of one instanton event can be incarnated by the effective vertex in eq. (3.30), which indeed violates, in a non-perturbative way, the chiral charge by $2N_f$ units.

In the PQ solution [14], $\overline{\theta}$ is promoted to $\overline{\theta} \to \overline{\theta} + 2Na/v_a$; therefore, eq. (3.30) is modified to (with $f_a \equiv v_a/2N$, and omitting the color indices i)

$$\begin{aligned}\Delta\mathcal{L}_{\text{inst}}(x) = c\, e^{i\overline{\theta}} e^{ia/f_a}\, \mathcal{K}^{(N_f)}_{N_c} \det_{s,t}\left[\bar{q}^s_R(x) q^t_L(x)\right] \\ + \text{h.c.}\,. \end{aligned} \tag{3.32}$$

One then can easily convince oneself that, closing the fermion legs using all the interactions at disposal contained in $S_{\text{matter}} + S_{\text{gauge}}$, obtains the instanton contribution to the axion potential; indeed eq. (3.32) is not invariant under the shifts $a(x)/f_a \to a(x)/f_a + \alpha$.

Following the methodology applied in the QCD case, we construct the gravitational analogue of 't Hooft vertex in eq. (3.30) by analyzing the Dirac zero-modes, *i.e.* the violation of the chiral charge, in the background of a gravitational instanton. That is to say, we have to solve for *normalizable* solutions of the covariant and massless Dirac equation:

$$\gamma^\mu \mathcal{D}_\mu \psi_f = 0\,, \tag{3.33}$$

where $\mathcal{D}_\mu$ is the Dirac operator evaluated in the gravitational instanton metric background twisted by the abelian gauge field $\mathcal{A}_\mu$, that is to say

$$\gamma^\mu \mathcal{D}_{\mu,\mathcal{A}} = \not{\mathcal{D}}_{\mathcal{A}} = \gamma^a E^\mu_a \left(\partial_\mu - \frac{1}{8}\omega_\mu{}^{bc}\left[\gamma^b, \gamma^c\right] + iQ^f_{\text{em}}\mathcal{A}_\mu\right).$$

An explicit computation (see appendix 3.5 for details), shows that, differently from what was found in ref. [110] and used in ref. [91], the number of zero modes in the AEH background is, instead [111]

$$|n_+ - n_-| = \sum_{2j+1=1}^{[2|Q^f_{\text{em}}p|+1]} (2j+1)\,, \tag{3.34}$$

in which Q^f_{em} is the electric charge of the fermion ψ_f in eq. (3.33) and $[\mathcal{N}]$ is the largest integer strictly smaller than $\mathcal{N}$ (for instance $[3] = 2$, etc). From topological arguments, see eq. (3.61), for a fermion in a AEH background, we have the Dirac string quantization condition

$$|Q_{\text{em}}p| = 0,\, 1,\, 2\, \dots\,. \tag{3.35}$$

Therefore, since $Q_{\text{em}}p$ is an integer, one AEH instanton event violates the chiral charge Q_5, associated with the axial current $J^\mu_5 = \sum_f \overline{\psi}_f \gamma^\mu\gamma_5\psi_f$, by

$$|\Delta Q_5| = 2|n_+ - n_-| = 2|Q^f_{\text{em}}p|\left(2|Q^f_{\text{em}}p| + 1\right) \tag{3.36}$$

units. Since the minimal electric charge of the Standard Model is $-\frac{1}{3}$, the instanton charge p has to be restricted to [91]

$$p = 3n, \quad \text{for some integer } n\,, \tag{3.37}$$

and eq. (3.29) becomes

$$\begin{aligned}\mathcal{Z}_{\rm E}\big|_{1-\rm inst} &= \sum_{p=3n} \int [\mathcal{D}\mathcal{A}]\,[\mathcal{D}\Psi]\,[\mathcal{D}h]\, e^{-\frac{\pi p^2}{\alpha}+i\,\frac{p^2}{2}\theta_{\rm em}+i\frac{\theta_{\rm grav}}{16}+\dots} + \mathcal{O}(e^{-M_{\rm Pl}^2\rho^2}) \\ &= \int [\mathcal{D}\mathcal{A}]\,[\mathcal{D}\Psi]\,[\mathcal{D}h]\, e^{-\frac{9\,\pi}{\alpha}+i\frac{9}{2}\theta_{\rm em}+i\frac{\theta_{\rm grav}}{16}+\dots} + \mathcal{O}\left(e^{-M_{\rm Pl}^2\rho^2},\, e^{-\frac{9\pi}{\alpha}}\right)\,,\end{aligned} \tag{3.38}$$

where, in the following, we will exclude $p = 0$ instantons, as they do not violate the chiral charge and therefore do not contribute to the axion potential. Therefore, the 't Hooft operator, generalizing the QCD one in eq. (3.30), associated with $p = 3$ AEH instantons will be

$$\begin{aligned}\Delta\mathcal{L}_{\rm AEH}(x) = \mathcal{K}\left(\frac{9\pi}{\alpha}\right)^{5/2} \int_{m_{\rm UV}^{-1}} \frac{d\rho}{\rho^5}\,\det\left[\prod_{f=\text{fermions}} \left(\overline{\psi}_{R,f}\psi_{L,f}\right)^{3|Q^f_{\rm em}|\left(6|Q^f_{\rm em}|+1\right)}\right] e^{-\frac{9\pi}{\alpha}+i\frac{9}{2}\theta_{\rm em}+i\frac{\theta_{\rm grav}}{16}} \\ + \text{h.c.}\,,\end{aligned} \tag{3.39}$$

where $\mathcal{K}$ is an $O(1)$ number, we have used the fact that the chiral charge in eq. (3.36) is violated by $\Delta Q_5 = 6|Q^f_{\rm em}|\left(6|Q^f_{\rm em}|+1\right)$ units, that the abelian gauge connection has 5 zero modes (see appendix 3.4 for details) and the product in eq. (3.39) runs over all the fermions at disposal. In the presence of an axion, the topological angles in eq. (3.26) are shifted to

$$\theta_{\rm em} \to \theta_{\rm em} + \frac{2Ea}{v_a}\,, \qquad \theta_{\rm grav} \to \theta_{\rm grav} + \frac{2Ga}{v_a}\,. \tag{3.40}$$

Therefore, the exponential in eq. (3.39) is modified to

$$\exp\left(-\frac{9\pi}{\alpha} + i\theta_{\rm AEH} + i\mathcal{E}_{\rm AEH}\frac{a}{f_a}\right)\,, \tag{3.41}$$

where, for simplicity, we have defined $\theta_{\rm AEH} \equiv \frac{9}{2}\theta_{\rm em} + \frac{\theta_{\rm grav}}{16}$ and $\mathcal{E}_{\rm AEH} \equiv \frac{9E}{2N} + \frac{G}{16N}$. As in the QCD case, since eq. (3.41) is not symmetric under continuous shifts $a(x)/f_a \to a(x)/f_a + \alpha$, it may be naturally interpreted as a gravitationally induced axion potential. In particular, it should be noted that in eq. (3.39) we are integrating up to (see eq. (3.8))

$$m_{\rm UV} < M_s = g_s M_{\rm Pl}\,, \tag{3.42}$$

because the instanton solution we are considering is a solution of Einstein's equations, and, as commonly believed, GR is not the complete theory of gravity. However, assuming that the UV completion of gravity is weakly coupled, $M_s \ll M_{\rm Pl}$, *i.e.* that the new degrees of freedom associated with quantum gravity must appear *before* $M_{\rm Pl}$, these non-perturbative effects arising from a UV completion of gravity will be weighted by the Euclidean action

$$\sim \exp\left(-\frac{\text{const}}{g_s}\right) \ll \exp\left(-\frac{9\pi}{\alpha}\right)\,, \tag{3.43}$$

where the inequality follows if we consider $g_s \ll \alpha$; under this assumption, $M_s^4/g_s^2\exp(-9\pi/g_s) \ll V_{\rm AEH}(a)$. We can depict this separation of scales as in fig. 3.3. This allows us to conclude that, under

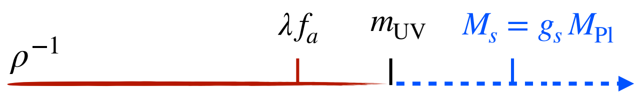

Figure 3.3: *The AEH solution is reliable up to some mass scale m_{UV}, after which corrections to GR become to be relevant due to the onset of particles of the UV-completion.*

the assumption that the UV completion of GR is weakly coupled, with $g_s \ll \alpha$, the gravitationally induced axion potential is dominated by effects of classical GR. That is to say

$$\Delta\mathcal{L}_{\mathrm{AEH}}(x) = \Delta\mathcal{L}_{\mathrm{AEH}}(x)|_{\mathrm{GR}} + \mathcal{O}\left(e^{-\frac{\mathrm{const}}{g_s}}\right) \simeq \Delta\mathcal{L}_{\mathrm{AEH}}(x)|_{\mathrm{GR}}\,. \tag{3.44}$$

In the following $\Delta\mathcal{L}_{\mathrm{AEH}}(x) = \Delta\mathcal{L}_{\mathrm{AEH}}(x)|_{\mathrm{GR}}$. Taking as a proxy $\lambda f_a \simeq 10^{12}$GeV, where λ is some coupling, we can compute numerically the axion potential induced by eq. (3.41). As long as we are at energy scales below $\lambda\, f_a$ we will not be able to probe the onset of the UV completion of the axion model, therefore the product in eq. (3.41) will run over Standard Model fermions. Therefore, omitting the color indices, the integral in eq. (3.39) separates into two distinct contributions, which we write as

$$\begin{aligned}
\Delta\mathcal{L}_{\mathrm{AEH}}(x) = \mathcal{K}\left(\frac{9\pi}{\alpha}\right)^{5/2} &\int_{(\lambda\, f_a)^{-1}} \frac{d\rho}{\rho^5} \det\left[\left\{\left(\bar{l}_R l_L\right)^{21}\left(\overline{u}_R u_L\right)^{10}\left(\bar{d}_R d_L\right)^{3}\right\}^{N_g}\right] e^{-\frac{9\pi}{\alpha}+i\theta_{\mathrm{AEH}}+i\mathcal{E}_{\mathrm{AEH}}\frac{a}{f_a}} \\
&+\mathcal{K}\left(\frac{9\pi}{\alpha}\right)^{5/2}\int_{m_{\mathrm{UV}}^{-1}}^{(\lambda\, f_a)^{-1}} \frac{d\rho}{\rho^5}\times \\
&\times \det\left[\left\{\left(\bar{l}_R l_L\right)^{21}\left(\overline{u}_R u_L\right)^{10}\left(\bar{d}_R d_L\right)^{3}\right\}^{N_g}\prod_{\mathcal{Q}}\left(\overline{\mathcal{Q}}_R\mathcal{Q}_L\right)^{3|Q^{\mathcal{Q}}_{\mathrm{em}}|\left(6|Q^{\mathcal{Q}}_{\mathrm{em}}|+1\right)}\right] e^{-\frac{9\pi}{\alpha}+i\theta_{\mathrm{AEH}}+i\mathcal{E}_{\mathrm{AEH}}\frac{a}{f_a}} \\
&+\mathrm{h.c.}\,,
\end{aligned} \tag{3.45}$$

where N_g is the number of generations of light fermions and we have taken into account, for $\lambda\, f_a < \rho^{-1} < m_{\mathrm{UV}}$ the onset of the axion model UV completion, *i.e.* the heavy fermions $\mathcal{Q}$, since there are additional heavy degrees of freedom (arising above m_{UV}) that we have integrated out in our treatment. Diagrammatically, this instanton vertex is represented on the left side of fig. 3.4.

We now examine how to translate this interaction into a potential for the axion. There are two important points to consider.

- Let us consider the first of the two integrals in eq. (3.45), the one bounded below by the length scale $(\lambda f_a)^{-1}$. Given our interest in computing the maximum contribution of this non-perturbative effect, we close the fermion legs in a way that optimally enhances the instanton contribution, thereby avoiding any mass suppression ($v_{\mathrm{EW}} \ll f_a$). Since we want the lower limit of integration to dominate, we close the fermion legs with Yukawa insertions, as depicted in the right panel of fig. 3.4.

- Let us now consider the second integral, defined over length scales in the range $\lambda\, f_a < \rho^{-1} < m_{\mathrm{UV}}$. To ensure the reliability of the contribution in the second line of eq. (3.41)—i.e., that the AEH solution remains unaffected by physics near M_s—we must close the fermion legs with mass insertions, resulting in an integral that exhibits dominant behavior near the scale $(\lambda\, f_a)^{-1}$. This is shown, in the corresponding range of lengths, in the right panel of fig. 3.4.

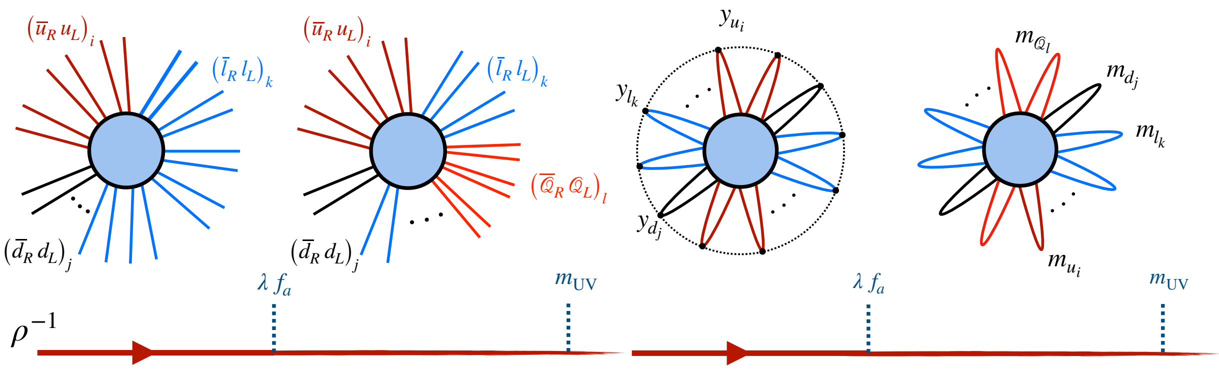

Figure 3.4: *Diagrammatic representation of AEH instanton vertex (on the left). AEH instanton contribution to the axion potential (on the right).*

All in all, we obtain the axion potential contribution (see appendix 3.6), up to $O(1)$ factors

$$
\begin{aligned}
V_{\rm AEH}(a) = & \lambda^3 \hbar^{17N_g} \left(\frac{9\pi}{\alpha}\right)^{5/2} \frac{(\lambda f_a)^4}{(\pi^2)^{17N_g}} \prod_{i=1}^{N_g} \left(y_l^{21}\, y_u^{10}\, y_d^{3}\right)_i e^{-\frac{9\pi}{\alpha}+i\theta_{\rm AEH}+i\mathcal{E}_{\rm AEH}\frac{a}{f_a}} \\
& + \lambda^3 \left(\frac{9\pi}{\alpha}\right)^{5/2} (\lambda f_a)^{4-34N_g-10N_{\mathcal{Q}}} \prod_{i=1}^{N_g} \left(m_l^{21} m_u^{10} m_d^{3}\right)_i \prod_{\mathcal{Q}=1}^{N_{\mathcal{Q}}} M_{\mathcal{Q}}^{10} \times \\
& \times e^{-\frac{9\pi}{\alpha}+i\theta_{\rm AEH}+i\tilde{\mathcal{E}}_{\rm AEH}\frac{a}{f_a}} + \text{h.c.}\,, \qquad (3.46)
\end{aligned}
$$

where, for dimensional reasons, we have one overall factor of λ^3, and, for concreteness, we consider the case in which $Q_{\rm em}^{\mathcal{Q}} = 2/3$. We find numerically that, since we want to enhance as much as possible this effect, taking $\lambda = O(1)$, $f_a = 10^{12}$ GeV and $\alpha = 10^{-1}$, because of loop and mass suppressions (see appendix 3.6)

$$
V_{\rm AEH}(a) \ll \underbrace{\lambda^3 \left(\frac{9\pi}{\alpha}\right)^{5/2} e^{-\frac{9\pi}{\alpha}} (\lambda f_a)^4}_{\simeq 10^{-70}\,\text{GeV}^4} \cos\left(\theta_{\rm AEH} + \mathcal{E}_{\rm AEH}\frac{a}{f_a}\right). \qquad (3.47)
$$

We may try to enhance this potential closing the fermion legs via Yukawa couplings associated with scalars that are not the Standard Model Higgs [45]. Nevertheless, we find that (taking the Yukawa couplings to be $O(1)$ numbers) this effect is still negligible compared to the QCD contribution.

3.2.4 Comment on the colored case

We notice that we could have taken into account in the Euclidean generating functional $\mathcal{Z}_{\rm E}$ in eq. (3.27) also the so-called CEH instantons [93]. CEH instantons have Euclidean action

$$
S_{\rm E}\left[\bar{g}_{\rm CEH}\right] = \frac{4\pi^2}{g_S^2} \times 3 + i\frac{3}{2}\bar{\theta} + i\frac{\theta_{\rm grav}}{16}\,. \qquad (3.48)
$$

Using similar arguments for the abelian case, one gets the 't Hooft vertex

$$\begin{aligned}\Delta\mathcal{L}_{\rm CEH}(x) = \tilde{\mathcal{K}}\left(\frac{3\pi}{\alpha_S}\right)^8 \int_{(\lambda\, f_a)^{-1}}^{\Lambda^{-1}} e^{-S_{\rm E}[\overline{g}_{\rm CEH}]}\,\frac{d\rho}{\rho^5} \prod_{\text{QCD quarks}} (\overline{q}_L\, q_R) \; + \\ + \tilde{\mathcal{K}}\left(\frac{3\pi}{\alpha_S}\right)^8 \int_{m_{\rm UV}^{-1}}^{(\lambda\, f_a)^{-1}} e^{-S_{\rm E}[\overline{g}_{\rm CEH}]}\,\frac{d\rho}{\rho^5} \prod_{\text{QCD quarks}} (\overline{q}_L\, q_R) \prod_{\mathcal{Q}} \left(\overline{\mathcal{Q}}_L\, \mathcal{Q}_R\right)^{f(R_{\mathcal{Q}})} \\ + \text{h.c.}\,, \end{aligned} \tag{3.49}$$

where $\tilde{\mathcal{K}}$ is a $O(1)$ number, g_S is the strong coupling, $f(R_{\mathcal{Q}})$ is the number of zero-modes associated to the color representation $R_{\mathcal{Q}}$ under which $\mathcal{Q}$ transforms [112], Λ is an infrared scale and, shifting $\overline{\theta} \to \overline{\theta} + \frac{a}{f_a}$, the exponential in eq. (3.49) is modified to

$$\exp\left(\frac{4\pi^2}{g_S^2}\times 3 + i\theta_{\rm CEH} + i\mathcal{A}_{\rm CEH}\frac{a}{f_a}\right)\,, \tag{3.50}$$

in which $\theta_{\rm CEH} = \frac{3}{2}\overline{\theta} + \frac{\theta_{\rm grav}}{16}$ and $\mathcal{A}_{\rm CEH} = \frac{3}{2} + \frac{G}{16N}$. All the calculations involving the 't Hooft operator in eq. (3.30), namely closing external fermion legs to get a potential, are valid as long as the coupling associated with the gauge connection is *perturbative*, since in the perturbative domain one-instanton contributions saturate the axion potential. In other words, closing the legs of the 't Hooft vertices in the strong coupling regime is unlikely to yield reliable results. Supporting this argument is the fact that the mass of the η' is not governed by large instanton effects, but rather by the confinement dynamics [113]. In light of these observations, in the second contribution in eq. (3.49), *i.e.* the one in which $\lambda\, f_a < \rho^{-1} < m_{\rm UV}$, the coupling is perturbative. Consequently, using 't Hooft operators to calculate the axion potential can yield meaningful results. For the instanton calculation to produce a reliable result, in the integration region $(\lambda\, f_a)^{-1} < \rho < \Lambda^{-1}$ where $\alpha_S(\Lambda) = O(1)$, the legs of the vertex in eq. (3.49) can be closed only through interactions that force the lower limit of integration to dominate, since for $\rho^{-1} = \lambda\, f_a$, g_S is perturbative. Therefore, to avoid the large instanton region, we must not introduce positive powers of ρ, differently from the analysis in [93]. The only way to do avoid the strong coupling regime is by closing the legs with Yukawa interactions. Because of the perturbativity of α_S and loop suppressions, we get, for $\lambda = O(1)$ and $\alpha_S = 10^{-2}$

$$V_{\rm CEH}(a) \lesssim \mathcal{O}(10^{-200})\, V_{\rm QCD}(a)\,, \tag{3.51}$$

where

$$V_{\rm QCD}(a) = -m_\pi^2 f_\pi^2 \sqrt{1 - \frac{4 m_u m_d}{(m_u+m_d)^2}\sin^2\left(\frac{a}{2f_a}\right)}\,.$$

This therefore shows that CEH instantons provide a subleading contribution to the axion potential compared to the abelian case.

3.2.5 Gravitational potential enhancement in *Nnatualness*

The only beyond the Standard Model scenario in which these gravitational effects can be significantly enhanced involves introducing multiple copies of the Standard Model to address the Higgs boson mass hierarchy problem [114]. Having N copies of the SM, naively implies that each copy has its own theta angle θ_i, however, if the S_N symmetry distinguishing among the different copies is only softly broken by Higgs mass terms (*i.e.* these copies differ only for the mass term in the Higgs potential), all these angles would be equal. Therefore, a shared axion would be able to set to zero all the θ_i's at the same time. Moreover, if one naively assumes the presence of an axion in each sector, this would elevate the number of light degrees of freedom, consequently worsening the constraints on N_{eff}. If a shared axion is the solution to the strong CP problem, then the number of copies is bounded to $N < 10^{10}$ [114]. In this case, the 't Hooft operator will be

$$\Delta\mathcal{L}_{\text{AEH}}(x) = \sum_{\text{SM=us}}^{10^{10}} \left\{ \left(\frac{9\pi}{\alpha}\right)^{5/2} \int_{m_{\text{UV}}^{-1}} \frac{d\rho}{\rho^5} \det\left[\prod_{f=\text{fermions}} \left(\overline{\psi}_{R,f}\psi_{L,f}\right)^{3|Q^f_{\text{em}}|\left(6|Q^f_{\text{em}}|+1\right)}\right] e^{-S_{\text{E}}} + \text{h.c.}\right\}\Bigg|_{\text{SM}} ,$$

where, as usual

$$S_{\text{E}} = e^{-\frac{9\pi}{\alpha} + i\theta_{\text{AEH}} + i\mathcal{E}_{\text{AEH}}\frac{a}{f_a}} .$$

Taking the Yukawa couplings to be $O(1)$ numbers, one gets that this contribution is still significantly small compared to the QCD contribution. Therefore, this gravitational contribution to the axion potential is still exceedingly small with respect to the axion potential generated by confinement dynamics in the strong interactions.

3.3 Conclusions

In this work, we analyzed the role of self-dual ALE solutions of the vacuum Euclidean Einstein equations in the Euclidean gravitational path integral. Our results indicate that low-energy physics potentially sensitive to these contributions—particularly the QCD axion—remains protected. This protection persists even across a range of beyond Standard Model scenarios, which might otherwise enhance these effects. Adopting a maximally inclusive definition of the path integral (as discussed in section 3.1.1), we derived an upper bound on the gravitational contribution to the axion potential. Our key findings are summarized as follows:

- **AEH instantons and weakly coupled string theory**: Assuming a weakly coupled string theory as the UV completion of gravity, we argued that AEH instantons saturate the gravitational contribution to the axion potential.

- **Zero modes and loop suppressions**: Following ref. [111], we identified zero modes previously overlooked in refs. [91, 115]. These additional zero modes, along with loop and mass suppressions, significantly reduce the AEH instanton contribution to the axion potential, see eq. (3.47). Specifically, the abelian contribution remains well below the current experimental bounds on the neutron electric dipole moment, independent of the axion model's UV completion.

- **CEH instantons and PQ protection**: By including CEH instantons in the sum over ALE manifolds in the gravitational path integral, see eq. (3.27), we showed that—contrary to the results of ref. [93]—these do not spoil the PQ solution. Instead, their contribution is subleading compared to the abelian case.

- **PQ quality problem in beyond the Standard Model scenarios**: Our analysis demonstrates that this non-perturbative contribution to the axion potential does not introduce a PQ quality problem, even in extended beyond the Standard Model scenarios. For instance, in the model discussed in ref. [114], where multiple Standard Model copies are coupled to a single $U(1)_{\text{PQ}}$, the PQ symmetry remains protected.

In conclusion, our findings suggest that gravitational effects do not pose a threat to the robustness of the QCD axion solution. This strengthens the viability of axion-based solutions to the strong CP problem across a wide range of UV completions and beyond the Standard Model frameworks.

3.4 Appendix A: Eguchi-Hanson manifold

Eguchi and Hanson discovered a non-trivial spherically symmetric solution of Einstein's equations in 4-dimensional Euclidean spacetime [82, 88], the so-called *Eguchi-Hanson instanton.* One would expect that the relevant instanton-like metrics would be those whose 2-form curvature R_{ab} is (anti)-self-dual, are localized in Euclidean spacetime and free of singularities. In fact, solutions have been found which have the interesting property that the metric approachs a flat metric at infinity, i.e. a vacuum configuration (as required for a tunneling interpretation). These solutions are called "asymptotically locally Euclidean" metrics, because as we shall see, at infinity, they are locally Euclidean. Apart for this solutions, the obvious metrics that seem to incarnate these features (self-dual, localized and free of singularities) are the standard solutions of black hole physics, which however in Euclidean spacetime are not asymptotically flat. The instanton metric is

$$
\begin{aligned}
ds^2_{\mathrm{EH}} &= \frac{\mathrm{d}r^2}{1-\frac{\rho^4}{r^4}} + + \frac{r^2}{4}(\sigma_x^2+\sigma_y^2) + \frac{r^2}{4}\sigma_z^2\left(1-\frac{\rho^4}{r^4}\right) \\
&= \frac{dr^2}{1-\frac{\rho^4}{r^4}} + \frac{r^2}{4}\left[d\theta^2+\sin^2\theta\, d\phi^2\right] + \frac{r^2}{4}\left(1-\frac{\rho^4}{r^4}\right)(d\psi+\cos\theta\, d\phi)^2\,, \quad r\geq\rho\,,
\end{aligned}
\tag{3.52}
$$

where we introduced the 1-forms

$$
\begin{aligned}
\sigma_1 &= \sin\psi\, d\theta - \cos\psi\sin\theta d\phi\,,\\
\sigma_2 &= \cos\psi d\theta + \sin\psi\sin\theta d\phi\,,\\
\sigma_3 &= d\psi + \cos\theta d\phi\,,
\end{aligned}
$$

(ϕ,θ,ψ) are the Euler angles on the S^3 sphere with ranges

$$
0\leq\theta<\pi\,,\ 0\leq\phi<2\pi\,,\ 0\leq\psi<4\pi\,,
$$

and ρ is the instanton core size. That is, in matrix form

$$
g^{\mathrm{EH}}_{\mu\nu} = \begin{pmatrix} \frac{r^2}{4} & 0 & 0 & 0 \\ 0 & -\frac{\rho^4\cos 2\theta+\rho^4-2r^4}{8r^2} & \frac{\left(r^4-\rho^4\right)\cos\theta}{4r^2} & 0 \\ 0 & \frac{\left(r^4-\rho^4\right)\cos\theta}{4r^2} & \frac{r^4-\rho^4}{4r^2} & 0 \\ 0 & 0 & 0 & \frac{1}{1-\frac{\rho^4}{r^4}} \end{pmatrix}.
$$

We have the vierblein

$$
\begin{aligned}
ds^2_{\mathrm{EH}} &= \sum_{a=1}^{4}\sum_{b=1}^{4} e^a e^b \eta_{ab}\,,\ e^a = e^a_\mu dx^\mu \\
e^a &= \left(\frac{r}{2}\sigma_x, \frac{r}{2}\sigma_y, \frac{u\,r}{2}\sigma_z, -\frac{dr}{u}\right)\,,\ u=\sqrt{1-\frac{\rho^4}{r^4}}\,,
\end{aligned}
\tag{3.53}
$$

where in the Euclidean $\eta_{ab} = \eta^{ab} = \text{diag}(1,1,1,1)$. We have the wedge products

$$
\begin{aligned}
e^1 \wedge e^2 &= \frac{r^2}{4} \sin\theta \, d\theta \wedge d\phi \,, \\
e^1 \wedge e^3 &= \frac{r^2}{4} u\big(-\cos\psi \sin\theta \, d\phi \wedge d\psi \\
&\quad + \sin\psi \, [d\theta \wedge d\psi + \cos\theta d\theta \wedge d\phi] \big) \,, \\
e^1 \wedge e^4 &= -\frac{r}{2u}\big(\sin\psi d\theta \wedge dr - \sin\theta \cos\psi d\phi \wedge dr \big) \,, \\
e^2 \wedge e^3 &= \frac{u\, r^2}{4}\big(\sin\theta \sin\psi \, d\phi \wedge d\psi \\
&\quad + \cos\psi \; [d\theta \wedge d\psi + \cos\theta \, d\theta \wedge d\phi] \big) \,, \\
e^2 \wedge e^4 &= -\frac{r}{2u}\big(\cos\psi \, d\theta \wedge dr + \sin\theta \sin\psi \, d\phi \wedge dr \big) \,, \\
e^3 \wedge e^4 &= -\frac{r}{2}\big(d\psi \wedge dr + \cos\theta \, d\phi \wedge dr \big) \,.
\end{aligned}
$$

We have the curvature 2-form

$$
R^a{}_b = R^a{}_b = \frac{1}{2} R^a{}_{b\mu\nu} dx^\mu \wedge dx^\nu \equiv d\omega^a{}_b + \omega^a{}_c \wedge \omega^c{}_b \,,
$$

where $\omega^a{}_b$ is the spin-connection 1-form [116, 117], and we find the self-dual curvature (for the flat indices a, b we are taking $\varepsilon_{1234} = +1$), $R_{mn} = +\frac{1}{2}\varepsilon_{mnab} R_{ab}$,

$$
\begin{aligned}
R_{14} = R_{23} &= -\frac{2\rho^4}{r^6} \left(e^1 \wedge e^4 + e^2 \wedge e^3 \right) \,, \\
R_{24} = -R_{13} &= -\frac{2\rho^4}{r^6} \left(e^2 \wedge e^4 + e^1 \wedge e^3 \right) \,, \\
R_{34} = R_{12} &= +\frac{4\rho^4}{r^6} \left(e^3 \wedge e^4 + e^1 \wedge e^2 \right) \,.
\end{aligned}
$$

To remove the coordinate singularity at $r = \rho$, we have to identify antipodal points of $r = a > \rho$ spherical surfaces. That is to say

$$
\begin{aligned}
&0 \le \theta < \pi, \\
&0 \le \phi < 2\pi, \\
&0 \le \psi < 2\pi \,.
\end{aligned}
\tag{3.54}
$$

This is an explicit example of a metric whose topology is asimptotically *locally* Euclidean, but not *globally* Euclidean (i.e., not S^3). We have the Pontryagin invariant

$$
p = -\frac{1}{16\pi^2} \int_{\mathcal{M}_{\text{EH}}} d^4x \, \sqrt{g} R_{\mu\nu\rho\sigma} \tilde{R}^{\mu\nu\rho\sigma} = \frac{1}{16\pi^2} \int_{\mathcal{M}_{\text{EH}}} d^4x \, \sqrt{g} \, \frac{384\rho^8}{r^{12}} = 3 \,.
$$

The EH metric (3.52) supports the self-dual $U(1)$ field

$$
\mathcal{A} = \frac{p\rho^2}{r^2} \sigma_z, \tag{3.55}
$$

which is to say

$$
\mathcal{A}_r = \mathcal{A}_\theta = 0, \quad \mathcal{A}_\psi = \frac{p\rho^2}{r^2}, \quad \mathcal{A}_\phi = \frac{p\rho^2}{r^2} \cos\theta \,. \tag{3.56}
$$

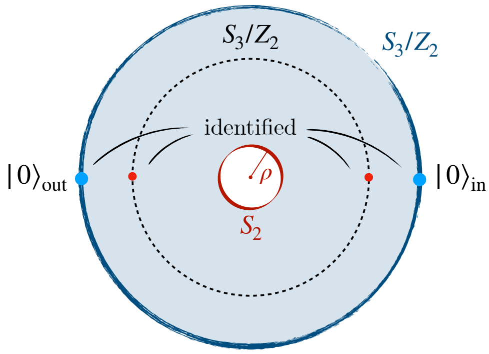

Figure 3.5: *Schematical representation of* $\mathcal{M}_{(\mathrm{A})\mathrm{EH}}$ *spacetime.*

This gauge field connection has 5 collective coordinates: 4 related to the instanton center x_0, 1 related to the integration constant ρ. We have the field-strength

$$\begin{aligned}\mathcal{F} &= d\mathcal{A} = \partial_\mu \mathcal{A}_\nu \, dx^\mu \wedge dx^\nu \\ &= -\frac{2p\rho^2\cos\theta}{r^3}\, dr\wedge d\phi - \frac{2p\rho^2}{r^3}\, dr\wedge d\psi - \frac{p\rho^2\sin\theta}{r^2}\, d\theta\wedge d\phi \\ &= -\frac{4p\rho^2}{r^4}\left(e^1\wedge e^2 - e^3\wedge e^4\right). \end{aligned} \tag{3.57}$$

That is, in matrix form

$$\mathcal{F}_{\mu\nu} = \begin{pmatrix} 0 & -\frac{p\rho^2\sin\theta}{r^2} & 0 & 0 \\ \frac{p\rho^2\sin\theta}{r^2} & 0 & 0 & \frac{2p\rho^2\cos\theta}{r^3} \\ 0 & 0 & 0 & \frac{2p\rho^2}{r^3} \\ 0 & -\frac{2p\rho^2\cos\theta}{r^3} & -\frac{2p\rho^2}{r^3} & 0 \end{pmatrix}$$

which is anti-self-dual, that is

$$\tilde{\mathcal{F}}^{\mu\nu} = \frac{1}{2\sqrt{g}}\,\varepsilon^{\mu\nu\rho\sigma}\mathcal{F}_{\rho\sigma} = -\mathcal{F}^{\mu\nu}\,, \quad \varepsilon^{0123} = 1\,.$$

Indeed, since (anti)self-dual Maxwell fields have vanishing energy-momentum tensor[7], the Einstein equations are undisturbed and, decorating the EH spacetime in eq. (3.52) with the gauge field in eq. (3.55), we have an automatic solution of the Einstein-Maxwell equations [118]. This is what we call an AEH spacetime. We have the action [119]

$$\begin{aligned} S_{\mathrm{AEH}} &= -\frac{1}{16\pi G_N}\int_M d^4x\,\sqrt{g}\,R - \frac{1}{8\pi G_N}\int_{\partial M} d^3\vec{x}\,\sqrt{k}\,[K] \\ &\quad + \frac{1}{4e^2}\int_{\mathcal{M}_{\mathrm{AEH}}} d^4x\,\sqrt{g}\,\mathcal{F}_{\mu\nu}\mathcal{F}^{\mu\nu} + i\int_{\mathcal{M}_{\mathrm{AEH}}} d^4x\,\sqrt{g}\,\frac{\theta_{\mathrm{em}}}{32\pi^2}\mathcal{F}_{\mu\nu}\tilde{\mathcal{F}}^{\mu\nu} \qquad (3.58) \\ &\quad - i\int_{\mathcal{M}_{\mathrm{AEH}}} d^4x\,\sqrt{g}\,\frac{\theta_{\mathrm{grav}}}{768\pi^2}R_{\mu\nu\rho\sigma}\tilde{R}^{\mu\nu\rho\sigma} = \frac{\pi p^2}{\alpha} - i\,\frac{p^2}{2}\theta_{\mathrm{em}} - i\frac{\theta_{\mathrm{grav}}}{16}\,. \qquad (3.59) \end{aligned}$$

Note that this action is independent of Newton's constant and rather similar to that of the Yang-Mills instanton except for a factor of 2. This can be traced back to the identification of antipodal points in EH space, which becomes a half of the (asymptotic) Euclidean space. We now ask whether the AEH

[7] One can easily verify that, using $\mathcal{F}_{12} = \mathcal{F}_{43} = -\frac{4p\rho^2}{r^4}$, obtains $T_{ab} = -\mathcal{F}_{ac}\mathcal{F}_{bc} + \frac{1}{4}\eta_{ab}\mathcal{F}_{cd}\mathcal{F}_{cd} = 0$.

space actually admits the existence of spin structures (Fermi fields) [120]. Consider a path γ at constant $r = a > \rho$ with $0 < \psi < 2\pi$ at fixed (θ, ϕ). Since at constant $r > \rho$, $\mathcal{M}_{\rm EH} \sim S_3/Z_2$, this path is indeed a loop. Furthermore this loop cannot be contracted to a point, since the loop encloses the S_2 sphere at $r = \rho$. Propagating a fermion field $\Psi(x)$ with charge $Q^f_{\rm em}$ along γ, one will obtain a new field $\Psi'(x)$ which is related to the original field by the abelian transformation

$$\Psi'(x) = e^{iQ^f_{\rm em} \oint_\gamma \mathcal{A}}\, \Psi(x)\,. \tag{3.60}$$

However, from the Stokes' theorem, in the limit $a \to \infty$,

$$\oint_\gamma \mathcal{A} = \int_{\mathcal{M}_\gamma} \mathcal{F} = -\int_{\mathcal{M}_\gamma} \frac{4p\rho^2}{r^4}\left(e^1 \wedge e^2 - e^3 \wedge e^4\right) = \int_{\mathcal{M}_\gamma} \frac{4p\rho^2}{r^4}\frac{r}{2} d\psi \wedge dr = -2\pi p\,,$$

where $\mathcal{M}_\gamma$ is the manifold lying over the loop contour γ. For the fermion $\Psi(x)$ to be consistently defined over the manifold, since antipodal points are identified, we have to impose the Dirac string quantization condition [120]

$$Q^f_{\rm em}\, p = \text{integer}\,. \tag{3.61}$$

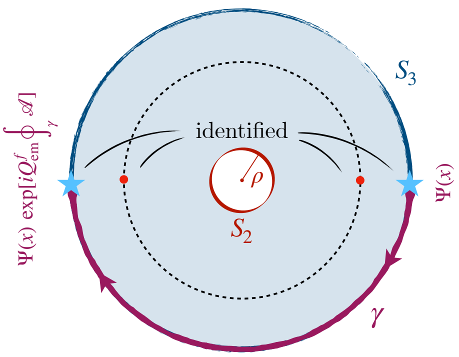

Figure 3.6: *Propagation of the fermion* $\Psi(x)$ *along the loop* γ*.*

3.5 Appendix B: Computation of Dirac zero-modes on AEH manifold

To make the analysis parallel to the Yang-Mills case and to give a precise estimate of all the loop factors we have to find explicitly the zero-modes of the Dirac operator $i\not{D}$ in the AEH background (see [111, 121] for a review). In this appendix we find the zero-modes of the Dirac operator for 4-manifolds with isometry group SO(3) and a self-dual Riemann tensor. Introducing the radial functions $f(r)$, $a(r)$, $b(r)$, $c(r)$, the metrics take the form

$$ds^2 = f^2 dr^2 + a^2\sigma_1^2 + b^2\sigma_2^2 + c^2\sigma_3^2\,. \tag{3.62}$$

We furthermore introduce the vierblein

$$e^1 = a\sigma_1, \quad e^2 = b\sigma_2, \quad e^3 = c\sigma_3, \quad e^4 = -f dr\,.$$

By definition, the inverse vierblein is given by

$$E^\mu_a = \eta_{ab} g^{\mu\nu} e^b_\nu \;\Leftrightarrow\; E^\mu_a e^b_\mu = \delta^b_a\,,$$

from which, inverting the 4×4 matrix e^a_μ, we straightforwardly find

$$E_1 = \frac{1}{a} X_1, \quad E_2 = \frac{1}{b} X_2, \quad E_3 = \frac{1}{c} X_3, \quad E_4 = -\frac{1}{f}\partial_r \,,$$

where

$$\begin{aligned} X_1 &= \sin\psi\, \partial_\theta + \cos\psi \,(\cot\theta\, \partial_\psi - \frac{1}{\sin\psi}\partial_\phi)\,, \\ X_2 &= \cos\psi\, \partial_\theta - \sin\psi \,(\cot\theta\, \partial_\psi - \frac{1}{\sin\theta}\partial_\phi)\,, \\ X_3 &= \partial_\psi \,. \end{aligned}$$

For many calculations it is convenient to use a proper radial coordinate R defined via

$$dR \equiv f\, dr \Leftrightarrow E_4 = -\partial_R \,.$$

We are interested in the general form of the Dirac operator in metrics like the one in eq. (3.62) and coupled to a spherically symmetric abelian $U(1)$ gauge connection with self-dual field strenght: indeed for (anti)-self-dual field strenght the energy momentum tensor identically vanishes. The gauge potential can then be written as

$$\mathcal{A} = \mathcal{A}_1\sigma_1 + \mathcal{A}_2\sigma_2 + \mathcal{A}_3\sigma_3 \,,$$

where $\mathcal{A}_1$, $\mathcal{A}_2$, $\mathcal{A}_3$ are functions of R only. The Dirac operator in the presence of the connection $\mathcal{A}$ is

$$\begin{aligned} \gamma^\mu \mathcal{D}_{\mu,\mathcal{A}} = \not{\mathcal{D}}_{\mathcal{A}} &= \gamma^a E^\mu_a \left(\partial_\mu - \frac{1}{8}\omega_\mu{}^{bc}\left[\gamma^b, \gamma^c\right] + iQ^f_{\mathrm{em}}\mathcal{A}_\mu\right) \\ &= \gamma^a \left(E_a - \frac{1}{8}\omega_a{}^{bc}\left[\gamma^b, \gamma^c\right] + iQ^f_{\mathrm{em}}\mathcal{A}(E_a)\right), \end{aligned}$$

where Q^f_{em} is the charge of the fermion under the U(1) connection $\mathcal{A}$, $\mathcal{A}(E_a) = E^\mu_a \mathcal{A}_\mu$ and we introduced the Euclidean γ matrices

$$\{\gamma_a, \gamma_b\} = -2\delta_{ab}\,, \quad a, b = 1, \ldots, 4\,, \tag{3.63}$$

where

$$\gamma^i = \begin{pmatrix} 0 & \tau_i \\ -\tau_i & 0 \end{pmatrix}, \quad \gamma^4 = -i\begin{pmatrix} 0 & \mathbf{1} \\ \mathbf{1} & 0 \end{pmatrix},$$

and we have the Pauli matrices $[\tau_i, \tau_j] = 2i\epsilon_{ijk}\tau_k\,, i = 1, 2, 3$. The self-duality of the Riemann tensor implies that the spin connection 2-form ω_{ab} is

$$\begin{aligned} \omega_{14} &= -\dot{a}\sigma_1, \quad \omega_{24} = -\dot{b}\sigma_2, \quad \omega_{34} = -\dot{c}\sigma_3\,, \\ \omega_{23} &= -A\sigma_1, \quad \omega_{31} = -B\sigma_2, \quad \omega_{12} = -C\sigma_3\,, \end{aligned} \tag{3.64}$$

where

$$A = \frac{b^2 + c^2 - a^2}{2bc},\ B = \frac{a^2 + c^2 - b^2}{2ac},\ C = \frac{a^2 + b^2 - c^2}{2ab}\,,$$

and $\dot{\varphi} = d\varphi/dR$. Using eq. (3.64), we obtain

$$\begin{aligned} \not{\mathcal{D}}_{\mathcal{A}} = \gamma^4 \Bigg\{ &\left[-\frac{\partial_r}{f} + iQ^f_{\mathrm{em}}\mathcal{A}(E_4) - \frac{1}{2}\left(\frac{\dot{a}}{a} + \frac{\dot{b}}{b} + \frac{\dot{c}}{c}\right)\right] I_4 \\ &+ \left[i(E_i + iQ^f_{\mathrm{em}}\mathcal{A}(E_i))\tau_i + \frac{1}{2}\left(\frac{A}{a} + \frac{B}{b} + \frac{C}{c}\right)\right]\begin{pmatrix} -\mathbf{1}_2 & 0 \\ 0 & \mathbf{1}_2 \end{pmatrix}\Bigg\}\,. \end{aligned}$$

Introducing

$$\mathcal{D}_i \equiv X_i + iQ^f_{\rm em}\mathcal{A}(X_i), \quad \mathcal{A}(X_i) = X_i^\mu \mathcal{A}_\mu\,, \quad i = 1,2,3\,,$$

we get

$$\not{D}_{\mathcal{A}} = \begin{pmatrix} 0 & T_{\mathcal{A}}^\dagger \\ T_{\mathcal{A}} & 0 \end{pmatrix}\,,$$

where

$$T_{\mathcal{A}} = \left[i\frac{\partial_r}{f} + Q^f_{\rm em}\mathcal{A}(E_4) + \frac{i}{2}\left(\frac{\dot{a}}{a} + \frac{\dot{b}}{b} + \frac{\dot{c}}{c}\right)\right]\mathbf{1}_2 + iB_{\mathcal{A}}\,,$$

$$B_{\mathcal{A}} = i\left(\frac{\tau_1\mathcal{D}_1}{a} + \frac{\tau_2\mathcal{D}_2}{b} + \frac{\tau_3\mathcal{D}_3}{c}\right) + \frac{1}{2}\left(\frac{A}{a} + \frac{B}{b} + \frac{C}{c}\right)\mathbf{1}_2\,,$$

and

$$T_{\mathcal{A}}^\dagger = \left[i\frac{\partial_r}{f} + Q^f_{\rm em}\mathcal{A}(E_4) + \frac{i}{2}\left(\frac{\dot{a}}{a} + \frac{\dot{b}}{b} + \frac{\dot{c}}{c}\right)\right]\mathbf{1}_2 - iB_{\mathcal{A}}\,.$$

The operator $T_{\mathcal{A}}^\dagger$ is the adjoint operator of $T_{\mathcal{A}}$ with respect to the scalar product

$$\langle\phi|\,|\psi\rangle = \int dV\ \phi^\dagger\psi = \int e^1\wedge e^2\wedge e^3\wedge e^4\,(\phi^*)^{\rm T}\psi\,,$$

where ϕ and ψ are $\mathcal{L}_2$ functions. Consider the metric

$$ds^2_{\rm hTN} \equiv {\rm V}ds^2_{\rm H^3L} + {\rm V}^{-1}\sigma_3^2\,,$$

where

$$ds^2_{\rm H^3L} = dr^2 + 4L^2\sinh^2\left(\frac{r}{2L}\right)(\sigma_1^2 + \sigma_2^2)\,,$$

and we have introduced the positive function

$${\rm V} \equiv \frac{1}{L}\left(\frac{1}{\beta} + \frac{1}{e^{r/L}-1}\right) = \frac{e^{r/L}+\beta-1}{\beta L(e^{r/L}-1)}\,,$$

where β and L are non-negative constant. If we conformally rescale the metric $ds^2_{\rm hTN}$ with the conformal factor

$$\Lambda \equiv \sqrt{\frac{4L}{\beta}}\frac{1}{(2-\beta)\cosh\left(\frac{r}{2L}\right) + \beta\sinh\left(\frac{r}{2L}\right)}\,,$$

we obtain a 1-parameter family of metrics

$$ds^2_\beta = \Lambda^2 ds^2_{\rm hTN}\,. \tag{3.65}$$

For $\beta \to 2$ we get, making the change of variables

$$r = \rho\,\mathrm{arccoth}\left(\frac{w^2}{\rho^2}\right), \quad \rho = 2L,$$

the AEH line element

$$ds^2_{\beta=2} = \frac{dw^2}{1-(\rho/w)^4} + \frac{w^2}{4}\left[\sigma_1^2 + \sigma_2^2 + \left(1-\left(\frac{\rho}{w}\right)^4\right)\sigma_3^2\right]\,, \tag{3.66}$$

while, for $\beta \to 0$ we get the Taub-NUT line element. We are now going to explicitly solve the Dirac zero-mode equation $\not{D}_{\mathcal{A}}\psi = 0$ on the manifold defined by the line element in eq. (3.65) with the connection of the kind (see eq. (3.55))[8]

$$\mathcal{A} = p\mathcal{A}_3\sigma_3 = p\frac{\sigma_3}{\beta L V} \xrightarrow[\text{AEH}]{} \frac{p\rho^2}{w^2}\sigma_3 \,, \tag{3.67}$$

where p is a real constant. We furthermore are interested in the case $a = b$. In the presence of the gauge connection given in eq. (3.67), after some algebra, eq. (3.65) becomes

$$T_p = i\left[\left(\frac{\partial_r}{f} + \frac{\dot{a}}{a} + \frac{\dot{c}}{2c}\right)\mathbf{1} + \frac{\sqrt{V}\lambda}{2\Lambda}P_p\right] \,,$$

where

$$P_p = \begin{pmatrix} \lambda^{-1}(2iX_3 - Q^f_{\text{em}}\tilde{p}) & 2iX_- \\ 2iX_+ & -\lambda^{-1}(2iX_3 - Q^f_{\text{em}}\tilde{p}) \end{pmatrix} + \left(\frac{\lambda^2+2}{2\lambda}\right)\mathbf{1}_2 \,, \tag{3.68}$$

$X_\pm = X_1 \pm iX_2$ and we have introduced the constants

$$\lambda^{-1} = 2LV\sinh\left(\frac{r}{2L}\right),$$
$$\tilde{p} = \frac{p}{\beta L V} \,.$$

Thus, in order to compute the eigenvectors of $\not{D}_{\mathcal{A}}\psi = 0$, we have to compute the eigenvectors of P_p [121]. The Laplace operator

$$\Delta_{S^3} = -X_1^2 - X_2^2 - X_3^2 \,,$$

commutes with iX_3, thus we can consider the basis of simultaneous eigenvectors

$$\left\{ |j, m, m'\rangle \,|\, 2j \in \mathbb{Z}, \quad 2m, 2m' \in \mathbb{Z}, \quad |m| \le j, |m'| \le j \right\} \,,$$

$$\Delta_{S^3}\,|j, m, m'\rangle = j(j+1)\,|j, m, m'\rangle \,,$$
$$iX_3\,|j, m, m'\rangle = m\,|j, m, m'\rangle \,.$$

iX_3 and $iX_\pm$ satisty the angular momentum algebra, which means

$$iX_+\,|j, m, m'\rangle = \sqrt{(j-m)(j+m+1)}\,|j, m+1, m'\rangle \,,$$
$$iX_-\,|j, m, m'\rangle = \sqrt{(j+m)(j-m+1)}\,|j, m-1, m'\rangle \,.$$

Given the expression for P_p it is quite natural to male the ansatz for its eigenvector to be of the form

$$\begin{pmatrix} \alpha\,|j, m, m'\rangle \\ \beta\,|j, m+1, m'\rangle \end{pmatrix} \,, \tag{3.69}$$

for some real constants α, β to be determined. Substituting eq. (3.69) in the eigenvalue equation for B_p one obtains

$$\frac{\alpha}{\beta} = \frac{1}{2\lambda\sqrt{(j-m)(j+m+1)}} \times \left[1 + 2m - Q^f_{\text{em}}\tilde{p} \pm \sqrt{(1 + 2m - Q^f_{\text{em}}\tilde{p})^2 + 4\lambda^2(j-m)(j+m+1)}\right] \,,$$

[8]We notice that, in the colored case, the gauge connection could be written as $\mathcal{A} = p\mathcal{A}_3^a\sigma_3\tau_a$, where τ_a is the color $SU(2)$ Pauli matrix.

and we have the eigenvalues, with multiplicity $2j+1$ (m' is a spectator at this level)

$$\frac{\lambda}{2} \pm \frac{1}{\lambda}\sqrt{(1+2m-Q^f_{\rm em}\tilde{p})^2+4\lambda^2(j-m)(j+m+1)}\,.$$

The above result holds for $-j \leq m \leq j-1$. Indeed, for $m=j$ we have the eigenvector

$$\begin{pmatrix} |j,j,m'\rangle \\ 0 \end{pmatrix},$$

with eigenvalue

$$\frac{\lambda}{2}+\frac{1}{\lambda}(2j+1-Q^f_{\rm em}\tilde{p}),$$

and multiplicity $2j+1$. For $m=-j-1$ we have the eigenvector

$$\begin{pmatrix} 0 \\ |j,-j,m'\rangle \end{pmatrix},$$

with eigenvalue

$$\frac{\lambda}{2}+\frac{1}{\lambda}(2j+1+Q^f_{\rm em}\tilde{p}),$$

and multiplicity $2j+1$.
We are now ready to solve the Dirac equation for the zero-modes over the backgrounds given by eq. (3.65)

$$\not{D}_p\psi=\not{D}_p\begin{pmatrix}\Psi\\ \Phi\end{pmatrix}=0\,,$$

where Ψ and Φ are 2-component Weyl spinors. Since

$$\not{D}_p\psi=\begin{pmatrix}0 & T_p^\dagger\\ T_p & 0\end{pmatrix}\begin{pmatrix}\Psi\\ \Phi\end{pmatrix}=0\Rightarrow\begin{cases}T_p\Psi=0,\\ T_p^\dagger\Phi=0\,.\end{cases}$$

It can be shown that $T_p^\dagger$ has trivial kernel, hence we can set $\Phi=0$. Using spherical symmetry, the spinor Ψ has the form

$$\Psi=\begin{pmatrix}K_1\\ K_2\end{pmatrix}h(r)\,|j,m,m'\rangle\ ,$$

where $K_{1,2}$ are arbitrary constants and $h(r)$ is a radial function. From the form of P_p in eq. (3.68) follows that, since for general $K_{1,2}\neq 0$,

$$P_p\begin{pmatrix}K_1\\ K_2\end{pmatrix}|j,m,m'\rangle \not\propto \begin{pmatrix}K_1\\ K_2\end{pmatrix}|j,m,m'\rangle\ ,$$

the equation $\not{D}_p\Psi=0$ has non-trivial solutions for

$$K_2=0\Rightarrow m=j\,,$$

or

$$K_1=0\Rightarrow m=-j\,.$$

As a consequence of eq. (3.65), we have

$$\begin{aligned} a=b=\Lambda a_{\rm hTN}&=2L\Lambda\sinh\left(\frac{r}{2L}\right)\ ,\\ c=\Lambda c_{\rm hTN}&=\frac{\Lambda}{\sqrt{V}}\,,\\ f=\Lambda f_{\rm hTN}&=\Lambda\sqrt{V}\,,\end{aligned}$$

and

$$
\begin{aligned}
T_p =& \frac{i}{2L\Lambda\sqrt{V}}\Bigg\{\Bigg[-2L\partial_r - \frac{LV_{,r}}{2V} - \coth\left(\frac{r}{2L}\right) \\
&+ \frac{3}{2}\left(\frac{(2-\beta)\sinh\left(\frac{r}{2L}\right)+\beta\cosh\left(\frac{r}{2L}\right)}{(2-\beta)\cosh\left(\frac{r}{2L}\right)+\beta\sinh\left(\frac{r}{2L}\right)}\right)\Bigg]\mathbf{1}_2 + \frac{P_p}{2\sinh\left(\frac{r}{2L}\right)}\Bigg\}\,.
\end{aligned}
\tag{3.70}
$$

For $K_2 = 0$

$$T_p\Psi = 0\,,$$

has the solution

$$h(r) = \mathcal{K}\frac{\left(e^{r/L}-1\right)^j\left(-\beta+e^{r/L}+1\right)^{3/2}}{\sqrt{\beta+e^{r/L}-1}}e^{-\frac{r}{4L}\left(3+4j+\frac{2}{\beta}(2Q^f_{\text{em}}p-2j-1)\right)}\,, \tag{3.71}$$

where $\mathcal{K}$ is a complex integration constant. In the case $K_1 = 0$, one obtains the solution in eq. (3.71) with p replaced by $-p$. Concentrating on the case $K_2 = 0$, for large r, $h(r)$ has the asymptotic behavior

$$h(r) \approx \exp[-\frac{r}{4L}\left(-1+\frac{2}{\beta}(2Q^f_{\text{em}}p-2j-1)\right)]\,.$$

We now impose this function to be square integrable with respect to the volume element

$$dV = fabc\,\sigma_1\wedge\sigma_2\wedge\sigma_3\wedge\,dr \approx e^{-r/L}\,\sigma_1\wedge\sigma_2\wedge\sigma_3\wedge\,dr\,,$$

therefore, for $h(r)$ to be $\mathcal{L}_2$ we must have

$$2j+1 < \frac{\beta}{2} + 2Q^f_{\text{em}}p\,,$$

that is

$$1 \le 2j+1 < \frac{\beta}{2} + 2Q^f_{\text{em}}p \quad\Rightarrow\quad 2Q^f_{\text{em}}p > 1-\frac{\beta}{2}\,.$$

Analogously, for $K_1 = 0$

$$1 \le 2j+1 < \frac{\beta}{2} - 2Q^f_{\text{em}}p \quad\Rightarrow\quad 2Q^f_{\text{em}}p < 1-\frac{\beta}{2}\,.$$

Therefore, for fixed j we have (remember that m' is a spectator at this level) $2j+1$ distinct solutions coming from the allowed values for m', giving

$$\dim(\text{Ker}(T_p)) = \sum_{2j+1=1}^{[2|Q^f_{\text{em}}p|+\beta/2]}(2j+1)\,,$$

where $[n]$ is the largest integer strictly smaller than n (so that $[3] = 2$ etc). In the AEH case, see eq. (3.61), $Q^f_{\text{em}}p$ is an integer, therefore the number of zero-modes of the Dirac operator is

$$
\begin{aligned}
|n_+ - n_-| &= \sum_{2j+1=1}^{[2|Q^f_{\text{em}}p|+1]}(2j+1) \\
&= |Q^f_{\text{em}}p|\left(2|Q^f_{\text{em}}p|+1\right)\,,
\end{aligned}
\tag{3.72}
$$

furthermore the zero-modes take the form

$$\psi_+^{(j)}(x) = \begin{pmatrix} h^{(j)}(r)\,|j,j,m'\rangle \\ 0 \\ 0 \\ 0 \end{pmatrix}, \quad Q^f_{\rm em} p > 0 \tag{3.73}$$

or

$$\psi_-^{(j)}(x) = \begin{pmatrix} 0 \\ h^{(j)}(r)\,|j,-j,m'\rangle \\ 0 \\ 0 \end{pmatrix}, \quad Q^f_{\rm em} p < 0\,, \tag{3.74}$$

where

$$h^{(j)}(r) = c_1 2^{3j+4}\left(\frac{L^2}{w^2-4L^2}\right)^{j+\frac{3}{2}}\left(\frac{w^2-4L^2}{w^2+4L^2}\right)^{\frac{1}{2}(j+|Q^f_{\rm em}p|+1)}\sqrt{\frac{w^2-4L^2}{w^2}}\,,$$

that is choosing $c_1 = 2^{-3j-4}L^{-2j-3}\mathcal{K}$, we obtain (see eq. (3.66))

$$h^{(j)}(r) = \mathcal{K}\,\frac{1}{w[w^4-\rho^4]^{(j+1)/2}}\left(\frac{w^2-\rho^2}{w^2+\rho^2}\right)^{\frac{|Q^f_{\rm em}p|}{2}}\,,$$
$$r = \rho\,\mathrm{arccoth}\left(\frac{w^2}{\rho^2}\right)\,,\quad \rho = 2L\,,$$

with $\mathcal{K}$ a normalization factor. That is, we have the normalized mode

$$h^{(j)}(r) = 2^{j+1}\sqrt{\frac{2}{\pi}}\left[\frac{\Gamma\left(j+|Q^f_{\rm em}p|+1\right)}{\Gamma(2j+1)\Gamma\left(|Q^f_{\rm em}p|-j\right)}\right]^{1/2}\frac{\rho^{2j+1}}{w[w^4-\rho^4]^{(j+1)/2}}\left(\frac{w^2-\rho^2}{w^2+\rho^2}\right)^{\frac{|Q^f_{\rm em}p|}{2}}\,, \tag{3.75}$$

where

$$r = \rho\,\mathrm{arccoth}\left(\frac{w^2}{\rho^2}\right)\,,\quad \rho = 2L\,, \tag{3.76}$$

and

$$j = 0,\ldots,\frac{2|p\,Q^f_{\rm em}|-1}{2}\,. \tag{3.77}$$

Analogously to SU(N) gauge group, the index $\not{D}_{\mathcal{A}}$, could also be computed – instead of computing explicitly and then counting the zero modes – in an integral form using the Atiyah-Patodi-Singer (APS) index theorem [111, 118, 122].

3.6 Appendix C: Closing fermion loops with Yukawa interactions in the AEH manifold

Having identified the 't Hooft vertex, we have to tie up the fermion zero-modes using all the interactions at disposal. For instance, allowing for a Yukawa-type interaction, we have to evaluate integrals of the kind

$$\mathcal{I} = \int d^4x_1\sqrt{g}\,d^4x_2\sqrt{g}\times$$
$$\times\,[h^{(j)}(x_1)]^2\mathcal{G}_F(x_1,x_2)[h^{(j')}(x_2)]^2\,, \tag{3.78}$$

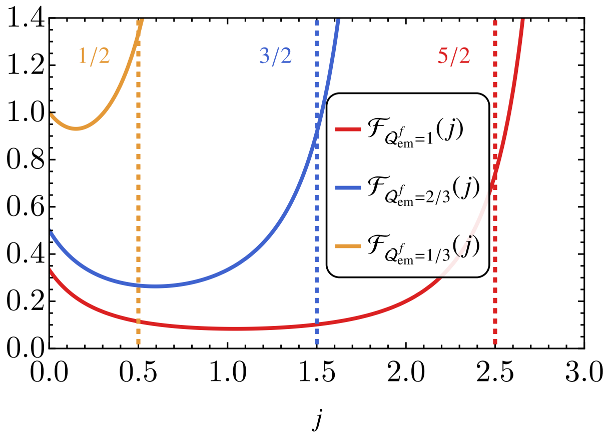

Figure 3.7: *Functions* $\mathcal{F}_{\mathcal{Q}^f}(j)$ *for* $\mathcal{Q}^f_{\rm em} = 1, 1/3, 2/3$, *where from* (3.75), $j_{\rm max}(\mathcal{Q}_{\rm em} = 1) = 5/2\,,\ j_{\rm max}(\mathcal{Q}_{\rm em} = 1/3) = 1/2\,,\ j_{\rm max}(\mathcal{Q}_{\rm em} = 2/3) = 3/2$.

where $\mathcal{G}_F(x_1, x_2)$ is the Euclidean scalar propagator in the AEH background, computed solving

$$\left(g^{\mu\nu}_{\rm EH}\nabla_\mu\nabla_\nu + m_s^2\right)\mathcal{G}_F(x,x') = -4\pi\,\sqrt{g_{\rm EH}}\delta^{(4)}(x-x')\,.$$

In principle, to do computations with $O(1)$ accuracy, we should compute numerically the integral in eq. (3.78); however we will discuss a counting rule for π^2 factors appearing in instanton diagrams. Indeed, as in the Yang-Mills case, one might think at first glance that instanton amplitudes are highly suppressed by loop factors, nonetheless the meaning of *loop* is not trivial in instanton calculus. Similarly to the flat spacetime case, from the integration over vertices we get

$$\int d^4x\sqrt{g} \propto \frac{8}{\pi^2}\int_\rho^\infty dr\, r^3\,, \tag{3.79}$$

in addition to the $1/\pi^2$ provided by momentum integration. Moreover, from the explicit expression of the zero modes on EH, see eq. (3.75), the zero-mode wavefunctions do not contain π factors other the ones coming from the normalization. Therefore, for $Q^f_{\rm em}p > 0$, we estimate

$$\begin{aligned}\mathcal{I} &\propto \left(\frac{8}{\pi^2}\right)^2\frac{1}{\pi^2}\left(\frac{8}{\pi^2}\right)^2\left[\frac{\Gamma(2j+1)\Gamma\left(Q^f_{\rm em}p-j\right)}{\Gamma\left(j+Q^f_{\rm em}p+1\right)}\right]\left[\frac{\Gamma(2j'+1)\Gamma\left(Q^f_{\rm em}p-j'\right)}{\Gamma\left(j'+Q^f_{\rm em}p+1\right)}\right]\\ &\approx \frac{1}{\pi^2}\mathcal{F}_{Q^f_{\rm em}}(j)\mathcal{F}_{Q^f_{\rm em}}(j')\,,\end{aligned} \tag{3.80}$$

where we introduced

$$\mathcal{F}_{Q^f_{\rm em}}(j) = \frac{\Gamma(2j+1)\Gamma\left(Q^f_{\rm em}p-j\right)}{\Gamma\left(j+Q^f_{\rm em}p+1\right)}\,. \tag{3.81}$$

Therefore, up to $O(1)$ factors, we can count a loop with a $1/\pi^2$ loop suppression factor.

3.7 Appendix D: One scale, one coupling

In the MKS system [123], there are three fundamental units: length [L], mass [M] and time [T]. From these three fundamental units, all other units (such as force, energy, pressure, etc.) can be derived. Specifically, the energy [E] is given by the combination [E] = [M][L]^2/[T]^2. Let us now consider a system of units in which $c = \epsilon_0 = 1$ (where ϵ_0 is the vacuum permittivity). In this case, we have [L]=[T] and, consequently only two fundamental units remain, namely [L] and [M]. Since now [E]=[M], we can work with [L]=[T] and [E]. The action $\mathcal{S}$ has the dimensions of energy multiplied by tume, $[\mathcal{S}] = [\mathrm{E}][\mathrm{L}]$, which corresponds to the dimensionality of the Planck constant. Therefore, we can write $[\mathcal{S}] = [\hbar] = [\mathrm{E}][\mathrm{L}]$. It follows that the dimension of a Lagrangian density is – in four dimensions – $[\mathcal{L}] = [\hbar]/[L]^4$. From the corresponding canonical kinetic terms, we therefore obtain the dimensions of a bosonic field ϕ and a fermionic field Ψ

$$\mathcal{L}_\phi \supset \frac{(\partial\phi)^2}{2} \Rightarrow [\phi]^2/[L]^2 = [\hbar]/[L]^4 \Leftrightarrow [\phi] = [\hbar]^{1/2}/[L]\,, \tag{3.82}$$

$$\mathcal{L}_\Psi \supset \overline{\Psi}\partial\!\!\!/\Psi \Rightarrow [\Psi]^2/[L] = [\hbar]/[L]^4 \Leftrightarrow [\Psi] = [\hbar]^{1/2}/[L]^{3/2}\,. \tag{3.83}$$

It then follows that a mass parameter m_*, whether bosonic of fermionic, appearing in the Lagrangian has the dimension $[m_*] = [\mathrm{L}]^{-1}$, that is, it corresponds to the inverse of a length scale (consequently, note that $[m_*] = [\mathrm{E}]/[\hbar]$). This sharply defines m_* as a scale, namely a length scale. A typical coupiling g_* in the Lagrangian, such as a Yukawa coupling or a gauge coupling, *i.e.* $g_*\phi\overline{\Psi}\Psi$, or $g_* A_\mu \overline{\Psi}\gamma^\mu\Psi$, has the dimension $[g_*] = [\hbar]^{-1/2}$. In natural units. the dimensionality of the coupling is obscured, and one might be tempted to treat g_* as if it were a dimensionelss numerical constant. However, by reinstating $\hbar$, the fundamental distinction between g_* and a pure number becomes evident. In gravity, the Ricci scalar R has the dimension of $[\mathrm{L}]^{-2}$ (since it is quadratic in the derivatives of the metric), thus from the Einstein-Hilbert action

$$\mathcal{S}_{\mathrm{E-H}} = \frac{\bar{M}_{\mathrm{Pl}}}{8\pi}\int d^4x\sqrt{-g}\,R \Rightarrow [\hbar] = [\mathrm{L}]^2[\bar{M}_{\mathrm{Pl}}]^2 \Leftrightarrow [\bar{M}_{\mathrm{Pl}}] = [\hbar]^{1/2}/[\mathrm{L}]\,. \tag{3.84}$$

Motivated by the previous relation, it is useful to introduce the coupling dimension [C] such that

$$[\mathrm{C}] = [\hbar]^{-1/2} = [\mathrm{E}]^{-1/2}[\mathrm{L}]^{-1/2}\,.$$

The Lagrangian density has then dimensions

$$[\mathcal{L}] = \frac{1}{[\mathrm{C}]^2[\mathrm{L}]^4}\,, \tag{3.85}$$

and also, we have

$$[\mathrm{C}][\bar{\mathrm{M}}_{\mathrm{Pl}}] = [\mathrm{L}]^{-1}\,, \tag{3.86}$$

that is, the product of the Planck mass times a fundamental coupling is sthe inverse of a length scale. Similarly, an object like the Goldstone decay constant f_π, where $U(x) = \exp(i\sigma^a\pi_a(x)/f_\pi)$, has then the dimensions

$$[\mathrm{C}][f_\pi] = [\mathrm{L}]^{-1}\,. \tag{3.87}$$

Assuming the existence of one fundamental coupling g_* and one fundamental scale m_*, we write the Lagrangian density in the form

$$\mathcal{L} = \frac{m_*^4}{g_*^2}\hat{\mathcal{L}}\left(\frac{\partial}{m_*}, \frac{g_*\phi}{m_*}, \frac{g_*\Psi}{m_*^{3/2}}, \frac{R}{m_*^2}\right)\,, \tag{3.88}$$

where, assuming all fields canonically normalized, $\hat{\mathcal{L}}$ is a dimensionless polynomial functional with arbitrary order-one numerical coefficients.

Part II

The strong CP problem: axion detection

CHAPTER

4

An Effective Field Theory for anisotropic antiferromagnets

4.1 Introduction

Antiferromagnets are magnetic materials which, below a certain temperature, exhibit long range order but no net magnetization. Contrary to ferromagnets, they were initially thought to have limited practical applications [124]. Recent years, however, have witnessed the development of a plethora of such applications, ranging from electron transport controlled by the spin degrees of freedom [e.g., 125, 126], the so-called spintronics, the development of quantum sensors [e.g., 127, 128], and, recently, light dark matter detection [129, 130]. Moreover, magnetic materials, both ferromagnets and antiferromagnets, are typically regarded as the textbook example for the phenomenon of spontaneous symmetry breaking and the emergence of Goldstone bosons [e.g., 131]. These are indeed nothing but the spin collective excitations of these systems, the so-called magnons.

Yet, in reality, the spectrum of most antiferromagnets feature tiny but non-zero gaps. This can be attributed to magneto-crystalline anisotropies, which provide small effects of explicit symmetry breaking. This is due to the presence of certain energetically favorable directions for the spins of the material, which are dictated by the underlying crystal structure of the antiferromagnet. These anisotropies, along with the exchange interaction, in turn determine the ground state of the system as well its behavior under the application of an external magnetic field.

In this work we extend the well known effective field theory (EFT) for magnons in antiferromagnet [e.g., 131–133] to include these anisotropic effects. In particular, we will consider the case where the system features two distinct anisotropies, the so-called "easy plane" antiferromagnets [134]. The other class of anisotropic antiferromagnets, so-called "easy axis", feature only one anisotropy, but their spectrum can be obtained from that the previous class, simply setting one of the parameters to zero. We will show that this extended EFT, while being eventually rather simple, features a number of interesting phenomena, such as the presence of the so-called gapped Goldstones [e.g., 135–138], their lifting to pseudo-Goldstones, as well as the presence of the so-called "spin flop" phase transition triggered by a varying external magnetic field, where the spin alignment in the ground state suddenly changes its direction [e.g., 134]. All this, is computable within the regime of validity of the EFT.

Moreover, in the presence of a magnetic field, as we will see, the theory cannot be diagonalized by a local redefinition. Hence it requires a careful quantization procedure, which we address in this work. Finally, we match our EFT to the short distance theory for a particular antiferromagnet, namely, nickel oxide (NiO). The latter, thanks to its simple structure and spin interactions, is often considered as the prototypical room-temperature antiferromagnet. Indeed, this material has been used to study a number of different processes, such as inelastic light scattering [e.g., 139, 140] and magnetic response to terahertz frequencies [141, 142]. Moreover, as mentioned, it has recently been realized that such a system offers an optimal target to look for the scattering of dark matter with spin-dependent interactions and masses as low as the keV [129], as well as to look for axion-like dark matter with masses in the meV range [143].

The goal of this work is also to present everything in a framework which can bridge the linguistic gap that is often present between the standard condensed matter and high energy physics literature. This is particularly important in light of the role that antiferromagnets might play in future searches for light dark matter, a genuinely high energy physics question which, however, requires condensed matter tools to be tackled. Moreover, an EFT formulation has the great advantage of allowing to neatly disentangle those phenomena that are universal, i.e. solely due to long-distance physics, from those that are, instead, due to a specific short-distance realization of the system.

Conventions: We adopt natural units, $\hbar = c = 1$, and an index notation such that $i, j, k = 1, 2, 3$ label spatial coordinates. We also employ Einstein's notation for summing over repeated indices.

4.2 The EFT

We now proceed to the construction of our EFT step-by-step, from the simplest instance to the most involved one. Throughout our manuscript, we assume to work at zero temperature. This is partially motivated by the phenomenological reasons highlighted in Ref. [143], but also due to the fact that the inclusion of thermal effects in a general quantum field theory is typically rather non-trivial and beyond the scope of this work.

4.2.1 The simplest EFT: the isotropic case

Let us start by reviewing the construction of the standard EFT for antiferromagnets, which has been discussed, for example, in Refs. [131–133]. We will go through this review rather thoroughly, in order to set the stage to the subsequent study, as well as highlight a few points which can make an easier connection between the high and low energy formalisms used to described antiferromagnets.

At distances comparable to its lattice spacing, an antiferromagnet is essentially a collection of magnetic moments, which antialign with respect to the neighboring ones. These magnetic moments typically arise from the fundamental spin of the unpaired electrons localized around each atom of the crystal. The exchange and superexchange interactions between electrons pertaining to different atoms give rise to a coupling between these spins. The simplest example of a short distance Hamiltonian describing such a system is given by the Heisenberg model [e.g., 144],

$$H_0 = \sum_{\boldsymbol{i},\boldsymbol{j}\in\mathbb{A}} J_{\boldsymbol{ij}}\, \boldsymbol{\mathcal{S}}_{\boldsymbol{i}} \cdot \boldsymbol{\mathcal{S}}_{\boldsymbol{j}} + \sum_{\boldsymbol{i},\boldsymbol{j}\in\mathbb{B}} J_{\boldsymbol{ij}}\, \boldsymbol{\mathcal{S}}_{\boldsymbol{i}} \cdot \boldsymbol{\mathcal{S}}_{\boldsymbol{j}}\,, \tag{4.1}$$

where $\boldsymbol{i}$ and $\boldsymbol{j}$ are positions on the lattice, which is usually seen as "bipartite", i.e., as composed of two sublattices, which we label as $\mathbb{A}$ and $\mathbb{B}$. $\boldsymbol{\mathcal{S}}_{\boldsymbol{i}}$ is the spin pertaining to a given lattice site, and $J_{\boldsymbol{ij}}$ are the above mentioned couplings. For an antiferromagnet, all the spins have the same magnitude, $|\boldsymbol{\mathcal{S}}_{\boldsymbol{i}}| = \mathcal{S}$.

In an antiferromagnet, the couplings J are such that the zero-temperature classical ground state, i.e., the state corresponding to the minimum classical energy,[1] corresponds to a configuration where all

[1]Contrary to ferromagnets, the exact *quantum* ground state of an antiferromagnet is unknown, and it is only approximated by its classical counterpart. Yet, the spin wave theory built out of this latter ground state gives a very accurate description of experimental results [e.g., 144].

the spins in the sublattice $\mathbb{A}$ are aligned parallel to each other, and those in the sublattice $\mathbb{B}$ are aligned in the opposite direction. The emergence of this ground state is quantified by an order parameter, the Néel vector, given by $\boldsymbol{\mathcal{N}} \equiv \sum_{i\in\mathbb{A}} \boldsymbol{\mathcal{S}}_{\boldsymbol{i}} - \sum_{i\in\mathbb{B}} \boldsymbol{\mathcal{S}}_{\boldsymbol{i}}$. On the classical ground state, the Néel vector acquires an expectation value parallel to the spins, $\langle\boldsymbol{\mathcal{N}}\rangle \neq 0$, which can in principle be aligned in *any* direction. The spin-wave excitations of the system, called magnons, are the long wavelength modulations of the order parameter around its equilibrium value.

From a symmetry viewpoint, the Hamiltonian (4.1) enjoys a global SO(3) symmetry, corresponding to the simultaneous rotation of all spins, $\boldsymbol{\mathcal{S}}_{\boldsymbol{i}} \to \mathcal{R}\cdot\boldsymbol{\mathcal{S}}_{\boldsymbol{i}}$, with $\mathcal{R}$ a 3×3 rotation matrix. Nonetheless, this symmetry is not respected by the ground state order parameter, which selects a specific direction. In other words, the original spin rotations are spontaneously broken down to the subgroup that leaves the order parameter unchanged, i.e., SO(3) $\to$ SO(2). In this respect, magnons are nothing but the associated Goldstone bosons and, as such, their dynamics can be described by an EFT valid at low energies and long wavelengths.

Beside the continuous symmetry just discussed, a central role is played by two discrete symmetries: time reversal, $\mathcal{T}$, and a discrete rotation of 180° in the plane where the spins lie, which we represent by $\mathcal{R}_\pi$. Both these transformations act on the spins by changing the direction of all of them. The order parameter thus changes sign under the separate action of $\mathcal{T}$ and $\mathcal{R}_\pi$, i.e.,

$$\boldsymbol{\mathcal{N}} \xrightarrow{\mathcal{T}} -\boldsymbol{\mathcal{N}}\,, \qquad \boldsymbol{\mathcal{N}} \xrightarrow{\mathcal{R}_\pi} -\boldsymbol{\mathcal{N}}\,. \tag{4.2}$$

Consequently, the theory must be invariant under their combined action, which leaves the order parameter unchanged.[2]. Here we prefer to phrase everything in terms of the rotation for two reasons: (1) it is better defined at long wavelengths, where one is insensitive to distances comparable to the lattice spacing, and (2) we believe that, phrased this way, it allows for a unified description of ferromagnets and antiferromagnets, as we explain in Appendix 4.7. The complete symmetry breaking pattern is then SO(3) $\times\,\mathcal{T} \to$ SO(2) $\times\,(\mathcal{T}\mathcal{R}_\pi)$. The EFT we present here is built in order to implement this pattern.

Now, magnons correspond to local modulations of the order parameter away from equilibrium, represented by a field $\hat{\boldsymbol{n}}(x)$, with $\langle\hat{\boldsymbol{n}}\rangle \propto \langle\boldsymbol{\mathcal{N}}\rangle$ and $\hat{\boldsymbol{n}}^2 = 1$.[3] With this at hand, the most general low energy EFT for magnons with at most two derivatives is simply given by [131],

$$\mathcal{L}_0 = \frac{c_1}{2}\left[(\partial_t\hat{\boldsymbol{n}})^2 - v_\theta^2(\nabla_i\hat{\boldsymbol{n}})^2\right]\,, \tag{4.3}$$

where c_1 is an effective coefficient that can be determined in terms of parameters of the microscopic Hamiltonian, as done in Ref. [129], while v_θ is the magnon propagation speed. All possible additional terms necessarily contain more derivatives and are therefore suppressed in the low energy/long wavelength limit.

Note that, by treating time derivatives and spatial gradients as completely independent from each other, we assumed the *explicit* breaking of boost invariance (whether Galileo or Lorentz is irrelevant). This is ultimately not what happens in Nature, as boosts are always *spontaneously* broken by the underlying lattice, and the ordinary gapless acoustic phonons are the corresponding Goldstones bosons necessary to recover the full symmetry, which they realize non-linearly [e.g., 145, 146]. Our approximation is valid as long as we are not interested in the phonon dynamics and their interplay with magnons. For an EFT including both, see Ref. [133].

[2] In the literature, instead of the discrete rotation we are using here, one often finds a discussion involving the action of a translation by a single lattice site [e.g., 131], which effectively exchanges the two sublattices, $\mathbb{A}$ and $\mathbb{B}$, thus changing the sign of the order parameter

[3] This can be understood from the fact that the coset space SO(3)/SO(2) $\simeq$ S^2, which is the unit 2-sphere, and $\hat{\boldsymbol{n}}$ denotes the unit vector on S^2.

In the presence of an external uniform magnetic field, $\mathbf{H}$, the microscopic Heisenberg Hamiltonian in Eq. (4.1) is modified by the Zeeman term,

$$H_{\mathrm{H}} = H_0 - \mu \sum_{\boldsymbol{i}} \mathbf{H} \cdot \boldsymbol{\mathcal{S}}_{\boldsymbol{i}} \,, \tag{4.4}$$

where μ is the gyromagnetic ratio of the spins. At the level of the EFT, as explained for example in Ref. [147], this can be included by promoting the time derivative in the Lagrangian $\mathcal{L}_0$ to a "covariant" derivative, $\partial_t \hat{\boldsymbol{n}} \to \partial_t \hat{\boldsymbol{n}} + \mu \mathbf{H} \times \hat{\boldsymbol{n}}$, i.e.,

$$\mathcal{L}_{\mathrm{H}} = \frac{c_1}{2} \left[(\partial_t \hat{\boldsymbol{n}} + \mu \mathbf{H} \times \hat{\boldsymbol{n}})^2 - v_\theta^2 (\nabla_i \hat{\boldsymbol{n}})^2 \right] . \tag{4.5}$$

The correctness of this procedure is guaranteed by the fact, when going to the associated Hamiltonian density, one indeed recovers a purely Zeeman term, as expected.

To determine the spectrum of this theory, we first need to find the background value for $\hat{\boldsymbol{n}}$. This is done by minimizing the Hamiltonian density, taken in the static and homogeneous limit, which reads

$$\mathcal{H}_{\mathrm{H}}\big|_{\text{stat., homog.}} = -\,\mathcal{L}_{\mathrm{H}}\big|_{\text{stat., homog.}} = -\frac{c_1}{2}(\mu \mathbf{H} \times \hat{\boldsymbol{n}})^2 = \frac{c_1}{2} \mu^2 \mathrm{H}^2 \left(\hat{n}_z^2 - 1 \right) , \tag{4.6}$$

where we take the magnetic field to be aligned along the z-axis, $\mathbf{H} = \mathrm{H}\, \hat{\boldsymbol{z}}$, a configuration we will assume in the rest of the work for simplicity. (A more general case is reported in Appendix 4.8.) The Hamiltonian above is clearly minimized by any configuration such that $\hat{n}_z = 0$. Therefore, while in absence of magnetic field the background value of the order parameter can be aligned along any direction, now this freedom is restricted to the plane perpendicular to the magnetic field itself. We will then take our background value to be, for example, $\langle \hat{\boldsymbol{n}} \rangle = \hat{\boldsymbol{y}}$.

Following the standard coset construction ideas [148, 149], the magnon fields can be parametrized as local broken transformations around equilibrium. Specifically, the background spontaneously breaks the rotations generated by S_1 and S_3, meaning that we can express the magnon fields as $\hat{\boldsymbol{n}}(x) = e^{i(\theta^1(x) S_1 + \theta^3(x) S_3)} \hat{\boldsymbol{y}}$. The corresponding quadratic Lagrangian is then,

$$\mathcal{L}_{\mathrm{H}} = \frac{c_1}{2} \left[\left(\dot{\theta}^1\right)^2 - v_\theta^2 \left(\boldsymbol{\nabla} \theta^1\right)^2 - \mu^2 \mathrm{H}^2 \left(\theta^1\right)^2 + \left(\dot{\theta}^3\right)^2 - v_\theta^2 \left(\boldsymbol{\nabla} \theta^3\right)^2 + \mathcal{O}\left(\theta^4\right) \right] , \tag{4.7}$$

and, the dispersion relations can be read off to be,

$$\omega_{q,-} = v_\theta q \,, \tag{4.8a}$$

$$\omega_{q,+} = \sqrt{\mu^2 \mathrm{H}^2 + v_\theta^2 q^2} \,. \tag{4.8b}$$

A comment about this spectrum is in order. In absence of magnetic field, the two modes are degenerate, and both gapless. This is because the background Hamiltonian of the system would be completely insensitive to the direction taken by $\langle \hat{\boldsymbol{n}} \rangle$. The two gapless modes are the Goldstone bosons reflecting this fact.

What happens at finite magnetic field? First of all, the existence of the gapless mode is the hallmark of the fact that the background Hamiltonian in Eq. (4.6) is still degenerate, but now only on the plane perpendicular to the z-axis. The gapless mode is the corresponding Goldstone boson. Secondly, the second mode, has a gap that is *universal*, meaning that it does not depend on the microscopic details of the system, which here are encoded in the effective coefficient c_1: it is solely dictated by the magnetic field. This is, instead, the hallmark of the so-called gapped Goldstones [135–138], which arise when a system has a finite density for one of its non-Abelian broken generators. This is indeed the case here for the broken charge S_3. In fact, the background value of the spin density, obtained from the SO(3) Noether current derived from the Lagrangian (4.5), is given by

$$\langle \boldsymbol{s} \rangle = \left\langle c_1 \left[\partial_t \hat{\boldsymbol{n}} \times \hat{\boldsymbol{n}} + \mathbf{H} - (\mathbf{H} \cdot \hat{\boldsymbol{n}})\, \hat{\boldsymbol{n}} \right] \right\rangle = c_1 \mathrm{H} \hat{\boldsymbol{z}} \,. \tag{4.9}$$

As another check of this, one can verify that the Lagrangian (4.5) can be obtained from the Lagrangian (4.3), valid in absence of magnetic field, by replacing $\hat{\boldsymbol{n}} \to e^{-i\mu \mathrm{H} t S_3} \cdot \hat{\boldsymbol{n}}$, which shows that the background under consideration also breaks time translations, but preserves a combination of them with a spin rotation generated by S_3. In other words, the symmetry breaking pattern in the presence of an external magnetic field is $\mathrm{SO}(3) \times H \to \bar{H} = H + \mu \mathbf{H} \cdot \boldsymbol{S}$.[4] One recognizes $\bar{H}$ to be precisely the modified Hamiltonian used to defined the ground state of a system at finite density for the operator $\mathbf{H} \cdot \boldsymbol{S}$. Crucially, gapped Goldstones are still *exact* Goldstone, meaning that they are needed to realize non-linearly the full SO(3) symmetry of the system.

4.2.2 EFT with anisotropies

As anticipated, we are interested in extending the EFT presented above to include the effects of tiny explicit breaking of the internal SO(3) symmetry, which are at the origin of the observed magnon gaps [e.g., 150, 151]. As mentioned in the Introduction, we are interested in the case of "easy plane" antiferromagnets, which involve two distinct anisotropies. (For a simpler illustrative case, see Ref. [147].) In particular, the microscopic Hamiltonian is modified to [151, 152]

$$H = H_{\mathrm{H}} + \sum_{\boldsymbol{i}} D_x \left(\boldsymbol{\mathcal{S}}^x_{\boldsymbol{i}}\right)^2 - \sum_{\boldsymbol{i}} D_z \left(\boldsymbol{\mathcal{S}}^z_{\boldsymbol{i}}\right)^2 , \tag{4.10}$$

where $D_x\,, D_z > 0$ are new anisotropic energies. The anisotropies along the x- and z-axes typically go under the name of, respectively, "hard axis" and "easy axis" anisotropy [134].

From the low energy viewpoint we again look at the symmetry breaking pattern. It is evident that the two anisotropies, if taken separately, would explicitly break the SO(3) spin rotations down to rotations around $\hat{\boldsymbol{x}}$, for the hard axis anisotropy, and around $\hat{\boldsymbol{z}}$, for the easy axis one. Since the additional terms in the Hamiltonian (4.10) are quadratic in the spins, they are also invariant under flipping of all the spins at the same time, $\boldsymbol{\mathcal{S}}_{\boldsymbol{i}} \to -\boldsymbol{\mathcal{S}}_{\boldsymbol{i}}$, which in turn corresponds to $\hat{\boldsymbol{n}} \to -\hat{\boldsymbol{n}}$. It follows, as it is probably reasonable to expect, that the additional terms in the effective Lagrangian are quadratic in the order parameter, i.e.,

$$\mathcal{L} = \frac{c_1}{2}\left[(\partial_t \hat{\boldsymbol{n}} + \mu \mathbf{H} \times \hat{\boldsymbol{n}})^2 - v_\theta^2 (\nabla_i \hat{\boldsymbol{n}})^2 + 2\lambda_z \hat{n}_z^2 - 2\lambda_x \hat{n}_x^2\right], \tag{4.11}$$

where $\lambda_x\,, \lambda_z > 0$ are two new effective coefficients, which can be determined in terms of the microscopic anisotropic energies (see Sec. 4.4). Their sign has been chosen for later convenience. In particular, the last two terms indeed explicitly break the full SO(3) group.

To define the ground state, we again consider static and homogeneous configurations in the Hamiltonian density,

$$\mathcal{H}\big|_{\text{stat., homog.}} = -\frac{c_1}{2}\left[(\mu \mathbf{H} \times \hat{\boldsymbol{n}})^2 + 2\lambda_z \hat{n}_z^2 - 2\lambda_x \hat{n}_x^2\right] = \frac{c_1}{2}\left[(\mu^2 \mathrm{H}^2 - 2\lambda_z)\hat{n}_z^2 + 2\lambda_x \hat{n}_x^2\right], \tag{4.12}$$

where we have dropped any irrelevant constant terms. Now, since $\lambda_x > 0$, the second term in the expression above is necessarily minimized by setting $\hat{n}_x = 0$. For the first term, instead, we have two possible configurations, depending on the relative strength between magnetic field effects and anisotropic ones. In particular, by defining a "spin-flop" field, $\mathrm{H}_{\text{s.f.}} \equiv \sqrt{2\lambda_z}/\mu$, we have

- for $\mathrm{H} > \mathrm{H}_{\text{s.f.}}$ the first terms is minimized by $\hat{n}_z = 0$, and the ground state is

$$\langle \hat{\boldsymbol{n}} \rangle = \hat{\boldsymbol{y}}\,;$$

  In this phase, the background value of the spin density in Eq. (5.6) — i.e., the total magnetization — is $\langle \boldsymbol{s} \rangle = c_1 \mathrm{H} \hat{\boldsymbol{z}}$. This is what is typically called the "spin-flop" phase [e.g., 134].

[4] To keep the notation light, we omit the discrete symmetries.

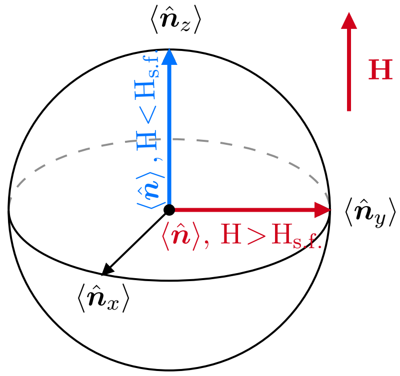

Figure 4.1: *Background configuration in the simultaneous presence of an external magnetic field* $\mathbf{H} = \mathrm{H}\hat{\boldsymbol{z}}$*, and both easy and hard axis anisotropies. Depending on the magnitude of the external magnetic field* H*, the system undergoes a phase transition, which, in the EFT framework, consists in a discontinuous change of the direction of the ground state.*

- for $\mathrm{H} < \mathrm{H}_{\rm s.f.}$ the first term is minimized by $\hat{n}_z = 1$, and the ground state is

$$\langle\hat{\boldsymbol{n}}\rangle = \hat{\boldsymbol{z}}\,.$$

  In this phase, instead, we have $\langle \boldsymbol{s}\rangle = 0$, which identifies this as the standard antiferromagnetic phase.

This situation is schematically represented in Fig. 4.1. Importantly, when the external magnetic field is varied across its spin-flop value, the order parameter, $\langle\hat{\boldsymbol{n}}\rangle$, is discontinuous. This is the hallmark of a first order phase transition [134, 153]. Let us study these two phases separately, starting with the instance where the anisotropies are a small correction to what done so far, and then consider the case where they become dominant over the magnetic field.

4.2.2.1 Small anisotropies: the $\mathrm{H} > \mathrm{H}_{\rm s.f.}$ phase

In this case the background is the same as in the absence of anisotropies, and we thus expect the explicit breaking effect to simply contribute to a small gap to the Goldstone modes. Indeed, by expanding again at quadratic order in the magnon fields, one gets,

$$\mathcal{L} = \frac{c_1}{2}\left[\left(\dot\theta^1\right)^2 - v_\theta^2\left(\boldsymbol{\nabla}\theta^1\right)^2 - \left(\mu^2\mathrm{H}^2 - 2\lambda_z\right)\left(\theta^1\right)^2 + \left(\dot\theta^3\right)^2 - v_\theta^2\left(\boldsymbol{\nabla}\theta^3\right)^2 - 2\lambda_x\left(\theta^3\right)^2 + \mathcal{O}\left(\theta^4\right)\right]. \tag{4.13}$$

The corresponding gaps are given by,

$$\omega_{q,+} = \sqrt{2\lambda_x + v_\theta^2 q^2}\,, \tag{4.14a}$$

$$\omega_{q,-} = \sqrt{\mu^2\mathrm{H}^2 - 2\lambda_z + v_\theta^2 q^2}\,. \tag{4.14b}$$

As anticipated, in this phase, the role of the anisotropies is that of turning the exact Goldstones described in Section 4.2.1 into *pseudo*-Goldstones. Moreover, the quadratic action above is simply a free theory for two independent real scalar fields. Consequently, it can be quantized in the standard way.

4.2.2.2 Large anisotropies: the $\mathrm{H} < \mathrm{H}_{\rm s.f.}$ phase

When the effects of the anisotropies are larger than those of the applied magnetic field, the background changes, and the system undergoes a phase transition. As an indication of this, the gap of the mode in

Eq. (4.14b) becomes imaginary, thus pointing to an instability. As anticipated, the new background is now $\langle \hat{\boldsymbol{n}} \rangle = \hat{\boldsymbol{z}}$. In this case, the broken generators are S_1 and S_2, and we must parametrize the magnon fields as $\hat{\boldsymbol{n}}(x) = e^{i\theta^a(x) S_a} \cdot \hat{\boldsymbol{z}}$, with $a = 1, 2$. Expanding Eq. (4.11) at quadratic order, one obtains

$$\mathcal{L} = \frac{c_1}{2} \left[\left(\dot{\theta}^a - \mu \mathrm{H} \epsilon^{ab} \theta^b \right)^2 - v_\theta^2 \left(\boldsymbol{\nabla} \theta^a \right)^2 - 2\lambda_z \left(\theta^a \right)^2 - 2\lambda_x \delta^{a2} \delta^{b2} \theta^a \theta^b + \mathcal{O}\left(\theta^4 \right) \right]. \tag{4.15}$$

In this phase, the quadratic Lagrangian is not diagonal in the magnon fields, θ^1 and θ^2. To determine the spectrum, we must write the linerized equations of motion in Fourier space, i.e. $\mathcal{M}^{ab}(\omega, q)\theta^b(\omega, \boldsymbol{q}) = 0$, with

$$\mathcal{M}^{ab}(q, \omega) = c_1 \left[\delta^{ab} \left(v_\theta^2 q^2 - \omega^2 + 2\lambda_z - \mu^2 \mathrm{H}^2 \right) + 2\lambda_x \delta^{a2} \, \delta^{b2} + 2\, i \mu \mathrm{H} \, \omega \, \epsilon^{ab} \right]. \tag{4.16}$$

The dispersion relations for the magnon modes are found by requiring that these equations of motion admit non-trivial solutions, that is to say, demanding that the determinant of the matrix above vanishes. After doing that, one obtains the following modes:

$$\omega_{q,\alpha=\pm}^2 = \mu^2 \mathrm{H}^2 + \lambda_x + 2\lambda_z + v_\theta^2 q^2 \pm \sqrt{\lambda_x^2 + 4\mu^2 \mathrm{H}^2 \left(\lambda_x + 2\lambda_z + v_\theta^2 q^2 \right)}\,. \tag{4.17}$$

The corresponding gaps are

$$\omega_{0,\pm}^2 = \mu^2 \mathrm{H}^2 + \lambda_x + 2\lambda_z \pm \sqrt{\lambda_x^2 + 4\mu^2 \mathrm{H}^2 \left(\lambda_x + 2\lambda_z \right)}\,, \tag{4.18}$$

which, for zero external field, are

$$\omega_{0,+}\big|_{\mathrm{H}=0} = \sqrt{2(\lambda_x + \lambda_z)}\,, \tag{4.19a}$$
$$\omega_{0,-}\big|_{\mathrm{H}=0} = \sqrt{2\lambda_z}\,. \tag{4.19b}$$

We can understand this spectrum using the following argument. For $\mathrm{H} = 0$ and neglecting the easy-axis anisotropy (indeed, as we will see, for NiO crystals $\lambda_z \ll \lambda_x$), the ground state must have $\hat{n}_x = 0$, i.e., performing rotations around the x-axis costs zero energy. There will thus be an exact Goldstone boson associated with this residual SO(2) invariance. However, introducing even a small anisotropy along the z-axis breaks this residual invariance, forcing the ground state along the z-direction.[5] We notice that the dispersion relations obtained in the isotropic case (4.8a) cannot be obtained taking the limit $\lambda_{x,z} \to 0$ in (4.17), since, in this limit, the background changes and the field parametrization must be re-evaluated.

4.3 Quantization of the EFT

We are now ready to proceed with the quantization of our theory in the non-trivial case of $\mathrm{H} < \mathrm{H}_{\mathrm{s.f.}}$. Lagrangian (4.15) contains both a term with a single time derivative and one with two time derivatives. This makes it impossible to diagonalize the quadratic action by a local field redefinition. (See Ref. [154] for a recent discussion.) This can be seen, for example, from the fact that the eigenvectors of the matrix in Eq. (4.16) present non-analyticities in the frequency ω. In order to deal with local fields, we then continue to work in the non-diagonal basis. In this basis, the magnon fields, θ^a, are not in one-to-one correspondence with the physical magnon states, $|\boldsymbol{q}, \alpha\rangle$, which are (approximately) asymptotic states with dispersion relations $\omega_{q,\alpha}$, given in Eq. (4.17).[6] This makes the quantization of the theory in the $\mathrm{H} < \mathrm{H}_{\mathrm{s.f.}}$ phase non-trivial.

[5] The high energy physicist would call this "vacuum selection".

[6] We remind the reader that the index $\alpha = \pm$ runs over the two possible magnon degrees of freedom.

In the following, we will denote with $a_{\boldsymbol{q},\alpha}$ the annihilation operator associated with the single magnon state $|\boldsymbol{q},\alpha\rangle$, that is to say that,

$$a^{\dagger}_{\boldsymbol{q},\alpha}\,|0\rangle = |\alpha,\boldsymbol{q}\rangle \;, \tag{4.20}$$

where the vacuum state is the one defined by the background configuration in presence of a magnetic field, as discussed in Sec. 4.2.2. We also adopt the relativistic normalization of the one-particle states, meaning the following commutation relation,

$$\left[a_{\boldsymbol{q},\alpha}, a^{\dagger}_{\boldsymbol{p},\beta}\right] = 2\omega_{\boldsymbol{q},\alpha}\,\delta_{\alpha\beta}(2\pi)^3\delta^{(3)}(\boldsymbol{q}-\boldsymbol{p})\,, \tag{4.21}$$

where the $\omega_{\boldsymbol{q},\alpha}$ are given in (4.17). We will also work with canonically normalized fields, which are achieved by simply replacing $\theta^a \to \theta^a/\sqrt{c_1}$ in Eq. (4.15).

Since the quadratic Lagrangian is non-diagonal, we have that $\langle 0|\theta^a|\boldsymbol{q},\alpha\rangle \not\propto \delta^a_\alpha$. To proceed with the quantization procedure, we first write the mode expansion of our fields,

$$\begin{aligned}\theta^a(x) = &\sum_{\alpha=\pm}\int\frac{d^3q}{(2\pi)^3 2\omega_{q,\alpha}}e^{-i\omega_{q,\alpha}t+i\boldsymbol{q}\cdot\boldsymbol{x}}\,\mathcal{Z}^a_{q,\alpha}\,a_{\boldsymbol{q},\alpha}\\ &+\text{h.c.}\,,\end{aligned} \tag{4.22}$$

where we introduced the overlap functions [e.g., 154–157], $\mathcal{Z}^a_{q,\alpha}$, which connect the θ^a fields to the physical magnon state, $|\boldsymbol{q},\alpha\rangle$. They are defined as,

$$\langle 0|\theta^a(x)|\boldsymbol{q},\alpha\rangle = e^{-i\omega_{q,\alpha}t+i\boldsymbol{q}\cdot\boldsymbol{x}}\,\mathcal{Z}^a_{q,\alpha}\,. \tag{4.23}$$

Since our theory is invariant under spatial rotations but not under boosts [157], the overlap functions will depend on q. To determine them, we impose the equal time commutators between the magnon fields and their conjugate momenta,

$$\left[\theta^a(\boldsymbol{x},t),\theta^b(\boldsymbol{y},t)\right] = 0\,, \tag{4.24a}$$

$$\left[\theta^a(\boldsymbol{x},t),\pi^b(\boldsymbol{y},t)\right] = i\,\delta^{ab}\,\delta^{(3)}(\boldsymbol{x}-\boldsymbol{y})\,, \tag{4.24b}$$

$$\left[\pi^a(\boldsymbol{x},t),\pi^b(\boldsymbol{y},t)\right] = 0\,, \tag{4.24c}$$

where $\pi^a \equiv \dot{\theta}^a - \mu\,\mathrm{H}\,\epsilon^{ab}\,\theta^b$. From the above commutators we get, respectively, the conditions,

$$\sum_{\alpha=\pm}\frac{\mathcal{Z}^a_{q,\alpha}\mathcal{Z}^{b*}_{q,\alpha} - \mathcal{Z}^{a*}_{q,\alpha}\mathcal{Z}^b_{q,\alpha}}{\omega_{q,\alpha}} = 0\,, \tag{4.25a}$$

$$\sum_{\alpha=\pm}\left[\mathcal{Z}^a_{q,\alpha}\mathcal{Z}^{b*}_{q,\alpha} + \mathcal{Z}^{a*}_{q,\alpha}\mathcal{Z}^b_{q,\alpha}\right] = 2\delta^{ab}\,, \tag{4.25b}$$

$$\sum_{\alpha=\pm}\omega_{q,\alpha}\left[\mathcal{Z}^a_{q,\alpha}\mathcal{Z}^{b*}_{q,\alpha} - \mathcal{Z}^{a*}_{q,\alpha}\mathcal{Z}^b_{q,\alpha}\right] = 4i\mu\mathrm{H}\epsilon^{ab}\,. \tag{4.25c}$$

Imposing the equations of motion for θ^a, we get the further constraint,

$$\mathcal{M}^{ab}(q,\omega_{q,\alpha})\mathcal{Z}^b_{q,\alpha} = 0\,,\quad\text{for}\quad\alpha=\pm\,, \tag{4.26}$$

where $\mathcal{M}^{ab}$ is defined in (4.16).

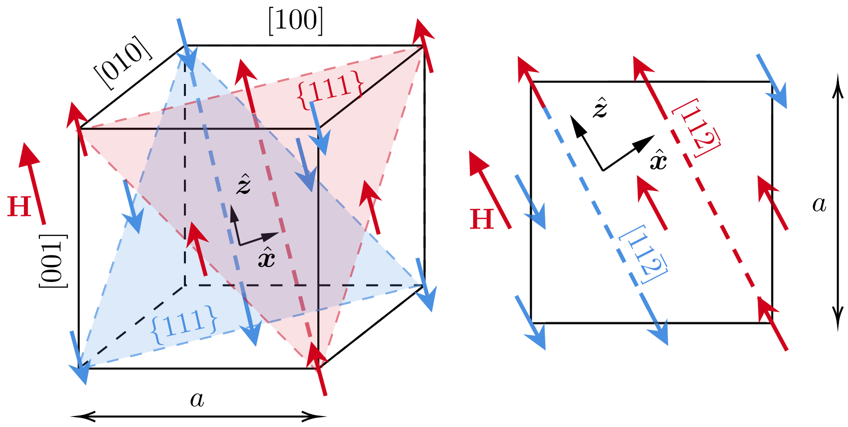

Figure 4.2: *The crystal structure and spin arrangements in NiO below the Néel temperature,* $T_{\rm N} \simeq$ 523 *K, are characterized by a face-centered-cubic arrangements of* $\rm Ni^{2+}$ *ions. The* $\rm Ni^{2+}$ *ions align ferromagnetically along the* $[11\bar{2}]$ *axis, indicated with bold dashed lines, lying within* $\{111\}$ *planes, depicted as colored triangular planes on the left. In this work, we consider the NiO sample in an external magnetic field,* **H***, that we choose oriented along the* $[11\bar{2}]$ *axis. In the following we will adopt a reference frame where the* $[111]$ *and* $[11\bar{2}]$ *axes, called hard and easy axes, coincide with the* x*- and* z*-axes, respectively.*

We can use the equation above to solve for one component of the overlap functions in terms of the other. In particular, we get

$$\mathcal{Z}^2_{q,\pm} = i \left(\frac{v_\theta^2 q^2 - \mu^2 \mathrm{H}^2 + 2\lambda_z - \omega^2_{q,\pm}}{2\mu \mathrm{H}\, \omega_{q,\pm}} \right) \mathcal{Z}^1_{q,\pm} \,. \tag{4.27}$$

Plugging this into the constraints reported in Eqs. (4.25) one finally finds

$$|\mathcal{Z}^1_{q,\pm}| = \sqrt{\frac{1}{2} \pm \frac{2\mu^2 \mathrm{H}^2 - \lambda_x}{2\sqrt{4\mu^2\mathrm{H}^2(v_\theta^2 q^2 + \lambda_x - 2\lambda_z) + \lambda_x^2}}} \,. \tag{4.28}$$

The overall phase, common to $\mathcal{Z}^1_{q,\alpha}$ and $\mathcal{Z}^2_{q,\alpha}$, is arbitrary.

We notice that, taking first the limit $\mathrm{H} \to 0$, and then $\lambda_z \to 0$, we get

$$\mathcal{Z}^a_{q,+} = \begin{pmatrix} 0 \\ -i \end{pmatrix} , \quad \mathcal{Z}^a_{q,-} = \begin{pmatrix} 1 \\ 0 \end{pmatrix} , \tag{4.29}$$

as a check of the fact that, in this limit, the quadratic action reduces to a diagonal form.

To make sure of the correctness of our results, in Appendix 4.9, we rederive the overlap functions using so-called "polology" arguments.

4.4 Matching to a short distance theory

Let us now give explicit values of the effective coefficients appearing in the effective theory. To do that, we match some observable quantities obtained within the EFT with the same quantity as obtained from the short distance Hamiltonian. In particular, we will focus on the case of NiO, which is of particular phenomenological relevance [e.g., 140, 143, 150].

In particular, the spin structure of NiO is dictated by that of its Ni^{2+} ions which, below its Néel temperature, $T_{\mathrm{N}} \simeq 523$ K, are ordered in stacked parallel planes. In each of these planes, the spins are aligned ferromagnetically, with each plane being antiferromagnetic with respect to the adjacent ones [e.g., 134]. In crystallographic jargon these are usually called $\{111\}$ planes — see Fig. 4.2. Moreover, in each plane, the spins are aligned along the so-called $[11\bar{2}]$ direction, as again showed in Figure 4.2. The spin structure just described is dictated by the presence of two anisotropies in spin space. The first one is along the direction perpendicular to the planes mentioned above, the so-called [111] direction, and is responsible precisely for forcing the spins to lie on these planes. This is the hard axis anisotropy. The second one, instead, is in the $[11\bar{2}]$ direction, and is responsible for the final orientation of the spins. This is the easy axis anisotropy.

For this material, the spins are arranged in a face centered cubic lattice with the nearest, next-to-nearest, and next-to-next-to-nearest neighbors separated, respectively, by the following distances,

$$|\boldsymbol{i}-\boldsymbol{j}| = \frac{a}{\sqrt{2}} \qquad (\text{nearest})\,, \tag{4.30a}$$

$$|\boldsymbol{i}-\boldsymbol{j}| = a \qquad (\text{next-to-nearest})\,, \tag{4.30b}$$

$$|\boldsymbol{i}-\boldsymbol{j}| = \sqrt{\frac{3}{2}}a \quad (\text{next-to-next-to-nearest})\,, \tag{4.30c}$$

where a is the cubic lattice parameter, see Fig. 4.2. As observed by neutron scattering experiments, the next-to-nearest spin-spin coupling is by far the dominant one [150, 151], and the corresponding Heisenberg Hamiltonian is well approximated by

$$H = 2\sum_{\langle \boldsymbol{i},\boldsymbol{j}\rangle} J_2\, \boldsymbol{\mathcal{S}}_{\boldsymbol{i}} \cdot \boldsymbol{\mathcal{S}}_{\boldsymbol{j}} + \sum_{\boldsymbol{i}} D_x \left(\boldsymbol{\mathcal{S}}_{\boldsymbol{i}}^x\right)^2 - \sum_{\boldsymbol{i}} D_z \left(\boldsymbol{\mathcal{S}}_{\boldsymbol{i}}^z\right)^2 + \mathcal{O}\left(J_1/J_2, J_3/J_2, \dots\right)\,, \tag{4.31}$$

where the sum over $\langle \boldsymbol{i},\boldsymbol{j}\rangle$ runs only over lattice positions such that $|\boldsymbol{i}-\boldsymbol{j}| = a$, J_2 is the corresponding next-to-nearest-neighbor coupling, and J_1, J_3, and so on are the remaining sub-leading couplings.

Let us now proceed with the matching. The magnon speed of propagation, v_θ, can be found from the dispersion relations in Eq. (4.17) in the case of zero applied field, $\mathrm{H} = 0$, since, for sufficiently large momenta, they become degenerate and linear, $\omega_{q,\alpha} \simeq v_\theta q$. The effective coefficient c_1, instead, is nothing but the so-called perpendicular magnetic susceptibility, $c_1 = \chi_\perp$, as one deduces from Eq. (5.6) (see also Refs. [158, 159]). Its expression in terms of the short distance parameters, instead, has been found in Ref. [129] by computing the rate of emission of one magnon by neutron scattering both within the EFT, as well as within the short distance theory, as done in Ref. [144]. The result is

$$c_1 = \frac{4\mathcal{S}^2}{a v_\theta^2} J_2\,. \tag{4.32}$$

The two anisotropic couplings, λ_x and λ_z, instead, can be determined by matching the values of the magnon gaps computed at zero magnetic field. In the short distance theory, these can be computed either by looking at the semiclassical solutions of the Landau-Lifshitz equations, or by actually quantizing the Hamiltonian and determining the spectrum of the corresponding magnon modes [e.g., 134]. Both methods return the same results:

$$\omega_{0,+}\big|_{\mathrm{H}=0} = \mu\sqrt{2\mathrm{H}_E\left(\mathrm{H}_{Az}+\mathrm{H}_{Ax}\right)}\,, \tag{4.33a}$$

$$\omega_{0,-}\big|_{\mathrm{H}=0} = \mu\sqrt{2\mathrm{H}_E\mathrm{H}_{Az}}\,, \tag{4.33b}$$

where H_E, H_{Az}, and H_{Ax} are microscopic magnetic fields built out of the parameters of the Heisenberg Hamiltonian. Specifically, they are given by

$$\mathrm{H}_E = \frac{2\mathcal{S}zJ_2}{\mu}\,, \quad \mathrm{H}_{Ax} = \frac{2\mathcal{S}D_x}{\mu}\,, \quad \mathrm{H}_{Az} = \frac{2\mathcal{S}D_z}{\mu}\,, \tag{4.34}$$

	Short distance						Long distance			
μ/μ_B	$\mathcal{S}$	a [Å]	H_E [kOe]	H_{Ax} [kOe]	H_{Az} [kOe]	$H_{s.f.}$ [kOe]	v_θ	c_1 [MeV/Å]	λ_x [meV^2]	λ_z [meV^2]
2.18	1	4.17	9684	6.35	0.11	46.3	1.3×10^{-4}	0.58	9.80	0.17

Table 4.1: *Summary of the relevant parameters for NiO, both for the short distance Hamiltonian and for the long distance EFT. All short distance values are taken from Ref. [134], except for the lattice parameter, a, which is taken from Ref. [150]. The propagation speeed, v_θ, is fitted from the dispersion relations measured in Ref. [150]. Finally, the effective coefficients c_1, λ_x and λ_z are determined from the matching conditions in Eqs. (4.32) and (4.35). In particular, in the expression for c_1 we traded the dominant coupling J_2 for the microscopic magnetic field H_E. For the sake of the more high energy oriented reader, we recall that magnetic fields in a material are typically measured in oersted (Oe). In these units, the vacuum permeability is given by $\mu_0 = 10^{-4}$ T/Oe.*

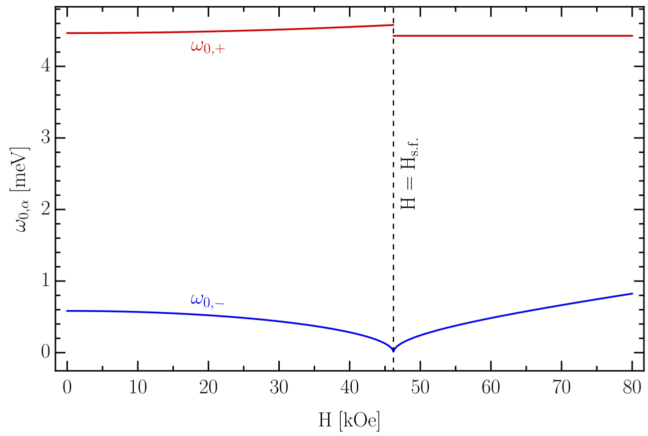

Figure 4.3: *Gaps of the lowest lying magnon modes, $\omega_{0,\pm}$, as a function of the external magnetic field. Across the critical value, $H = H_{s.f.}$, the lightest mode becomes gapless, while the higher one has a discontinuity.*

where z is the number of next-to-nearest neighbors coupled by J_2, the so-called "coordination number", which for NiO is $z = 6$. With this at hand, the low energy anisotropic couplings are found to be

$$\lambda_x = \mu^2 H_E H_{Ax} \,, \tag{4.35a}$$
$$\lambda_z = \mu^2 H_E H_{Az} \,. \tag{4.35b}$$

In Table 4.1, we summarize the numerical values of both the short and long distance parameters for NiO. In Fig. 4.3, instead, we plot the gaps of the two lowest lying magnon modes of NiO as a function of the magnitude of the external magnetic field.

Note also that the value of the critical spin-flop magnetic field can also be determined in the short distance theory. In particular, it is given by [134],

$$H_{s.f.} \simeq \sqrt{2 H_E H_{Az}} \,, \tag{4.36}$$

where the approximation comes from considering the limit $H_{Ax,Az} \ll H_E$. Using Eqs. (4.35), this reproduces exactly what was found independently within the EFT, as discussed below Eq. (4.12).

4.5 The regime of validity of the EFT

As any effective theory, our EFT is valid only within certain conditions on the momenta and energies under consideration. Indeed, the Lagrangian in Eq. (4.11) is just the leading order in a systematic expansion in small momenta and energies. We then conclude our discussion by determining the limits of our EFT.

First of all, the theory is applicable as long as the wavelengths of interest are much larger than the typical distance characterizing the microscopic system. This translates into a cutoff on the momenta that one can consider: for momenta larger than this cutoff, one starts being sensitive to the short distance details of the material at hand. In a lattice, the natural momentum cutoff is given by the inverse lattice spacing, which means that our EFT is valid as long as the momenta are such that $q \ll 1/a$. As far as the energy cutoff is concerned, instead, the natural energy cutoff is given by the dominant spin-spin coupling, i.e., the theory is valid for $\omega \ll J_2$. Physically, this is the energy that one must provide to the system in order to be able to completely flip one of the spins.

Moreover, our theory also accounts for the effects of explicit symmetry breaking. This can be done consistently only as long as these effects are consistent with the regime of applicability of the EFT, and can therefore be included in the power counting. In detail, this can be quantified by requiring for the gaps induced by the anisotropies to be substantially smaller than the energy cutoff. This means to require that $\sqrt{\lambda_{x,z}} \ll J_2$. Using Eqs. (4.34) and (4.35), this can be rephrased in terms of microscopic magnetic fields, corresponding to requiring $\mathrm{H}_{Ax,Az} \ll \mathrm{H}_E$. This condition is indeed well satisfied by our prototypical antiferromagnet, NiO (see Table 4.1).

Finally, since our setup also features an external magnetic field, we also need to make sure that this is sufficiently small not to cause drastic changes is the short distance structure of the material. Similarly as above, we can estimate the maximum magnetic field, beyond which the theory loses validity, as the value for which the gap of one of the magnon modes becomes comparable to the energy cutoff. When the magnetic field becomes large, it dominates the expression for the largest gap in Eq. (4.14), which then become simply $\omega_{0,-} \simeq \mu\mathrm{H}$. When this is comparable to the energy cutoff, the theory is not applicable anymore. In other words, we must further make sure that the applied magnetic field satisfies $\mathrm{H} \ll J_2/\mu$. Note that, up to order one factors, this coincides with $\mathrm{H} \ll \mathrm{H}_E$.

4.6 Conclusions

In this work, we have built a low energy EFT for anisotropic antiferromagnets. We showed that the introduction of small anisotropies induces the emergence of a number of interesting phenomena, especially in the presence of a magnetic field, which can nonetheless be studied analytically within the regime of applicability of the EFT. This contributed to elucidate which of these phenomena are universal, meaning that they do not depend on the precise details of the short distance physics.

Moreover, an EFT description of this class of systems can help phrase the question in a language that can be understood from both a condensed matter and a high energy physics viewpoint. Such a description also makes it straightforward to compute magnon scattering amplitudes, which play an important role in determining the magnon lifetime in magnetic materials where traditional methods encounter difficulties [160]. This is also relevant in light of recent proposals to employ antiferromagnets as a target for light dark matter detection [129, 130, 143].

Various additional effects are, however, still left out of the present treatment. These are, for example, the inclusion of the long distance effects of dipolar interactions between spins. These are believed to be at the root of a richer spectrum observed in NiO, which features six additional light modes [140]. These modes all have gaps substantially below the energy cutoff of our EFT and, thus, it should be possible to systematically account for them. Furthermore, it is known that the magnon gaps can be varied by straining the antiferromagnetic sample [161]. This requires a treatment which includes interactions with phonons in our EFT. We leave these and other interesting direction for future work.

4.7 Appendix A: On the role of discrete symmetries in ferromagnets and antiferromagnets

We now take a moment to discuss systematically the role played by discrete symmetries and, in particular, how to employ them in the low energy EFT to discriminate between ferromagnets and antiferromagnets. In doing so, we will revisit some of the arguments that are typically found in the literature, rephrasing them in a way that, in our opinion, offers a viewpoint that is fully consistent with the proper low energy EFT ideology — see also Ref. [147].

Consider again a bipartite lattice of spins, as discussed in Sec. 4.2.1. Regardless of what magnetic system one is actually considering, the presence of long range order is indicated by the existence of a given order parameter, say $\boldsymbol{\mathcal{O}}$, which transforms linearly under the SO(3) group of spin rotations, $\boldsymbol{\mathcal{O}} \to \mathcal{R} \cdot \boldsymbol{\mathcal{O}}$, and acquires a non-zero expectation value on the ground state, $\langle \boldsymbol{\mathcal{O}} \rangle \neq 0$. This fact alone tells us that the original spin rotation symmetry is spontaneously broken to the subgroup that leaves $\langle \boldsymbol{\mathcal{O}} \rangle$ unchanged. At this level, there is no distinction between ferromagnets and antiferromagnets. In both instances, their low energy EFT will be formulated in terms of a 3-vector field, $\hat{\boldsymbol{n}}(x)$, such that $|\hat{\boldsymbol{n}}(x)| = 1$ and $\langle \hat{\boldsymbol{n}}(x) \rangle \neq 0$. The difference arises when one wants to express the order parameter in terms of the degrees of freedom of the short distance theory, i.e., the spins of the material. In particular, one has

$$\boldsymbol{\mathcal{O}} = \begin{cases} \sum_{i \in \mathbb{A}} \boldsymbol{\mathcal{S}}_{\boldsymbol{i}} + \sum_{i \in \mathbb{B}} \boldsymbol{\mathcal{S}}_{\boldsymbol{i}} \equiv \boldsymbol{\mathcal{M}} \,, & \text{ferromagn.} \\ \sum_{i \in \mathbb{A}} \boldsymbol{\mathcal{S}}_{\boldsymbol{i}} - \sum_{i \in \mathbb{B}} \boldsymbol{\mathcal{S}}_{\boldsymbol{i}} \equiv \boldsymbol{\mathcal{N}} \,, & \text{antiferromagn.} \end{cases} ,$$

where $\boldsymbol{\mathcal{M}}$ is the magnetization and $\boldsymbol{\mathcal{N}}$ is the Néel vector.

How about discrete symmetries? As mentioned again in Sec. 4.2.1, both time reversal, $\mathcal{T}$, and the discrete rotation of 180° in the plane containing the spins, $\mathcal{R}_\pi$, flip the direction of all the spins. But then, the order parameter also changes sign under either of these transformations,

$$\boldsymbol{\mathcal{O}} \xrightarrow{\mathcal{T}} -\boldsymbol{\mathcal{O}} \,, \qquad \boldsymbol{\mathcal{O}} \xrightarrow{\mathcal{R}_\pi} -\boldsymbol{\mathcal{O}} \,, \qquad \boldsymbol{\mathcal{O}} \xrightarrow{\mathcal{T}\mathcal{R}_\pi} \boldsymbol{\mathcal{O}} \,. \tag{4.37}$$

Again, this is true regardless of whether one is dealing with a ferromagnet or an antiferromagnet. It then follows that both these systems feature *the same symmetry breaking pattern*, i.e. $\mathrm{SO}(3) \times \mathcal{T} \to \mathrm{SO}(2) \times (\mathcal{T}\mathcal{R}_\pi)$.

The rules of the game to build a low energy EFT for either of these systems are then exactly the same.

1. Consider the field $\hat{\boldsymbol{n}}(x)$ such that,
   - it rotates under SO(3), $\hat{\boldsymbol{n}}(x) \xrightarrow{\mathrm{SO}(3)} \mathcal{R} \cdot \hat{\boldsymbol{n}}(x)$;
   - it changes sign under either time reversal or the discrete rotation of 180°, $\hat{\boldsymbol{n}}(x) \xrightarrow{\mathcal{T}} -\hat{\boldsymbol{n}}(x)$ and $\hat{\boldsymbol{n}}(x) \xrightarrow{\mathcal{R}_\pi} -\hat{\boldsymbol{n}}(x)$;
   - it has unit norm and acquires a non-zero expectation value on the ground state, $\langle \hat{\boldsymbol{n}}(x) \rangle \neq 0$.
2. Write the most general theory for $\hat{\boldsymbol{n}}(x)$ that is invariant under the full SO(3) and under the combined action of $(\mathcal{T}\mathcal{R}_\pi)$.
3. Organize the theory in a derivative expansion.

Following this, the most general leading-order Lagrangian respecting these rules is the one reported also in [133],

$$\mathcal{L} = \frac{c_1}{2}(\partial_t \hat{\boldsymbol{n}})^2 - \frac{c_2}{2}(\nabla_i \hat{\boldsymbol{n}})^2 + c_3\,(\partial_t \phi)\cos\theta \,, \tag{4.38}$$

where $\theta(x)$ and $\phi(x)$ are the polar and azimuthal angles defining $\hat{\boldsymbol{n}} = (\sin\theta\cos\phi,\, \sin\theta\sin\phi,\, \cos\theta)$. As shown in Ref. [133], under an infinitesimal SO(3) rotation, the Lagrangian above changes by a total derivative, thus ensuring the invariance of the theory (modulo possible non-trivial topologies).

What discriminates a ferromagnet from an antiferromagnet then? The difference between the two systems lies in the behavior of the *magnetization*. First of all, for a ferromagnet, the magnetization changes sign under time reversal or, equivalently, under $\mathcal{R}_\pi$. For an antiferromagnet, instead, it does not. Moreover, the background value of the magnetization of a ferromagnet is non-zero, while it vanishes for an antiferromagnet.

Starting from the above low energy EFT, the magnetization is simply found as the temporal component of the Noether current associated to the original SO(3) symmetry, i.e., the spin density. From Eq. (4.38), one gets

$$\boldsymbol{s} = c_1\, \partial_t \hat{\boldsymbol{n}} \times \hat{\boldsymbol{n}} + c_3\, \hat{\boldsymbol{n}} \,. \tag{4.39}$$

Now it is clear that the only way that one has to reproduce the correct behavior of the magnetization described above must be if $c_1 = 0$ for ferromagnets, and $c_3 = 0$ for antiferromagnets, thus reducing the Lagrangian in Eq. (4.38) to the known ones for these two systems.

In light of the discussion above, we stress what we believe is an important conceptual point. The conditions $c_1 = 0$ or $c_3 = 0$ do not follow from different symmetry breaking patterns distinguishing ferromagnets from antiferromagnets. At low energies they have the same symmetry breaking pattern. What is happening here is different. The magnetization in Eq. (4.39), which is a long distance observable, is an output of our EFT, not an input. By comparing the behavior of $\boldsymbol{s}$ under time reversal to that obtained from the microscopic theory of ferromagnets and antiferromagnets, we are rather performing a *matching* procedure which determines the values of the effective coefficients, as per usual. Alternatively, if we would have included the single-time derivative term in the Lagrangian for antiferromagnets, we would have arrived at the conclusion that they have a non-zero background magnetization, which is at odds with experiment.

4.8 Appendix B: Background and quadratic theory for a more general magnetic field

It is interesting to study what happens to the ground state of our theory, and to its quadratic Lagrangian, in the more general case of a magnetic field in the anisotropy plane, i.e., for $\mathbf{H} = \mathrm{H}\cos\theta\,\hat{\boldsymbol{x}} + \mathrm{H}\sin\theta\,\hat{\boldsymbol{z}}$. For simplicity we limit ourself to the range $\theta \in [0, \pi/2]$. In this instance, the Hamiltonian obtained from Eq. (4.11), computed on static and homogeneous configurations, reads

$$\begin{aligned}\mathcal{H}|_{\text{stat., homog.}} = \frac{c_1}{2}\big[&(2\lambda_x + \mu^2\mathrm{H}^2\cos^2\theta)\hat{n}_x^2 - (2\lambda_z - \mu^2\mathrm{H}^2\sin^2\theta)\hat{n}_z^2 \\ &+ 2\mathrm{H}^2\hat{n}_x\hat{n}_z\sin\theta\cos\theta\big]\,,\end{aligned} \tag{4.40}$$

where again we omit irrelevant constant terms. One can verify that the background configuration that minimizes the Hamiltonian depends on the value taken by the projection of the magnetic field along the easy axis. In particular, for $\mathrm{H}\sin\theta > \mathrm{H}_{\text{s.f.}}$ the background is $\langle\hat{\boldsymbol{n}}\rangle = \hat{\boldsymbol{y}}$, while for $\mathrm{H}\sin\theta < \mathrm{H}_{\text{s.f.}}$ it is $\langle\hat{\boldsymbol{n}}\rangle = \hat{\boldsymbol{z}}$.

In this more general case, the quadratic Lagrangian is always non-diagonal, in each of the two phases. The Fourier space linear equations of motion for the magnon fields are again given by $\mathcal{M}^{ab}(\omega, q)\theta^b(\omega, \boldsymbol{q})$, where now the kinetic matrix is given by

$$
\begin{aligned}
\mathcal{M}^{ab} &= \begin{pmatrix} v_\theta^2 q^2 - \omega^2 + \mu^2 \mathrm{H}^2 \sin^2\theta - 2\lambda_z & -\mu^2 \mathrm{H}^2 \cos\theta \sin\theta \\ -\mu^2 \mathrm{H}^2 \cos\theta \sin\theta & v_\theta^2 q^2 - \omega^2 + \mu^2 \mathrm{H}^2 \cos^2\theta + 2\lambda_x \end{pmatrix}, \mathrm{H}\sin\theta > \mathrm{H}_{\text{s.f.}}\,, \\
\mathcal{M}^{ab} &= \begin{pmatrix} v_\theta^2 q^2 - \omega^2 - \mu^2 \mathrm{H}^2 \sin^2\theta + 2\lambda_z & 2i\mu \mathrm{H}\omega \sin\theta \\ -2i\mu \mathrm{H}\omega \sin\theta & v_\theta^2 q^2 - \omega^2 + \mu^2 \mathrm{H}^2 \cos 2\theta + 2(\lambda_x + \lambda_z) \end{pmatrix}, \mathrm{H}\sin\theta < \mathrm{H}_{\text{s.f.}}\,.
\end{aligned}
\tag{4.41}
$$

Now, while neither of them is diagonal, the off-diagonal terms for the $\mathrm{H}\sin\theta > \mathrm{H}_{\text{s.f.}}$ case do not depend on frequency. This means that the quadratic theory can be diagonalized by a simple, local field redefinition. In other words, one can simply work with a linear combination of the magnon fields, chosen to diagonalize the matrix. For $\mathrm{H}\sin\theta < \mathrm{H}_{\text{s.f.}}$, instead, the off-diagonal terms are frequency dependent, and one thus need to follow the same procedure discussed in Sec. 4.3.

The spectrum of the theory is found again by requiring that the matrices above have vanishing determinant. The final expressions can be found analytically, but they are considerably more involved than what was found in the main text. We thus omit them.

4.9 Appendix C: Overlap functions from "polology"

To verify our procedure, we rederive the overlap functions with an alternative method, using the so-called "polology" technique [162], in a way analogous to what has been recently done in Ref. [154, 157]. As usual for such kind of manipulations, we will be using the completeness relation,

$$
\mathbb{1} = \sum_{\alpha=\pm} \int \frac{d^3q}{(2\pi)^3 2\omega_{q,\alpha}} \left|\boldsymbol{q},\alpha\right\rangle \left\langle \boldsymbol{q},\alpha\right| + \dots\,, \tag{4.42}
$$

where the ellipsis stands for multi-particle states. The latter will not play any role as long as one is interested in *tree level* S-matrix elements, for which one considers the on-shell limit of the external *one*-particle states. Inserting the above relation in the time-ordered two-point function (or, alternatively, the correlator) of the magnon field, one gets

$$
\begin{aligned}
\langle 0|\mathcal{T}\left\{\theta^a(\boldsymbol{x},t)\theta^b(\boldsymbol{y},t')\right\}|0\rangle &= \langle 0|\theta^a(\boldsymbol{x},t)\theta^b(\boldsymbol{y},t')|0\rangle\, \theta(t-t') + \langle 0|\theta^b(\boldsymbol{y},t')\theta^a(\boldsymbol{x},t)|0\rangle\, \theta(t'-t) \\
&= \sum_{\alpha=\pm}\int \frac{d^3q}{(2\pi)^3 2\omega_{q,\alpha}} \big[\langle 0|\theta^a(\boldsymbol{x},t)|\boldsymbol{q},\alpha\rangle\langle \boldsymbol{q},\alpha|\theta^b(\boldsymbol{y},t')|0\rangle\theta(t-t') \\
&\quad + \langle 0|\theta^b(\boldsymbol{y},t')|\boldsymbol{q},\alpha\rangle\langle \boldsymbol{q},\alpha|\theta^a(\boldsymbol{x},t)|0\rangle\theta(t'-t)\big] + \dots \\
&= \int \frac{d^4q}{(2\pi)^4} e^{-i\omega(t-t') + i\boldsymbol{q}\cdot(\boldsymbol{x}-\boldsymbol{y})} \times \\
&\quad \times \sum_{\alpha=\pm}\frac{1}{2\omega_{q,\alpha}}\left[\frac{i\mathcal{Z}^a_{q,\alpha}\mathcal{Z}^{b*}_{q,\alpha}}{\omega - \omega_{q,\alpha} + i\varepsilon} - \frac{i\mathcal{Z}^{a*}_{q,\alpha}\mathcal{Z}^{b}_{q,\alpha}}{\omega + \omega_{q,\alpha} - i\varepsilon}\right] + \dots\,, \\
&\equiv \int \frac{d^4q}{(2\pi)^4} e^{-i\omega(t-t') + i\boldsymbol{q}\cdot(\boldsymbol{x}-\boldsymbol{y})} \mathcal{K}^{ab}(\omega,q) + \dots\,,
\end{aligned}
\tag{4.43}
$$

where $d^4q = d\omega d^3q$, $|0\rangle$ is the vacuum in the presence of external magnetic field and anisotropies (see Sec. 4.2.2), and we used the identity $\theta(t) = \int \frac{d\omega}{2\pi}\frac{i}{\omega + i\varepsilon}e^{-i\omega t}$.

Now, at tree level, the Fourier transform of the two-point function is the inverse of the kinetic matrix, which we reported in Eq. (4.16), i.e.,

$$
\begin{aligned}
\mathcal{K}^{ab}(\omega,q) &= -i\left[\mathcal{M}^{ab}(\omega,q)\right]^{-1} \\
&= \frac{-i}{\det\left[\mathcal{M}(\omega,q)\right]}\Big(\delta^{ab}\big[v_\theta^2 q^2 - \mu^2\mathrm{H}^2 - \omega^2 + 2(\lambda_z + \lambda_z)\big] - \delta^{a2}\,\delta^{b2} 2\lambda_x - 2i\mu\mathrm{H}\omega\,\epsilon^{ab}\Big)\,.
\end{aligned}
\tag{4.44}
$$

Since this is an identity between Fourier coefficients, it must hold true for any value of ω, and should thus be solved by comparing terms with the same powers of the frequency. Specifically, setting $a = b = 1, 2$, we can extract the absolute values of the overlap functions. Indeed, for $a = b = 1$, we get $|\mathcal{Z}^1_{q,-}|^2 + |\mathcal{Z}^1_{q,+}|^2 = 1$ and

$$\sum_{\alpha=\pm} |\mathcal{Z}^1_{q,\alpha}|^2 \omega^2_{q,-\alpha} = v_\theta^2 q^2 - \mu^2 \mathrm{H}^2 + 2(\lambda_z + \lambda_z)\,, \tag{4.45}$$

where $\omega_{-\alpha} = \omega_{\mp}$, for $\alpha = \pm$. Analogously, for $a = b = 2$, we get $|\mathcal{Z}^2_{q,-}|^2 + |\mathcal{Z}^2_{q,+}|^2 = 1$ and

$$\sum_{\alpha=\pm} |\mathcal{Z}^2_{q,\alpha}|^2 \omega^2_{q,-\alpha} = v_\theta^2 q^2 - \mu^2 \mathrm{H}^2 + 2\lambda_z\,. \tag{4.46}$$

Therefore we find that

$$|\mathcal{Z}^1_{q,\pm}| = \sqrt{\frac{1}{2} \pm \frac{2\mu^2\mathrm{H}^2 - \lambda_x}{2\sqrt{4\mu^2\mathrm{H}^2(v_\theta^2 q^2 + \lambda_x - 2\lambda_z) + \lambda_x^2}}}\,,$$
$$|\mathcal{Z}^2_{q,\pm}| = \sqrt{\frac{1}{2} \pm \frac{2\mu^2\mathrm{H}^2 + \lambda_x}{2\sqrt{4\mu^2\mathrm{H}^2(v_\theta^2 q^2 + \lambda_x - 2\lambda_z) + \lambda_x^2}}}\,,$$

in agreement with Eqs. (4.27) and (4.28). To determine the relative phase between $\mathcal{Z}^1_{q,\alpha}$ and $\mathcal{Z}^2_{q,\alpha}$ we write them as

$$\mathcal{Z}^a_{q,\alpha} = \left|\mathcal{Z}^a_{q,\alpha}\right| e^{i\varphi^a_\alpha}\,. \tag{4.47}$$

By taking $a = 1$, $b = 2$ in Eq. (4.44), we obtain the following equation for the relative phase, $\Delta\varphi_\alpha \equiv \varphi^1_\alpha - \varphi^2_\alpha$,

$$\begin{aligned}\sum_\alpha \frac{i|\mathcal{Z}^1_{q,\alpha}||\mathcal{Z}^2_{q,\alpha}|}{\omega_{q,\alpha}\left(\omega^2 - \omega^2_{q,\alpha}\right)} &\left[i\,\omega \sin\Delta\varphi_\alpha + \omega_{q,\alpha}\cos\Delta\varphi_\alpha\right] \\ &= -\frac{2\mu\mathrm{H}\omega}{\det\left[\mathcal{M}(\omega,\boldsymbol{q})\right]}\,.\end{aligned} \tag{4.48}$$

Equating again terms with the same powers of ω, we find $\Delta\varphi_\pm = \pm\pi/2$, which again agrees with Eq. (4.27).

CHAPTER

5

Axion detection with anisotropic antiferromagnets

5.1 Introduction

Direct dark matter searches for both heavy Weakly Interacting Massive Particles [e.g., 163–167] and axions [e.g., 168–178], have so far reported null results. Concerning the axion, in particular, only a handful of experiments have (or will have) enough sensitivity to probe the QCD axion region, i.e. the right masses and couplings to potentially offer a solution to the strong CP problem. In order to keep expanding the scope of our searches, and probe yet unexplored regions in parameter space, new ideas and detection strategies are needed.

A good deal of work has been recently devoted toward taking advantage of the rich spectrum of collective excitations featured by different condensed matter systems, trying to employ them to look for sub-MeV dark matter scattering and axion absorption, probing new values of their possible mass [e.g., 130, 179–202]. For a review, see [203, 204].

In this work we show that nickel oxide (NiO), a well studied antiferromagnet [e.g., 140, 205, 206], offers an optimal target to probe the electron coupling of axion dark matter with masses in the unexplored range $m_a \sim \mathcal{O}(0.1-10)$ meV. (Other proposals valid for similar masses are [194, 195, 201].) It has already been shown that NiO provides an ideal target also to look for sub-MeV dark matter scattering from spin-dependent interactions [200]. Among other reasons, this is because its vanishing magnetization ensures that the emission of multiple collective excitations (the so-called magnons) is allowed. This enables the transfer of a large fraction of the dark matter energy even at masses as low as the keV.

As we will argue, NiO is also very efficient at absorbing axions, with masses in the same range as the typical energies of its magnon modes. In particular, the process of axion conversion into a single excitation provides (at least) two resonant values for a narrowband search, corresponding to the two lowest lying magnon modes. By tuning an external magnetic field one can also make one of the magnons arbitrarily light, giving access to axion masses even below the meV range. The conversion into two magnons, instead, offers the possibility for a *broadband* channel: the system is able to absorb axions in a wide range of masses by simply adjusting the total energy and relative momentum of the two outgoing excitations.

We work within an effective field theory (EFT) for the description of magnons and their interactions, valid at low energies and long wavelengths [131, 132, 147, 207], which we extend to incorporate the rich phenomenology of NiO [208]. In this framework, magnons are the (pseudo-)Goldstone bosons associated with the breaking of non-relativistic spin symmetry, as induced by the antiferromagnetic ground state.

v_θ	c_1 [MeV/]	μ/μ_B	λ_x [meV^2]	λ_z [meV^2]	Λ_UV [keV]	ρ_T [g/cm^3]
1.3×10^{-4}	0.58	2.18	9.80	0.17	0.6	6.7

Table 5.1: Parameters for the EFT of magnons in NiO [208]. μ_B is the Bohr magneton, and the mass density, ρ_T is taken from [210]. Λ_UV is estimated from [205] as the momentum for which the dispersion relation deviates from linear by 10%. Note that while the EFT is general for any antiferromagnet with the same symmetry breaking pattern, the value of the parameters crucially depends on the microscopic structure of the order parameter and of the crystal.

The main advantage of this EFT is that it is completely dictated by symmetry, thus bypassing the need for a microscopic description of the system. The intricacies of the short distance physics are encoded in a few effective coefficients, which we match from data. This has a twofold advantage. On the one hand, the EFT formulation allows one to clearly disentangle those phenomena that are universal, i.e., common to a broad class of systems, to those that are specific to a given short distance realization of these systems. On the other hand, it helps formulating the current problem in a language that is closer to high energy physics, thus allowing one to borrow concepts and techniques from this field.

Conventions: We use natural units, $\hbar = c = 1$, and follow an index notation with $i, j, k = 1, 2, 3$ and $a, b = 1, 2$.

5.2 The EFT

We start by summarizing the EFT for magnons in NiO, which has been developed in full detail in [208]. After that, we introduce the axion, and describe how to incorporate it into the above mentioned EFT. Throughout our treatment, we will assume to work at zero temperature, as motivated by the standard setup for direct dark matter searches.

5.2.1 Magnons in NiO

A magnetic material can be thought of as a collection of spins arising from the elementary spins of the unpaired electrons localized around each lattice site, with the exchange and superexchange interaction between these electrons providing an effective coupling between different spins. In an antiferromagnet, these couplings are such that, below a certain critical temperature, the ground state of the system develops a long-range order, with neighboring spins antiparallel to each other and all aligned along one direction. We take this to be the z-axis. For NiO, this happens below the temperature $T_\mathrm{N} \simeq 523$ K, called the Néel temperature [e.g., 205, 209].

In this context, one can define an order parameter, the so-called Néel vector, consisting of a staggered sum of all the spins in the material, i.e., $\boldsymbol{\mathcal{N}} \equiv \sum_i (-1)^i \boldsymbol{\mathcal{S}}_i$, where $\boldsymbol{\mathcal{S}}_i$ is the spin of the i-th lattice site and $(-1)^i$ is positive for spins on even sites, and negative for those on odd sites. In the ordered ground state, the Néel vector acquires a non-zero expectation value, $\langle \boldsymbol{\mathcal{N}} \rangle \propto \hat{\boldsymbol{z}}$. From the symmetry viewpoint, this spontaneously breaks the internal spin rotations to the subgroup of rotations that leave the order parameters unchanged, i.e. those around the z-axis. The symmetry breaking pattern is then SO(3) $\to$ SO(2), and magnons are nothing but the associated Goldstone bosons. As such, they can be described by an EFT.

A convenient way of parametrizing them is in terms of local modulations of the order parameter, $\hat{\boldsymbol{n}} = e^{i\theta^a S_a} \cdot \hat{\boldsymbol{z}}$, where $S_a = \{S_1, S_2\}$ are the broken SO(3) generators, with $(S_i)_{jk} = -i\epsilon_{ijk}$, and $\theta^a(x)$ are the magnon fields. The most general, lowest order Lagrangian describing magnons at low energies and small momenta is simply given by [e.g., 131]

$$\mathcal{L}_\theta = \frac{c_1}{2}\left[(\partial_t\hat{\boldsymbol{n}})^2 - v_\theta^2\,(\nabla_i\hat{\boldsymbol{n}})^2\right] . \tag{5.1}$$

Here v_θ is the magnon propagation speed, and it can be determined from their dispersion relation, obtaining $v_\theta \simeq 1.3\times10^{-4}$ [200]. The coefficient c_1 can instead be matched to the parameters of the microscopic spin Hamiltonian using neutron scattering data [200]. We report the values of all the effective coefficients in Table 5.1.

The phenomenology of NiO is, however, richer than this. Specifically, its magnon modes actually present a small but non-zero gap. This is due to tiny explicit breaking effects, turning the magnons into *pseudo*-Goldstones. To the best of our knowledge, the microscopic mechanism generating these gaps has not been completely understood. Data from Raman and Brillouin scattering experiments seem to point to magneto-crystalline anisotropies and dipolar interactions between spins as the most plausible explanation [140]. Yet, the simplest model which correctly reproduces the spectrum of the two lowest lying magnon modes only includes two anisotropic terms with no dipole interactions, as done, for example, in [205, 206]. These anisotropies explicitly break the internal SO(3), and are encoded in the EFT by two additional operators [208],

$$\mathcal{L}_{\text{anis}} = c_1\left[\,\lambda_z\,\hat{n}_z^2 - \lambda_x\,\hat{n}_x^2\,\right] , \tag{5.2}$$

where $\lambda_z, \lambda_x > 0$. The anisotropic couplings can also be matched to the parameters of the microscopic Hamiltonian [208], and their values are again in Table 5.1. The anisotropies in the x- and z-directions are often dubbed "hard" and "easy" axis anisotropies, respectively [206].

In order to scan different axion masses, one needs to vary the magnon gap. This can be achieved by placing the NiO sample in a constant magnetic field, which we take to be aligned with the easy axis, $\mathbf{H} = \mathrm{H}\,\hat{\boldsymbol{z}}$. This can be accounted for in the EFT by promoting the ordinary time derivative to a covariant one in the Lagrangian (5.1), $\partial_t\hat{\boldsymbol{n}} \to \partial_t\hat{\boldsymbol{n}} + \mu\mathbf{H}\times\hat{\boldsymbol{n}}$, such that the Lagrangian is now invariant under simultaneous gauge transformations of $\hat{\boldsymbol{n}}$ and $\mathbf{H}$, with the latter playing the role of a vector potential. Indeed, at the level of the Hamiltonian, this procedure returns the standard Zeeman coupling [147, 208, 211]. Here μ is the gyromagnetic ratio, again given in Table 5.1.

All together, the EFT for magnons in NiO is given by

$$\begin{aligned}\mathcal{L}_{\text{EFT}} &= \frac{c_1}{2}\left[\big(\partial_t\hat{\boldsymbol{n}} + \mu\mathbf{H}\times\hat{\boldsymbol{n}}\big)^2 - v_\theta^2\big(\nabla_i\hat{\boldsymbol{n}}\big)^2\right] + \mathcal{L}_{\text{anis}} \\ &= \frac{c_1}{2}\left[\big(\dot{\theta}^a - \mu\mathrm{H}\epsilon^{ab}\theta^b\big)^2 - v_\theta^2\big(\boldsymbol{\nabla}\theta^a\big)^2 - 2\lambda_z\big(\theta^a\big)^2 - 2\lambda_x\delta^{a2}\delta^{b2}\theta^a\theta^b + \mathcal{O}\big(\theta^4\big)\right],\end{aligned} \tag{5.3}$$

where we expanded in fluctuations around equilibrium.

From the solutions to the linearized equations of motion one finds that there are, as expected, two physical magnon modes, with dispersion relations given by [208],

$$\omega_{q,\pm}^2 = \mu^2\mathrm{H}^2 + \lambda_x + 2\lambda_z + v_\theta^2 q^2 \pm \sqrt{4\mu^2\mathrm{H}^2(\lambda_x + 2\lambda_z + v_\theta^2 q^2) + \lambda_x^2}\,. \tag{5.4}$$

The quantization of this theory is complicated by the presence of a one-derivative kinetic term, which does not allow one to diagonalize the quadratic Lagrangian (5.3) by a local field redefinition. The details of the quantization procedure have been developed in [208].

Importantly, as the magnetic field increases, the gaps of the + and − modes in Eq. (5.4) respectively increase and decrease. This feature can be used to scan over different axion masses. At $\mu_0\mathrm{H} = \mu_0\sqrt{2\lambda_z}/\mu \simeq 4.62$ T,[1] the lightest modes becomes gapless and, for larger fields, the system undergoes a

[1]In the presence of a material, the magnetic field H is typically reported in oersted (Oe). In this work, we use $\mu_0 = 10^{-4}$ T/Oe to convert to Tesla, which is more common in the high energy literature.

(first order) "spin-flop" phase transition to a different ground state, characterized by $\langle \hat{\boldsymbol{n}} \rangle = \hat{\boldsymbol{y}}$ [e.g., 206, 208]. In this work, we are not interested in this regime. However, we notice that thermal and radiative corrections are expected to change both the magnon dispersion relation, as well as the value of the critical magnetic field, but not too dramatically [212]. They are also expected to induce a small gap even at the phase transition point.

It is also interesting to note that in the absence of magnetic fields, the magnon gaps are $\omega_{0,+/-} \sim \sqrt{\lambda_{x/z}}$, corresponding to $\mathcal{O}(\text{meV})$ energies. This is in contrast to ferrimagnets [194], where the gaps are $\mathcal{O}(\mu\text{eV})$, and hence are more suitable to probe axion masses in that range.

Finally, our EFT breaks down for momenta larger than a strong coupling scale, Λ_{UV}, when the details of microscopic system become relevant. This cutoff can be estimated, for example, as the momentum for which the dispersion relation sensibly deviates from linearity, indicating that higher derivative terms in the effective Lagrangian become relevant. In the rest of this work, we always ensure that momenta and energies are below, respectively, Λ_{UV} and $v_\theta \Lambda_{\text{UV}}$, the latter being the typical microscopic energy scale.

5.2.2 Axion-magnon coupling

We are interested in the axion-electron coupling, which is ultimately responsible for the interaction between axions and magnons. The corresponding Lagrangian is

$$\begin{aligned}\mathcal{L}_a = \frac{g_{aee}}{2m_e}\partial_\mu a\, \bar{e}\gamma^\mu\gamma^5 e &\xrightarrow{\text{n.r.}} -\frac{g_{aee}}{m_e}\boldsymbol{\nabla} a \cdot \left(e^\dagger_{\text{nr}}\frac{\boldsymbol{\sigma}}{2}e_{\text{nr}}\right) \\ &\xrightarrow{\text{IR}} -\frac{g_{aee}}{m_e}\boldsymbol{\nabla} a \cdot \boldsymbol{s}\end{aligned} \tag{5.5}$$

where we first took the non-relativistic limit as described in [200] (see also [213]), with e_{nr} the non-relativistic electron field, neglecting terms suppressed by the ratio of the axion mass to the electron mass. In going to the second line, we used the fact that $e^\dagger_{\text{nr}}\boldsymbol{\sigma} e_{\text{nr}}/2$ is the electron spin density. At low energies, it must be expressed in the terms of the relevant degrees of freedom, which in this case are the magnons. Note that we have neglected an additional term, which scales as the electron velocity. For most materials, this is subleading with respect to the coupling included here. For a more detailed discussion we refer the reader to [201, 214]. The inclusion of this additional effect is beyond the scope of the present work.

Now, the spin density is nothing but the Noether current associated with the original SO(3) symmetry which, given the Lagrangian (5.3), reads as

$$\begin{aligned}s^i &= c_1\left[\left(\partial_t\hat{\boldsymbol{n}} \times \hat{\boldsymbol{n}}\right)^i + \mu(\mathbf{H}\cdot\hat{\boldsymbol{n}})\,\hat{n}^i\right] \\ &\simeq c_1\left[\delta^{ia}\left(\dot{\theta}^a - \mu\text{H}\epsilon^{ab}\theta^b\right) - \delta^{i3}\theta^a\left(\epsilon^{ab}\dot{\theta}^b + \mu\text{H}\,\theta^a\right)\right] ,\end{aligned} \tag{5.6}$$

where we omitted constant terms and neglected higher order contributions in the small fluctuations.

With this at hand, and given the expression for the canonical fields reported in [208], one easily finds the amplitudes, $i\mathcal{M}$, for the axion-magnon conversions:

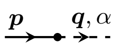

$$= i\frac{g_{aee}\sqrt{c_1}}{m_e}p_a\left[i\omega_{q,\alpha}\mathcal{Z}^a_{q,\alpha} + \mu\text{H}\epsilon^{ab}\mathcal{Z}^b_{q,\alpha}\right]^*, \tag{5.7a}$$

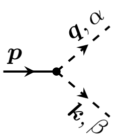

$$= i\,\frac{g_{aee}}{m_e}\,p_z\left[i\left(\omega_{q,\alpha} - \omega_{k,\beta}\right)\epsilon^{ab}\mathcal{Z}^a_{q,\alpha}\mathcal{Z}^b_{k,\beta} + 2\mu\text{H}\mathcal{Z}^a_{q,\alpha}\mathcal{Z}^b_{k,\beta}\right]^*, \tag{5.7b}$$

where $\alpha, \beta = \pm$ run over the physical magnon states, with dispersion relations as in Eq. (5.4). The coefficients $\mathcal{Z}^a_{q,\alpha} \equiv \langle 0|\theta^a(0)|\boldsymbol{q}, \alpha\rangle$ are the overlap functions between the magnon fields and the physical magnon states. They are given by [208]

$$|\mathcal{Z}^1_{q,\pm}| = \sqrt{\frac{1}{2} \pm \frac{2\mu^2\mathrm{H}^2 - \lambda_x}{2\sqrt{4\mu^2\mathrm{H}^2(v_\theta^2 q^2 + \lambda_x + 2\lambda_z) + \lambda_x^2}}}\,, \tag{5.8a}$$

$$\mathcal{Z}^2_{q,\pm} = i\left(\frac{v_\theta^2 q^2 - \mu^2\mathrm{H}^2 + 2\lambda_z - \omega^2_{q,\pm}}{2\mu\mathrm{H}\,\omega_{q,\pm}}\right)\mathcal{Z}^1_{q,\pm}\,, \tag{5.8b}$$

where the common overall phase is arbitrary.

5.3 Event rates

We can now compute the axion absorption event rates per unit target mass. For a target material of density ρ_T (see Table 5.1), this is given by

$$R(\hat{\boldsymbol{v}}_\mathrm{e}) = \frac{\rho_a}{\rho_\mathrm{T} m_a}\int d^3v\, f(|\boldsymbol{v} + \boldsymbol{v}_\mathrm{e}|)\,\Gamma(\boldsymbol{v})\,. \tag{5.9}$$

Here $f(v)$ is the dark matter velocity distribution in the Milky Way. To compare with other proposals, we take this as a truncated Maxwellian as in the standard halo model, with dispersion $v_0 = 230$ km/s, escape velocity $v_\mathrm{esc} = 600$ km/s and boosted with respect to the Galactic rest frame by the Earth velocity, $v_\mathrm{e} = 240$ km/s [215, 216]. We also take the axion dark matter density to be $\rho_a = 0.4$ GeV/cm^3 [215, 217].

One of the advantages of employing an EFT approach like we do, and thus formulating the problem in terms of local Lagrangians, lies in the fact that the rate Γ can now be computed in the standard way, as explained in any particle physics textbook.

5.3.1 One-magnon absorption and directionality

For the conversion into a single magnon, momentum conservation enforces its momentum to be equal to the axion one, $\boldsymbol{q} = m_a\boldsymbol{v}$. Since we will be interested in masses $m_a \lesssim 1$ eV, this momentum is always extremely small, and can be set to zero everywhere without any appreciable corrections, as one can check explicitly. In light of this, the absorption rate is

$$\begin{aligned}\Gamma_\alpha &= \frac{\pi m_a|g_{aee}|^2}{2m_e^2}\frac{c_1}{\omega_{0,\alpha}}\left|v^a V^a_\alpha\right|^2\delta(m_a - \omega_{0,\alpha}) \\ &\to \frac{m_a|g_{aee}|^2}{m_e^2}\frac{c_1}{\omega_{0,\alpha}}\left|v^a V^a_\alpha\right|^2\frac{m_a\omega_{0,\alpha}\gamma_\alpha}{\left(m_a^2 - \omega_{0,\alpha}^2\right)^2 + \left(\omega_{0,\alpha}\gamma_\alpha\right)^2}\,,\end{aligned} \tag{5.10}$$

where $V^a_\alpha \equiv i\omega_{0,\alpha}\mathcal{Z}^a_{0,\alpha} + \mu\mathrm{H}\epsilon^{ab}\mathcal{Z}^b_{0,\alpha}$, and we regulated the energy δ-function with a Breit-Wigner distribution, accounting for the magnon finite width, γ_α. This width is roughly $\gamma_\alpha = \mathcal{O}(1{-}100)$ μeV [218, 219], and it depends on various properties of the material, such as Umklapp scattering, temperature, and boundary effects [219]. To the best of our knowledge, this information is not available for NiO. We thus follow the conservative approach of [194] and treat $\gamma_\alpha/\omega = \gamma_\alpha/m_a$ as a free parameter.

The event rate has a non-trivial dependence on the direction of the Earth velocity. This is because antiferromagnets feature a preferential direction, as set by the order parameter. This directionality can be exploited as an efficient strategy to discriminate between signal and background [e.g., 220, 221]. As we show, in NiO this feature is quite remarkable, with a modulation following the direction of the Earth velocity of about 300%.

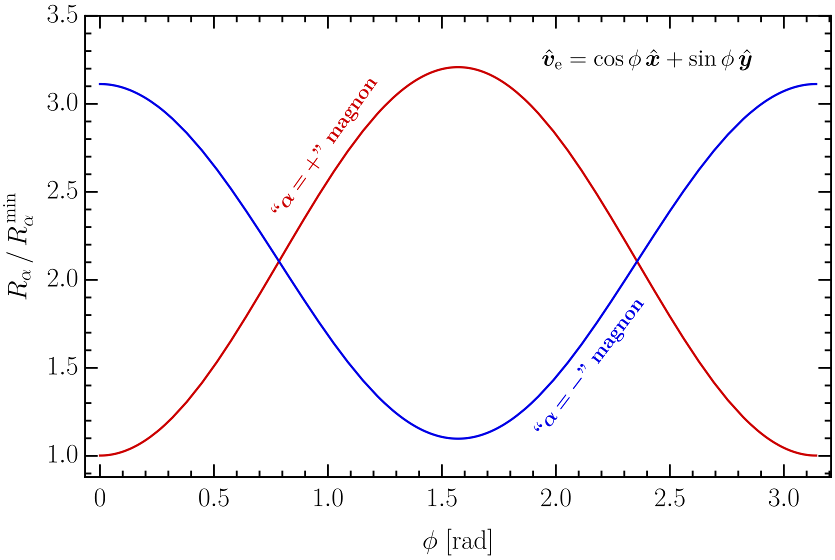

Figure 5.1: *One-magnon event rate as a function of the direction of the Earth velocity, taken to be on the xy-plane, i.e.* $\hat{\boldsymbol{v}}_\mathrm{e} = \cos\phi\,\hat{\boldsymbol{x}} + \sin\phi\,\hat{\boldsymbol{y}}$*, at* $\mu_0 H = 1$ *T. The rate is normalized to its minimum value, achieved for* $\hat{\boldsymbol{v}}_\mathrm{e} = \hat{\boldsymbol{z}}$*. Note that the minima of the curve lie very close to* $R_\alpha/R_\alpha^{\mathrm{min}} = 1$*. This means, for example, that the* R_+ *rates evaluated at* $\boldsymbol{v}_\mathrm{e} = \hat{\boldsymbol{z}}$ *and* $\boldsymbol{v}_\mathrm{e} = \hat{\boldsymbol{x}}$ *are very similar. This is because the* V_α^a *vectors have one component much larger than the other, as a consequence of the large hierarchy between the effects due to the external magnetic field, and those due to the intrinsic anisotropies.*

After averaging Eq. (5.10) over the dark matter velocity distribution, the rate depends on the Earth velocity as

$$R_\alpha(\hat{\boldsymbol{v}}_\mathrm{e}) \propto \frac{\langle \boldsymbol{v}_\perp^2 \rangle}{2} V_\alpha^a (V_\alpha^a)^* + \left| v_\mathrm{e}^a V_\alpha^a \right|^2 , \tag{5.11}$$

where $\boldsymbol{v}_\perp$ is a velocity perpendicular to the order parameter (i.e., on the xy-plane), and directionality is due to the second term. If the axion has the right mass to emit an $\alpha = +$ magnon, the rate is maximum when $\hat{\boldsymbol{v}}_\mathrm{e} = \hat{\boldsymbol{y}}$, while for $\alpha = -$, this happens when $\hat{\boldsymbol{v}}_\mathrm{e} = \hat{\boldsymbol{x}}$. In Fig. 5.1 we report the directional dependence of the event rate. As anticipated, the signal modulation is very strong. However, we point out that realistic materials present various domains, each with a different orientation of the order parameter. This effect could decrease the modulation.[2]

In Fig. 5.2 we instead show the projected reach obtained assuming three events per year for a kilogram of NiO, in the ideal absence of background. The total rate is given by $R = R_+ + R_-$, and we evaluate it in the $\hat{\boldsymbol{v}}_\mathrm{e} = \hat{\boldsymbol{x}}$ configuration. The result obtained for the $\hat{\boldsymbol{v}}_\mathrm{e} = \hat{\boldsymbol{y}}$ is analogous, differing by no more than order 1. We show results for both $\gamma_\alpha/\omega = 10^{-3}$ and 10^{-5}, with the second one being rather optimistic and likely achievable only in very pure samples. We also scan different values of the external magnetic field, in the range $\mu_0\mathrm{H} \in [0, 4.5]$ T. Crucially, when this approaches the critical value (see Sec. 5.2.1), the one-magnon process probes lower and lower values of the axion mass, as again shown in Fig. 5.2. This makes the H-field scanning in NiO potentially a very powerful avenue to cover a large portion of the parameter space.

5.3.2 Two-magnon absorption

As explained also in [200], antiferromagnets offer the possibility of multi-magnon events, which are instead strongly suppressed by symmetry in ferrimagnets [188]. In the context of axion absorption,

[2] We are grateful to G. Marocco for pointing this out.

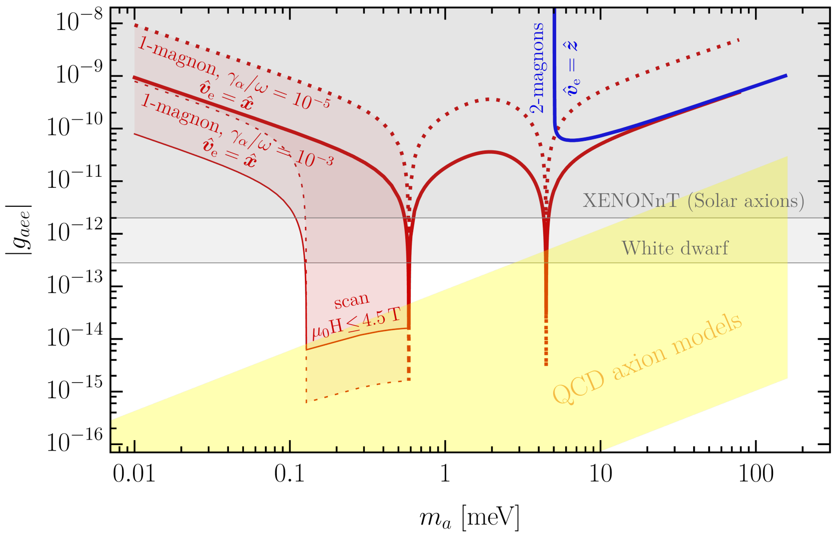

Figure 5.2: *Projected reach at 95% CL for a kilogram of material and a year of exposure, assuming no background. For single magnon absorption, we treat γ_α/ω as a free parameter. The one- and two-magnon channels have been computed, respectively, for $\hat{\boldsymbol{v}}_e = \hat{\boldsymbol{x}}$ and $\hat{\boldsymbol{v}}_e = \hat{\boldsymbol{z}}$. The red shaded regions are obtained for a magnetic field varying in the range $\mu_0 H \in [0, 4.5]$ T. The same scan for the higher magnon mode is not visible in logarithmic scale. The projections are interrupted when the energy/momenta involved exceed the EFT cutoff. The yellow band corresponds to the QCD axion models reviewed, for example, in [99, 222], and is stopped in correspondence to the cosmological bound determined in [223]. The white dwarf bound is taken from [224], and the XENONnT one from [176] (see also [225]).*

these allow for a broadband channel, since the system can absorb axions with different masses by simply changing the energy and relative momentum of the multiple excitations, without the need for any external tuning. In our EFT language, the matrix element for two-magnon absorption is in Eq. (5.7b).

In this case the magnons are effectively emitted back-to-back, $\boldsymbol{p} \simeq -\boldsymbol{k}$, since again the axion momentum is irrelevant. This considerably simplifies the calculation of the event rate, which is now the sum over all possible outgoing magnons $R = R_{++} + R_{+-} + R_{-+} + R_{--}$. Moreover, contrary to the one-magnon case, the maximum rate in this case is obtained for $\hat{\boldsymbol{v}}_e = \hat{\boldsymbol{z}}$. The resulting projections are again reported in Fig. 5.2. As one can see, the absorption into two magnons provides a broadband channel, which can be dominant when the magnons are particularly long-lived.

5.4 Conclusions

NiO can be employed as an optimal target to probe the electron coupling of axion dark matter with masses around the meV and couplings down to the QCD axion ones, a region still experimentally uncharted. The one-magnon channel features a strongly directional signal, which can be key to an efficient background rejection strategy. Moreover, by varying the external magnetic field toward its critical "spin-flop“ value, it is possible to probe axion masses that are, in principle, arbitrarily small, thus covering a large portion of the unexplored parameter space. Finally, the excitation of multiple magnons in the final state provides a broadband channel for axion absorption, which is the dominant signature in samples that allow for an especially narrow magnon mode.

Our results, together with the previous proposal to employ NiO as a target for sub-MeV dark matter scattering from spin-dependent interactions [200], make a strong physics case for the employment of this material as a *multi-purpose* target for light dark matter searchers, covering a brand new region of parameter space.

This also paves the way to a number of further investigations. For instance, our study does not deal with magnetic fields that are arbitrarily close to the critical point, as other effects might become relevant when the magnon becomes sufficiently light. It is also important to understand how the possible directional signal is affected by the presence of multiple domains in a realistic material, or if other material might perform better than NiO (see, e.g., [226]). In this second instance, one will have to work out another EFT, if useful. Moreover, it is known that NiO features a number of additional light excitations [140], and that the magnon gaps can also be varied (quite a lot) by applying an external strain to the sample [e.g., 161]. Neither of these features are currently included in our EFT, and their implications for light dark matter searches have not been explored. In particular, if not suppressed by possible selection rules, the other light magnon modes could provide additional channels for axion absorption, which would allow one to cover an even larger region in parameter space. Finally, to turn this into a concrete proposal, one must address the question of what are the observable signatures associated with the emission of magnons in the NiO sample. This is also relevant in light of the fact that, once a concrete detection strategy is in place, the final excluded region could be different from the ideal one presented here. We leave these and other interesting directions for future work.

Part III

Naturalness and inflation

CHAPTER

6

Highest natural scale and inflation

6.1 Introduction

Whether the Standard Model is a *natural* theory or not remains an open question—one that has fueled remarkably theoretical development (see e.g. the review [227] and the references cited therein). In a nutshell, a theory is *natural* if the contribution to the Higgs mass δm_h arising from quantum corrections is not larger than Higgs pole mass $M_h \approx 125\,\mathrm{GeV}$. However, it is less clear how to implement the naturalness principle concretely. For example, if we assume some unknown scale of new physics $\Lambda_{\rm NP}$ and compute the one-loop correction to the Higgs mass coming from the top quark using cutoff regularization, we would get $\delta m_h^2 \sim y_t^2/(4\pi)^2\Lambda_{\rm NP}^2$, where $y_t \approx 1$ is the top Yukawa coupling. The condition $\delta m_h^2 \lesssim M_h^2$ would imply $\Lambda_{\rm NP} \lesssim \mathrm{TeV}$. However, no new physics has been so far seen at LHC with $\sqrt{s} \approx 14\,\mathrm{TeV}$. This argument invests the regulator with a physical meaning [24, 228], namely $\Lambda_{\rm NP}$ is the scale where the Higgs mass becomes calculable. Although this physical interpretation, quadratic divergences are regulator-dependent artifacts and do not manifest in all regularization schemes—for example, they are absent in dimensional regularization, where power-law divergences are systematically set to zero.

A practical, bottom-up possibility for reconciling the naturalness principle with experimental constraints is provided by the criterion of *finite naturalness*, introduced in Ref. [229] (see also [234]). The basic idea is that we should ignore quadratic divergences in loop computations. From the UV perspective, such an assumption may be justified in models where an infinite tower of states at the new-physics scale cancels power divergences [235, 236], or where the Planck scale arises from spontaneous symmetry breaking [229]. The finite naturalness principle guarantees that the Higgs mass remains small if there are no new heavy mass particles sizably coupled to the Higgs boson. Indeed, the Standard Model alone satisfies the criterion of finite naturalness, without demanding new physics up to the Planck scale [229]. However, in extensions of the Standard Model that introduce particles with masses far above the weak scale, the Higgs mass generally acquires a quadratic dependence on these heavy scales—independent of the chosen regularization or subtraction scheme. Fig. 6.1 schematically illustrates the finite naturalness bound in relation to the presence of a mass scale M, directly or loop-coupled to the Higgs, as motivated by beyond-the-Standard-Model scenarios.

Hereafter, we define the Planck mass through $G = M_{\rm Pl}^{-2}$, and the reduced Planck mass as $\bar{M}_{\rm Pl} = M_{\rm Pl}/\sqrt{8\pi}$.

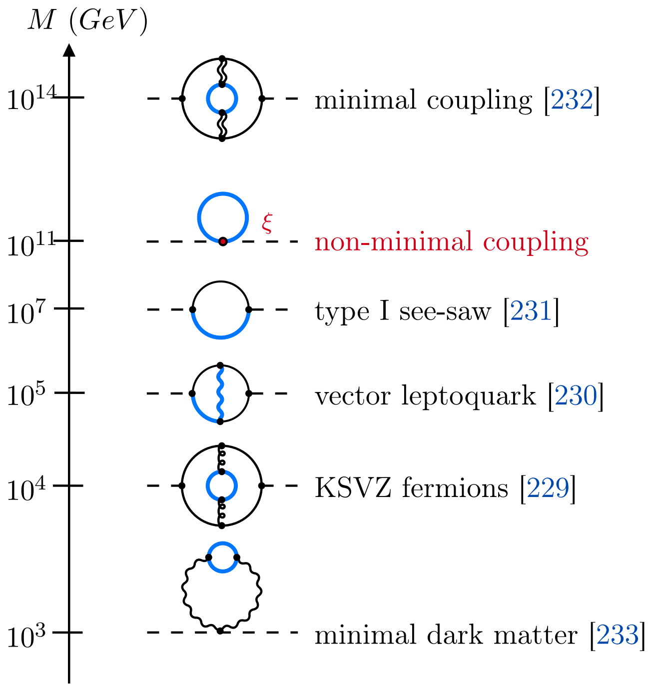

Figure 6.1: *Finite naturaleness limits for new physics scenarios. Thick blue lines show heavy states with mass M coupled to Standard Model particles (thin black lines in loops).*

6.2 The SM with a decoupled heavy scale

As a proxy for the existence of a heavy mass scale, we introduce a Dirac fermion Ψ with mass M_Ψ and without direct coupling to the Higgs boson. Therefore, contributions to the Higgs running mass m_H proceeds through the exchange of virtual gravitons. The common lore is that one needs (at least) three loops to produce an additive contribution to the Higgs running mass involving the new heavy scale [229, 232], $\delta m_h^2 \sim y_t^2 M_\Psi^6/\bar{M}_{\rm Pl}^4(4\pi)^6$, resulting in a finite naturalness bound [232] $M_\Psi \lesssim 10^{14}\,$GeV.

This result is derived assuming that the Higgs boson is minimally coupled to gravity. However, quantum fluctuations will unavoidably generate a dimension-four operator $\xi H^\dagger H R$, even if set to zero at some scale [237, 238]. Thus, the principle of renormalizability demands the addition of this operator to the original action from the beginning, inducing a non-minimal coupling to gravity.

We start with the Jordan frame action

$$\begin{aligned}\mathcal{S} = \int d^4x\sqrt{-g}\Big\{\frac{1}{2}\left[\bar{M}_{\rm Pl}^2+\xi(h+v)^2\right]R+\frac{1}{2}(\partial_\mu h)(\partial^\mu h)-\left(\frac{1}{2}m^2h^2+\lambda v h^3+\frac{\lambda}{4}h^4\right)\Big\}\\ + S_m(\Psi, g_{\mu\nu}; M_\Psi)\,, \end{aligned} \tag{6.1}$$

that combines the Einstein-Hilbert term (R is the Ricci scalar), the Higgs sector of the SM after spontaneous symmetry breaking and the matter action S_m describing the Dirac fermion Ψ (decoupled from the SM). The Higgs mass is $m^2 = 2\lambda v^2$. We work in the unitary gauge and neglect the interaction terms in the covariant derivatives.

The non-minimal coupling gives rise to a kinetic mixing between the Higgs and the graviton. The propagation of these two degrees of freedom is decoupled by means of a conformal transformation

$$g_{\mu\nu} \to \Omega^2 g_{\mu\nu}\,, \qquad \text{with:} \quad \Omega^2 \equiv 1+\frac{\xi(h+v)^2}{\bar{M}_{\rm Pl}^2}\,. \tag{6.2}$$

Together with suitable field redefinitions, Eq. (6.2) brings the original action Eq. (6.1) into the Einstein frame, where the Higgs field becomes indeed minimally coupled to gravity, but the scalar potential and the matter action are transformed (see Supplementary Materials for details). The key aspect is that the fermion mass term becomes

$$-\frac{M_\Psi}{\Omega}\bar{\Psi}\Psi\,, \tag{6.3}$$

with Ω given in Eq. (6.2). In the Einstein frame, therefore, the Ψ mass generates a tower of interaction terms that couples Ψ to the Higgs field. The leading correction to the Higgs mass in the limit $\xi \ll 1$ comes from the following effective operator

$$\frac{\xi M_\Psi}{2\bar{M}_{\rm Pl}^2}h^2\bar{\Psi}\Psi\,. \tag{6.4}$$

In Supplementary Materials we also derive the same result working directly in the Jordan Frame, showing consistency among various approaches.

At one loop, the finite contribution to the Higgs mass from the vertex Eq. (6.4) is

$$\delta m_h^2 = \xi\frac{4M_\Psi^4}{(4\pi)^2\bar{M}_{\rm Pl}^2}\,, \tag{6.5}$$

that gives the following bound of naturalness on the mass-scale M_Ψ

$$M_\Psi \lesssim 10^{10}\,\xi^{-1/4}\,\text{GeV}\,. \tag{6.6}$$

This is more stringent than the bound given in Refs. [229, 232]. Of course, Eq. (6.6) depends on the non-minimal coupling ξ; however, it should be noted that the latter only enters with the scaling $\xi^{-1/4}$ which makes the dependence mild. Thus, even when ξ is loop generated, i.e. $\xi \sim 1/(4\pi)^2$, the corresponding bound is $M_\Psi \lesssim 10^{11}$.

The bound in Eq. (6.6) holds also if we consider a scalar field instead of a Dirac fermion in the original action Eq. (6.1), since the resulting mass term in going from the Jordan to the Einstein frame will again acquire a factor Ω^{-1}.

6.3 Application to inflationary theories.

We consider an inflaton field ϕ with canonically normalized kinetic term and potential given, at the renormalizable level, by

$$V(\phi) = \sum_{k=2}^{4}\frac{a_k}{k!}\frac{g^{k-2}\phi^k}{M^{k-4}}\,, \tag{6.7}$$

where g is some fundamental coupling, M a mass scale and a_k dimensionless coefficients. We find it advantageous to keep track of the correct powers of coupling, along with those of mass, in the various terms of the potential. We further assume that the mass M and the Planck scale are related by the equation $g\bar{M}_{\rm Pl} = M$. The potential takes the form

$$V(\phi) = M^2\bar{M}_{\rm Pl}^2\sum_{k=2}^{4}\frac{a_k}{k!}\left(\frac{\phi}{\bar{M}_{\rm Pl}}\right)^k\,. \tag{6.8}$$

We further define $c_k \equiv a_k/k!$, and $\bar{c}_k \equiv c_k/c_4$. We thus rewrite our potential in the form

$$V(x) = c_4M^2\bar{M}_{\rm Pl}^2\left[\bar{c}_2x^2 + \bar{c}_3x^3 + x^4\right]\,, \tag{6.9}$$

with $x \equiv \phi/\bar{M}_{\rm Pl}$. The expression in square brackets is purely dimensionless, while the dimensionful part of the potential is completely captured by the factorized product $M^2\bar{M}_{\rm Pl}^2$. Field values are naturally given in units of the reduced Planck mass. The potential in Eq. (6.9) is nothing but a linear combination of monomial terms, each of which, if analyzed individually, is in tension with the upper limit on the tensor-to-scalar ratio. To overcome this issue, we consider a specific combination that yields the presence of an exact stationary inflection point at some field value ϕ_0. In other words, we impose the conditions $V'(\phi_0) = V''(\phi_0) = 0$. Solving the corresponding system of equations, we write

$$V(x) = c_4 M^2 \bar{M}_{\rm Pl}^2 \left[2x_0^2 x^2 - \frac{8x_0}{3}x^3 + x^4\right] , \tag{6.10}$$

with $x_0 \equiv \phi_0/\bar{M}_{\rm Pl}$. In this form, the model features two free parameters. The overall scale of the potential, $V_0 \equiv c_4 M^2 \bar{M}_{\rm Pl}^2$, and the parameter x_0 that controls the position of the stationary inflection point. In particular, only x_0 enters into the description of the inflationary dynamics, while V_0 is an overall normalization essentially determined by ensuring the match with the measured value of A_s.

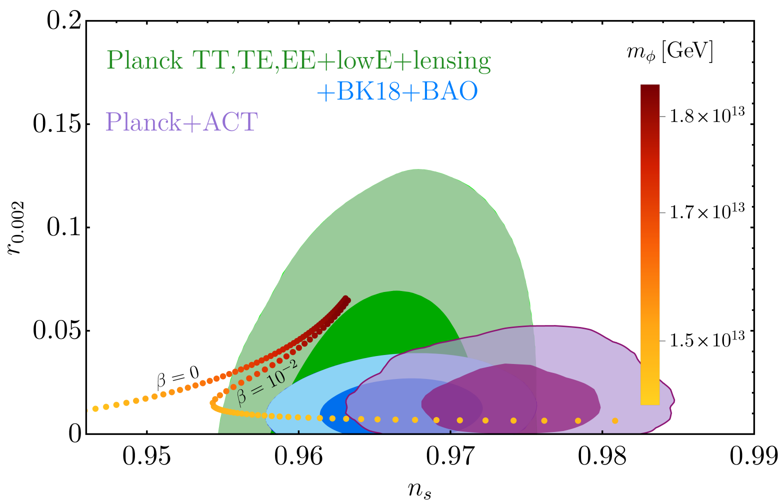

Figure 6.2: *Prediction in the (n_s, r) plane for the model given in Eq. (6.14). We fix two characteristic values $\beta = 0, 10^{-2}$ while varying the parameter x_0. We keep track of the latter in the color bar, treating it as the mass of the inflaton m_ϕ. We require $N = 55$ e-folds of inflation after CMB modes exited the horizon. Experimental constraints are shown using the Planck 2018 baseline analysis (green regions) and including BICEP/Keck and baryon acoustic oscillation (BAO) data (blue regions), cf. Ref. [239]. We also show (purple regions) the recent results from the Atacama Cosmology Telescope (ACT), cf. Ref. [240]. We show the 65% and 95% confidence contours. When the inflection point is exact ($\beta = 0$) the model is in tension with BK18+BAO and ACT data.*

In Fig. 6.2, we plot the model's prediction in the (n_s, r) plane for the two characteristic values of $N = 50, 60$ e-folds, varying the parameter x_0 (see the Appendix for details about the procedure we use to extract cosmological observables). We keep track of the latter in the legend, treating it as the mass of the inflaton m_ϕ, which we define as

$$m_\phi^2 \equiv 4x_0^2 \left(\frac{c_4 M^2}{\bar{M}_{\rm Pl}^2}\right) \bar{M}_{\rm Pl}^2 . \tag{6.11}$$

We read the combination of parameters $c_4 M^2/\bar{M}_{\rm Pl}^2$ directly from the measured value of A_s since in the slow-roll approximation we just have

$$A_s = \frac{V(\phi_*)}{24\pi^2 \epsilon_V(\phi_*)\bar{M}_{\rm Pl}^4}\,, \tag{6.12}$$

Besides being in tension with the recent ACT data (see purple region in Fig. 6.2), this model has a more severe problem. The slow-roll trajectory identified by the solutions analyzed in Fig. 6.2 is not an attractor. The simplest way to convince oneself of this point is to calculate the number of e-folds. In slow-roll approximation, we find

$$N = -\int_{x_*}^{x_{\rm end}} \frac{V(x)}{V'(x)}dx = -\int_{x_*}^{x_{\rm end}} \frac{x(3x^2 - 8xx_0 + 6x_0^2)}{12(x-x_0)^2}dx\,, \tag{6.13}$$

where $x_* = \phi_*/\bar{M}_{\rm Pl}$ and $x_{\rm end} = \phi_{\rm end}/\bar{M}_{\rm Pl}$. The integrand function in Eq. (6.13) features a singularity at $x = x_0$. Since, by construction, $x_{\rm end} < x_0$, we are compelled to choose $x_* < x_0$ to avoid encountering the singularity. Indeed, in the analysis leading to Fig. 6.2, we imposed the condition $0 < x_{\rm end} < x_* < x_0$. Clearly, there is nothing mathematically wrong in restricting our analysis to this choice. $x_* < x_0$.

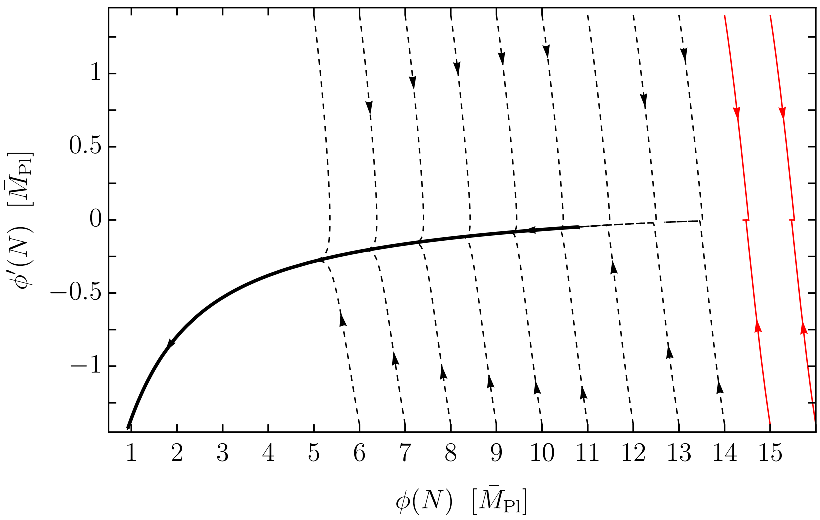

Figure 6.3: *Phase-space portrait of the classical inflationary dynamics for $x_0 = 15$ ($\beta = 0$). The slow-roll trajectory associated to observable inflation is indicated in solid bold black. The trajectories marked in red are disconnected from the rest of the phase space.*

We confirm the previous findings in slow-roll approximation by showing in Fig. 6.3 a phase-space portrait of the classical inflationary dynamics, obtained solving exactly Eq. (6.34) with arbitrary initial conditions. As a benchmark value, we consider $x_0 = 15$. The trajectories marked in red are disconnected from the rest of the phase space. Following these trajectories, the inflaton stops at around the inflection point, and inflation never ends. On the contrary, all trajectories indicated with dashed black lines converge onto the slow-roll trajectory, indicated in solid bold black, rolling along which the inflaton first reaches the condition $\epsilon > 1$ where the accelerated expansion ends and subsequently the minimum at $x = 0$ where reheating oscillations begin.

In the next section, we show that is it possible to modify the model in such a way that slow-roll becomes an attractor of the dynamics.

6.3.1 Quasi-stationary inflection point inflation.

We perturb the stationary inflection point [241] allowing the cubic term in Eq. (6.10) to deviate by a factor $1-\beta$, i.e.

$$V(x) = c_4 M^2 \bar{M}_{\rm Pl}^2 \left[2x_0^2 x^2 - \frac{8x_0}{3}(1-\beta)x^3 + x^4 \right] . \tag{6.14}$$

With this expression, both $V'(x_0)$ and $V''(x_0)$ are proportional to β. Thus, assuming $\beta \ll 1$, x_0

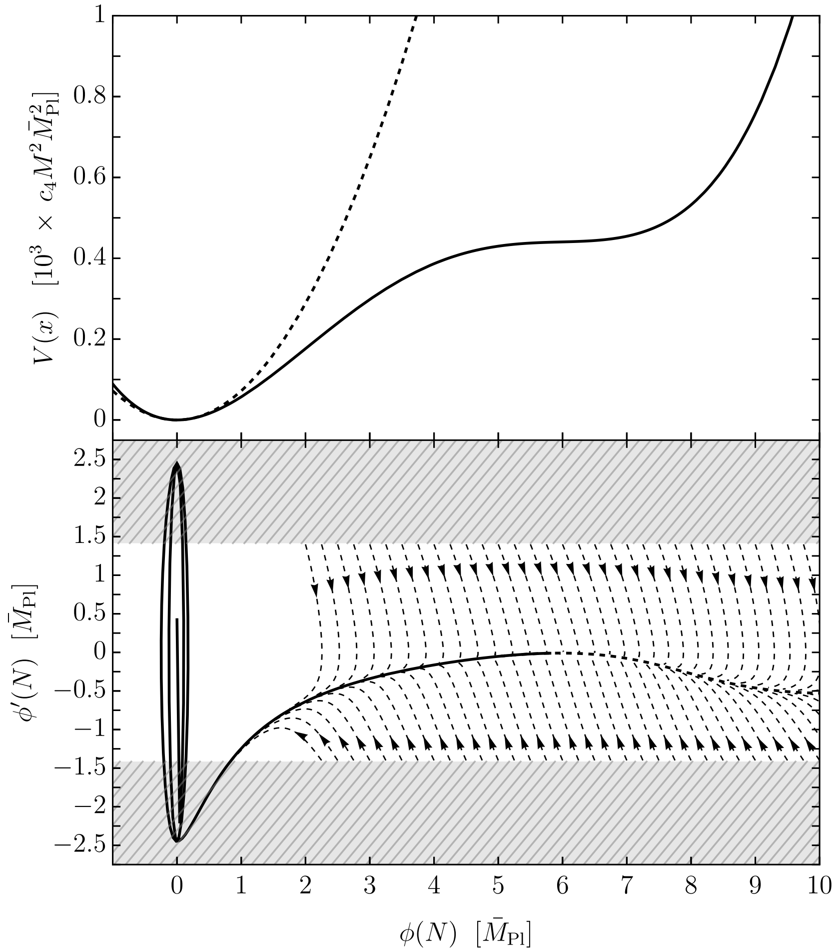

Figure 6.4: *Phase-space portrait of the classical inflationary dynamics for $x_0 = 6$ and $\beta = 10^{-3}$. Varying β does not qualitatively change the behaviors of the dynamics. The point along the slow-roll trajectory which marks the transition between the continuous and dashed part corresponds to x_*, i.e. the field value at which the CMB modes exited the horizon during inflation.*

becomes an approximate inflection point. This simple generalization introduces new features into the model. In particular, in Fig. 6.4 we show the phase-space portrait of the classical inflationary dynamics using the benchmark value $x_0 = 6$. At the variance with the previous case, there are no more curves disconnected from the slow-roll trajectory, meaning that the latter becomes an attractor of the dynamics. Hence, we conclude that in the large-field regime ($x_0 > 1$) the inflationary dynamics is robust against perturbations of the initial condition. However, this conclusion has to be changed in the limit of small-field values ($x_0 \lesssim 1$). In Fig. 6.5, we show again the phase-space portrait of the inflationary dynamics, but fixing $x_0 = 1$. Remarkably, there are two distinct trajectories that contains a phase of slow-roll inflation. The first one, marked in blue, acts as an attractor for trajectories with initial position $\phi(N=0) \lesssim 2\,\bar{M}_{\rm Pl}$, whereas the second one, highlighted in orange, is an attractor when

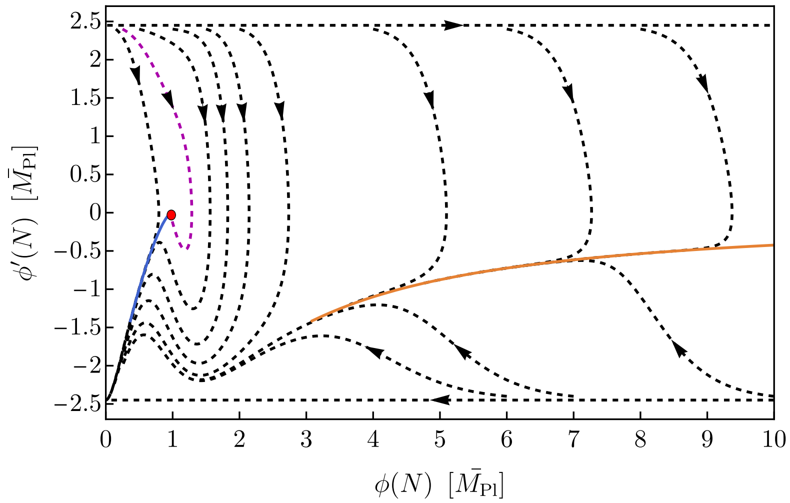

Figure 6.5: *Phase-space portrait of the classical inflationary dynamics for $x_0 = 1$ and $\beta = 1.85 \times 10^{-6}$. Varying β does not qualitatively change the behaviors of the dynamics. There are two distinct trajectories that contains a phase of slow-roll inflation, marked in blue and in orange. The red point along the blue trajectory corresponds to $x_* \approx 0.9992$, i.e. the field value at which the CMB modes exited the horizon during inflation. The resulting observables are $n_s = 0.965$ and $r = 2 \times 10^{-8}$.*

the initial position is $\phi(N = 0) \gtrsim 2\,\bar{M}_{\rm Pl}$. In the latter case, the slow-roll parameters are kept small since the field goes through super-Planckian values and the quasi-inflection point in $x_0 = 1$ does not play any role. Indeed, the orange curve in Fig. 6.5 is qualitatively the same slow-roll phase generated by a generic combination of monomials, incompatible with the Planck measurements. Viceversa, the slow-roll parameters associated to the blue curve in Fig. 6.5 are small thanks to the quasi-stationary inflection point. In this case, $N \approx 55$ e-folds of observed inflation requires the CMB modes to exit the horizon at $x_* \approx 0.9992$ (see the red point in Fig. 6.5), i.e. slightly smaller than x_0. However, the latter point is not generically reached for trajectories with initial position $\phi(N = 0) \lesssim 2$ and thus the model requires fine-tuning. To clarify this property of the model, let us consider the dashed magenta curve depicted in Fig. 6.5, which goes through x_* and gives rise to inflationary observables compatible with Planck data. We see from Fig. 6.5 that a small perturbation on this trajectory generates a new curve which does not go through x_* (even if it will generically fall onto the slow-roll trajectory in blue). These results highlight that the small-field regime is not robust against perturbation on the initial conditions, even if capable of reproducing experimental data.

The presence of two distinct slow-roll trajectories in the small-field regime is better understood by studying the solutions to the equation $\epsilon_V = 1$, where ϵ_V is defined in Eq. (6.37). It turns out that for $x_0 \gg 1$ there is only one positive solution, confirming the existence of just one slow-roll trajectory. On the other hand, for $x_0 \lesssim 1$ different solutions arise, allowing for the existence of a second slow-roll trajectory. In particular, it is possible to analytically compute the point where the equation $\epsilon_V = 1$ develops multiple positive solutions for $\beta \ll 1$ as $x_0 \approx 2.3$.

6.3.2 How robust is single-field inflation?

In Fig. 6.6 we show the allowed parameter space of the model, together with different values of the inflaton mass. In the large-field regime ($x_0 \gtrsim 1$), as pointed out in the previous section, inflation is robust against perturbations of the initial conditions. However, Fig. 6.6 shows that the corresponding values of inflaton mass violate the naturalness bound Eq. (6.6), resulting in a destabilization of the running Higgs mass. To avoid this problem, we are forced to work in the small-field regime ($x_0 \lesssim 1$), where $m_\phi \lesssim 10^{11}$ GeV. Nevertheless, we already highlighted that in this regime a successful inflationary dynamics requires a considerable amount of fine-tuning. Furthermore, the recent results from ACT [240] pushes the viable region in the parameter space even further into the disfavored regime, as visible in Fig. 6.6. We emphasize that introducing a direct coupling between the inflaton and the Standard Model, such as $\lambda\phi^2 h^2$, worsens this issue, as the bound in Eq. (6.6) would become even more stringent.

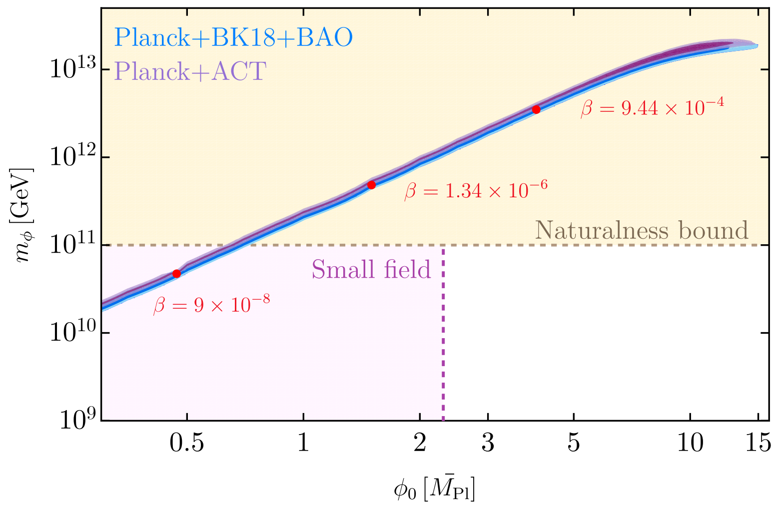

Figure 6.6: *Parameter space of the model considered in Eq. (6.14), shown for different values of the β parameter. We fix $\xi = 1/(4\pi)^2$, assuming it is loop-generated. The resulting excluded region, corresponding to $m_\phi \gtrsim 10^{11}$, GeV, is shown in beige. The small-field regime, $x_0 \lesssim 2.3$, is indicated in light pink. The region of parameter space compatible with Planck data (blue/azure region), for $N \approx 55$ e-folds of inflation, either lies within the region excluded by finite naturalness or falls into the small-field regime, where inflationary dynamics requires significant fine-tuning (see Fig. 6.5). The ACT data (purple region) further accentuate this trend. As highlighted in the discussion, the naturalness bound depends only mildly on ξ.*

6.4 Conclusions

In this work, we showed that in the limiting case of an inflationary sector $\mathcal{L}_\phi$ that couples only gravitationally to the SM, fine-tuning is not an option. In particular, in the large field regime inflationary dynamics provides a compelling dynamical solution to the origin of the observed universe. However, the required inflaton mass – assuming a finite naturalness criterion – is in conflict with the weak scale, even if direct couplings to the Standard Model are absent. This is because the principle of renormalizability demands a non-minimal coupling of the Higgs to gravity, resulting in a contribution to the runnig Higgs mass well before the three-loop diagrams previously discussed in the literature [232]. On the other hand, a light inflation would pacifically coesist with the weak scale, but implies a considerable amount of fine-tuning on the inflationary dynamics, as also shown in Ref. [242].

There are numerous avenues for future research. First of all, we note that although $\phi(N)$ and $\phi'(N)$ define an effective phase space, they do not constitute canonical variables [243]. Consequently, a rigorous quantification of the fine-tuning in the small-field regime requires introducing a suitable canonical measure (see e.g. Ref. [244]). Additionally, our findings might be used as a theoretical guide for classes of models that elegantly evade the naturalness bound while still operating in the large-field regime. In this regard, our work motivates the exploration of alternative cosmological scenarios, such as bouncing cosmologies [245–247], and may represent a first step toward rethinking the origin of the universe. These questions, however, are beyond the scope of the present work and are left for future investigation.

6.5 Appendix A: Transformation from the Jordan to the Einstein frame

We start with the Jordan frame action

$$\mathcal{S}_{\mathrm{EH}+H} = \int d^4x\sqrt{-g}\left[\left(\frac{1}{2}\bar{M}_{\mathrm{Pl}}^2 + \xi H^\dagger H\right)R + (D_\mu H)^\dagger (D^\mu H) - V(H^\dagger H)\right], \tag{6.15}$$

that combines the Einstein-Hilbert term (R is the Ricci scalar) and the Higgs sector of the SM. The Higgs potential is $V(H^\dagger H) = -\mu^2 H^\dagger H + \lambda(H^\dagger H)^2$ and $D_\mu H$ is the $SU(2)_L \otimes U(1)_Y$ covariant derivative acting on the Higgs doublet. For simplicity's sake, we omit the subscript indicating bare parameters and fields. The potential $V(H^\dagger H)$ induces spontaneous symmetry breaking, and, after expanding around the minimum of the potential, we get

$$\mathcal{S}_{\mathrm{EH}+H} \ni \int d^4x\sqrt{-g}\left\{\frac{1}{2}\left[\bar{M}_{\mathrm{Pl}}^2 + \xi(h+v)^2\right]R + \frac{1}{2}(\partial_\mu h)(\partial^\mu h) - \left(\frac{1}{2}m^2h^2 + \lambda v h^3 + \frac{\lambda}{4}h^4\right)\right\}, \tag{6.16}$$

where $m^2 = 2\lambda v^2$. We only focus on the Higgs field (i.e. we work in the unitary gauge and neglect the interaction terms in the covariant derivatives). Next, we move to the Einstein frame (further details can be found in Ref. [248]). The Lagrangian density for the Higgs field reads

$$\mathcal{L}_H = \frac{1}{2}\left[\frac{1}{\Omega^2} + \frac{3\bar{M}_{\mathrm{Pl}}^2}{2\Omega^4}\left(\frac{d\Omega^2}{dh}\right)^2\right](\partial_\mu h)(\partial^\mu h) - \frac{1}{\Omega^4}\left(\frac{1}{2}m^2h^2 + \lambda v h^3 + \frac{\lambda}{4}h^4\right),$$

with:

$$\Omega^2 \equiv 1 + \frac{\xi(h+v)^2}{\bar{M}_{\mathrm{Pl}}^2}\,. \tag{6.17}$$

This Lagrangian density describes a non-renormalizable scalar theory. This is the prize to pay, in the Einstein frame, for the non-minimal coupling of the scalar H to gravity – that is, a non-renormalizable theory – in the Jordan frame. We expand the above Lagrangian up to dimension-four operators in the field h. We find

$$\begin{aligned}\mathcal{L}_H =& \frac{1}{2}\left[\frac{1+\xi(1+6\xi)v^2/\bar{M}_{\mathrm{Pl}}^2}{(1+\xi v^2/\bar{M}_{\mathrm{Pl}}^2)^2}\right](\partial_\mu h)(\partial^\mu h) \\ &- \left[\frac{1}{2}\frac{m^2}{(1+\xi v^2/\bar{M}_{\mathrm{Pl}}^2)^2}h^2 + \frac{v\lambda(1-3\xi v^2\bar{M}_{\mathrm{Pl}}^2)^2)}{(1+\xi v^2/\bar{M}_{\mathrm{Pl}}^2)^3}h^3\right. \\ &\left. + \frac{\lambda(1-22\xi v^2/\bar{M}_{\mathrm{Pl}}^2 + 25\xi^2v^4/\bar{M}_{\mathrm{Pl}}^4)}{4(1+\xi v^2/\bar{M}_{\mathrm{Pl}}^2)^4}h^4\right] \\ &+ \text{higher dim operators}\,.\end{aligned} \tag{6.18}$$

The field h in Eq. (6.18) is not canonically normalized. If we rescale

$$h \to a h\,, \qquad \text{with:} \quad a \equiv \frac{1+\xi v^2/\bar{M}_{\mathrm{Pl}}^2}{[1+\xi(1+6\xi)v^2/\bar{M}_{\mathrm{Pl}}^2]^{1/2}}\,, \tag{6.19}$$

we find the Lagrangian density

$$\begin{aligned}\mathcal{L}_H =& \frac{1}{2}(\partial_\mu h)(\partial^\mu h) - \left\{\frac{1}{2}\frac{m^2}{[1+\xi(1+6\xi)v^2/\bar{M}_{\rm Pl}^2]}h^2 + \frac{v\lambda(1-3\xi v^2/\bar{M}_{\rm Pl}^2)}{[1+\xi(1+6\xi)v^2/\bar{M}_{\rm Pl}^2]^{3/2}}h^3\right. \\ &\left. + \frac{\lambda(1-22\xi v^2/\bar{M}_{\rm Pl}^2+25\xi^2v^4/\bar{M}_{\rm Pl}^4)}{4[1+\xi(1+6\xi)v^2/\bar{M}_{\rm Pl}^2]^2}h^4\right\}, \end{aligned} \tag{6.20}$$

with additional higher-dimensional operators that are not shown. In the limit $\xi \to 0$, Eq. (6.20) reproduces the Lagrangian density of the SM describing the massive Higgs excitation and its self-interactions in the broken phase of the electroweak symmetry. The Higgs mass is now given by

$$M_h^2 \equiv \frac{m^2}{[1+\xi(1+6\xi)v^2/\bar{M}_{\rm Pl}^2]} = m^2\left[1 - \frac{2\xi(1+6\xi)v^2}{\bar{M}_{\rm Pl}^2} + O\left(\frac{v^4}{\bar{M}_{\rm Pl}^4}\right)\right], \tag{6.21}$$

and equals the tree-level Higgs mass in the SM (that is, $M_h^2 = m^2$) plus small gravitational corrections. Similarly, the trilinear and qurtic Higgs couplings take the form

$$\begin{aligned} &\text{trilinear:}\ \ \lambda v\left[1-\frac{3}{4}\xi(5+6\xi)\frac{v^2}{\bar{M}_{\rm Pl}^2}+O\left(\frac{v^4}{\bar{M}_{\rm Pl}^4}\right)\right]h^3\,, \\ &\text{quartic:}\ \ \frac{\lambda}{4}\left[1-\xi(23+6\xi)\frac{v^2}{\bar{M}_{\rm Pl}^2}+O\left(\frac{v^4}{\bar{M}_{\rm Pl}^4}\right)\right]h^4\,. \end{aligned} \tag{6.22}$$

We now add to the Jordan frame action in Eq. (6.15) the action for a free Dirac fermion Ψ with mass M_Ψ minimally coupled to gravity and decoupled from the Higgs field H. In the Einstein frame, the key aspect is that the mass term becomes

$$-\frac{M_\Psi}{\Omega}\bar{\Psi}\Psi\,, \tag{6.23}$$

with Ω given in Eq. (6.17). If we expand Ω^{-1} and rescale the field h according to Eq. (6.19), we find

$$\begin{aligned}\frac{M_\Psi}{\Omega}\bar{\Psi}\Psi =& \frac{M_\Psi}{(1+\xi v^2/\bar{M}_{\rm Pl}^2)^{1/2}}\left\{1 - \frac{\xi v h}{\bar{M}_{\rm Pl}^2[1+\xi(1+6\xi)v^2/\bar{M}_{\rm Pl}^2]^{1/2}}\right. \\ &\left. - \frac{\xi(1-2\xi v^2/\bar{M}_{\rm Pl}^2)}{2\bar{M}_{\rm Pl}^2[1+\xi(1+6\xi)v^2/\bar{M}_{\rm Pl}^2]}h^2 + O(h^3)\right\}\bar{\Psi}\Psi\,. \end{aligned} \tag{6.24}$$

In the Einstein frame, therefore, the Ψ mass generates a tower of interaction terms that couples Ψ to the Higgs field. The leading term that survives, as expected, even if we take the limit $v \to 0$, is the effective operator

$$\frac{\xi M_\Psi}{2\bar{M}_{\rm Pl}^2}h^2\bar{\Psi}\Psi\,, \tag{6.25}$$

which destabilizes the Higgs mass.

6.6 Appendix B: A Jordan Frame Analysis

It is possible to obtain Eq. (6.5) working directly in the Jordan frame. For the sake of simplicity, we focus directly on terms quadratic in h. We further assume $g_{\mu\nu} = \eta_{\mu\nu} + \kappa\, l_{\mu\nu}$, where $\kappa \equiv 2/\bar{M}_{\rm Pl}$. Since we are interested in the naturalness problem that arises in the present universe, we expand around a flat background. It is straightforward to generalized the discussion to an FRLW background, relevant for early-universe considerations. The main difference would be a shift in the pole Higgs mass due to the cosmological constant contribution, but the analysis about quantum corrections still holds.

At first order in κ, the graviton-scalar mixing induced by the non-minimal coupling is described by the term

$$\sqrt{-g}\,\frac{\xi}{2}R\,h^2 = \kappa\frac{\xi}{2}(l^{\mu\alpha}\partial_\mu\partial_\alpha - l\,\Box)h^2\,, \tag{6.26}$$

where $l = \eta^{\mu\nu}l_{\mu\nu}$. The overall graviton-scalar interaction can be written as

$$\sqrt{-g}\mathcal{L}_H^{(1)} = \frac{\kappa}{2}l^{\mu\nu}T_{\mu\nu}\,, \tag{6.27}$$

where $T_{\mu\nu}$ is the effective energy-momentum tensor associated to the scalar field, i.e.

$$T_{\mu\nu} = -\partial_\mu h\partial_\nu h + \eta_{\mu\nu}\Big(\frac{1}{2}\partial_\alpha h\partial^\alpha h - \frac{1}{2}m^2h^2\Big) - \xi(\eta_{\mu\nu}\Box - \partial_\mu\partial_\nu)h^2\,. \tag{6.28}$$

The corresponding amplitude is

$$\frac{-i\kappa}{2}\Big[p_{1\mu}p_{2\nu} + p_{1\nu}p_{2\mu} - \eta_{\mu\nu}(p_1\cdot p_2 - m^2) + 2\,\xi\Big(\eta_{\mu\nu}\,q^2 - q_\mu q_\nu\Big)\Big]\,, \tag{6.29}$$

and the associated Feynman diagram is

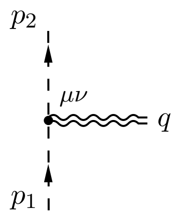

Figure 6.7: *Feynman diagram for the graviton-scalar vertex.*

The fact that the non-minimal interaction sources a contribution that involves only q_μ, the graviton momentum, is understood by noticing that the derivatives in Eq. (6.26) can be conveniently carried on $l_{\mu\nu}$, up to irrelevant boundary terms. The only diagrams that gives a contribution $\sim M_\Psi^4/\bar{M}_{\rm Pl}^2$ is the following tadpole

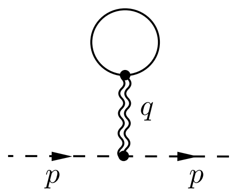

Figure 6.8: *Tadpole contribution to the Higgs propagator.*

Due to momentum conservation only the zero graviton modes mediate this tadpole, leading to an infrared divergence. We regularize this object by assuming $q^2 \neq 0$ and subsequently taking the limit $q^2 \to 0$. The contribution to the Higgs-self energy is then

$$i\Sigma_{grav} = \frac{i\kappa^2}{2(4\pi)^2}\frac{1}{q^2}M_\Psi^2 A_0(M_\Psi^2)\Big(3\xi q^2 + m_H^2\Big)\,. \tag{6.30}$$

As expected, the contribution coming from the standard vertex, obtained in the minimally coupled case, is proportional to m_H^2 and thus vanishes if we send $m_H^2 \to 0$. On the contrary the contribution from the non-minimal coupling cancels the soft graviton momentum at the denominator, leaving a finite contribution for $q^2 \to 0$, and does not vanish in the $m_H^2 \to 0$ limit. Thus, the additive contribution to the running Higgs mass is again

$$\delta m_H^2 \sim \xi \frac{1}{(4\pi)^2} \frac{M_\Psi^4}{\bar{M}_{\rm Pl}^2} \tag{6.31}$$

in agreement with Eq. (6.5).

Finally, we point out that an alternative way to cure the infrared divergence in Fig. 6.8 is to use a cosmological constant [249]. Indeed, an additional term $\sqrt{-g}\,\Lambda$ gives at fist order the following vertex proportional to $\eta_{\mu\nu}$

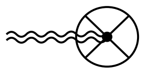

Figure 6.9: *Counterterm generated by the addition of a cosmological constant.*

Thus, the constant Λ can be fine-tuned in such a way that the tadpole (without including the graviton propagator) vanishes. However, this works only in the minimal case, since Λ can cancel only a constant quantity and not a momentum-dependent one. Therefore, the contribution proportional to ξ in Eq. (6.30) will unavoidably survive.

6.7 Appendix C: Inflaton dynamics and relation to cosmological observables

For the sake of clarity, let us take advantage of this point to define our notation. The Hubble rate is $H \equiv \dot{a}/a$, with $\dot{} \equiv d/dt$ where t is the cosmic time and a the scale factor of the flat Friedmann-Lemaître-Robertson-Walker (FLRW) metric $ds^2 = dt^2 - a^2(t)d\vec{x}^2$, with $\vec{x}$ comoving coordinates. The e-fold time N is defined by $dN = Hdt$. The Hubble-flow parameters ϵ_i (for $i \geqslant 1$) are defined by the recursive relation

$$\epsilon_i \equiv \frac{\dot{\epsilon}_{i-1}}{H\epsilon_{i-1}}\,, \qquad \text{with:} \quad \epsilon_0 \equiv \frac{1}{H}\,. \tag{6.32}$$

As customary, we simply indicate as ϵ the first Hubble parameter, $\epsilon \equiv \epsilon_1 = -\dot{H}/H^2$. Instead of the second Hubble parameter ϵ_2, sometimes it is useful to introduce the Hubble parameter η defined by

$$\eta \equiv -\frac{\ddot{H}}{2H\dot{H}} = \epsilon - \frac{1}{2}\frac{d\log\epsilon}{dN}\,, \qquad \text{with:} \quad \epsilon_2 = 2\epsilon - 2\eta\,. \tag{6.33}$$

Using the number of e-folds as time variable, the inflaton equation of motion reads

$$\frac{d^2\phi}{dN^2} + \left[3 - \frac{1}{2\bar{M}_{\rm Pl}^2}\left(\frac{d\phi}{dN}\right)^2\right]\left[\frac{d\phi}{dN} + \bar{M}_{\rm Pl}^2 \frac{d\log V(\phi)}{d\phi}\right] = 0\,, \tag{6.34}$$

and, in turn, the Hubble parameters take the form

$$\epsilon = \frac{1}{2\bar{M}_{\rm Pl}^2}\left(\frac{d\phi}{dN}\right)^2, \quad \eta = 3 + \frac{\bar{M}_{\rm Pl}^2(3-\epsilon)V'(\phi)}{V(\phi)(d\phi/dN)}\,, \tag{6.35}$$

while the Hubble rate is related to the inflaton potential by means of the Friedmann equation

$$(3-\epsilon)H^2 = V(\phi)\,. \tag{6.36}$$

We indicate the slow-roll approximation of ϵ and $\eta+\epsilon$ as ϵ_V and η_V. We have

$$\epsilon_V(\phi) = \frac{\bar{M}_{\rm Pl}^2}{2}\left(\frac{V'(\phi)}{V(\phi)}\right)^2 , \quad \eta_V(\phi) = \bar{M}_{\rm Pl}^2 \frac{V''(\phi)}{V(\phi)} . \tag{6.37}$$

As is well-known, the comparison of the theory's predictions with cosmological observables in the slow-roll limit consists of three steps.

* By imposing $\epsilon = 1$, we find the field value at the end of the accelerated phase of inflationary expansion, $\phi_{\rm end}$.
* Integrating $dN = Hdt$ in field space, we find the duration of inflation in the interval $(\phi_{\rm end}, \phi_*)$. In the slow-roll approximation, we have

$$N = -\frac{1}{\bar{M}_{\rm Pl}^2}\int_{\phi_*}^{\phi_{\rm end}} \frac{V(\phi)}{V'(\phi)} d\phi . \tag{6.38}$$

  We indicate with ϕ_* the field value at which the long-scale CMB modes exited the Hubble horizon during inflation. By requiring $N \in (50, 60)$ e-folds of inflation, we extract ϕ_* using Eq. (6.38).
* Finally, we compute

$$n_s = 1 + 2\eta_V(\phi_*) - 6\epsilon_V(\phi_*) , \qquad r = 16\epsilon_V(\phi_*) , \tag{6.39}$$

  and compare with cosmological data.

Acknowledgments

I thank my family, in particular my mother, Antonella, and my brothers, Edoardo, Orlando and Macchia.
I thank my mentors, Angelo Esposito and Alfredo Urbano, who guided me through research and for the many discussions on physics in which little was needed to understand each other.
I thank Roberto Contino, whose teachings and discussions permeate this thesis.
I thank Mauro Valli for the physics discussions and for his constant encouragements.
I thank Sidney Coleman, whose lectures on quantum field theory sparked my passion for Fundamental Interactions.
I thank all the other people I met along this journey.
Finally, I thank the waves of the Atlantic Ocean, among which this thesis was completed.

Ringraziamenti

Ringrazio la mia famiglia, in particolare mia madre, Antonella, ed i miei fratelli, Edoardo, Orlando e Macchia.
Ringrazio i miei mentori, Angelo Esposito e Alfredo Urbano che mi hanno guidato attraverso la ricerca e per le molteplici discussioni di fisica, dove per capirsi bastava poco.
Ringrazio Roberto Contino, i cui insegnamenti e discussioni permeano questa tesi.
Ringrazio Mauro Valli per le discussioni di fisica e per gli incoraggiamenti costanti.
Ringrazio Sidney Coleman, le cui lezioni di teoria dei campi hanno acceso in me la passione per le Interazioni Fondamentali.
Ringrazio tutte le altre persone che ho incontrato lungo questo cammino.
Ringrazio le onde dell'oceano Atlantico, tra le quali questa tesi ha avuto la sua conclusione.

Bibliography

[1] P. G. Catinari and A. Urbano. "Gravitational instantons and the quality problem of the QCD axion: Facts, speculations, and statements in between". In: *Phys. Rev. D* 111.12 (2025), p. 125007. DOI: 10.1103/n5nz-8232. arXiv: 2410.12741 [hep-th].

[2] P. G. Catinari, A. Esposito, and S. Pavaskar. "Effective field theory for anisotropic antiferromagnets: Gapped Goldstone bosons, pseudo-Goldstone excitations, and phase transitions". In: *Phys. Rev. B* 112.6 (2025), p. 064408. DOI: 10.1103/msy3-ztxr. arXiv: 2411.09761 [cond-mat.str-el].

[3] P. G. Catinari, A. Esposito, and S. Pavaskar. "Hunting axion dark matter with antiferromagnets: A case study with nickel oxide". In: *Phys. Rev. D* 112.3 (2025), p. 035007. DOI: 10.1103/k6pg-bkwh. arXiv: 2411.11971 [hep-ph].

[4] P. G. Catinari, L. Del Grosso, L. Di Giovanni, and A. Urbano. "Insights into the highest natural scale: Finite naturalness challenges inflationary dynamics". In: (Apr. 2025). arXiv: 2504.17846 [hep-ph].

[5] H. K. Dreiner, H. E. Haber, and S. P. Martin. In: *Phys. Rept.* 494 (2010), pp. 1–196. DOI: 10.1016/j.physrep.2010.05.002. arXiv: 0812.1594 [hep-ph].

[6] C. Abel et al. "Measurement of the Permanent Electric Dipole Moment of the Neutron". In: *Phys. Rev. Lett.* 124.8 (2020), p. 081803. DOI: 10.1103/PhysRevLett.124.081803. arXiv: 2001.11966 [hep-ex].

[7] J. R. Ellis and M. K. Gaillard. "Strong and Weak CP Violation". In: *Nucl. Phys. B* 150 (1979), pp. 141–162. DOI: 10.1016/0550-3213(79)90297-9.

[8] C. Vafa and E. Witten. "Parity Conservation in QCD". In: *Phys. Rev. Lett.* 53 (1984), p. 535. DOI: 10.1103/PhysRevLett.53.535.

[9] P. Di Vecchia and G. Veneziano. "Chiral Dynamics in the Large n Limit". In: *Nucl. Phys. B* 171 (1980), pp. 253–272. DOI: 10.1016/0550-3213(80)90370-3.

[10] E. Witten. "Large N Chiral Dynamics". In: *Annals Phys.* 128 (1980), p. 363. DOI: 10.1016/0003-4916(80)90325-5.

[11] S. R. Coleman and E. Witten. "Chiral Symmetry Breakdown in Large N Chromodynamics". In: *Phys. Rev. Lett.* 45 (1980), p. 100. DOI: 10.1103/PhysRevLett.45.100.

[12] P. Di Vecchia, F. Nicodemi, R. Pettorino, and G. Veneziano. "Large n, Chiral Approach to Pseudoscalar Masses, Mixings and Decays". In: *Nucl. Phys. B* 181 (1981), pp. 318–334. DOI: 10.1016/0550-3213(81)90356-4.

[13] R. Dashen. "Some Features of Chiral Symmetry Breaking". In: *Phys. Rev. D* 3 (8 Apr. 1971), pp. 1879–1889. DOI: 10.1103/PhysRevD.3.1879. URL: https://link.aps.org/doi/10.1103/PhysRevD.3.1879.

[14] R. D. Peccei and H. R. Quinn. "CP Conservation in the Presence of Pseudoparticles". In: *Phys. Rev. Lett.* 38 (25 June 1977), pp. 1440–1443. DOI: 10.1103/PhysRevLett.38.1440. URL: https://link.aps.org/doi/10.1103/PhysRevLett.38.1440.

[15] S. Weinberg. "A New Light Boson?" In: *Phys. Rev. Lett.* 40 (1978), pp. 223–226. DOI: 10.1103/PhysRevLett.40.223.

[16] F. Wilczek. "Problem of Strong P and T Invariance in the Presence of Instantons". In: *Phys. Rev. Lett.* 40 (1978), pp. 279–282. DOI: 10.1103/PhysRevLett.40.279.

[17] H. Georgi, D. B. Kaplan, and L. Randall. "Manifesting the Invisible Axion at Low-energies". In: *Phys. Lett. B* 169 (1986), pp. 73–78. DOI: 10.1016/0370-2693(86)90688-X.

[18] D. Y. Cheong, N. L. Rodd, and L.-T. Wang. "Quantum description of wave dark matter". In: *Phys. Rev. D* 111.1 (2025), p. 015028. DOI: 10.1103/PhysRevD.111.015028. arXiv: 2408.04696 [hep-ph].

[19] M. Dine and W. Fischler. "The Not So Harmless Axion". In: *Phys. Lett. B* 120 (1983). Ed. by M. A. Srednicki, pp. 137–141. DOI: 10.1016/0370-2693(83)90639-1.

[20] D. J. Gross, R. D. Pisarski, and L. G. Yaffe. "QCD and instantons at finite temperature". In: *Rev. Mod. Phys.* 53 (1 Jan. 1981), pp. 43–80. DOI: 10.1103/RevModPhys.53.43. URL: https://link.aps.org/doi/10.1103/RevModPhys.53.43.

[21] I. Affleck. "On Constrained Instantons". In: *Nucl. Phys. B* 191 (1981). Ed. by M. A. Shifman, p. 429. DOI: 10.1016/0550-3213(81)90307-2.

[22] M. Shifman. *Advanced Topics in Quantum Field Theory: A Lecture Course*. 2nd ed. Cambridge University Press, 2022.

[23] G. Grilli di Cortona, E. Hardy, J. Pardo Vega, and G. Villadoro. "The QCD axion, precisely". In: *JHEP* 01 (2016), p. 034. DOI: 10.1007/JHEP01(2016)034. arXiv: 1511.02867 [hep-ph].

[24] K. G. Wilson. In: *Rev. Mod. Phys.* 55 (3 July 1983), pp. 583–600. DOI: 10.1103/RevModPhys.55.583. URL: https://link.aps.org/doi/10.1103/RevModPhys.55.583.

[25] S. Weinberg. In: *Phys. Lett. B* 91 (1980), pp. 51–55. DOI: 10.1016/0370-2693(80)90660-7.

[26] V. F. Weisskopf. "On the Self-Energy and the Electromagnetic Field of the Electron". In: *Phys. Rev.* 56 (1 July 1939), pp. 72–85. DOI: 10.1103/PhysRev.56.72. URL: https://link.aps.org/doi/10.1103/PhysRev.56.72.

[27] H. Murayama. "Supersymmetry phenomenology". In: *ICTP Summer School in Particle Physics*. Feb. 2000, pp. 296–335. arXiv: hep-ph/0002232.

[28] A. Hook. "New Solutions to the Gauge Hierarchy Problem". In: *Ann. Rev. Nucl. Part. Sci.* 73.1 (2023), pp. 23–39. DOI: 10.1146/annurev-nucl-102422-080830.

[29] C. P. Burgess. *Introduction to Effective Field Theory: Thinking Effectively about Hierarchies of Scale*. Cambridge University Press, 2020.

[30] T. Cohen. "As Scales Become Separated: Lectures on Effective Field Theory". In: *PoS* TASI2018 (2019), p. 011. arXiv: 1903.03622 [hep-ph].

[31] H. K. Dreiner, H. E. Haber, and S. P. Martin. *From Spinors to Supersymmetry*. Cambridge, UK: Cambridge University Press, July 2023. ISBN: 978-1-139-04974-0. DOI: 10.1017/9781139049740.

[32] M. D. Schwartz. *Quantum Field Theory and the Standard Model*. Cambridge University Press, Mar. 2014. ISBN: 978-1-107-03473-0, 978-1-107-03473-0.

[33] C. G. Callan Jr, R. Dashen, and D. J. Gross. "The structure of the gauge theory vacuum". In: *Physics Letters B* 63.3 (1976), pp. 334–340. DOI: 10.1016/0370-2693(76)90277-X.

[34] R. Jackiw and C. Rebbi. "Vacuum Periodicity in a Yang-Mills Quantum Theory". In: *Phys. Rev. Lett.* 37 (3 July 1976), pp. 172–175. DOI: 10.1103/PhysRevLett.37.172. URL: https://link.aps.org/doi/10.1103/PhysRevLett.37.172.

[35] R. Jackiw. "Introduction to the Yang-Mills quantum theory". In: *Rev. Mod. Phys.* 52 (4 Oct. 1980), pp. 661–673. DOI: 10.1103/RevModPhys.52.661. URL: https://link.aps.org/doi/10.1103/RevModPhys.52.661.

[36] K. Huang. *Quarks, leptons & gauge fields*. World Scientific, 1992.

[37] S. Weinberg. *The quantum theory of fields: Volume 2, Modern applications*. Cambridge University Press, 2005.

[38] G. 't Hooft. "Computation of the quantum effects due to a four-dimensional pseudoparticle". In: *Phys. Rev. D* 14 (12 Dec. 1976), pp. 3432–3450. DOI: 10.1103/PhysRevD.14.3432. URL: https://link.aps.org/doi/10.1103/PhysRevD.14.3432.

[39] A. I. Vainshtein, V. I. Zakharov, V. A. Novikov, and M. A. Shifman. "ABC's of Instantons". In: *Sov. Phys. Usp.* 25 (1982), p. 195. DOI: 10.1070/PU1982v025n04ABEH004533.

[40] C. G. Callan, R. Dashen, and D. J. Gross. "Toward a theory of the strong interactions". In: *Phys. Rev. D* 17 (10 May 1978), pp. 2717–2763. DOI: 10.1103/PhysRevD.17.2717. URL: https://link.aps.org/doi/10.1103/PhysRevD.17.2717.

[41] K. Fujikawa. "Path Integral for Gauge Theories with Fermions". In: *Phys. Rev. D* 21 (1980). [Erratum: Phys.Rev.D 22, 1499 (1980)], p. 2848. DOI: 10.1103/PhysRevD.21.2848.

[42] S. Coleman. *Aspects of Symmetry: Selected Erice Lectures*. Cambridge University Press, 1985. DOI: 10.1017/CBO9780511565045.

[43] G. 't Hooft. "Symmetry Breaking through Bell-Jackiw Anomalies". In: *Phys. Rev. Lett.* 37 (1 July 1976), pp. 8–11. DOI: 10.1103/PhysRevLett.37.8. URL: https://link.aps.org/doi/10.1103/PhysRevLett.37.8.

[44] M. Shifman, A. Vainshtein, and V. Zakharov. "Instanton density in a theory with massless quarks". In: *Nuclear Physics B* 163 (1980), pp. 46–56. ISSN: 0550-3213. DOI: https://doi.org/10.1016/0550-3213(80)90389-2. URL: https://www.sciencedirect.com/science/article/pii/0550321380903892.

[45] J. M. Flynn and L. Randall. "A computation of the small instanton contribution to the axion potential". In: *Nuclear Physics B* 293 (1987), pp. 731–739. ISSN: 0550-3213. DOI: https://doi.org/10.1016/0550-3213(87)90089-7. URL: https://www.sciencedirect.com/science/article/pii/0550321387900897.

[46] C. Csáki, M. Ruhdorfer, and Y. Shirman. 2020. arXiv: 1912.02197 `[hep-ph]`.

[47] C. Csáki, R. T. D'Agnolo, E. Kuflik, and M. Ruhdorfer. 2024. arXiv: 2311.09285 `[hep-ph]`. URL: https://arxiv.org/abs/2311.09285.

[48] M. Kamionkowski and J. March-Russell. "Planck scale physics and the Peccei-Quinn mechanism". In: *Phys. Lett. B* 282 (1992), pp. 137–141. DOI: 10.1016/0370-2693(92)90492-M. arXiv: hep-th/9202003.

[49] T. Banks and N. Seiberg. "Symmetries and Strings in Field Theory and Gravity". In: *Phys. Rev. D* 83 (2011), p. 084019. DOI: 10.1103/PhysRevD.83.084019. arXiv: 1011.5120 `[hep-th]`.

[50] R. Bousso. "A Covariant entropy conjecture". In: *JHEP* 07 (1999), p. 004. DOI: 10.1088/1126-6708/1999/07/004. arXiv: hep-th/9905177.

[51] R. Bousso. "The Holographic principle". In: *Rev. Mod. Phys.* 74 (2002), pp. 825–874. DOI: 10.1103/RevModPhys.74.825. arXiv: hep-th/0203101.

[52] J. D. Bekenstein. "Black holes and the second law". In: *Lett. Nuovo Cim.* 4 (1972), pp. 737–740. DOI: 10.1007/BF02757029.

[53] S. W. Hawking. "Gravitational Radiation from Colliding Black Holes". In: *Phys. Rev. Lett.* 26 (21 May 1971), pp. 1344–1346. DOI: 10.1103/PhysRevLett.26.1344. URL: https://link.aps.org/doi/10.1103/PhysRevLett.26.1344.

[54] R. Bousso. "Holography in general space-times". In: *JHEP* 06 (1999), p. 028. DOI: 10.1088/1126-6708/1999/06/028. arXiv: hep-th/9906022.

[55] T. Banks and M. Dine. "The Cosmology of string theoretic axions". In: *Nucl. Phys. B* 505 (1997), pp. 445–460. DOI: 10.1016/S0550-3213(97)00413-6. arXiv: hep-th/9608197.

[56] P. Svrcek and E. Witten. "Axions In String Theory". In: *JHEP* 06 (2006), p. 051. DOI: 10.1088/1126-6708/2006/06/051. arXiv: hep-th/0605206.

[57] T. Banks and L. J. Dixon. "Constraints on String Vacua with Space-Time Supersymmetry". In: *Nucl. Phys. B* 307 (1988), pp. 93–108. DOI: 10.1016/0550-3213(88)90523-8.

[58] D. Harlow and H. Ooguri. "Symmetries in quantum field theory and quantum gravity". In: *Commun. Math. Phys.* 383.3 (2021), pp. 1669–1804. DOI: 10.1007/s00220-021-04040-y. arXiv: 1810.05338 [hep-th].

[59] I. Antoniadis, N. Arkani-Hamed, S. Dimopoulos, and G. R. Dvali. "New dimensions at a millimeter to a Fermi and superstrings at a TeV". In: *Phys. Lett. B* 436 (1998), pp. 257–263. DOI: 10.1016/S0370-2693(98)00860-0. arXiv: hep-ph/9804398.

[60] S. H. Shenker. "The Strength of Nonperturbative Effects in String Theory". In: *Random Surfaces and Quantum Gravity*. Ed. by O. Alvarez, E. Marinari, and P. Windey. Boston, MA: Springer US, 1991, pp. 191–200. ISBN: 978-1-4615-3772-4. DOI: 10.1007/978-1-4615-3772-4_12. URL: https://doi.org/10.1007/978-1-4615-3772-4_12.

[61] F. Larsen and F. Wilczek. "Renormalization of black hole entropy and of the gravitational coupling constant". In: *Nucl. Phys. B* 458 (1996), pp. 249–266. DOI: 10.1016/0550-3213(95)00548-X. arXiv: hep-th/9506066.

[62] X. Calmet, S. D. H. Hsu, and D. Reeb. "Quantum gravity at a TeV and the renormalization of Newton's constant". In: *Phys. Rev. D* 77 (2008), p. 125015. DOI: 10.1103/PhysRevD.77.125015. arXiv: 0803.1836 [hep-th].

[63] G. Dvali. "Black Holes and Large N Species Solution to the Hierarchy Problem". In: *Fortsch. Phys.* 58 (2010), pp. 528–536. DOI: 10.1002/prop.201000009. arXiv: 0706.2050 [hep-th].

[64] G. Dvali and M. Redi. "Black Hole Bound on the Number of Species and Quantum Gravity at LHC". In: *Phys. Rev. D* 77 (2008), p. 045027. DOI: 10.1103/PhysRevD.77.045027. arXiv: 0710.4344 [hep-th].

[65] D. Baumann and L. McAllister. *Inflation and String Theory*. Cambridge Monographs on Mathematical Physics. Cambridge University Press, May 2015. ISBN: 978-1-107-08969-3, 978-1-316-23718-2. DOI: 10.1017/CBO9781316105733. arXiv: 1404.2601 [hep-th].

[66] S. B. Giddings and A. Strominger. "Axion Induced Topology Change in Quantum Gravity and String Theory". In: *Nucl. Phys. B* 306 (1988), pp. 890–907. DOI: 10.1016/0550-3213(88)90446-4.

[67] L. F. Abbott and M. B. Wise. "Wormholes and Global Symmetries". In: *Nucl. Phys. B* 325 (1989), pp. 687–704. DOI: 10.1016/0550-3213(89)90503-8.

[68] R. Kallosh, A. D. Linde, D. A. Linde, and L. Susskind. "Gravity and global symmetries". In: *Phys. Rev. D* 52 (1995), pp. 912–935. DOI: 10.1103/PhysRevD.52.912. arXiv: hep-th/9502069.

[69] R. Alonso and A. Urbano. "Wormholes and masses for Goldstone bosons". In: *JHEP* 02 (2019), p. 136. DOI: 10.1007/JHEP02(2019)136. arXiv: 1706.07415 [hep-ph].

[70] P.-S. Hsin, L. V. Iliesiu, and Z. Yang. "A violation of global symmetries from replica wormholes and the fate of black hole remnants". In: *Class. Quant. Grav.* 38.19 (2021), p. 194004. DOI: 10.1088/1361-6382/ac2134. arXiv: 2011.09444 [hep-th].

[71] J. Alvey and M. Escudero. "The axion quality problem: global symmetry breaking and wormholes". In: *JHEP* 01 (2021). [Erratum: JHEP 11, 223 (2023)], p. 032. DOI: 10.1007/JHEP01(2021)032. arXiv: 2009.03917 [hep-ph].

[72] A. Hebecker, T. Mikhail, and P. Soler. "Euclidean wormholes, baby universes, and their impact on particle physics and cosmology". In: *Front. Astron. Space Sci.* 5 (2018), p. 35. DOI: 10.3389/fspas.2018.00035. arXiv: 1807.00824 [hep-th].

[73] T. Hertog, B. Truijen, and T. Van Riet. "Euclidean axion wormholes have multiple negative modes". In: *Phys. Rev. Lett.* 123.8 (2019), p. 081302. DOI: 10.1103/PhysRevLett.123.081302. arXiv: 1811.12690 [hep-th].

[74] S. W. Hawking. "Gravitational Instantons". In: *Phys. Lett. A* 60 (1977), p. 81. DOI: 10.1016/0375-9601(77)90386-3.

[75] G. W. Gibbons and S. W. Hawking. "Classification of Gravitational Instanton Symmetries". In: *Commun. Math. Phys.* 66 (1979), pp. 291–310. DOI: 10.1007/BF01197189.

[76] T. Eguchi, P. B. Gilkey, and A. J. Hanson. "Gravitation, Gauge Theories and Differential Geometry". In: *Phys. Rept.* 66 (1980), p. 213. DOI: 10.1016/0370-1573(80)90130-1.

[77] J. W. York Jr. "Role of conformal three geometry in the dynamics of gravitation". In: *Phys. Rev. Lett.* 28 (1972), pp. 1082–1085. DOI: 10.1103/PhysRevLett.28.1082.

[78] G. W. Gibbons and S. W. Hawking. "Action Integrals and Partition Functions in Quantum Gravity". In: *Phys. Rev. D* 15 (1977), pp. 2752–2756. DOI: 10.1103/PhysRevD.15.2752.

[79] R. Schon and S.-T. Yau. "On the Proof of the positive mass conjecture in general relativity". In: *Commun. Math. Phys.* 65 (1979), pp. 45–76. DOI: 10.1007/BF01940959.

[80] E. Witten. "A Simple Proof of the Positive Energy Theorem". In: *Commun. Math. Phys.* 80 (1981), p. 381. DOI: 10.1007/BF01208277.

[81] G. W. Gibbons and C. N. Pope. "The Positive Action Conjecture and Asymptotically Euclidean Metrics in Quantum Gravity". In: *Commun. Math. Phys.* 66 (1979), pp. 267–290. DOI: 10.1007/BF01197188.

[82] T. Eguchi and A. J. Hanson. "Selfdual Solutions to Euclidean Gravity". In: *Annals Phys.* 120 (1979), p. 82. DOI: 10.1016/0003-4916(79)90282-3.

[83] G. W. Gibbons and S. W. Hawking. "Gravitational Multi - Instantons". In: *Phys. Lett. B* 78 (1978), p. 430. DOI: 10.1016/0370-2693(78)90478-1.

[84] A. H. Taub. "Empty space-times admitting a three parameter group of motions". In: *Annals Math.* 53 (1951), pp. 472–490. DOI: 10.2307/1969567.

[85] E. Newman, L. Tamburino, and T. Unti. "Empty space generalization of the Schwarzschild metric". In: *J. Math. Phys.* 4 (1963), p. 915. DOI: 10.1063/1.1704018.

[86] A. A. Belavin and D. E. Burlankov. "The Renormalizable Theory of Gravitation and the Einstein Equations". In: *Phys. Lett. A* 58 (1976), pp. 7–8. DOI: 10.1016/0375-9601(76)90530-2.

[87] W. J. Marciano, H. Pagels, and Z. Parsa. "Multiply Charged Magnetic Monopoles, SU(3) Pseudoparticles and Gravitational Pseudoparticles". In: *Phys. Rev. D* 15 (1977), p. 1044. DOI: 10.1103/PhysRevD.15.1044.

[88] T. Eguchi and P. G. O. Freund. "Quantum Gravity and World Topology". In: *Phys. Rev. Lett.* 37 (1976), p. 1251. DOI: 10.1103/PhysRevLett.37.1251.

[89] A. Hebecker and P. Henkenjohann. "Gauge and gravitational instantons: From 3-forms and fermions to Weak Gravity and flat axion potentials". In: *JHEP* 09 (2019), p. 038. DOI: 10.1007/JHEP09(2019)038. arXiv: 1906.07728 [hep-th].

[90] S. Deser, M. J. Duff, and C. J. Isham. "GRAVITATIONALLY INDUCED CP EFFECTS". In: *Phys. Lett. B* 93 (1980), pp. 419–423. DOI: 10.1016/0370-2693(80)90356-1.

[91] R. Holman, T. W. Kephart, and S.-J. Rey. "Semiclassical gravity and invisible axions". In: *Phys. Rev. Lett.* 71 (1993), pp. 320–323. DOI: 10.1103/PhysRevLett.71.320. arXiv: hep-ph/9207208.

[92] S.-J. Rey. "Protecting invisible axion from Planck scale physics". In: *7th Meeting of the APS Division of Particles Fields*. Nov. 1992, pp. 1565–1567.

[93] Z. Chen and A. Kobakhidze. "Coloured gravitational instantons, the strong CP problem and the companion axion solution". In: *Eur. Phys. J. C* 82.7 (2022), p. 596. DOI: 10.1140/epjc/s10052-022-10542-3. arXiv: 2108.05549 [hep-ph].

[94] Z. Chen, A. Kobakhidze, C. A. J. O'Hare, Z. S. C. Picker, and G. Pierobon. "Phenomenology of the companion-axion model: photon couplings". In: *Eur. Phys. J. C* 82.10 (2022), p. 940. DOI: 10.1140/epjc/s10052-022-10909-6. arXiv: 2109.12920 [hep-ph].

[95] Z. Chen, A. Kobakhidze, C. A. J. O'Hare, Z. S. C. Picker, and G. Pierobon. "Cosmology of the companion-axion model: dark matter, gravitational waves, and primordial black holes". In: (Oct. 2021). arXiv: 2110.11014 [hep-ph].

[96] H. Boutaleb-Joutei, A. Chakrabarti, and A. Comtet. "Gauge Field Configurations in Curved Space-times. 3. Selfdual SU(2) Fields in Eguchi-hanson Space". In: *Phys. Rev. D* 21 (1980), pp. 979–983. DOI: 10.1103/PhysRevD.21.979.

[97] A. Chakrabarti. "Classical Solutions of Yang-Mills Fields. (Selected Topics)". In: *Fortsch. Phys.* 35 (1987), pp. 1–64.

[98] L. Alvarez-Gaume and E. Witten. "Gravitational Anomalies". In: *Nucl. Phys. B* 234 (1984). Ed. by A. Salam and E. Sezgin, p. 269. DOI: 10.1016/0550-3213(84)90066-X.

[99] L. Di Luzio, M. Giannotti, E. Nardi, and L. Visinelli. "The landscape of QCD axion models". In: *Phys. Rept.* 870 (2020), pp. 1–117. DOI: 10.1016/j.physrep.2020.06.002. arXiv: 2003.01100 [hep-ph].

[100] L. Di Luzio, F. Mescia, and E. Nardi. "Redefining the Axion Window". In: *Phys. Rev. Lett.* 118.3 (2017), p. 031801. DOI: 10.1103/PhysRevLett.118.031801. arXiv: 1610.07593 [hep-ph].

[101] K. Choi and S. H. Im. "Realizing the relaxion from multiple axions and its UV completion with high scale supersymmetry". In: *JHEP* 01 (2016), p. 149. DOI: 10.1007/JHEP01(2016)149. arXiv: 1511.00132 [hep-ph].

[102] D. E. Kaplan and R. Rattazzi. "Large field excursions and approximate discrete symmetries from a clockwork axion". In: *Phys. Rev. D* 93.8 (2016), p. 085007. DOI: 10.1103/PhysRevD.93.085007. arXiv: 1511.01827 [hep-ph].

[103] M. Farina, D. Pappadopulo, F. Rompineve, and A. Tesi. "The photo-philic QCD axion". In: *JHEP* 01 (2017), p. 095. DOI: 10.1007/JHEP01(2017)095. arXiv: 1611.09855 [hep-ph].

[104] S. Hawking. "Spacetime foam". In: *Nuclear Physics B* 144.2 (1978), pp. 349–362. ISSN: 0550-3213. DOI: https://doi.org/10.1016/0550-3213(78)90375-9. URL: https://www.sciencedirect.com/science/article/pii/0550321378903759.

[105] G. W. Gibbons, S. W. Hawking, and M. J. Perry. "Path Integrals and the Indefiniteness of the Gravitational Action". In: *Nucl. Phys. B* 138 (1978), pp. 141–150. DOI: 10.1016/0550-3213(78)90161-X.

[106] D. N. Page. "The Positive Action Conjecture". In: *Phys. Rev. D* 18 (1978), p. 2733. DOI: 10.1103/PhysRevD.18.2733.

[107] J. W. York Jr. "Gravitational degrees of freedom and the initial-value problem". In: *Phys. Rev. Lett.* 26 (1971), pp. 1656–1658. DOI: 10.1103/PhysRevLett.26.1656.

[108] A. Belavin, A. Polyakov, A. Schwartz, and Y. Tyupkin. "Pseudoparticle solutions of the Yang-Mills equations". In: *Physics Letters B* 59.1 (1975), pp. 85–87. ISSN: 0370-2693. DOI: https://doi.org/10.1016/0370-2693(75)90163-X. URL: https://www.sciencedirect.com/science/article/pii/037026937590163X.

[109] S. Weinberg. *The quantum theory of fields. Vol. 2: Modern applications.* Cambridge University Press, Aug. 2013. ISBN: 978-1-139-63247-8, 978-0-521-67054-8, 978-0-521-55002-4. DOI: 10.1017/CBO9781139644174.

[110] G. 't Hooft. "A physical interpretation of gravitational instantons". In: *Nuclear Physics B* 315.2 (1989), pp. 517–527. ISSN: 0550-3213. DOI: https://doi.org/10.1016/0550-3213(89)90366-0. URL: https://www.sciencedirect.com/science/article/pii/0550321389903660.

[111] G. Franchetti. "Harmonic spinors on a family of Einstein manifolds". In: *Nonlinearity* 31.6 (Apr. 2018), p. 2419. DOI: 10.1088/1361-6544/aab0bd. URL: https://dx.doi.org/10.1088/1361-6544/aab0bd.

[112] M. Bianchi, F. Fucito, G. Rossi, and M. Martellini. "ALE instantons in string effective theory". In: *Nuclear Physics B* 440.1–2 (Apr. 1995), pp. 129–170. ISSN: 0550-3213. DOI: 10.1016/0550-3213(94)00552-p. URL: http://dx.doi.org/10.1016/0550-3213(94)00552-P.

[113] C. Csáki et al. "On the dynamical origin of the η' potential and the axion mass". In: *JHEP* 10 (2023), p. 139. DOI: 10.1007/JHEP10(2023)139. arXiv: 2307.04809 `[hep-ph]`.

[114] N. Arkani-Hamed et al. "Solving the Hierarchy Problem at Reheating with a Large Number of Degrees of Freedom". In: *Phys. Rev. Lett.* 117 (25 Dec. 2016), p. 251801. DOI: 10.1103/PhysRevLett.117.251801. URL: https://link.aps.org/doi/10.1103/PhysRevLett.117.251801.

[115] S.-J. Rey. "Spontaneous CP violation: Small instanton and invisible axion". In: *Phys. Rev. D* 47 (1993), R2652–R2655. DOI: 10.1103/PhysRevD.47.R2652. arXiv: hep-ph/9209295.

[116] N. D. Birrell and P. C. W. Davies. *Quantum Fields in Curved Space.* Cambridge Monographs on Mathematical Physics. Cambridge, UK: Cambridge Univ. Press, Feb. 1984. ISBN: 978-0-521-27858-4, 978-0-521-27858-4. DOI: 10.1017/CBO9780511622632.

[117] T. Ortin. *Gravity and Strings.* 2nd ed. Cambridge Monographs on Mathematical Physics. Cambridge University Press, July 2015. ISBN: 978-0-521-76813-9, 978-0-521-76813-9, 978-1-316-23579-9. DOI: 10.1017/CBO9781139019750.

[118] T. Eguchi, P. B. Gilkey, and A. J. Hanson. "Gravitation, gauge theories and differential geometry". In: *Physics Reports* 66.6 (1980), pp. 213–393. ISSN: 0370-1573. DOI: https://doi.org/10.1016/0370-1573(80)90130-1. URL: https://www.sciencedirect.com/science/article/pii/0370157380901301.

[119] Z. Xiao. "Scalar Flat Metrics of Eguchi- Hanson Type*". In: *Communications in Theoretical Physics* 42.2 (Aug. 2004), p. 235. DOI: 10.1088/0253-6102/42/2/235. URL: https://dx.doi.org/10.1088/0253-6102/42/2/235.

[120] S. Hawking and C. Pope. "Generalized spin structures in quantum gravity". In: *Physics Letters B* 73.1 (1978), pp. 42–44. ISSN: 0370-2693. DOI: https://doi.org/10.1016/0370-2693(78)90167-3. URL: https://www.sciencedirect.com/science/article/pii/0370269378901673.

[121] C. N. Pope. "The eta invariant for charged spinors in Taub-NUT". In: *Journal of Physics A: Mathematical and General* 14.5 (May 1981), p. L133. DOI: 10.1088/0305-4470/14/5/007. URL: https://dx.doi.org/10.1088/0305-4470/14/5/007.

[122] M. F. Atiyah, V. K. Patodi, and I. M. Singer. "Spectral asymmetry and Riemannian Geometry. I". In: *Mathematical Proceedings of the Cambridge Philosophical Society* 77.1 (1975), pp. 43–69. DOI: 10.1017/S0305004100049410.

[123] G. Panico and A. Wulzer. *The Composite Nambu-Goldstone Higgs*. Vol. 913. Springer, 2016. DOI: 10.1007/978-3-319-22617-0. arXiv: 1506.01961 [hep-ph].

[124] L. Néel. "Magnetism and local molecular field". In: *Science* 174.4013 (1971), pp. 985–992. DOI: 10.1126/science.174.4013.985.

[125] M. N. Baibich et al. "Giant magnetoresistance of (001) Fe/(001) Cr magnetic superlattices". In: *Physical review letters* 61.21 (1988), p. 2472. DOI: 10.1103/PhysRevLett.61.2472.

[126] G. Binasch, P. Grünberg, F. Saurenbach, and W. Zinn. "Enhanced magnetoresistance in layered magnetic structures with antiferromagnetic interlayer exchange". In: *Physical review B* 39.7 (1989), p. 4828. DOI: 10.1103/PhysRevB.39.4828.

[127] D. Lachance-Quirion, Y. Tabuchi, A. Gloppe, K. Usami, and Y. Nakamura. "Hybrid quantum systems based on magnonics". In: *Applied Physics Express* 12.7 (2019), p. 070101. DOI: 10.7567/1882-0786/ab248d.

[128] D. Lachance-Quirion et al. "Resolving quanta of collective spin excitations in a millimeter-sized ferromagnet". In: *Science Advances* 3.7 (2017), e1603150. DOI: 10.1126/sciadv.1603150.

[129] A. Esposito and S. Pavaskar. "Optimal antiferromagnets for light dark matter detection". In: *Phys. Rev. D* 108 (1 July 2023), p. L011901. DOI: 10.1103/PhysRevD.108.L011901. URL: https://link.aps.org/doi/10.1103/PhysRevD.108.L011901.

[130] D. J. E. Marsh, K.-C. Fong, E. W. Lentz, L. Smejkal, and M. N. Ali. "Proposal to Detect Dark Matter using Axionic Topological Antiferromagnets". In: *Phys. Rev. Lett.* 123.12 (2019), p. 121601. DOI: 10.1103/PhysRevLett.123.121601. arXiv: 1807.08810 [hep-ph].

[131] C. P. Burgess. "Goldstone and pseudoGoldstone bosons in nuclear, particle and condensed matter physics". In: *Phys. Rept.* 330 (2000), pp. 193–261. DOI: 10.1016/S0370-1573(99)00111-8. arXiv: hep-th/9808176.

[132] P. Chandra, P. Coleman, and A. Larkin. "A quantum fluids approach to frustrated Heisenberg models". In: *Journal of Physics: Condensed Matter* 2.39 (1990), p. 7933. DOI: 10.1088/0953-8984/2/39/008.

[133] S. Pavaskar, R. Penco, and I. Rothstein. "An effective field theory of magneto-elasticity". In: *SciPost Physics* 12.5 (May 2022). ISSN: 2542-4653. DOI: 10.21468/scipostphys.12.5.155. URL: http://dx.doi.org/10.21468/SciPostPhys.12.5.155.

[134] S. M. Rezende, A. Azevedo, and R. L. Rodríguez-Suárez. "Introduction to antiferromagnetic magnons". In: *Journal of Applied Physics* 126.15 (2019), p. 151101. DOI: 10.1063/1.5109132. URL: https://doi.org/10.1063/1.5109132.

[135] A. Nicolis and F. Piazza. "Implications of Relativity on Nonrelativistic Goldstone Theorems: Gapped Excitations at Finite Charge Density". In: *Phys. Rev. Lett.* 110.1 (2013). [Addendum: Phys.Rev.Lett. 110, 039901 (2013)], p. 011602. DOI: 10.1103/PhysRevLett.110.011602. arXiv: 1204.1570 [hep-th].

[136] A. Nicolis, R. Penco, F. Piazza, and R. A. Rosen. "More on gapped Goldstones at finite density: More gapped Goldstones". In: *JHEP* 11 (2013), p. 055. DOI: 10.1007/JHEP11(2013)055. arXiv: 1306.1240 [hep-th].

[137] H. Watanabe, T. Brauner, and H. Murayama. "Massive Nambu-Goldstone Bosons". In: *Phys. Rev. Lett.* 111.2 (2013), p. 021601. DOI: 10.1103/PhysRevLett.111.021601. arXiv: 1303.1527 [hep-th].

[138] G. Cuomo et al. "Gapped Goldstones at the cut-off scale: a non-relativistic EFT". In: *JHEP* 02 (2021), p. 068. DOI: 10.1007/JHEP02(2021)068. arXiv: 2005.12924 [hep-th].

[139] M. Grimsditch, L. McNeil, and D. Lockwood. "Unexpected behavior of the antiferromagnetic mode of NiO". In: *Physical Review B* 58.21 (1998), p. 14462. DOI: 10.1103/PhysRevB.58.14462.

[140] J. Milano, L. Steren, and M. Grimsditch. "Effect of dipolar interaction on the antiferromagnetic resonance spectra of NiO". In: *Physical review letters* 93.7 (2004), p. 077601. DOI: 10.1103/PhysRevLett.93.077601.

[141] A. Sievers III and M. Tinkham. "Far infrared antiferromagnetic resonance in MnO and NiO". In: *Physical Review* 129.4 (1963), p. 1566. DOI: 10.1103/PhysRev.129.1566.

[142] T. Satoh et al. "Spin oscillations in antiferromagnetic NiO triggered by circularly polarized light". In: *Physical review letters* 105.7 (2010), p. 077402. DOI: 10.1103/PhysRevLett.105.077402.

[143] P. G. Catinari, A. Esposito, and S. Pavaskar. "Hunting axion dark matter with antiferromagnets: A case study with nickel oxide". In: *Phys. Rev. D* 112 (3 Aug. 2025), p. 035007. DOI: 10.1103/k6pg-bkwh. URL: https://link.aps.org/doi/10.1103/k6pg-bkwh.

[144] S. Lovesey. *Theory of Neutron Scattering from Condensed Matter. Vol. 2: Polarization Effects and Magnetic Scattering*. International series of monographs on physics. Clarendon Press, 1984. ISBN: 9780198520177. URL: https://global.oup.com/academic/product/theory-of-neutron-scattering-from-condensed-matter-9780198520290?cc=in&lang=en&.

[145] H. Leutwyler. "Phonons as goldstone bosons". In: *Helv. Phys. Acta* 70 (1997), pp. 275–286. arXiv: hep-ph/9609466.

[146] A. Nicolis, R. Penco, F. Piazza, and R. Rattazzi. "Zoology of condensed matter: Framids, ordinary stuff, extra-ordinary stuff". In: *JHEP* 06 (2015), p. 155. DOI: 10.1007/JHEP06(2015)155. arXiv: 1501.03845 [hep-th].

[147] T. Brauner. *Effective Field Theory for Spontaneously Broken Symmetry*. Springer Nature, 2024. ISBN: 978-3-031-48378-3, 978-3-031-48377-6. DOI: 10.1007/978-3-031-48378-3. arXiv: 2404.14518 [hep-th].

[148] C. G. Callan Jr, S. Coleman, J. Wess, and B. Zumino. "Structure of phenomenological Lagrangians. II". In: *Physical Review* 177.5 (1969), p. 2247. DOI: 10.1103/PhysRev.177.2247.

[149] S. Coleman, J. Wess, and B. Zumino. "Structure of phenomenological Lagrangians. I". In: *Physical Review* 177.5 (1969), p. 2239. DOI: 10.1103/PhysRev.177.2239.

[150] M. T. Hutchings and E. J. Samuelsen. "Inelastic neutron scattering measurement of spin waves and magnetic interactions in NiO". In: *Solid State Communications* 9.13 (1971), pp. 1011–1014. ISSN: 0038-1098. DOI: https://doi.org/10.1016/0038-1098(71)90451-0. URL: https://www.sciencedirect.com/science/article/pii/0038109871904510.

[151] M. T. Hutchings and E. J. Samuelsen. "Measurement of Spin-Wave Dispersion in NiO by Inelastic Neutron Scattering and Its Relation to Magnetic Properties". In: *Phys. Rev. B* 6 (9 Nov. 1972), pp. 3447–3461. DOI: 10.1103/PhysRevB.6.3447. URL: https://link.aps.org/doi/10.1103/PhysRevB.6.3447.

[152] F. Keffer and C. Kittel. "Theory of Antiferromagnetic Resonance". In: *Phys. Rev.* 85 (2 Jan. 1952), pp. 329–337. DOI: 10.1103/PhysRev.85.329. URL: https://link.aps.org/doi/10.1103/PhysRev.85.329.

[153] F. L. A. Machado et al. "Spin-flop transition in the easy-plane antiferromagnet nickel oxide". In: *Phys. Rev. B* 95 (10 Mar. 2017), p. 104418. DOI: 10.1103/PhysRevB.95.104418. URL: https://link.aps.org/doi/10.1103/PhysRevB.95.104418.

[154] L. Hui, I. Kourkoulou, A. Nicolis, A. Podo, and S. Zhou. "S-matrix positivity without Lorentz invariance: a case study". In: *JHEP* 04 (2024), p. 145. DOI: 10.1007/JHEP04(2024)145. arXiv: 2312.08440 [hep-th].

[155] A. Esposito, E. Geoffray, and T. Melia. "Effective field theory for acoustic and pseudoacoustic phonons in solids". In: *Phys. Rev. D* 102.10 (2020), p. 105009. DOI: 10.1103/PhysRevD.102.105009. arXiv: 2006.05429 [hep-th].

[156] C. Cheung, A. Helset, and J. Parra-Martinez. "Geometric soft theorems". In: *JHEP* 04 (2022), p. 011. DOI: 10.1007/JHEP04(2022)011. arXiv: 2111.03045 [hep-th].

[157] P. Creminelli, M. Delladio, O. Janssen, A. Longo, and L. Senatore. "Non-analyticity of the S-matrix with spontaneously broken Lorentz invariance". In: *JHEP* 06 (2024), p. 201. DOI: 10.1007/JHEP06(2024)201. arXiv: 2312.08441 [hep-th].

[158] S. Chakravarty, D. R. Nelson, and B. I. Halperin. "Low temperature behavior of two-dimensional quantum antiferromagnets". In: *Phys. Rev. Lett.* 60 (1988), pp. 1057–1060. DOI: 10.1103/PhysRevLett.60.1057.

[159] E. Manousakis. "The spin-1/2 Heisenberg antiferromagnet on a square lattice and its application to the cuprous oxides". In: *Reviews of Modern Physics* 63.1 (1991), p. 1. DOI: 10.1103/RevModPhys.63.1.

[160] F. J. Dyson. "General theory of spin-wave interactions". In: *Phys. Rev.* 102 (1956), pp. 1217–1230. DOI: 10.1103/PhysRev.102.1217.

[161] H.-H. Kim et al. "Giant stress response of terahertz magnons in a spin-orbit Mott insulator". In: *Nature Communications* 13.1 (2022), p. 6674. DOI: 10.1038/s41467-022-34375-6.

[162] S. Weinberg. *The Quantum theory of fields. Vol. 1: Foundations*. Cambridge University Press, June 2005. ISBN: 978-0-521-67053-1, 978-0-511-25204-4. DOI: 10.1017/CBO9781139644167.

[163] D. S. Akerib et al. "Results from a search for dark matter in the complete LUX exposure". In: *Phys. Rev. Lett.* 118.2 (2017), p. 021303. DOI: 10.1103/PhysRevLett.118.021303. arXiv: 1608.07648 [astro-ph.CO].

[164] R. Agnese et al. "First Dark Matter Constraints from a SuperCDMS Single-Charge Sensitive Detector". In: *Phys. Rev. Lett.* 121.5 (2018). [Erratum: Phys.Rev.Lett. 122, 069901 (2019)], p. 051301. DOI: 10.1103/PhysRevLett.121.051301. arXiv: 1804.10697 [hep-ex].

[165] E. Aprile et al. "Light Dark Matter Search with Ionization Signals in XENON1T". In: *Phys. Rev. Lett.* 123.25 (2019), p. 251801. DOI: 10.1103/PhysRevLett.123.251801. arXiv: 1907.11485 [hep-ex].

[166] A. H. Abdelhameed et al. "First results from the CRESST-III low-mass dark matter program". In: *Phys. Rev. D* 100.10 (2019), p. 102002. DOI: 10.1103/PhysRevD.100.102002. arXiv: 1904.00498 [astro-ph.CO].

[167] Q. Wang et al. "Results of dark matter search using the full PandaX-II exposure". In: *Chin. Phys. C* 44.12 (2020), p. 125001. DOI: 10.1088/1674-1137/abb658. arXiv: 2007.15469 [astro-ph.CO].

[168] R. Barbieri et al. "Searching for galactic axions through magnetized media: the QUAX proposal". In: *Phys. Dark Univ.* 15 (2017), pp. 135–141. DOI: 10.1016/j.dark.2017.01.003. arXiv: 1606.02201 [hep-ph].

[169] N. Crescini et al. "Axion search with a quantum-limited ferromagnetic haloscope". In: *Phys. Rev. Lett.* 124.17 (2020), p. 171801. DOI: 10.1103/PhysRevLett.124.171801. arXiv: 2001.08940 [hep-ex].

[170] C. P. Salemi et al. "Search for Low-Mass Axion Dark Matter with ABRACADABRA-10 cm". In: *Phys. Rev. Lett.* 127.8 (2021), p. 081801. DOI: 10.1103/PhysRevLett.127.081801. arXiv: 2102.06722 [hep-ex].

[171] C. Bartram et al. "Search for Invisible Axion Dark Matter in the 3.3–4.2 μeV Mass Range". In: *Phys. Rev. Lett.* 127.26 (2021), p. 261803. DOI: 10.1103/PhysRevLett.127.261803. arXiv: 2110.06096 [hep-ex].

[172] C. Goodman et al. "ADMX Axion Dark Matter Bounds around 3.3 μeV with Dine-Fischler-Srednicki-Zhitnitsky Discovery Ability". In: *Phys. Rev. Lett.* 134.11 (2025), p. 111002. DOI: 10.1103/PhysRevLett.134.111002. arXiv: 2408.15227 [hep-ex].

[173] A. Rettaroli et al. "Search for axion dark matter with the QUAX–LNF tunable haloscope". In: *Phys. Rev. D* 110.2 (2024), p. 022008. DOI: 10.1103/PhysRevD.110.022008. arXiv: 2402.19063 [physics.ins-det].

[174] K. Altenmüller et al. "New Upper Limit on the Axion-Photon Coupling with an Extended CAST Run with a Xe-Based Micromegas Detector". In: *Phys. Rev. Lett.* 133.22 (2024), p. 221005. DOI: 10.1103/PhysRevLett.133.221005. arXiv: 2406.16840 [hep-ex].

[175] H. Yan et al. "Constraining exotic spin dependent interactions of muons and electrons". In: *Eur. Phys. J. C* 79.11 (2019), p. 971. DOI: 10.1140/epjc/s10052-019-7442-8.

[176] E. Aprile et al. "Search for New Physics in Electronic Recoil Data from XENONnT". In: *Phys. Rev. Lett.* 129.16 (2022), p. 161805. DOI: 10.1103/PhysRevLett.129.161805. arXiv: 2207.11330 [hep-ex].

[177] F. Capozzi and G. Raffelt. "Axion and neutrino bounds improved with new calibrations of the tip of the red-giant branch using geometric distance determinations". In: *Phys. Rev. D* 102.8 (2020), p. 083007. DOI: 10.1103/PhysRevD.102.083007. arXiv: 2007.03694 [astro-ph.SR].

[178] C. O'Hare. *cajohare/AxionLimits: AxionLimits*. https://cajohare.github.io/AxionLimits/. Version v1.0. July 2020. DOI: 10.5281/zenodo.3932430.

[179] W. Guo and D. N. McKinsey. "Concept for a dark matter detector using liquid helium-4". In: *Phys. Rev. D* 87.11 (2013), p. 115001. DOI: 10.1103/PhysRevD.87.115001. arXiv: 1302.0534 [astro-ph.IM].

[180] Y. Hochberg, T. Lin, and K. M. Zurek. "Detecting Ultralight Bosonic Dark Matter via Absorption in Superconductors". In: *Phys. Rev. D* 94.1 (2016), p. 015019. DOI: 10.1103/PhysRevD.94.015019. arXiv: 1604.06800 [hep-ph].

[181] K. Schutz and K. M. Zurek. "Detectability of Light Dark Matter with Superfluid Helium". In: *Phys. Rev. Lett.* 117.12 (2016), p. 121302. DOI: 10.1103/PhysRevLett.117.121302. arXiv: 1604.08206 [hep-ph].

[182] S. Knapen, T. Lin, and K. M. Zurek. "Light Dark Matter in Superfluid Helium: Detection with Multi-excitation Production". In: *Phys. Rev. D* 95.5 (2017), p. 056019. DOI: 10.1103/PhysRevD.95.056019. arXiv: 1611.06228 [hep-ph].

[183] Y. Hochberg, T. Lin, and K. M. Zurek. "Absorption of light dark matter in semiconductors". In: *Phys. Rev. D* 95.2 (2017), p. 023013. DOI: 10.1103/PhysRevD.95.023013. arXiv: 1608.01994 [hep-ph].

[184] S. Knapen, T. Lin, M. Pyle, and K. M. Zurek. "Detection of Light Dark Matter With Optical Phonons in Polar Materials". In: *Phys. Lett. B* 785 (2018), pp. 386–390. DOI: 10.1016/j.physletb.2018.08.064. arXiv: 1712.06598 [hep-ph].

[185] S. A. Hertel, A. Biekert, J. Lin, V. Velan, and D. N. McKinsey. "Direct detection of sub-GeV dark matter using a superfluid ^{4}He target". In: *Phys. Rev. D* 100.9 (2019), p. 092007. DOI: 10.1103/PhysRevD.100.092007. arXiv: 1810.06283 [physics.ins-det].

[186] S. Griffin, S. Knapen, T. Lin, and K. M. Zurek. "Directional Detection of Light Dark Matter with Polar Materials". In: *Phys. Rev. D* 98.11 (2018), p. 115034. DOI: 10.1103/PhysRevD.98.115034. arXiv: 1807.10291 [hep-ph].

[187] F. Acanfora, A. Esposito, and A. D. Polosa. "Sub-GeV Dark Matter in Superfluid He-4: an Effective Theory Approach". In: *Eur. Phys. J. C* 79.7 (2019), p. 549. DOI: 10.1140/epjc/s10052-019-7057-0. arXiv: 1902.02361 [hep-ph].

[188] T. Trickle, Z. Zhang, and K. M. Zurek. "Detecting Light Dark Matter with Magnons". In: *Phys. Rev. Lett.* 124.20 (2020), p. 201801. DOI: 10.1103/PhysRevLett.124.201801. arXiv: 1905.13744 [hep-ph].

[189] A. Caputo, A. Esposito, and A. D. Polosa. "Sub-MeV Dark Matter and the Goldstone Modes of Superfluid Helium". In: *Phys. Rev. D* 100.11 (2019), p. 116007. DOI: 10.1103/PhysRevD.100.116007. arXiv: 1907.10635 [hep-ph].

[190] A. Caputo, A. Esposito, E. Geoffray, A. D. Polosa, and S. Sun. "Dark Matter, Dark Photon and Superfluid He-4 from Effective Field Theory". In: *Phys. Lett. B* 802 (2020), p. 135258. DOI: 10.1016/j.physletb.2020.135258. arXiv: 1911.04511 [hep-ph].

[191] T. Trickle, Z. Zhang, K. M. Zurek, K. Inzani, and S. M. Griffin. "Multi-Channel Direct Detection of Light Dark Matter: Theoretical Framework". In: *JHEP* 03 (2020), p. 036. DOI: 10.1007/JHEP03(2020)036. arXiv: 1910.08092 [hep-ph].

[192] S. M. Griffin, K. Inzani, T. Trickle, Z. Zhang, and K. M. Zurek. "Multichannel direct detection of light dark matter: Target comparison". In: *Phys. Rev. D* 101.5 (2020), p. 055004. DOI: 10.1103/PhysRevD.101.055004. arXiv: 1910.10716 [hep-ph].

[193] G. Baym, D. H. Beck, J. P. Filippini, C. J. Pethick, and J. Shelton. "Searching for low mass dark matter via phonon creation in superfluid ^{4}He". In: *Phys. Rev. D* 102.3 (2020). [Erratum: Phys.Rev.D 104, 019901 (2021)], p. 035014. DOI: 10.1103/PhysRevD.104.019901. arXiv: 2005.08824 [hep-ph].

[194] A. Mitridate, T. Trickle, Z. Zhang, and K. M. Zurek. "Detectability of Axion Dark Matter with Phonon Polaritons and Magnons". In: *Phys. Rev. D* 102.9 (2020), p. 095005. DOI: 10.1103/PhysRevD.102.095005. arXiv: 2005.10256 [hep-ph].

[195] S. Chigusa, T. Moroi, and K. Nakayama. "Detecting light boson dark matter through conversion into a magnon". In: *Phys. Rev. D* 101.9 (2020), p. 096013. DOI: 10.1103/PhysRevD.101.096013. arXiv: 2001.10666 [hep-ph].

[196] A. Caputo, A. Esposito, F. Piccinini, A. D. Polosa, and G. Rossi. "Directional detection of light dark matter from three-phonon events in superfluid ^{4}He". In: *Phys. Rev. D* 103.5 (2021), p. 055017. DOI: 10.1103/PhysRevD.103.055017. arXiv: 2012.01432 [hep-ph].

[197] K. T. Matchev, J. Smolinsky, W. Xue, and Y. You. "Superfluid effective field theory for dark matter direct detection". In: *JHEP* 05 (2022), p. 034. DOI: 10.1007/JHEP05(2022)034. arXiv: 2108.07275 [hep-ph].

[198] Y. You et al. "Signatures and detection prospects for sub-GeV dark matter with superfluid helium". In: *JHEP* 07 (2023), p. 009. DOI: 10.1007/JHEP07(2023)009. arXiv: 2208.14474 [hep-ph].

[199] B. Campbell-Deem, S. Knapen, T. Lin, and E. Villarama. "Dark matter direct detection from the single phonon to the nuclear recoil regime". In: *Phys. Rev. D* 106.3 (2022), p. 036019. DOI: 10.1103/PhysRevD.106.036019. arXiv: 2205.02250 [hep-ph].

[200] A. Esposito and S. Pavaskar. “Optimal antiferromagnets for light dark matter detection”. In: *Phys. Rev. D* 108.1 (2023), p. L011901. DOI: 10.1103/PhysRevD.108.L011901. arXiv: 2210.13516 [hep-ph].

[201] A. Berlin, A. J. Millar, T. Trickle, and K. Zhou. “Physical signatures of fermion-coupled axion dark matter”. In: *JHEP* 05 (2024), p. 314. DOI: 10.1007/JHEP05(2024)314. arXiv: 2312.11601 [hep-ph].

[202] S. Chigusa, D. Kondo, H. Murayama, R. Okabe, and H. Sudo. “Axion detection via superfluid ^{3}He ferromagnetic phase and quantum measurement techniques”. In: *JHEP* 09 (2024), p. 191. DOI: 10.1007/JHEP09(2024)191. arXiv: 2309.09160 [hep-ph].

[203] Y. Kahn and T. Lin. “Searches for light dark matter using condensed matter systems”. In: *Rept. Prog. Phys.* 85.6 (2022), p. 066901. DOI: 10.1088/1361-6633/ac5f63. arXiv: 2108.03239 [hep-ph].

[204] K. M. Zurek. “Dark Matter Candidates of a Very Low Mass”. In: *Ann. Rev. Nucl. Part. Sci.* 74 (2024), pp. 287–319. DOI: 10.1146/annurev-nucl-101918-023542. arXiv: 2401.03025 [hep-ph].

[205] M. T. Hutchings and E. Samuelsen. “Measurement of spin-wave dispersion in NiO by inelastic neutron scattering and its relation to magnetic properties”. In: *Physical Review B* 6.9 (1972), p. 3447. DOI: 10.1103/PhysRevB.6.3447.

[206] S. M. Rezende, A. Azevedo, and R. L. Rodríguez-Suárez. “Introduction to antiferromagnetic magnons”. In: *Journal of Applied Physics* 126.15 (2019). DOI: 10.1063/1.5109132.

[207] S. Pavaskar, R. Penco, and I. Z. Rothstein. “An effective field theory of magneto-elasticity”. In: *SciPost Phys.* 12.5 (2022), p. 155. DOI: 10.21468/SciPostPhys.12.5.155. arXiv: 2112.13873 [hep-th].

[208] P. G. Catinari, A. Esposito, and S. Pavaskar. “An EFT for anisotropic anti-ferromagnets: gapped Goldstones, pseudo-Goldstones, and phase transitions”. In: (Nov. 2024). arXiv: 2411.09761 [cond-mat.str-el].

[209] J. Tomlinson, L. Domash, R. Hay, and C. Montgomery. “The high temperature heat content of nickel oxide”. In: *Journal of the American Chemical Society* 77.4 (1955), pp. 909–910. DOI: 10.1021/ja01609a032.

[210] K. Kannan, D. Radhika, K. K. Sadasivuni, K. R. Reddy, and A. V. Raghu. “Nanostructured metal oxides and its hybrids for photocatalytic and biomedical applications”. In: *Advances in Colloid and Interface Science* 281 (2020), p. 102178. DOI: 10.1016/j.cis.2020.102178.

[211] H. Leutwyler. “Nonrelativistic effective lagrangians”. In: *Physical Review D* 49.6 (1994), p. 3033. DOI: 10.1103/PhysRevD.49.3033.

[212] F. Machado et al. “Spin-flop transition in the easy-plane antiferromagnet nickel oxide”. In: *Physical Review B* 95.10 (2017), p. 104418. DOI: 10.1103/PhysRevB.95.104418.

[213] G. Krnjaic, D. Rocha, and T. Trickle. “The non-relativistic effective field theory of dark matter-electron interactions”. In: *JHEP* 03 (2025), p. 165. DOI: 10.1007/JHEP03(2025)165. arXiv: 2407.14598 [hep-ph].

[214] Z. Wang and L. Shao. “Axion induced spin effective couplings”. In: *Phys. Rev. D* 103.11 (2021), p. 116021. DOI: 10.1103/PhysRevD.103.116021. arXiv: 2102.04669 [hep-ph].

[215] T. Piffl et al. “The RAVE survey: the Galactic escape speed and the mass of the Milky Way”. In: *Astron. Astrophys.* 562 (2014), A91. DOI: 10.1051/0004-6361/201322531. arXiv: 1309.4293 [astro-ph.GA].

[216] G. Monari et al. “The escape speed curve of the Galaxy obtained from Gaia DR2 implies a heavy Milky Way”. In: *Astronomy & Astrophysics* 616 (2018), p. L9. DOI: 10.1051/0004-6361/201833748.

[217] X. Ou, A.-C. Eilers, L. Necib, and A. Frebel. “The dark matter profile of the Milky Way inferred from its circular velocity curve”. In: *Monthly Notices of the Royal Astronomical Society* 528.1 (2024), pp. 693–710. DOI: 10.1093/mnras/stae034.

[218] S. Bayrakci, T. Keller, K. Habicht, and B. Keimer. “Spin-wave lifetimes throughout the Brillouin zone”. In: *Science* 312.5782 (2006), pp. 1926–1929. DOI: 10.1126/science.1127756.

[219] S. Bayrakci et al. “Lifetimes of Antiferromagnetic Magnons in Two and Three Dimensions:<? format?> Experiment, Theory, and Numerics”. In: *Physical review letters* 111.1 (2013), p. 017204. DOI: 10.1103/PhysRevLett.111.017204.

[220] D. N. Spergel. “The Motion of the Earth and the Detection of Wimps”. In: *Phys. Rev. D* 37 (1988), p. 1353. DOI: 10.1103/PhysRevD.37.1353.

[221] F. Mayet et al. “A review of the discovery reach of directional Dark Matter detection”. In: *Phys. Rept.* 627 (2016), pp. 1–49. DOI: 10.1016/j.physrep.2016.02.007. arXiv: 1602.03781 [astro-ph.CO].

[222] I. G. Irastorza and J. Redondo. “New experimental approaches in the search for axion-like particles”. In: *Prog. Part. Nucl. Phys.* 102 (2018), pp. 89–159. DOI: 10.1016/j.ppnp.2018.05.003. arXiv: 1801.08127 [hep-ph].

[223] F. Bianchini, G. G. di Cortona, and M. Valli. “QCD axion: Some like it hot”. In: *Phys. Rev. D* 110.12 (2024), p. 123527. DOI: 10.1103/PhysRevD.110.123527. arXiv: 2310.08169 [hep-ph].

[224] M. M. Miller Bertolami, B. E. Melendez, L. G. Althaus, and J. Isern. “Revisiting the axion bounds from the Galactic white dwarf luminosity function”. In: *JCAP* 10 (2014), p. 069. DOI: 10.1088/1475-7516/2014/10/069. arXiv: 1406.7712 [hep-ph].

[225] A. Caputo and G. Raffelt. “Astrophysical Axion Bounds: The 2024 Edition”. In: *PoS* COSMICWISPers (2024), p. 041. DOI: 10.22323/1.454.0041. arXiv: 2401.13728 [hep-ph].

[226] G. Marocco and J. Wheater. “Spin-dependent dark matter scattering in quasi-two-dimensional magnets”. In: (Jan. 2025). arXiv: 2501.18120 [hep-ph].

[227] N. Craig. “Naturalness: past, present, and future”. In: *Eur. Phys. J. C* 83.9 (2023), p. 825. DOI: 10.1140/epjc/s10052-023-11928-7. arXiv: 2205.05708 [hep-ph].

[228] C. Branchina, V. Branchina, and F. Contino. “Physical tuning and naturalness”. In: *Phys. Rev. D* 107.9 (2023), p. 096012. DOI: 10.1103/PhysRevD.107.096012. arXiv: 2208.05431 [hep-ph].

[229] M. Farina, D. Pappadopulo, and A. Strumia. “A modified naturalness principle and its experimental tests”. In: *JHEP* 08 (2013), p. 022. DOI: 10.1007/JHEP08(2013)022. arXiv: 1303.7244 [hep-ph].

[230] P. Fileviez Pérez, C. Murgui, S. Patrone, A. Testa, and M. B. Wise. “Finite naturalness and quark-lepton unification”. In: *Phys. Rev. D* 109.1 (2024), p. 015011. DOI: 10.1103/PhysRevD.109.015011. arXiv: 2308.07367 [hep-ph].

[231] F. Vissani. “Do experiments suggest a hierarchy problem?” In: *Phys. Rev. D* 57 (1998), pp. 7027–7030. DOI: 10.1103/PhysRevD.57.7027. arXiv: hep-ph/9709409.

[232] A. de Gouvea, D. Hernandez, and T. M. P. Tait. “Criteria for Natural Hierarchies”. In: *Phys. Rev. D* 89.11 (2014), p. 115005. DOI: 10.1103/PhysRevD.89.115005. arXiv: 1402.2658 [hep-ph].

[233] M. Cirelli, N. Fornengo, and A. Strumia. “Minimal dark matter”. In: *Nucl. Phys. B* 753 (2006), pp. 178–194. DOI: 10.1016/j.nuclphysb.2006.07.012. arXiv: hep-ph/0512090.

[234] G. F. Giudice. “Naturalness after LHC8”. In: *PoS* EPS-HEP2013 (2013), p. 163. DOI: 10.22323/1.180.0163. arXiv: 1307.7879 [hep-ph].

[235] K. R. Dienes. “Solving the hierarchy problem without supersymmetry or extra dimensions: An Alternative approach”. In: *Nucl. Phys. B* 611 (2001), pp. 146–178. DOI: 10.1016/S0550-3213(01)00344-3. arXiv: hep-ph/0104274.

[236] G. E. Volovik. “Vacuum energy: Quantum hydrodynamics versus quantum gravity”. In: *JETP Lett.* 82 (2005), pp. 319–324. DOI: 10.1134/1.2137368. arXiv: gr-qc/0505104.

[237] J. R. Espinosa et al. “The cosmological Higgstory of the vacuum instability”. In: *JHEP* 09 (2015), p. 174. DOI: 10.1007/JHEP09(2015)174. arXiv: 1505.04825 [hep-ph].

[238] I. L. Buchbinder, S. D. Odintsov, and I. L. Shapiro. *Effective action in quantum gravity.* 1992.

[239] P. A. R. Ade et al. “Improved Constraints on Primordial Gravitational Waves using Planck, WMAP, and BICEP/Keck Observations through the 2018 Observing Season”. In: *Phys. Rev. Lett.* 127.15 (2021), p. 151301. DOI: 10.1103/PhysRevLett.127.151301. arXiv: 2110.00483 [astro-ph.CO].

[240] E. Calabrese et al. “The Atacama Cosmology Telescope: DR6 Constraints on Extended Cosmological Models”. In: (Mar. 2025). arXiv: 2503.14454 [astro-ph.CO].

[241] M. Drees and Y. Xu. “Small field polynomial inflation: reheating, radiative stability and lower bound”. In: *JCAP* 09 (2021), p. 012. DOI: 10.1088/1475-7516/2021/09/012. arXiv: 2104.03977 [hep-ph].

[242] K. Clough et al. “Robustness of Inflation to Inhomogeneous Initial Conditions”. In: *JCAP* 09 (2017), p. 025. DOI: 10.1088/1475-7516/2017/09/025. arXiv: 1608.04408 [hep-th].

[243] G. N. Remmen and S. M. Carroll. “Attractor Solutions in Scalar-Field Cosmology”. In: *Phys. Rev. D* 88 (2013), p. 083518. DOI: 10.1103/PhysRevD.88.083518. arXiv: 1309.2611 [gr-qc].

[244] G. N. Remmen and S. M. Carroll. “How Many e-Folds Should We Expect from High-Scale Inflation?” In: *Phys. Rev. D* 90.6 (2014), p. 063517. DOI: 10.1103/PhysRevD.90.063517. arXiv: 1405.5538 [hep-th].

[245] D. Battefeld and P. Peter. “A Critical Review of Classical Bouncing Cosmologies”. In: *Phys. Rept.* 571 (2015), pp. 1–66. DOI: 10.1016/j.physrep.2014.12.004. arXiv: 1406.2790 [astro-ph.CO].

[246] R. Brandenberger and P. Peter. “Bouncing Cosmologies: Progress and Problems”. In: *Found. Phys.* 47.6 (2017), pp. 797–850. DOI: 10.1007/s10701-016-0057-0. arXiv: 1603.05834 [hep-th].

[247] L. Del Grosso et al. “Cosmological Consequences of Unconstrained Gravity and Electromagnetism”. In: (May 2024). arXiv: 2405.06374 [hep-ph].

[248] Y. Fujii and K. Maeda. *The scalar-tensor theory of gravitation.* Cambridge Monographs on Mathematical Physics. Cambridge University Press, July 2007. ISBN: 978-0-521-03752-5, 978-0-521-81159-0, 978-0-511-02988-2. DOI: 10.1017/CBO9780511535093.

[249] B. de Wit and R. Gastmans. “On the Induced Cosmological Term in Quantum Gravity”. In: *Nucl. Phys. B* 128 (1977), pp. 294–312. DOI: 10.1016/0550-3213(77)90033-5.